

Acquisitions and Bibliographic Services Branch

395 Wellington Street Ottawa, Ontario K1A 0N4 Bibliothèque nationale du Canada

Direction des acquisitions et des services bibliographiques

395, rue Wellington Ottawa (Ontano) K1A 0N4

Your fac. Voter interesce

Our Ne. Notice reference

NOTICE

The quality of this microform is heavily dependent upon the quality of the original thesis submitted for microfilming. Every effort has been made to ensure the highest quality of reproduction possible.

La qualité de cette microforme dépend grandement de la qualité de la thèse soumise au microfilmage. Nous avons tout fait pour assurer une qualité supérieure de reproduction.

AVIS

If pages are missing, contact the university which granted the degree.

S'il manque des pages, veuillez communiquer avec l'université qui a conféré le grade.

Some pages may have indistinct print especially if the original pages were typed with a poor typewriter ribbon or if the university sent us an inferior photocopy.

La qualité d'impression de certaines pages peut laisser à désirer, surtout si les pages originales ont été dactylographiées à l'aide d'un ruban usé ou si l'université nous a fait parvenir une photocopie de qualité inférieure.

Reproduction in full or in part of this microform is governed by the Canadian Copyright Act, R.S.C. 1970, c. C-30, and subsequent amendments. La reproduction, même partielle, de cette microforme est soumise à la Loi canadienne sur le droit d'auteur, SRC 1970, c. C-30, et ses amendements subséquents.



CHARACTERIZATION OF POLYSTYRENE BASED DIBLOCK COPOLYMER MICELLES

by

Karine Khougaz

Submitted to the Faculty of Graduate Studies and Research in partial fulfillment of the requirements for the degree of

Doctor of Philosophy

Department of Chemistry McGill University Montreal, Quebec Canada H3A 2K6

© Karine Khougaz, 1995



Acquisitions and Bibliographic Services Branch

395 Wellington Street Ottawa, Ontario K1A 0N4 Bibliothèque nationale du Canada

Direction des acquisitions et des services bibliographiques

395, rue Wellington Ottawa (Ontario) K1A 0N4

Your file. Vicely reference

Our life. Notice references

The author has granted an irrevocable non-exclusive licence allowing the National Library of Canada to reproduce, loan, distribute or sell copies of his/her thesis by any means and in any form or format, making this thesis available to interested persons.

L'auteur a accordé une licence irrévocable et non exclusive permettant à la Bibliothèque nationale du Canada reproduire, prêter, distribuer ou vendre des copies de sa thèse de quelque manière et sous quelque forme que ce soit pour mettre des exemplaires de cette thèse à disposition la personnes intéressées.

The author retains ownership of the copyright in his/her thesis. Neither the thesis nor substantial extracts from it may be printed or otherwise reproduced without his/her permission. L'auteur conserve la propriété du droit d'auteur qui protège sa thèse. Ni la thèse ni des extraits substantiels de celle-ci ne doivent être imprimés ou autrement reproduits sans son autorisation.

ISBN 0-612-12402-9



ABSTRACT

The micellization of polystyrene based block copolymers was investigated in aqueous and in organic media. Micelles formed from polystyrene-b-poly(sodium acrylate) (PS-b-PANa) in sodium chloride solutions were investigated by static light scattering (SLS). The aggregation numbers (Nagg) were influenced by low salt concentrations (< 0.10 M) and they were essentially independant of the soluble block lengths. The core radii (R_c) agreed well with previous solid state results on similar samples studied by small-angle X-ray scattering (SAXS). It was thus concluded that no supermicellar aggregates were present and that the cores were solvent free.

A method to evaluate the critical micelle concentrations (cmc's) of block copolymer micelles by SLS was developed to account for the effects of polydispersity on the cmc. It was found that for block copolymers which have a significant dependence of the cmc on the insoluble block length and which are polydisperse only the present approach was able to evaluate the cmc.

The micellization of PS-b-PANa and PS-b-poly(acrylic acid) (PS-b-PAA) block copolymers were investigated in organic solvents. The cmc's were found to range from 1 x 10-7 to 5 x 10-9 M for insoluble block lengths ranging from 2.6 to 18 units. The N_{agg} and R_c values for four PS-b-PANa series in tetrahydrofuran, were found to be a function of the length of both blocks. The effect of the degree of neutralization of the PAA block on micellization was probed by SLS and SAXS; micelle formation was found to commence at 5% neutralization. The distribution of water between toluene and the polar cores of block ionomer and sodium bis(2-ethylhexyl)sulfosuccinate (AOT) reverse micelles was investigated by proton chemical shift measurements as a function of temperature. The amount of water solubilized and the thermodynamic parameters of transfer were found to be a function of the core nature.

RÉSUMÉ

La micellisation des copolymères disséquencés basés sur le motif styrènique a été étudiée en milieu aqueux et organiques. Les micelles formées par le polystyrène-b-poly(acrylates de sodium) (PS-b-PANa) dans des solutions contenant du chlorure de sodium ont été étudiées par la diffusion lumineuse en mode statique (DLMS). Les indices d'aggrégation (I_{agg}) sont influencés par la présence d'une concentration peu élevée de sel (< 0.10 M), mais ils ne varient pas en fonction des longueurs des séquences solubles dans le média. Pour des échantillons similaires, les rayons du coeur des micelles (Rc) déterminés à l'aide de la DLMS sont en bon accord avec ceux déterminés ultérieurement en phase solide par la diffusion des rayons-X aux petits angles (SAXS). Il est donc possible de conclure qu'aucun super-aggrégats micellaires sont présents et que le solvant est absent du coeur des micelles.

Une méthode basée sur la DLMS, permettant l'évaluation la concentration critique de micelle (CCM) pour des micelles de copolymères disséquencés, a été développée pour tenir compte de l'effet de la polydispersité sur la CCM. Il a été trouvé que cette méthode est la seule qui permet d'évaluer la CCM pour des copolymères disséquencés dont la longueur de la séquence insoluble a un effet marqué sur la CMC et où la polydispersité est présente.

La micellisation des copolymères disséquencés, comme le PS-b-PANa et le PS-b-poly(acrylate acide) (PS-b-PAA), a été étudiée dans des solvants organiques. Les CCM's varient entre 1 x 10⁻⁷ et 1 x 10⁻⁹ M pour des séquences insolubles ayant une longueur variant entre 2.6 et 18 unités. Il a été observé que les valeurs d'I_{agg} et de R_C, pour quatre séries de PS-b-PANa dans le tetrahydrofurane, varient en fonction de la longueur des deux séquences. L'effet du degré de neutralisation de la séquence PAA sur la micellisation a été étudié par la DLMS et la SAXS; il a été observé que la formation des micelles débute lorsque le degré de neutralisation atteint 5%. La distribution de l'eau entre le toluène et les coeurs polaires des micelles inverses, basées sur des ionomères disséquencés ou du bis(2-ethylhexyl) sulfosuccinate de sodium (AOT), a été étudiée à l'aide du déplacement chimique du proton en fonction de la température. La quantité d'eau solubilisée et les paramètres thermodynamiques de transfert varient en fonction de la nature du coeur de la micelle.

FOREWORD

In accordance with guideline 7 of the "Guidelines Concerning Thesis Preparation" (Faculty of Graduate Studies and Research), the following text is cited.

"The candidate has the option, subject to the approval of the Department, of including as part of the thesis the text, or duplicated published text (see below), of an original paper, or papers. In this case the thesis must still conform to all other requirements explained in Guidelines Concerning Thesis Preparation. Additional material (procedural and design data as well as descriptions of equipment) must be provided in sufficient detail (e.g. in appendices) to allow a clear an precise judgment to be made of the importance and originality of the research reported. The thesis should be more than a mere collection of manuscripts published or to be published. It must include a general abstract, a full introduction and literature review and a final overall conclusion. Connecting texts which provide logical bridges between different manuscripts are usually desirable in the interests of cohesion.

It is acceptable for these to include as chapters authentic copies of papers already published, provided these are duplicated clearly on regulation thesis stationery and bound as an integral part of the thesis. Photographs or other materials which do not duplicate well must be included in their original form. In such instances, connecting texts are mandatory and supplementary explanatory material is almost always necessary.

The inclusion of manuscripts co-authored by the candidate and others is acceptable but the candidate is required to make an explicit statement on who contributes to such a work and to what extent, and supervisors must attest to the accuracy of the claims, e.g., before the Oral Committee. Since the task of the Examiners is made more difficult in these cases, it is the candidate's interest to make the responsibilities of authors perfectly clear. Candidates following this option must inform the Department before it submits the thesis for review."

This dissertation is written in the form of six papers. The papers each comprise one chapter, with a introduction of this work in a first chapter and general conclusions contained in an eighth chapter. Following normal procedure, the papers have been either published or submitted or will be submitted shortly for publication in scientific journals. A list of the papers is given below:

Chapter 2: Accounts of Chemical Research (in press)

Chapter 3: Macromolecules 1995, 25, 7135 - 7147.

Chapter 4: Macromolecules 1994, 27, 6341 - 6346.

Chapter 5: Macromolecules (submitted)

Chapter 6: Canadian Journal of Chemistry (in press)

Chapter 7: Langmuir (to be submitted)

All of the papers include the research director, Dr. Adi Eisenberg, as co-author. Chapter 2 also includes Mr. Matthew Moffitt who co-wrote this review article. Chapter 3 includes Dr. Irina Astafieva as a co-author, recognizing discussions and her expertise in polyelectrolytes. Chapter 4 includes Dr. Zhisheng Gao, recognizing his advice and important discussions regarding the method of cmc determination using his micellization model. Chapter 5 includes Dr. Xing Fu Zhong as a co-author recognizing the synthesis of the samples used in the study. Chapter 6 includes Dr. Diep Nguyen and Dr. Claudine Williams as co-authors, they measured the small-angle X-ray data. Chapter 7, includes Dr. Zhisheng Gao who performed some of the NMR relaxation time measurements. All the block copolymer samples were synthesized by other people, for instance by Dr. Xing Fu Zhong (Chapters 3, 4, 5, and 7), Dr. Sunil K. Varshney (Chapters 5, 6 and 7) and Dr. Alain Desjardins (Chapter 7). Other than the supervision, advice and direction of Dr. Eisenberg and the aforementioned contribution to the chapters, all of the work presented in this dissertation was performed by the author.

ACKNOWLEDGMENT

This work would not have been so enjoyable if it was not for Dr. Eisenberg who has a tremendous enthusiasm for science. He is an excellent and dedicated teacher and gives special attention to the growth of scientists.

I would especially like to thank my mother, my father, and my sister for their endless support, encouragement and love which I have received throughout my life. I also thank Lee for his love, companionship, and endless support. (Ti Amo!)

In addition, I would like to thank ...

- Joon, (an angel who fell off a cloud) for being a great best friend and for enriching my life forever. I also thank him for his support, all his advice and help, and for proof reading my thesis.
- Michelle, (my twin!) for her wonderful and special friendship, great humor, coffee breaks, encouragement and many happy moments.
- © Francis, for his friendship, for being my very own personal computer wiz, and for the translation of my abstract.
- © Angela, for being my oldest and dearest friend and for her encouragement.
- Matthew, for useful discussions, his terrific jokes and for reading parts of this thesis.
- Diep, for her friendship and advice
- ② Zhisheng for his many insights and guidance, Xing Fu for synthesizing most of the polymers used in my thesis, and Ray for his valuable opinions.
- Special friends: Antonella, Ariane, Darlene, Larry, Louis, Louise, Shaune, Joanne, and Phil.
- In addition, I would like to thank all the persons in my group, past and present who made my work place very enjoyable as well as other persons in the department;

present: Bruce, Chris, Hongwei, Kui, Lifeng, Matthew, Neil, Sheng, Yisong, Zhimei and past: Alain, Attila, Gaoming, George, Irina, Ishrat, Jean Pierre, Jianming, Katsu, Monali, Mario, Nishi, Sabrina, Stan, Sunil.

others in the department: Anmar, Jean, Kathy, Laura, Tanya, Tara, Dr. R. Brown, Dr. B. Lennox, and Dr. G. Darling, Renée, Françoise, and the secretaries in the department, in particular, Paulette, Carol B., and Aline.

Finally, I am very gratefully for scholarship funding which I have received from the Natural Sciences and Engineering Research Council of Canada and Le Fonds pour La Formation de Chercheurs et L'Aide à la Recherche for scholarship funding.

Abst	ract		ii
Résu	mé		iii
Fore	ward		iv
Ackr	nowledgn	eent	xiii
Table	e of Cont	ents	xiv
List	of Freque	ntly Used Symbols	xx
List	of Tables		xxvi
List	of Figures		xxviii
Cha	pter 1.	General Introduction	
1.1.	Introduc	tion	1
	1.1.1.	General Overview of Polymers	2
		1.1.1.1. Average and Distribution of Molecular Weights	2
		1.1.1.2. Types of Polymers	5
1.2.	Features	of Block Copolymers	6
	1.2.1.	Synthesis of Block Copolymers	6
	1.2.2.	Phase Separation in Bulk	7
1.3.	Micelliz	ation of Block Copolymers in Solution	8
	1.3.1.	Dependence of the Free Energy of Micellization on the Insoluble Block Length	13
	1.3.2.	Influence of Polydispersity on the cmc	13
	1.3.3.	Dynamics of Block Copolymer Micelles	15
	1.3.4.	Equilibrium Versus Near Equilibrium Conditions of Micelle Formation	15
1.4.	Theoreti	cal Analysis of Block Copolymer Micelles	16
1.5.	Methods	of Micellar Characterization	19
	1.5.1.	Static Light Scattering	2
		1.5.1.1. General Light Scattering Theory	21

		1.5.1.2. Application to Block Copolymers	24
		1.5.1.3. Application to Polyelectrolytes	25
		1.5.1.4. SLS Analysis	26
		1.5.1.5. Instrumentation	28
	1.5.2.	Dynamic Light Scattering	29
	1.5.3.	Size Exclusion Chromatography	30
1.6.	Focus ar	nd Purpose of Present Thesis	31
1.7.	Reference	es	37
Cha	apter 2.	Micellization of Ionic Block Copolymers	
2.1.	Introduc	tion	41
2.2.	Ionic Bl	ock Copolymers in Organic Solvents (Block Ionomer Micelles)	45
	2.2.1.	Characterization of Fundamental Parameters	46
	2.2.2.	Critical Micelle Concentrations of Block Ionomers	50
	2.2.3.	Characterization of Water Solubilization and Chain Dynamics by NMR	52
	2.2.4.	Semiconductor Nanoparticles in Block Ionomer Micelles	53
2.3.	Ionic Bl	ock Copolymers in Aqueous Media (Block Polyelectrelyte Micelles)	55
	2.3.1.	Characterization of Star Micelles	56
	2.3.2.	Characterization of Crew Cut Micelles	59
2.4.	Conclus	ions	61
2.5.	Acknow	rledgment	61
2.6.	Referen	ces	62
Cha	apter 3.	Characterization of Polystyrene-b-Poly(sodium	
		acrylate) Block Polyelectrolyte Micelles by Static Light Scattering	
	ABSTR		67
2 1		·	
	Introduc		68
3.2.	Expenin	nental Section	7

	3.2.1.	Materials	71
	3.2.2.	Sample Preparation for Static Light Scattering (SLS)	72
	3.2.3.	SLS Measurement	73
	3.2.4.	Specific Refractive Index Increment Measurement (dn/dc)	73
3.3.	Results	and Discussion	74
	3.3.1.	Theory	74
	3.3.2.	Time Dependence of SLS Data - Kinetics of Disentanglement	78
	3.3.3.	Aggregation Numbers and Micellar Sizes as a Function of Salt	
		Concentration	85
		3.3.3.1. Specific Refractive Index Increment	85
		3.3.3.2. Typical Zimm Plots	88
		3.3.3.3. Influence of Salt Concentration	90
	3.3.4.	Characterization in 2.5 M NaCl	96
		3.3.4.1. Aggregation Numbers and Calculated Core Radii	96
		3.3.4.2. Second Virial Coefficient Values	100
		3.3.4.3. Radius of Gyration Values	100
	3.3.5.	Applications of Scaling Theories	101
		3.3.5.1. Star Model	101
		3.3.5.2. Mean Field Models	104
	3.3.6.	Comparison with Solid State Results and with those for PS-b-PEO in Water	108
3.4.	Conclus	ions	109
3.5.	Acknow	rledgment	110
3.6.	Reference	œs	113
Cha	apter 4.	Determination of the Critical Micelle Concentration of	
		Block Copolymer Micelles by Static Light Scattering	
	ABSTR	ACT	117
4.1.	Introduc	tion	118
4.2.	Theory		122
4.3.	Experim	ental	126
	4.3.1.	Sample Preparation	126

	4.3.2.	Static Light Scattering	127
4.4.	Results a	nd Discussion	127
	4.4.1.	PS-b-PANa System	127
	4.4.2.	PS-b-P4VP System	131
	4.4.3.	PS-b-PI System	134
4.5.	Conclusi	ons	139
4.6.	Acknowl	edgment	140
4.7.	Referenc	es	142
Cha	pter 5.	Aggregation and Critical Micelle Concentrations of	
		Polystyrene-b-Poly(sodium acrylate) and Polystyrene-	
		b-Poly(acrylic acid) Micelles in Organic Media	
	ABSTR	ACT	144
5.1.	Introduc	tion	145
5.2.	Experim	ental	150
	5.2.1.	Synthesis	150
	5.2.2.	Size Exclusion Chromatography	152
	5.2.3.	Sample Preparation for Light Scattering	152
	5.2.4.	Static Light Scattering Measurements	153
	5.2.5.	Dynamic Light Scattering Measurements	156
5.3.	Results a	and Discussion	157
	5.3.1.	cmc's for PS(660)-b-PANa(x) and PS(660)-b-PAA(x) Block Copolymer Micelles	158
		5.3.1.1. Solvent and Insoluble Block Effects	158
		5.3.1.2. Theoretical applications of the Mixed Micelle Model	163
		5.3.1.3. Correlations of the a and b Constants with Interaction Parameters	165
	5.3.2.	Aggregation of PS(660)-b-PANa(x) and PS(660)-b-PAA(x) Block Copolymer Micelles	172
		5.3.2.1. Size Exclusion Chromatography	172
		5.3.2.2. Static Light Scattering	175
		5.3.2.3. Dynamic Light Scattering	180

	5.3.3.	Effect of PS block lengths on the Aggregation of PS-b-PANa block ionomers	183
5.4.	Conclus	ions	190
5.5.	Acknow	ledgment	192
5.6.	Reference	ees ees	194
Cha	pter 6.	Effect of the Degree of Neutralization on the Micellization of Block Ionomers	
	ABSTR	ACT	199
6.1.	Introduc	tion	200
6.2.	Experim	ental ental	202
	6.2.1.	Materials	202
	6.2.2.	Sample Preparation for SLS	203
	6.2.3.	Static Light Scattering and Specific Refractive Index Increment (dn/dc) Measurement	204
	6.2.4.	Sample Preparation for SAXS	205
	6.2.5.	SAXS Measurement	205
6.3.	Results a	and Discussion	205
	6.3.1.	Titration of PS-b-PAA with CsOH/MeOH	206
	6.3.2.	SLS Results on Freeze Dried Samples	211
	6.3.3.	SAXS Results on Freeze Dried Samples	214
6.4.	Conclusi	ons	216
6.5.	Acknow	ledgment	217
6.6.	Dedicati	on	217
6.7.	Reference	es es	219
Cha	pter 7.	Distribution of Water in Solutions of Reverse Micelles	
		of AOT and Block Ionomers in Toluene	
	ABSTR	ACT	22]
7.1.	Introduc	tion	222

Anı	nex A	Program for cmc Determination	A- 1
8.2.	Sugges	stions for Future Work	267
		Block Copolymer Reverse Micelles	263
		Cmc Determination of Block Copolymer Micelles by SLS	262
0.1.		Block Polyelectrolyte Micelles	260
ጸ 1	Conclu	sions and Contributions to Original Knowledge	260
Cha	apter 8.	. Conclusions, Contributions to Original Knowledge and Suggestions for Future Work	.
7.7.	Referen	nces	256
7.6.	Acknov	wledgment	255
7.5.	Conclus	sions	254
	7.4.2.	Relaxation Studies of Nuclei in the Ion-Water Core	252
		7.4.1.5. Possible Structure of the hydrated core in block ionomers	
		7.4.1.4. Counterion Effect	250
		7.4.1.3. Comparison of Thermodynamic Parameters for the Reverse Micelle Systems	244
		7.4.1.2. Block Ionomers	239
		7.4.1.1. AOT	233
	7.4.1.		232
		and Discussion	232
7.3.	Theoret	tical Aspects of Water Transfer	229
		NMR Measurement	229
		Sample Preparation	228
l sáns	7,2,1.		226
7.2	Experin	nental	226

θ Angle

Γ Decay rate

α Degree of neutralization

ρ Density (g/mL)

β Optical constant (for DLS)

σ Standard deviation of the MWD curve

η Viscosity

φ Volume fraction of monomers in a chain

λ Wavelength (nm)

 λ_0 Wavelength in vacuum (nm)

χ Flory-Huggins interaction parameter

χ_{AB} Interaction parameter between the A and B blocks

χ_{core-sol} Interaction parameter of the polymer forming the core and

the solvent

Xcorona-sol Interaction parameter of polymer forming the corona and

the solvent

χ_{ps} Polymer-solvent interaction parameter

ΔGatt Free energy of attraction

 ΔG_{m} Free energy of micelle formation

 ΔG_t^o Free energy of transfer ΔH_t^o Enthalpy of transfer $\Delta v_{1/2}$ Line width at half height

 α_i Mole fraction of *i*th component in the mixture

 δ_{mic} Chemical shift of solute in micelle

(M_N)_w Weight-average molecular weight of an aggregate

 $\delta_{\rm obs}$ Observed chemical shift

 δ_p Solubility parameter for the polymer δ_s Solubility parameter for the solvent

 δ_{sol} Chemical shift of solute in the solvent phase

 $\Delta S_{\bullet}^{\circ}$ Entropy of transfer

<R_e²>, Square z-average radius of gyration

[η] Intrinsic viscosity

[D_M] Concentration of micellized surfactant

[D_T] Total surfactant concentration or concentration of ionic

block on a repeat unit basis

4VP 4-vinylpyridine a Monomer size

A-b-B Diblock copolymer; polymer A attached to polymer B

 A_2 Second virial coefficient (mL mol/g²))

A_H Hamaker constant

AOT Sodium bis(2-ethylhexyl)sulfosuccinate

B Baseline

c Concentration

c* Overlap concentration (units)

cal Calculated

C_i cmc for a monodisperse system cmc Critical micelle concentration cmc(mix) cmc for a polydisperse system

CML Critical micelle length

CMT Critical micelle temperature
C_s Salt concentration (M)

Cs⁺ Cesium ion

CsOH Cesium hydroxide

CTAB Cetyltrimethylammonium bromide

D Translational diffusion coefficient

Dh Hydrodynamic diameter
DLS Dynamic light scattering
DMF Dimethylformamide

dn/dc Specific refractive index increment (mL/g)

DP Degree of Polymerization

DP_n Number average degree of polymerization
DP_w Weight average degree of polymerization

E_{coh} Cohesive energy

ESR Electron spin resonance

expt Experimental

f_i Activity coefficient

 $f_{\rm mic}$ Percent of micellized chains

FT-IR Fourier-transform infrared spectroscopy

G₂(t) Correlation function

H Distance between surfaces of two particles

h Hour

I Scattered intensity

 $I(\theta)$ Scattered intensity (mV) at an angle θ

 $I(\theta)_{solvent}$ Solvent intensity

I₀ Intensity of incident light

IR Infrared

K Distribution coefficient of solute or Optical constant (for

SLS)

k Scaling factor

k_B Boltzmann constant
LiBr Lithium bromide

In Logarithm to the base e (=2.303)

LOW Leibler, Orland and Wheeler

M Molarity (moles/liter) m_{θ} Slope of c=0 line m_{c} Slope of $\theta = 0$ line

m; Mass of material in the *i*th fraction

M_i Molecular weight of molecules of the *i*th fraction

M_n Number-average molecular weight
 M_v Viscosity-average molecular weight

MW Repeat unit molecular weight

 M_w Weight-average molecular weight (g/mol) M_w (mic) Weight-average molecular weight of micelles $M_w(s)$ Weight-average molecular weight of single chains

M_{w,app} Apparent weight-average molecular weight
M_{w,total} Total weight-average molecular weight

MWD Molecular weight distribution
M, Z-average molecular weight

N Number average degree of polymerization

n Refractive index

N_A Number of monomeric units in copolymer block forming the

corona

NaCl Sodium chloride

Nagg Aggregation number

Nav Avogadro's number

N_B Number of monomeric units in copolymer block forming the

core

N_i Number average degree of polymerization of ith component

NMR Nuclear Magnetic Resonance

N_{PANa} Number of monomeric or repeat units in PANa N_{PS} Number of monomeric or repeat units in PS N_{py}+(Me)I⁻ Pyridine quarternized with methyl iodide

p Fraction of solute in a micelle
 P(θ) Particle scattering function
 P(t-BuA) Poly(tert-butylacrylate)
 P.I. Polydispersity Index
 P2VP Poly(2-vinylpyridine)
 P4VP Poly(4-vinylpyridine)

P4VPEtBr Poly(4-vinylpyridinium ethyl bromide)
P4VPMeI Poly(4-vinylpyridinium methyl iodide)

PAA Poly(acrylic acid)
PACs Poly(cesium acrylate)
PANa Poly(sodium acrylate)
PBO Poly(butylene oxide)
PEO Poly(ethylene oxide)

PEP Poly(ethylene-co-propylene)

PI Polyisoprene

PMAA poly(methacrylic acid)
PMACs Poly(cesium methacrylate)
PMANa Poly(sodium methacrylate)
PMtMA Poly(metal methacrylate)
PPO Poly(propylene oxide)

PS Polystyrene

PS-COONa Sodium carboxylate-terminated polystyrene

Pt-BS Poly(tert-butylstyrene)
PTFE Poly(tetrafluoroethylene)

q Scattering vector

r Distance between center of scattering medium

R Gas constant (8.314 J K⁻¹ mol⁻¹) or Molar ratio of water to

number of moles of surfactant or Molar ratio of water to the

number of moles of ionic repeat unit (for the block

ionomers)

R₁ Spin-lattice relaxation rateR₂ Spin-spin relaxation rate

R(θ) Rayleigh ratio

r² Linear least-squares correlation coefficient

R_c Core radius (nm)

R_{cmc} Rayleigh ratio at the cmc
R_g Radius of gyration (nm)
R_b Hydrodynamic radius (nm)

 $R_{\rm m}$ Micelle radius $R_{\rm p}$ Particle radius

RPI Radii polydispersity indices

R_t Equivalent thermodynamic radius

S Single chain concentration

S/N_{agg} Surface area per chain (nm² / chain)
SANS Small-angle neutron scattering
SAXS Small-angle X-ray scattering

sec Secondary

SEC Size exclusion chromatography

SLS Static light scattering

S_{mic} Concentration of solute in the micelle

S_{sol} Concentration of solute in the solvent phase

T Temperature

t Time

t-BuA tert-butyl acrylate

t-BuMA tert-butyl methacrylate

TEM Transmission electron microscopy

tert Tertiary

T_g Glass transition temperature

THF Tetrahydrofuran

V Molar volume or Volts or Volume of scattering medium

V_c Core volume

 V_i Elution volume of the *i*th species V_s Molar volume of the solvent

W/O Water in oil

wt. %	Weight percent
$x_{\mathbf{i}}$	Mole fraction in the micelle
Z_d	Dissymmetry ratio

List of Tables

Table 1.1.	Methods for the Characterization of Block Copolymer Micelles	20
Table 3.1.	Characterization of Poly(styrene-b-sodium acrylate) in 0.10 and	
	2.5 M NaCl by SLS for Different Heating Periods at 100°C	84
Table 3.2.	Specific Refractive Index of Poly(styrene-b-sodium acrylate) in	
	Water and in NaCl Solutions	86
Table 3.3.	Micellar Properties of Some Poly(styrene-b-sodium acrylate)	
	Block Polyelectrolytes Micelles in Different Salt Concentrations	91
Table 3.4.	Summary of Results Obtained for Different Theoretical Scaling	
	Relations	107
Table 4.1.	Critical Micelle Concentration for the Poly(styrene-b-sodium	
	acrylate) Series in THF	130
Table 5.1.	Composition and Polydispersity Index of the PS homopolymers	
	and the Block Copolymers	151
Table 5.2.	Specific Refractive Index Increments of PS(660)-b-PANa(x) in	
	Different Solvents at 630 nm and 25°C	154
Table 5.3.	Summary of the a and b Constants for Different Block	
	Copolymer Systems and the Hildebrand Solubility Parameters 50	
	used in the Evaluation of Core-Solvent Interactions	164
Table 5.4.	Summary of the Weight Average Molecular Weights and	
	Aggregation Numbers for PS(660)-b-PANa(x) and PS(660)-b-	
	PAA(x) as Determined by SLS in Different Solvents	173
Table 5.5.	Summary of the Results Obtained for PS(660)-b-PANa(x) and	
	PS(660)-b-PAA(x) by SLS and DLS in Different Solvents	179
Table 5.6.	Summary of SLS Results for PS(x)-b-PANa(y) in THF	184

List of Tables

Table 5.7.	Comparison of Aggregation Numbers Determined by SLS and	
	SAXS ⁴¹	190
Table 6.1.	Results for Different Percent Neutralization for PS-b-PAA in	
	Toluene	212
Table 7.1.	Cmc values for AOT Reverse Micelles in Toluene for R = 6 at	
	Different Temperatures	236
Table 7.2.	Composition, Polydispersity Indices (P.I.) and Mole % of the	
	Ionic Block for the Block Ionomers	240
Table 7.3.	Thermodynamic Results for the Systems Studied as a Function	
	of the Ionic Group Moeity at 25°C for a Constant Water Ratio	
	of 6 and the Thermodynamic Parameters for the Transfer of	
	Water from Toluene to a Water Phase	246

List of Figures

Figure 1.1.	Distribution of molecular weights in a typical polymer.	2
Figure 1.2.	Molecular weight distributions of polymers with an average	
	chain length of 50 repeat units and P.I. values of 1.03, 1.05 and	
	1.10.	4
Figure 1.3.	Types of copolymers prepared from monomers A and B.	5
Figure 1.4.	Morphologies of PS-b-PB as a function of the volume fraction	
	of PS.	8
Figure 1.5.	Schematic representation of block copolymer (a) star and (b)	
	crew cut micelles.	9
Figure 1.6.	Structure of a monomolecular micelle formed by an AB block	
	copolymer molecule in a nonsolvent for the B block.	12
Figure 1.7.	Single chain concentration as a function of total block	
	copolymer concentration at different polydispersity indices in	
	the PS-b-PI / n-hexadecane system.	14
Figure 1.8.	Angular dependence of the Rayleigh ratio for small and large	
	particles.	23
Figure 1.9.	Representation of redistribution of solvent components A and	
	B, in which A is selectively sorbed by the polymer.	26
Figure 1.10.	Schematic Illustration of a Zimm plot	28
Figure 1.11.	Structures of PS based block copolymers used in the present	
	work.	32
Figure 2.1.	SAXS profiles of PS(600)-b-PACs(45) diblock ionomer in	
	toluene in the concentration range from 0.01 g/mL to 0.10	
	g/mL_38	49

List of Figures

Figure 2.2.	Typical cmc values for different micellar systems in aqueous	
	media: sodium alkyl sulfonate surfactants (•).44 poly(ethylene	
	oxide)-b-poly(butylene oxide)-b-poly(ethylene oxide) (PEO-b-	
	PBO-b-PEO) (\spadesuit),46 PS-b-PANa (\blacksquare),26 PS-b-PEO (\blacksquare) and	
	PEO-b-PS-b-PEO ($lacktriangledown$) ⁴⁵ and in nonaqueous media: AOT	
	(Δ), ⁴⁴ polystyrene-b-poly(isoprene) (PS-b-PI) (\square), ⁴³ PS-b-	
	PANa (O). ²⁷	51
Figure 2.3.	Plot of CdS particle diameter vs. diameter of original core	
	(calculated from $R_c = 6.5 N_B^{3/5}$ Å). Dotted circles indicate	
	CdS particles synthesized within the microdomains of random	
	ionomers. ⁵¹	54
Figure 3.1.	Effect of different heating times on the normalized plot of the	
	Rayleigh ratio as a function of $\sin^2(\theta/2)$ for PS(40)-b-	
	PANa(520).	81
Figure 3.2.	Typical Zimm plots for (a) PS(23)-b-PANa(44) and (b) PS(23)-	
	b-PANa(300) in 2.5 M NaCl.	89
Figure 3.3.	Second virial coefficient values for samples PS(6)-b-PANa(180)	
	(O), PS(23)-b-PANa(300) (O) and poly(sodium acrylate)	
	$(\mathbf{m})^{50}$ as a function of the inverse salt concentration on a	
	semilog plot. The inset graph shows the relation on a linear	
	plot.	95
Figure 3.4.	Aggregation number as a function of insoluble PS block length	
	for almost constant PANa block lengths of 85 (O), 170 (1)	
	and 350 (Δ) units as well as the samples PS(23)-b-PANa(44)	
	(V) and PS(71)-b-PANa(120) (V). The inset graph shows the	
	aggregation number as a function of PANa block length for	

	constant PS block lengths. The points in parentheses represent	
	the samples PS(50)-b-PANa(330) and PS(23)-b-PANa(780).	97
Figure 3.5.	Radius of the core as a function of the PS block length to the	
	power of 3/5, according to the star model for PS-b-PANa in 2.5	
	M NaCl (•), PS-b-PMACs and PS-b-P4VPMeI in the solid	
	state (\square),60 and PS-b-PEO in water (\triangle).54 The solid line	
	represents the linear regression through the data, and the dashed	
	line represents the 95% confidence limits.	103
Figure 3.6.	Radius of gyration (Rg(b)) according to the scaling predictions	
	of the star model for PS-b-PANa in 2.5 M NaCl for different PS	
	block lengths of 6 (○), 11(△), 23 (●), 40 (♦), 50 (■), and 71	
	(□) units. The lines represent linear regressions through the	
	data; the dashed line is the best fit, and the solid line is forced	
	through the origin.	105
Figure 4.1.	Range of existence of different species in solution as a function	
	of concentration according to the closed association model. ³³	121
Figure 4.2.	Typical cmc determination for PS(660)-b-PANa(8.9) in THF	
	from the program calculations (-) and with intentional	
	deviations of 20 % () and 50 % ().	129
Figure 4.3.	Effect of the polydispersity index on the cmc determination of	
	PS(660)-b-PANa(8.9) in THF.	132
Figure 4.4.	Cmc determination for PS(470)-b-P4VP(52) in toluene; the	
	lines () and () represent the fits obtained from the	
	current method and the Debye equation, respectively.	133
Figure 4.5.	Single chain concentrations as a function of total concentration	
	at different polydispersity indices for (a) PS-b-PANa in THF	
	and (h) PS-b-IVP in tolinene	125

Figure 4.6.	Effect of polydispersity index on the cmc values for simulated	
	data of a PS-b-PI system. The symbols represent the data	
	generated for different polydispersities: (A) 1.0, (O) 1.1 and	
	(•) 1.2. The lines represent the fit from the Debye equation	
	through the simulated data for the different polydispersity	
	indices () 1.0, () 1.1, () 1.2, respectively.	136
Figure 4.7.	Debye equation fit for the simulated data of the PS-b-PI sytem	
	with a polydispersity index of 1.2. The solid line indicates the	
	fit when the first point on the unimer line is included. The other	
	lines represent the fits for different ranges of Kc/R(0) values	
	used. These ranges are indicated by numbers which refer to the	
	ratio of the Kc/R(0) value for the unimer to the cutoff value.	
	The inset graph is a magnification of the 7 and 10 times ratio,	
	respectively.	138
Figure 5.1.	Plots of Kc/R(0) used in cmc determinations for PS(660)-b-	
	PANa(x) for different PANa block lengths in THF.	159
Figure 5.2.	Cmc values of PS(660)-b-PANa(x) in chloroform, THF and	
	toluene, and of PS(660)-b-PAA(x) in toluene, as a function of	
	the insoluble block length. The inset represents the data plotted	
	as the log of the cmc as a function of NpANa 1/3.	161
Figure 5.3.	Molecular weight distribution of the single chains (S) and the	
	micelle fraction (M) at 5 times the cmc for PS(660)-b-	
	PANa(8.9) in THF.	166
Figure 5.4.	Correlations of the a and b constants with the interaction	
	parameters of the polymer forming the core and the solvent.	170
Figure 5.5.	Aggregation numbers for PS(660)-b-PANa(x) and PS(660)-b-	
	PAA(x) in different solvents plotted as a function of the	

List of Figures

	insoluble block length. The solid and the dashed lines represent	
	linear regressions and 95 % confidence intervals.	177
Figure 5.6.	Hydrodynamic radii for PS(660)-b-PANa(x) in different	
	solvents plotted according to the scaling relation of the star	
	model.	182
Figure 5.7.	Aggregation numbers of PS(x)-b-PANa(y) in THF plotted as a	
	function of the PANa block length for different PS block	
	ler gths.	185
Figure 5.8.	Calculated core radii for the PS(x)-b-PANa(y) samples	
	investigated in THF plotted as a function of the PS and PANa	
	block lengths for the series with PS block lengths of 190 (\spadesuit),	
	630 (●), 660 (▲) and 2300 (■) units. The inset is a plot of	
	the surface area per chain as a function of NPANa ^{2/5} .	188
Figure 6.1.	Summary of results for PS(600)-b-PAA(45) as a function of	
	percent neutralization; (a) aggregation numbers (Nagg) for	
	freeze dried samples measured in toluene; (b) core radii (Rc) for	
	freeze dried samples measured in toluene (A) and scattered	
	light intensity at 90° normalized to polymer concentration	
	(I90/c) as a function of the percent neutralization with	
	CsOH/methanol measured in dioxane (O). The inset shows	
	Igo/c for low percent of neutralization. The lines are shown as	
	a guide for the eye.	207
Figure 6.2.	Scattered light intensity at 90° normalized to polymer	
	concentration (190/c) as a function of the percent neutralization	
	with CsOH/methanol in benzene/methanol (90/10 (v/v)) for	
	PS(600)-b-PAA(34) (●) and PS(600)-b-PAA(13) (▲). The	
	lines are shown as a guide for the eye.	209

Figure 7.1.	Structure of AOT	223
Figure 7.2.	Typical NMR Spectra of (a) PS-b-PMANa in benzene-d6 and	
	(b) water in benzene-d ₆ at 25°C.	231
Figure 7.3.	Plots for the evalutation of the distribution coefficients using	
	[DT] (see text) for AOT in toluened8 at different temperatures	
	and using $[D_M]$ at 25°C (O). The solid and dashed lines	
	represent second order and first order regressions through the	
	points, respectively.	234
Figure 7.4.	Semilog Plot of observed ¹ H chemical shift of water as a	
	function the inverse total surfactant concentration.	235
Figure 7.5.	Typical evaluation of the distribution coefficients of water for	
	PS(310)-b-PANa(17) in toluene-d8 at different temperatures.	241
Figure 7.6.	Plot of the ln of the distribution coefficients as a function of	
	inverse temperature for PS(440)-b-PMANa(18) (O), PS(440)-	
	b-PMANa(40) (◊), PS(310)-b-PMANa(42) (Δ), PS(310)-b-	
	PMANa(17) (□), PS(382)-b-PANa(27) (•), and PS(660)-b-	
	PANa(21) (A) block ionomers. The solid line represents the	
	linear regression through all the data points and the dashed line	
	is the 99% confidence interval.	243
Figure 7.7.	The free energy for the water transfer process as a function of	
	temperature for the different systems; polystyrene-b-poly(4-	
	vinylpyridine) (●,◆), polystyrene-b-poly(sodium	
	methylacrylate) (0) and polystyrene-b-(sodium acrylate) (0),	
	and AOT (■) in toluene-d8. The solid lines represent the linear	
	regression through the respective reverse micelle systems.	248
Figure 7.8.	Relaxation rates of different nuclei in the aqueous core of	
	PS(440)-b-PANa(40) reverse micelles.	253

The important thing is not to stop questioning.

Curiosity has its own reason for existing. One cannot help but be in awe when one contemplates the mysteries of eternity, of life, and of the marvelous structure of reality.

- Albert Einstein

For my parents,

CHAPTER 1

General Introduction

1.1. INTRODUCTION

In recent years, considerable interest has focused on the self-assembly of polymers which form a wide array of structures. For instance, block copolymers have been shown to form microphase separated regions of different morphologies in the solid state. The association of these polymers in solution and on surfaces has also been investigated. In the focus of this thesis is on the characterization of amphiphilic block copolymers which associate in both aqueous and organic media to form micelle structures. This chapter is divided into six sections. The first section discusses the averages and distributions of molecular weights in polymers. Second, the synthesis and phase behavior of block copolymers in the solid state are addressed. In the third part, certain aspects of the micellization of block copolymers in solution are discussed such as the model of association, the dependence of the critical micelle concentration (cmc) on the length and polydispersity of the insoluble block, the dynamics, and the conditions of micelle preparation. The fourth part describes some theories pertaining to the structure of block copolymer micelles. The fifth part is devoted to a description of general methods of block copolymer micelles characterization with special emphasis on static light scattering, which

is the principal method used in this work. In the final section, the purpose of the thesis and a brief summary of each chapter is given.

1.1.1. General Overview of Polymers

1.1.1.1. Average and Distribution of Molecular Weights

Polymers are large molecules (macromolecules) that are built up of smaller units or monomers. The length of the polymer chain can be described by the degree of polymerization (DP), which is the number of repeat units in a molecule. It is given by the ratio of the molecular weight of the polymer to that of the repeat unit. An important feature which distinguishes polymers from low molecular weight molecules is the existence of a distribution of chain lengths and thus of molecular weights. As a result, experimental measurements can only give average values which depend on the particular method employed. Figure 1.1 shows a plot of the molecular weight distribution (MWD); in the figure the amount of polymer is plotted as a function of the molecular weight. The characteristic molecular weights which can be obtained are shown in the figure and are defined below.

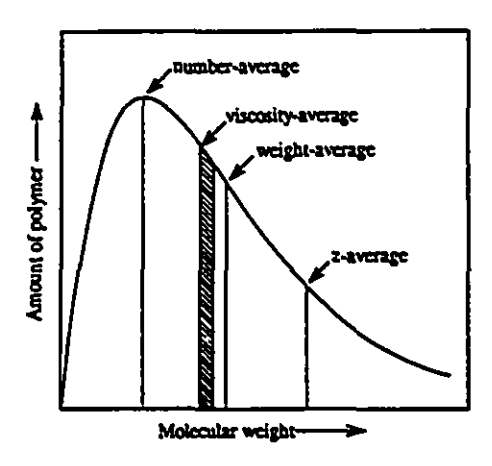


Figure 1.1. Distribution of molecular weights in a typical polymer.⁶

The number-average molecular weight (M_n), can be obtained by methods which measure colligative properties such as osmotic and vapor pressure.⁸ It is defined as,

$$M_{n} = \frac{\sum_{i} N_{i} M_{i}}{\sum_{i} N_{i}} \tag{1}$$

where N_i and M_i refer to the number and molecular weight of the molecules in the *i*th fraction, respectively.

The weight-average molecular weight (M_w) can be measured by absolute methods such as light scattering. It is given as,

$$M_{w} = \frac{\sum_{i} m_{i} M_{i}}{\sum_{i} m_{i}}$$
 (2)

where m_i is the mass of material in the *i*th fraction. The mass of material is given by the product of the molecular weight and the number of molecules, i.e. $m_i = N_i M_i$, thus eq. 2 can be written as,

$$M_{w} = \frac{\sum_{i} N_{i} M_{i}^{2}}{\sum_{i} N_{i} M_{i}}$$
(3)

Since each molecule contributes to M_w in proportion to the square of its mass, heavier molecules contribute more to M_w than lighter ones.

The viscosity-average molecular weight (M_v) can be obtained by viscosity measurements. It is defined as

$$M_{v} = \left(\frac{\sum_{i} N_{i} M_{i}^{1+a}}{\sum_{i} N_{i} M_{i}}\right)^{1/a}$$
(4)

where a is the Mark-Houwink exponent, which is characteristic of the system and lies in the range 0.5 < a < 1.0. When a is equal to unity, then $M_v = M_w$. It should be noted that M_v is not an absolute value and its determination is based on prior calibration with known molecular weights for the same system and conditions.

The z-average molecular weight (M_z) can be obtained by methods such as sedimentation equilibrium. It is defined as

$$M_z = \frac{\sum_i N_i M_i^3}{\sum_i N_i M_i^2}$$
 (5)

The MWD curve can be characterized by the *polydispersity index* (P.I.) which is defined as

$$P.L = \frac{M_w}{M_p} \tag{6}$$

When P.I. is equal to unity, the sample is said to be *monodisperse*. A range of polydispersity indices can be obtained depending on the methods of polymerization. The breadth or the standard deviation (σ) of the MWD can be evaluated from the P.I. by the following equation⁷

$$\sigma = M_n \left(\frac{M_w}{M_n} - 1 \right)^{0.5} \tag{7}$$

There are methods such as size exclusion chromatography (SEC), which can measure the molecular weight distribution. The principles and features of this method will be discussed later in section 1.5.3.

The relationship between the P.I. and the MWD is illustrated in Figure 1.2 for P.I. of 1.03, 1.05 and 1.10. In this figure, the MWD was represented by a Gaussian function with an average chain length of 50 units. The standard deviations of the MWD curves for P.I. values of 1.03, 1.05 and 1.10 are 9, 11 and 16, respectively.

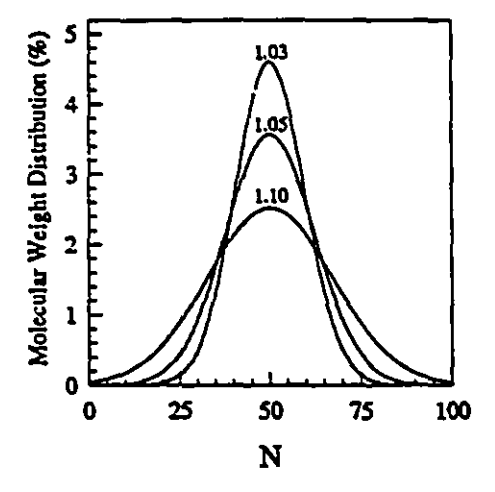


Figure 1.2. Molecular weight distributions of polymers with an average chain length of 50 repeat units and P.L values of 1.03, 1.05 and 1.10.

1.1.1.2. Types of Polymers

Different types of polymers can be synthesized depending on the number and distribution of the monomers. When a single monomer is involved, the polymer is referred to as a homopolymer. When the polymer is composed of more than one repeat unit, it is referred to as a copolymer. In copolymers, the monomer units can be distributed along the chain in various arrangements, resulting in polymers of different structures and properties. Several different structures composed of two monomers A and B, are shown in Figure 1.3. In random copolymers, the A-B sequence is governed by statistics, depending only on the relative abundances of each monomer and their reactivity ratios. In alternating copolymers, the A and B monomers are distributed in a regular alternating pattern. For block copolymers, a sequence of A monomers is attached to a sequence of B monomers. If one sequence of A blocks is attached to one sequence of B blocks, the polymer is called a diblock copolymer. It is also possible to have a polymer with a central B block attached with terminal A blocks which is referred to a triblock copolymer. In graft copolymers, a polymer of one repeat unit (backbone) is branched with chains composed of a different repeat unit. The present thesis focuses on block copolymers, and certain aspects such as the synthesis and phase separation behavior will now be discussed.

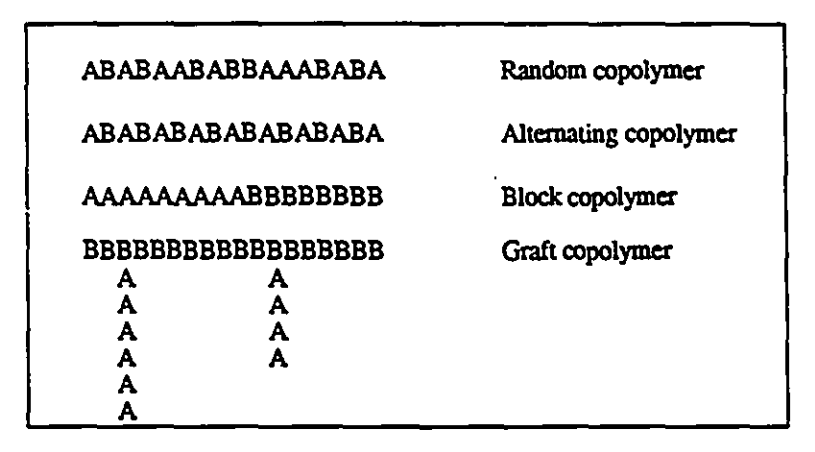


Figure 1.3. Types of copolymers prepared from monomers A and B.

1.2. FEATURES OF BLOCK COPOLYMERS

1.2.1. Synthesis of Block Copolymers

Block copolymers can be synthesized by sequential anionic living polymerization.⁹ Living polymerization processes consist of only initiation and propagation steps, since there are essentially no terminating side reactions. A typical reaction scheme using this polymerization technique, in which a block copolymer of styrene and *tert*-butylacrylate (PS-b-Pt-BuA) is synthesized, is described below. In this scheme, the initiator is the reaction product of *sec*-butyllithium with the α-methylstyrene monomer.

The resulting compound is used to initiate the styrene monomer. Propagation continues until all the styrene monomer is consumed, and the carbanions remain active.

This step is followed by the sequential addition and polymerization of the second monomer, tert-butylacrylate (t-BuA).

It should be noted that in this synthesis procedure, α -methylstyrene is used as an end capping agent which decreases the nucleophilicity of the polystyryl carbanions. This reduces the attack at the ester functional group of the acrylate monomer. The reaction can be terminated by the addition of an alcohol, water or carbon dioxide. The types of monomers which can be polymerized by this method are those containing electron withdrawing substituent groups such as nitrile, carboxyl and phenyl. These groups act to stabilize the carbanion.

Certain features of this polymerization method should be noted. First, it is essential to remove all active impurities such as water and oxygen from the reaction medium in order to obtain a termination-free system. Second, since there is no terminating side reaction, the block length depends only on the monomer to initiator ratio and is thus easily controlled. Third, since the initiation step is rapid compared to that of propagation, a very low degree of polydispersity can be achieved in these polymerizations. ¹⁰

1.2.2. Phase Separation in Bulk

In general, polymer pairs are not compatible since the entropy of mixing is very small for polymers, and the enthalpy is generally positive unless favorable interactions are involved between the two components. One way to enhance miscibility is by introducing specific interactions between the polymers such as the incoporation of ionic groups in the chain. Similarly, block copolymers which are composed of two incompatible blocks, will also prefer to segregate. However, since the blocks are attached to each other, the extent of phase separation is restricted. The effect of these two competing factors results in microphase separation. The length scale of phase separation is comparable to the size of the block copolymer chain and is ca. tens of nanometers. In comparison, phase separated regions of incompatible homopolymers are typically in the micron range.

An interesting feature of block copolymers is the range of morphologies which can occur during phase separation. For instance, the microdomain formation in block copolymers of polystyrene-b-polybutadiene (PS-b-PB) and polystyrene-b-polyisoprene (PS-b-PI) has been very well characterized. Figure 1.4 illustrates the morphologies which are obtained as the volume fraction of PS increases. For instance, different morphologies can be observed, such as spherical, cylindrical, ordered bicontinuous double diamond (OBDD), or lamellar, depending on the volume fraction of the blocks.

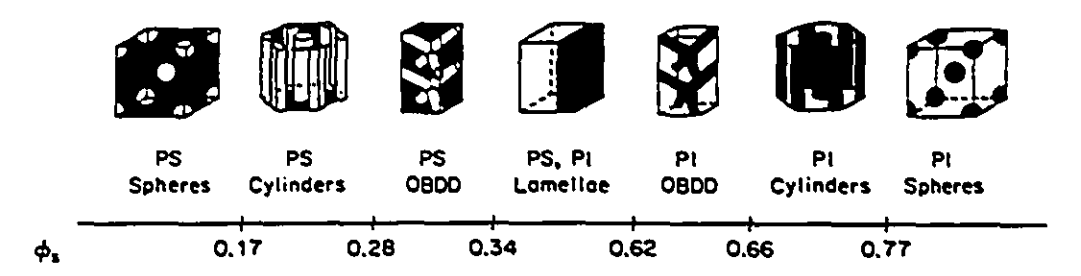


Figure 1.4. Morphologies of PS-b-PI as a function of the volume fraction of PS.¹³

Several theories have been developed to describe the phase separation of block copolymers, and these have been reviewed.¹ A universal phase diagram has been proposed, in which the phase separation depends on two parameters, the volume fraction of monomers in a chain (ϕ) and the product of the interaction parameter between the A and B blocks (χ_{AB}) and the polymerization index (N).¹⁴ An increase in χ_{AB} , induced by changing the temperature or the chemical nature of the blocks, will result in morphological changes occurring at different volume fractions.

1.3. MICELLIZATION OF BLOCK COPOLYMERS IN SOLUTION

When block copolymers are dissolved in a solvent which is selective for one of the blocks, the chains associate to form micelle structures. Different morphologies can be

Chapter 1. General Introduction

obtained depending on the chemical nature and the volume fraction of the blocks as well as the conditions of preparation. Most studies have concentrated on the characterization of spherical block copolymer micelles. The structure of these micelles consists of a core formed by the insoluble blocks, surrounded by a corona which is composed of the soluble blocks. In general, two types of spherical block copolymer micelles can be distinguished, star and crew cut micelles. Star micelles have a relatively small core compared to the corona, while crew cut micelles have a relatively large core compared to the corona. These micelle structures are shown schematically in Figure 1.5.

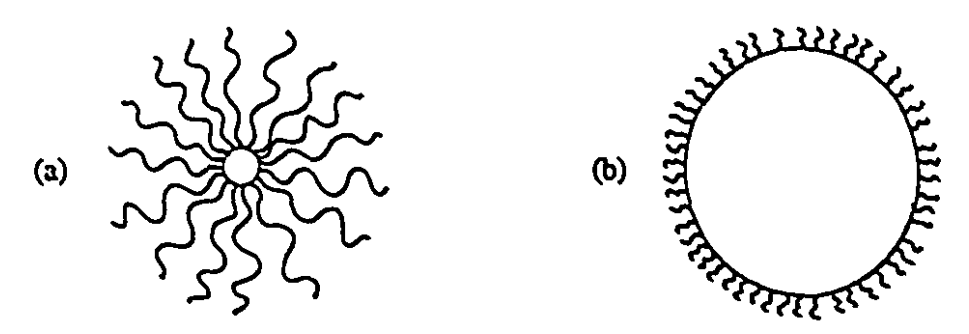


Figure 1.5. Schematic representation of block copolymer (a) star and (b) crew cut micelles.

Under equilibrium conditions, block copolymers can micellize in principle by two mechanisms, open or closed association.

15 Open association is characterized by a series of equilibria between unimers, dimers, trimers, etc. On the other hand, closed association is characterized by an equilibrium between unimers and micelles, and can be represented by

$$\mathbf{M} \rightleftharpoons \mathbf{M}_{\mathbf{n}} \tag{8}$$

where n is the number of unimers, and M and M_n are the molecular weights of the unimers and micelles, respectively. In general, it has been found that the micellization of block

copolymers occurs by the closed association mechanism, which is also the case in low molecular weight surfactants.

The model of closed association implies the existence of a *critical micelle* concentration (cmc). The cmc is the concentration at which micelles begin to form. From this value, the free energy of micelle formation (ΔG_m) can be evaluated from,

$$\Delta G_{\rm m} = -R \, T \, \ln(\rm cmc) \tag{9}$$

where R is the gas constant and T is the temperature. From the temperature dependence of the cmc, the enthalpy and entropy of micellization can be determined. The thermodynamic parameters of micellization can also be determined from the concentration dependence of the *critical micelle temperature* (CMT), which is the temperature at which micelles form.

The driving force for the micellization of block copolymers in organic or aqueous media can be determined from the thermodynamic parameters. On the one hand, the driving force for block copolymer micellization in organic solvents was found to be governed by the enthalpic contribution to the free energy of micellization. ¹⁶ This negative enthalpy change results from the replacement of unfavorable polymer-solvent interactions by polymer-polymer and solvent-solvent interactions. On the other hand, for block copolymers as well as low molecular weight surfactants in water, the driving force for micellization is dominated by the entropic contribution. ¹⁷ This result arises from the change in the water structure due to the hydrophobic interactions. For instance, the presence of hydrophobic blocks in water causes a significant decrease in the entropy of water. Upon micellization, the structure of water is restored, and the entropy due to the localization of the hydrophobic blocks in the cores.

There are several similarities between the micellization of block copolymers and low molecular weight surfactants, some of which were discussed above. However, there are also certain important differences between the micellization of these two species. Examples of these differences are listed below.

- In general, the cmc's of block copolymer micelles are lower than those of low molecular weight surfactants, and the molecular weights of block copolymer micelles are higher than those of low molecular weight surfactants.
- 2. Block copolymers when present in single chains form structures referred to as monomolecular micelles. 18 In a nonsolvent or poor solvent for the B block, the B block adopts a collapsed conformation. 19 It is expected that the thermodynamics of association of these insoluble blocks will be different from those of low molecular weight surfactants.
- 3. The molecular weights of block copolymers are not monodisperse in contrast to low molecular weight surfactants. The polydispersity has been found to significantly effect certain micellar parameters such as the cmc.
- 4. The dynamics of micelle systems are much slower in block copolymer micelles compared to low molecular weight surfactants. In fact, in some block copolymer micelles, the structures are said to be kinetically "frozen".
- Block copolymer micelles often form structures which may not be under full equilibrium conditions.

In the following sections, points 2 to 5 will be discussed further, since they address important features of block copolymer micelles which are relevant to the present work.

1.3.1. Dependence of the Free Energy of Micellization on the Insoluble Block Length

For low molecular weight surfactants, the free energy of micellization has been found to be proportional to the length of the alkyl chain.²⁰ However, for block copolymers, the free energy of micellization is expected to be different since it involves the

association of collapsed or contracted insoluble blocks, shown schematically in Figure 1.6, illustrating the structure of monomolecular micelles. It should be noted that several theories have developed relations between the free energy of micellization and the insoluble block length for block copolymer micelles. 21-24 For the present discussion, one such theory by Gao and Eisenberg²⁴ will be described. This theory is addressed and applied in the present thesis.

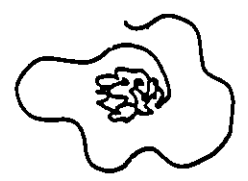


Figure 1.6. Structure of a monomolecular micelle formed by an AB block copolymer molecule in a nonsolvent for the B block. 18

The driving force for micellization of block copolymers can be considered as being due to Van der Waals interactions.²⁵ For the association of two spherical particles, the free energy of interaction (ΔG^{att}) can be given by the Hamaker equation,²⁶

$$\Delta G^{\text{att}} = \frac{-A_{\text{H}}R_{\text{p}}}{12\text{H}} \tag{10}$$

where A_H is the Hamaker constant, which depends on the material, solvent and temperature, R_p is the particle radius and H is the distance between the surfaces of the two particles. Equation 10 is valid only when two particles are in proximity of each other, i.e. when $H/R_p << 1$. If more than two spheres are interacting, the total interaction energy should be proportional to R_p .

For a monodisperse block copolymer, it has been suggested by the Gao and Eisenberg theory, that the free energy of micellization is proportional to the radius of the collapsed insoluble block.²⁴ Since the radius is proportional to the cube root of the insoluble block length (N_B) , the free energy of micellization can be given as

$$\frac{-\Delta G_{\rm m}}{RT} = \log C_{\rm i} = aN_{\rm B}^{1/3} + b \tag{11}$$

where C_i is the cmc of a monodisperse polymer, and a and b are constants. This equation is valid only when the insoluble block is in a collapsed state. Satisfactory results were obtained for two micelle systems investigated, 24 PS- 24 PS- 24 PS- 24 PS- 24 and polystyrene- 24 PS- 24

1.3.2. Influence of Polydispersity on the cmc

The effect of polydispersity on the micellization of block copolymers has been recently investigated in a theory by Gao and Eisenberg.²⁴ In this theory, the micellization of polydisperse block copolymers is treated in a manner analogous to that used in low molecular weight mixed micelles. Figure 1.7 shows plots of the single chain concentration (S) versus the total concentration for different polydispersity indices. The plots represent theoretical calculations for a typical block copolymer, PS-b-PI in n-hexadecane with an average insoluble block (PS) length of 67 units. When the polymer concentration is below the cmc (shown by arrows in Figure 1.7), S is equal to the total polymer concentration. Above the cmc for a monodisperse system, S remains constant with increasing polymer concentration. However, for polydisperse block copolymers, S increases with total concentration. Experimental evidence for the change in S with concentration has been reported, for instance in polystyrene-b-polybutadiene-b-polystyrene triblock copolymers in tetrahydrofuran/allyl alcohol mixtures.²⁹

Other interesting aspects of the effects of polydispersity can be seen in Figure 1.7. First, the cmc values are found to decrease as the polydispersity index (P. I.) increases. This phenomenon occurs because block copolymer chains which are shorter than 67 units are more soluble and contribute less to the cmc than chains which are larger than 67 units.

Thus, it is important to establish the P.I. of the insoluble block, (especially, if this value is large) when reporting cmc values. Second, the discontinuity in the single chain concentration at the cmc becomes less noticable at higher polydispersity indices. Therefore, techniques which evaluate the cmc by monitoring the properties of the single chains may not be as precise as those monitoring the changes in the micelles.

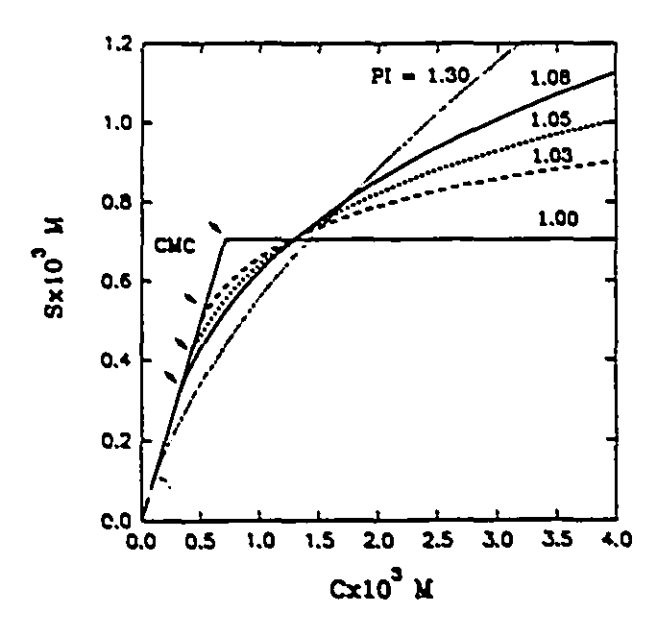


Figure 1.7. Single chain concentration as a function of total block copolymer concentration at different polydispersity indices in the PS-b-PI / n-hexadecane system.²⁴

The fraction of different polymer components of the micelles was also found to depend strongly on the concentration. For instance, at concentrations close to the cmc, micelles were predominantly formed from polymers with the longest insoluble blocks. At higher polymer concentrations, the solutions became strongly depleted of the long polymer components.

1.3.3. Dynamics of Block Copolymer Micelles

The closed association model (see eq. 8) implies the existence of a dynamic equilibrium between single chains and micelles and also between micelles themselves. The dynamic process probing the exchange of chains between micelles has been investigated by fluorescence^{30,31} and by sedimentation velocity experiments.^{32,33} This process was found to depend on the nature of the solvent quality for the insoluble block. For instance, the dynamics of micelle exchange vas studied in polystyrene-b-poly(methacrylic acid) (PS-b-PMAA) block copolymers by sedimentation velocity.³² In these experiments, micelles of different molar masses were mixed and the solvent quality was changed. For instance, the solvent mixture used was water and dioxane, which is a nonsolvent and a solvent, respectively, for the PS core. It was found that exchange occurred between micelles when the PS core was swollen with dioxane, for instance for a solvent composition of water/dioxane (20/80 v/v). However, when the percent of dioxane in the solvent mixture decreased, no exchange occurred between the micelles, and the micelle structures were regarded as being "frozen", i.e. dynamics of exchange was extremely slow or non-existent.

1.3.4. Equilibrium Versus Near Equilibrium Conditions of Micelle Formation

Block copolymer micelles can be prepared by two methods. In the first method, the block copolymer in single chain form is dissolved in a solvent which is good for both blocks. By changing the temperature or the solvent composition, one of the blocks collapses and associates above the cmc to form micelle structures. The second method involves direct dissolution of block copolymers in a selective solvent. The block copolymer micelle prepared in this manner can be left to anneal by standing or heating.

It is interesting to examine which conditions of micelle preparation result in the formation of equilibrium structures. For instance, if block copolymer micelles are prepared by the second method, i.e. direct dissolution in a selective solvent, equilibrium

structures may form if the block forming the core is swollen with solvent. This aspect was addressed in the previous section, in which a swollen micelle core would allow the exchange between single chains and micelles to proceed, and a thermodynamic equilibrium state could be attained. Another condition for exchange would be the case if the glass transition (T_g) of the block forming the core is below room temperature (i.e. the temperature of measurement). If the T_g of the core is higher than room temperature, then the core would be glassy, and the dynamics would be extremely slow.

Other situations of micelle preparation from direct dissolution can be envisaged. For instance, if a bulk sample is prepared by solvent evaporation or by freeze drying from a micellar solution, it is expected that the morphology of the micelles would be retained when redissolved in a selective solvent. This phenomenon has been addressed in several studies. 34,35 If the micellar solution which was recovered consisted of swollen cores, then some rearrangement could occur during the solvent evaporation or the freeze drying process.

1.4. THEORETICAL ANALYSIS OF BLOCK COPOLYMER MICELLES

Several theories have been proposed to describe block copolymer micelles. In general, these theories can be divided into two categories, star and mean-field theories. The star models describe the case in which the core is relatively small compared to the corona. In this case, the density of the corona decreased with increasing distance from the core. On the other hand, mean-field models describe micelles which have relatively large cores and thin coronas. 21,22,38-40 The density of the corona is assumed to be uniform. Some of the theories which are relevant to the studies presented in the thesis will be reviewed.

The star model has first been proposed by Daoud and Cotton to describe the conformations of star shaped polymers. In this region, the following scaling relations were developed relating micelle characteristics to the number of units in the soluble and insoluble blocks (N_A and N_B). Scaling relations such as for the core radius (R_c), corona thickness, aggregation number (N_{agg}) were developed for four regions, depending on the relative block lengths. A star model was also developed by Halperin. In this model, the scaling relations for one region, where $N_A >> N_B$, were proposed and were in agreement with those of Zhulina and Birstein. In this region, the following scaling relations were proposed to describe N_{agg} , R_c and the micelle radius (R_m)

$$N_{agg} \sim N_B^{4/5}$$
 $R_c \sim a N_B^{3/5}$
 $R_m \sim a N_B^{4/25} N_A^{3/5}$
(12)

where a is the length of the monomer unit.

The mean field theories of de Gennes³⁸ and Leibler, Orland and Wheeler (LOW)²¹ proposed that N_{agg} and R_c were dominated by the insoluble block. Scaling relations were developed by de Gennes for cases in which the interfacial energy between the core and solvent was large,

$$N_{agg} \sim N_B$$
 and $R_c \sim N_B^{2/3}$ (13)

Relations were also developed for systems with small interfacial energies

$$N_{agg} \sim N_B^{1/2}$$
 and $R_c \sim N_B^{1/2}$ (14)

The LOW theory proposed the following scaling relations,

$$N_{agg} \sim N_B^{0.6}$$
 and $R_c \sim N_B^{0.53}$ (15)

Other mean field theories such as those by Whitmore and Noolandi⁴⁰ and Nagarajan and Ganesh²² found a dependence of N_{agg} and R_c on the soluble block length. The dependence was described by two exponents (α and β),

$$N_{agg} \sim N_A^{\alpha} N_B^{\beta}$$
 and $R_c \sim N_A^{\alpha} N_B^{\beta}$ (16)

On the one hand, Whitmore and Noolandi found that the exponents for R_c were $-0.1 \le \alpha \le 0$ and $0.67 \le \beta \le 0.76$, i.e. there was only a weak dependence of R_c on the soluble block. On the other hand, Nagarajan and Ganesh found that the soluble block can have a strong influence on the micellar properties, depending on the nature of the interactions with the solvent. For instance, the influence of the soluble block becomes more significant in systems in which the solvent is very good for the soluble block.

In addition to these theories, there are two theories which specifically address the micellization of block polyelectrolyte micelles; those of Marko and Rabin²³ and of Dan and Tirrell.⁴² The first theory describes the microphase-separation properties of chargedneutral diblocks using a mean-field approach. Due to the large energy cost of contacts between the neutral block and the solvent, it is favorable for the chains to aggregate; however, Coulombic repulsion sets a preferred size for these aggregates which take the form of spherical micelles. The cmc, micelle size, and Nagg values were calculated for long polyelectrolyte chains. Two situations were considered: the weakly charged case where there is no charge condensation either for the isolated chains or for the micelles, and the case of highly charged diblocks, for which counterion condensation on the micelles reduces their Coulombic energy. It was shown that when strong condensation occurs, the osmotic pressure of the confined counterion strongly stretches the polyelectrolyte chains in the corona. In this case, the theory predicts that highly charged diblocks will not form stable micelles with high aggregation numbers, and that micelle formation will predominantly occur in dilute solutions of weakly charged diblocks. Therefore, according to the theoretical prediction of Marko and Rabin, 23 micellization of highly charged block polyelectrolytes in dilute salt solutions will not occur unless the charged block is short as compared to the hydrophobic block forming the micelle core.

In the theory by Dan and Tirrell, ⁴² scaling relations for block copolymer micelles in the region of moderate salt concentration were investigated. In this salt concentration region, the range of excluded volume interactions is higher than that of the electrostatic correlation length, such that the conformation of the polymer chain is a function of both factors. Therefore, this region lies between the low salt concentration where electrostatic effects dominate and the high salt concentration where the screening effects reduce the range of electrostatic interactions, and the conformation of charged chains in block polyelectrolyte micelles is indistinguishable from that of neutral ones. It was found that the aggregation number, cmc, and chemical potential of the micellar solution are deminated by the core block properties and are identical, within a logarithmic factor, to those calculated for the star model. ⁵⁷ It was also suggested that changes in salt concentration do not affect either the cmc or aggregation number, though the corona size decreases with increasing salt concentration.

1.5. METHODS OF MICELLAR CHARACTERIZATION

A variety of methods have been used to characterize the structure and the properties of block copolymer micelles. Some of these methods, such as static and dynamic light scattering, and viscosity probe macroscopic events, while others such as fluorescence spectroscopy and nuclear magnetic resonance probe microscopic events. A summary of some of these methods and the information which can be obtained on block copolymer micelles is given in Table 1.1. In this thesis, four methods were mainly used in the characterization of block copolymer micelles, static light scattering (SLS), dynamic light scattering (DLS), size exclusion chromatography (SEC) and nuclear magnetic resonance (NMR). These methods will be discussed in the following sections at a level of

Chapter 1: General Introduction

detail relative to their importance in the thesis, with the exception of NMR which is a well known technique.

Table 1.1. Methods for the Characterization of Block Copolymer Micelles

Method	Information Obtained		
Static light scattering (SLS)	-cmc, Mw, radius of gyration, second virial		
	coefficient		
Dynamic light scattering (DLS)	-cmc, diffusion coefficient, hydrodynamic		
	radius, size distribution		
Small-angle X-ray and neutron scattering	-Core radius, Mw, radius of gyration,		
(SAXS and SANS)	lattice structure		
Size exclusion chromatography (SEC)	-MWD, fraction of micelles to unimers,		
	dynamics of equilibrium.		
Sedimentation velocity	-Fraction of micelles to unimers, dynamics		
	of equilibrium.		
Transmission electron microscopy (TEM)	-Morphology, size, size distribution		
Viscosity	-cmc, M _v , hydrodynamic radius		
Fluorescence	-cmc, dynamics of micelle equilibrium,		
	dynamics on a segmental level		
Nuclear magnetic resonance (NMR)	-Microscopic motions and environments		

1.5.1. Static Light Scattering

1.5.1.1. General Light Scattering Theory

Static light scattering (SLS) is an invaluable method for the characterization of polymers in solution. The M_{w} , the dimension and thermodynamic information such as virial coefficients can be obtained by this absolute technique. Light scattering can be classified into three categories depending on the relative size of the particles compared to the wavelength of light in the scattering medium (λ) .⁴³ These three categories are given below,

Rayleigh $D/\lambda < 1/20$

Debye $1/20 < D/\lambda < 1$

Mie $D/\lambda > 1$

where D is the major dimension of the particle. The present section will focus only on Rayleigh and Debye scattering.

Rayleigh scattering describes the light scattered by small particles, i.e. $D < \lambda/20$. In this case, particles scatter light *isotropically*, i.e. the scattered intensity is equal in all directions. In a typical light scattering experiment, the intensity of scattered light (I) is measured over a range of different angles (θ). The *Rayleigh ratio* R(θ) describes the angle-dependent light scattering; it is defined as

$$R(\theta) = \frac{I(\theta)r^2}{I_0V}$$
 (17)

where $I(\theta)$ is the intensity of light at different scattering angles, r is the distance between the center of the scattering medium and the detector, I_0 is the intensity of the incident light, and V is the volume of the scattering medium. Light is scattered from both the polymer and the solvent. In order to obtain information on the polymer alone, the scattering due to the solvent molecules $(I(\theta)_{solvent})$ is subtracted, and the quantity $R(\theta)$ is used to represent the excess Rayleigh ratio given by

$$R(\theta) = \frac{(I(\theta) - I(\theta)_{solvent})r^2}{I_0V}$$
 (18)

For vertically polarized light, the light scattering data can be represented by the following equation

$$\frac{\mathrm{Kc}}{\mathrm{R}(\theta)} = \frac{1}{\mathrm{M_w}} + 2\mathrm{A}_2\mathrm{c} \tag{19}$$

where A_2 is the second virial coefficient, K is an optical constant and c is the concentration. The optical constant is defined as

$$K = \frac{2\pi^2 n_o^2 (dn / dc)^2}{\lambda_o^4 N_{av}}$$
 (20)

when n_0 is the refractive index of the solvent medium, (dn/dc) is the specific refractive index increment, λ_0 is the wavelength in vacuum, and N_{av} is Avogadro's number. The specific refractive index increment is a measure of the change of the solution refractive index with respect to a change in the concentration of the molecular species being measured. It can be determined using a differential refractometer or an interferometer. It should be noted that eq. 19 is valid for dilute solutions, in which the terms with higher powers of concentration can be neglected.

When the particle size is larger than $\lambda/20$, light is scattered from different parts of the molecule. As a result, scattered light reaches the detector in different phases. This effect is referred to as intramolecular interference. The path difference is larger in the backward direction (large θ) than in the forward direction (small θ), and destructive interference increases with θ . At an angle of zero, there is no interference effect. The asymmetric scattering envelope for large particles is compared to that of small particles (Debye scatterers) in Figure 1.8.

The angular dependence of scattered light for a large particle is described by the particle scattering function $(P(\theta))$. It is given by the ratio of the scattered intensity for large particles to the scattered intensity in the absence of interference, i.e.

$$P(\theta) = \frac{R(\theta)}{R(0)} \tag{21}$$

where R(0) is the Rayleigh ratio at a scattering angle of zero, and $P(\theta)$ is equal to unity at a scattering angle of 0° . The asymmetric scattering from large particles can be described by the dissymmetry ratio (Z_d) , which is given by the following ratio

$$Z_{\rm d} = \frac{R(45)}{R(135)} = \frac{P(45)}{P(135)} \tag{22}$$

In general, it is possible to use any angles which are symmetric about 90°, however, 45 and 135° are most frequently used.

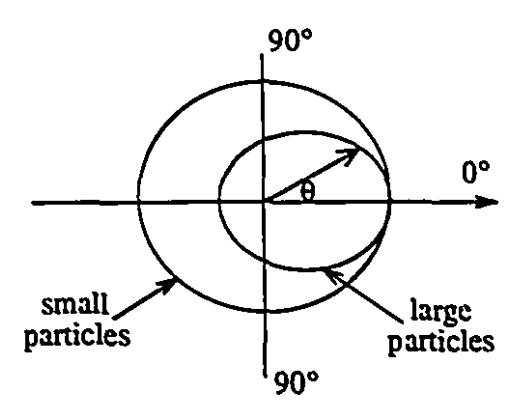


Figure 1.8. Angular dependence of the Rayleigh ratio for small and large particles.

Equation 19 can be amended to take into account the intraparticle interference, and the equation becomes

$$\frac{\mathrm{Kc}}{\mathrm{R}(\theta)} = \frac{1}{\mathrm{M_w}\mathrm{P}(\theta)} + 2\mathrm{A}_2\mathrm{c} \tag{23}$$

The particle scattering function is given as 45

$$P(\theta) = 1 - \frac{2\mu^2 < R_g^2 >}{3!} + \dots$$
 (24)

where μ is equal to $(4\pi/\lambda)\sin(\theta/2)$. This equation gives the relation between $P(\theta)$ and the radius of gyration for any molecule independent of the molecular conformation. For polydisperse samples, $\langle R_g^2 \rangle$ is the square z-average radius of gyration usually written as $\langle R_g^2 \rangle_z$. In the present work it will also be represented using the notation R_g .

The inverse particle scattering function for small angles can be given as. 44,45

$$\lim_{\theta \to 0} P(\theta)^{-1} = 1 + \frac{16\pi^2 < R_g^2 > \sin^2(\theta/2)}{3\lambda^2}$$
 (25)

Therefore, a plot of $P(\theta)^{-1}$ versus $\sin^2(\theta/2)$, would give a straight line at small angles; the slope of which is proportional to $\langle R_g^2 \rangle$. This equation can be employed only when $Kc/R(\theta)$ is linear in $\sin^2(\theta/2)$. Therefore, the data for larger angles which departs significantly from linearity cannot be used. Alternatively, a wide range of angles can be used to determine R_g if $P(\theta)$ is expanded to include higher terms in $\sin^2(\theta/2)$. The first linear term in $\sin^2(\theta/2)$ for this non-linear regression analysis would be proportional to the radius of gyration (eq. 24).

1.5.1.2. Application to Block Copolymers

SLS measurements on block copolymers can be complicated by the fact that they often are polydisperse in chemical composition. A polydispersity in composition results in a polydispersity in the dn/dc values, since there are different contributions of each fraction to the total dn/dc.⁴⁷ In this case, the M_w refers to an apparent value (M_{w,app}), since it depends, through the refractive index increments, on the nature of the solvent. However, there are certain situations in which M_{w,app} is equal to the true M_w.⁴⁵ This occurs, for instance, when the parent homopolymers of the copolymers have equal refractive index increments. Also, this result is found for copolymers which have low heterogeneities in

composition, such as copolymers with a small content of one component or if the difference of the refractive index increments of the parent homopolymers is small.

1.5.1.3. Application to Polyelectrolytes.

Polyelectrolytes are polymers containing ionizable groups. When polyelectrolytes are dissolved in an ionizing solvent at low concentrations and in the absence of salt, the chains expand due to the repulsive forces of the charges along the polymer backbone. This phenomenon is referred to as the *polyelectrolyte effect*. Light scattering measurements of polyelectrolytes in the absence of salt are anomalous, since dilution is accompanied by increasing expansion of macro-ions. The addition of a low molecular weight electrolyte increases the concentration of ions in solution. As a result, there are more counterions present to screen the charges on the polyions, and thus the expansion of the chains decreases. In general, 0.01 to 0.1 M salt is sufficient to supress the polyelectrolyte effect.⁴⁵

Polyelectrolyte solutions, in the presence of salt, consist of multicomponent or mixed solvents. In mixed solvents, selective adsorption can occur because the polymer generally has a higher affinity for one of the solvent components. The concentration of that component will therefore be higher within the domain of the polymer molecules compared to the surrounding polymer free solvent. In order to measure equilibrium properties of solutions, the solution must be in thermodynamic equilibrium with the solvent. This equilibrium can be achieved by dialysis in which the solution is separated from the solvent by a semipermeable membrane. The redistribution of the solvent components is shown schematically in Figure 1.9.

Chapter 1. General Introduction

		Solution		Solvent
	Time	Domain of macromolecules	Bulk solvent	V -> ∞
	(1) t ₀	2 A:B > 1	A:B<1	Membra
	(2) t >	<i>t</i> o	В —	AA
	(3) t_	(A:B > 1)	A:B=1	A: B = 1

Figure 1.9. Representation of redistribution of solvent components A and B, in which A is selectively sorbed by the polymer.⁴⁵

1.5.1.4. SLS Analysis

In a typical light scattering measurement, the scattered intensity is monitored as a function of different angles and different concentrations. The M_w , A_2 and R_g can then be evaluated by solving equation 23 graphically. This method is referred to as a Zimm plot, ⁴⁸ and a typical plot is shown in Figure 1.10, in which $Kc/R(\theta)$ is plotted versus $\sin^2(\theta/2)$ + kc, where k is scaling factor. This factor is adjusted such that the contributions from c are ca. equal to those from the contributions from $\sin^2(\theta/2)$. Usually, this value is chosen as the reciprocal of the maximum concentration. The inverse value of M_w can be evaluated by extrapolating the data points to zero concentration and zero angle, at which point eq. 23 becomes,

$$\lim_{\theta,c\to 0} \frac{Kc}{R(\theta)} = \frac{1}{M_w} \tag{26}$$

The second virial coefficient can be obtained from the slope (m_c) of the extrapolated line of $\theta = 0$ given by

$$m_{c} = \frac{d}{dc} \left(\lim_{\theta \to 0} \frac{Kc}{R(\theta)} \right) = 2A_{2} / k$$
 (27)

The R_g value, can be evaluated from the initial slope (m_θ) of the c=0 line at low angles where $P(\theta)^{-1}$ is given by eq. 25.

$$m_{\theta} = \frac{d}{d\sin^2(\theta/2)} \left(\lim_{c \to 0} \frac{Kc}{R(\theta)} \right) = \frac{1}{M_w} \frac{16\pi^2 < R_g^2 >}{3\lambda^2}$$
 (28)

On the other hand, as discussed in section 1.5.1.1.(eq.24), it can also be determined from a polynomial regression of the c = 0 line as a function of $\sin^2(\theta/2)$. Since the extrapolations are made to zero concentration and zero angle, it is important to make the measurements at dilute concentrations and at a number of small angles.

In addition to Zimm plots, Debye and Berry plots have also been used to analyze light scattering data. In the Debye plot, the y axis is the reciprocal of that used in the Zimm plot, i.e. $R(\theta)/Kc$ is plotted as a function of $\sin^2(\theta/2) + kc$. In general, when the M_w and R_g of the particle are very large, Zimm plots have uncertainties in extracting these values. This fact can be considered, for instance, for a polymer of $M_w = 1 \times 10^7$ g/mol, for which the intercept of the Zimm plot (after double extrapolations of c and $\theta \to 0$) will be close to zero. Therefore, because of slight experimental uncertainties in the data points and the large polymer size, the exact location of the intercept is uncertain. In these cases, the Debye plot is preferable to extract the values for high M_w and large R_g . Berry plots have also been employed to analyze light scattering data. These plots consist of using the square roots of the x and y axis of the Zimm plots. The resulting graphs are more linear and allow for easier extrapolations.⁴³

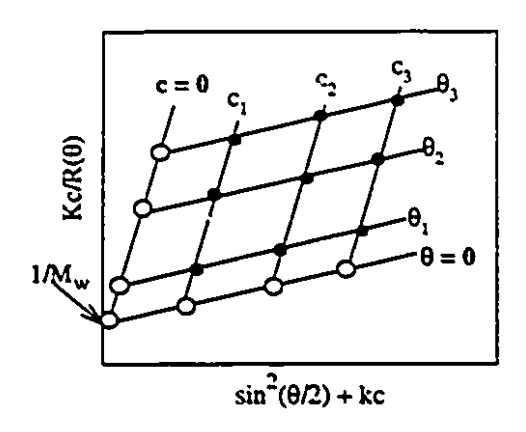


Figure 1.10. Schematic Illustration of a Zimm plot

1.5.1.5. Instrumentation

The instrument employed in the SLS experiments was a multiangle light scattering photometer (Wyatt Technology Corp., Santa Barbara, California, U.S.A.). It consists of 15 fixed detectors ranging from 26 to 129° surrounding a thermostated cell. This instrument allows the measurement of the scattered intensity at several angles in a short period of time.

Perhaps the most tedious part of a light scattering measurement is sample preparation. It is important to have very accurate concentrations, since most of light scattering analysis depends on this value. Elimination of dust from the polymer solution is also crucial, since these particles will increase the scattered intensity and lead to incorrect results. In order to remove dust particles, the samples can be filtered through a membrane, or, alternatively, the solutions can be centrifuged. When the samples are filtered, it is important to ensure that no polymer is retained on the filters, which would change the concentrations. Also, it is important to use filters of appropriate pore size. As

a general guideline, polymers with molecular weights less than 3 x 10^6 g/mol can be filtered through 0.2 μ m filters and larger particles through 0.45 μ m filters.⁴⁹

1.5.2. Dynamic Light Scattering

In contrast to SLS, which measures time averaged or static properties, dynamic light scattering (DLS) measures time dependent properties of particles. Several books⁵⁰⁻⁵² and review articles^{53,54} have focused on the principles and applications of this method. Since particles in solution are in constant, random or Brownian motion, their positions are continuously changing.⁵³ Thus, the distance that the scattered waves travel to the detector varies as a function of time. These scattered waves can interfere constructively or destructively depending on the distances traveled to the detector. This results in an average intensity with superimposed fluctuations. The frequencies of these fluctuations are related to the speed and therefore the size of the particles. For instance, small particles move rapidly and cause high frequency fluctuations, while large particles move slowly, causing low frequency fluctuations.

The fluctuating signals are processed from the autocorrelation function $(G_2(t))$ as a function of the time (t). As t increases, the correlation is low, and the function approaches the background or baseline (B). For short times, the correlation is high. The function decays exponentially with t, and it is given by the following

$$G_2(t) = \beta e^{-2\Gamma t} + B \tag{29}$$

where β is an optical constant which depends on the instrument, and Γ is the decay rate for the process. This rate is given by

$$\Gamma = Dq^2 \tag{30}$$

where D is the translation diffusion coefficient, and q is the scattering vector equal to $(4\pi \text{ n sin } (\theta/2)/\lambda_0)$. The diffusion coefficient (D) for spherical particles is related to the hydrodynamic radius (R_h) by the Stokes-Einstein equation,

$$D = k_B T / (6 \pi \eta R_b)$$
 (31)

where k_B is the Boltzmann constant, T is the absolute temperature, and η is the viscosity of the solvent medium. This equation assumes that particles are moving independent of each other; therefore, measurements should be made in dilute solution, or the results should be extrapolated to zero concentration.

1.5.3. Size Exclusion Chromatography

Size exclusion chromatography (SEC) is a separation method which is widely used in the determination of the MWD of polymers. 7,10,55 This method consists of passing a polymer solution through a column which is packed with porous materials. As the polymer molecules flow through the column, they can diffuse into the pore structures depending on the polymer size. For instance, small molecules can diffuse into the pores, more readily than large molecules. On the other hand, large molecules can enter only a small portion of the pores or they may even be totally excluded if their size is too large. Since the larger molecules spend less time in the columns, they are eluted first. The eluted material is thus separated as a function of size, and the separation can be monitored by a detector such as a refractometer.

SEC is not an absolute method and requires calibration. The universal calibration method can be used.⁵⁶ In this method, the product of the intrinsic viscosity and the molecular weight ($[\eta]M$) is plotted as a function of the elution volume. All polymers, regardless of their chemical composition or architecture, should fit on this curve. This

curve is based on the concept that the elution of polymer molecules in SEC columns is determined by their hydrodynamic volume which is proportional to the $[\eta]M$ product.

The molecular weight distribution (MWD) for a polydisperse sample can be determined by dividing the experimental SEC curve into slices of equal volume. If enough slices are taken, each slice can be considered to be monodisperse and the total area of the curve can be represented by the sum of the heights of the individual slices. The molecular weight of the ith species (Mi) is obtained from the calibration plot for the elution volume of the ith species (Vi). The M_n and M_w values can then be evaluated.

1.6. FOCUS AND PURPOSE OF PRESENT THESIS

The focus of this thesis is on the characterization of block copolymer micelles formed from the association of PS based block copolymers. These block copolymers were synthesized by sequential anionic polymerization, and the structures of the blocks are given in Figure 1.11. The block copolymers were composed of a nonionic polystyrene (PS) block attached to either nonionic blocks of poly(acrylic acid) (PAA) or poly(4-vinylpyridine)(P4VP) or ionic blocks of poly(sodium acrylate) (PANa), poly(sodium methacrylate) (PMANa), or poly(4-vinylpyridinium methyl iodide) (P4VPMeI).

Due to the amphiphilic nature of these block copolymers, micellization can occur in either aqueous or organic media. For instance, PS-b-PANa, when dissolved in water, will form block polyelectrolyte or regular micelles in which the PS blocks associate to form the micelle core which is surrounded by the soluble PANa corona. A systematic study on the aggregation numbers and sizes of these block polyelectrolytes in aqueous media has not yet been reported. The other type of micelle which can form from PS-b-PANa are block ionomer or reverse micelles. The micelle structure consists of an ionic core composed of PANa blocks surrounded by nonionic PS blocks which form the corona.

Figure 1.11. Structures of PS based block copolymers used in the present work.

Several aspects of these block copolymer micelles have not yet been investigated. For instance, the cmc's of block polyelectrolyte micelles formed from PS-b-PANa have been measured by fluorescence spectroscopy as a function of block lengths and salt content.⁵⁷ However, the aggregation numbers and micelle size have not yet been determined as a function of these parameters.

Several studies have focused on the characterization of block ionomer micelles. However, the cmc's of these micelles have not yet been evaluated. It would be of interest to examine the dependence of these values on the insoluble block length, the nature of the core (i.e. ionic versus nonionic), and the solvent medium. In general, methods used for cmc determination such as SLS do not take into account the effects of polydispersity on the cmc's which were discussed in section 1.3.2. The development of a method for the cmc determination of polydisperse block copolymer micelles would be useful.

The N_{agg} and R_c have been determined for polystyrene-b-poly(cesium acrylate) (PS-b-PACs) block ionomers in the solid state and in concentrated solutions by SAXS.³⁵ However, the N_{agg}, R_c and micelle size of PS-b-PANa in dilute solution have not yet been investigated. The effects of block lengths can be systematically investigated by SLS and compared to scaling theories mentioned in section 1.4. Comparison of the results obtained from dilute solution could then be made with those determined by SAXS. Another interesting feature of block ionomers would be to probe the effect of neutralizing the PAA block forming the core to different degrees on N_{agg} and R_c. The degree of neutralization at which micellization begins could also be determined.

Water can be easily solubilized into the polar cores of block ionomers. The amount of water solubilized has been investigated by NMR measurements of the proton chemical shifts of water for one block ionomer sample, PS(440)-b-PMANa(40), in different solvents.⁵⁸ It would be of interest to determine the amount of water solubilized as a function of the block lengths, core nature and temperature. Information could then be

obtained on the nature of the hydrated ionic cores which would be pertinent for catalysis in these systems.

The purpose of the present thesis is to investigate several unexplored aspects of block copolymer micelles which were discussed in the preceding paragraphs, in order to achieve better understanding of the micellization of PS based block copolymers. In the following section, the contents of each chapter are briefly outlined.

In Chapter 2 of this thesis, a literature survey of the relevant studies pertaining to these micelles is presented including some of the work presented in this thesis. Chapter 3 focuses on a systematic study of the micellization of PS-b-PANa block copolymers by SLS in aqueous media. The effects of salt content and block lengths on the micellar parameters such as Nagg, R_c, and R_g were investigated. Comparison of these values with scaling models was also made.

Chapter 4 addresses the determination of cmc's of block copolymer micelles by SLS. As discussed previously in section 1.3.2., the polydispersity of the insoluble block influences the cmc. Therefore, a method was developed to account for these polydispersity effects in order to correctly evaluate the cmc's.

Chapters 5 and 6 concentrate on the micellization of PS-b-PANa and PS-b-PAA block copolymer micelles in organic solvents. The cmc's, N_{agg} and sizes were determined as a function of the insoluble block length. A systematic study on the effects of the soluble and insoluble block lengths on the aggregation numbers was performed using 4 PS-b-PANa block copolymer series. Scaling relations were developed to describe the N_{agg} and R_c values as a function of the block lengths.

Chapter 7 focuses on the solubilization of water into the polar cores of an anionic low molecular weight surfactant, sodium bis(2-ethylhexyl)sulfosuccinate (AOT), and block ionomer micelles by measuring the proton chemical shift of water using NMR. The block ionomers investigated were PS-b-PANa, PS-b-PMANa and PS-b-P4VPMeI. The effects of the block lengths and core nature on the distribution and thermodynamics of the

Chapter 1. General Introduction

water transfer process were probed. Relaxation rates of different nuclei in the hydrated core of a block ionomer were also investigated.

Chapter 8 presents the conclusions of the thesis, the contributions to original knowledge, and suggestions for future work. Annex A contains the program written in BASIC which was developed to determine the cmc's of block copolymer micelles.

1.7. REFERENCES

- Brown, R. A.; Masters, A. J.; Price, C.; Yuan, X. F. In Comprehensive Polymer Science. The Synthesis, Characterization, Reactions and Applications of Polymers; Booth C.; Price, C. Eds.; Pergamon Press: Oxford, 1989; Vol. 2, Chapter 6.
- Price, C. In *Development in Block Copolymers*: Goodman, I., Ed.; Elsevier Applied Science: London, U.K., 1982; Vol. 1, p. 39.
- Tuzar, Z.; Kratochvil, P. Surface and Colloid. Sci. Series, Matijevic Ed.; Plenum Press: New York, 1993; Vol. 1, p.1.
- (a) Zhu, J.; Eisenberg, A.; Lennox, R. B. Macromolecules 1992, 9, 2243. (b) Li,
 S.; Hanley, S.; Khan, I.; Eisenberg, A.; Lennox, R. B. Langmuir 1995, 9, 2243.
- Meszaros, M.; Eisenberg, A.; Lennox, R. B. Faraday Discuss. 1994, 98, 283.
- van Krevelen, D. W. Properties of Polymers: Their Correlation with Chemical Structure; Their Numerical Estimations and Prediction from Additive Group Contributions; Elsevier: Amsterdam, 1990, 3rd edition.
- Hiemenz, P. C. Polymer Chemistry: The Basic Concepts; Marcel Dekker: New York, 1984.
- Sperling, L. H. Introduction to Physical Polymer Science; John Wiley and Sons: New York, 1986.
- Noshay, A.; McGrath, J. E. Block Copolymers Overview and Critical Survey;
 Academic Press: New York, 1977.
- Painter, P.C.; Coleman, M. M. Fundamentals of Polymer Science: An Introductory Text; Technomic Publishing: Lancaster, 1994.

- (a) Smith, P.; Hara, M.; Eisenberg, A. In Current Topics of Polymer Science, Volume II; Ottenbrite, R. M.; Utracki, L. A.; Inoue, S. Eds.; Hanser Publishers: Munich, 1987, p. 256. (b) Natansohn, A.; Murali, R.; Eisenberg, A. Makromol. Chem., Makromol Symp. 1988, 16, 175.
- 12 Thomas, E. L.; Lescanec, R. L. Phil. Trans. R. Soc. Lond. A 1994, 348, 149.
- 13 Bates, F. S.; Fredrickson, G. H. Annu. Rev. Phys. Chem. 1990, 41, 525.
- (a) Leibler, L. Macromolecules 1980, 13, 1602. (b) Fredrickson, G. H.; Helfand,
 E. J. Chem. Phys. 1987, 87, 697.
- Elias, H. G., In Light Scattering from Polymer Solutions; Huglin, M. B., Ed.;

 Academic Press: New York, 1972, Chapter 9.
- (a) Price, C.; Chan, E. K. M.; Stubbersfield, R. B. Eur. Polym. J. 1987, 23, 649.
 (b) Quintana, J. R.; Villacampa, M.; Munoz, M.; Andrio, A.; Katime, I. A. Macromolecules, 1992, 25, 3125. (c) Zhou, Z.; Chu, B.; Peiffer, D. C. Macromolecules 1993, 26, 1876.
- (a) Deng, Y.; Yu, G.-E.; Price, C.; Booth, C. J. Chem. Soc., Faraday Trans.
 1992, 88, 1441. (b) Alexandridis, P.; Holtzwarth, J. F.; Hatton, T.A.
 Macromolecules 1994, 27, 2414. (c) Zhou, Z.; Chu, B. Macromolecules 1994,
 27, 2025.
- 18 Sadron, C. Pure Appl. Chem. 1962, 4, 347.
- 19 Chu, B. Langmuir 1995, 11, 414.
- (a) Lindman, B.; Wennerstrom, H. Top. Curr. Chem. 1980, 87, 1. (b) Tanford,
 C. The Hydrophobic Effect: Formation of Micelles and Biological Membranes;
 John Wiley & Sons: New York, 1980. (c) Mayers, D. Surfactant Science and
 Technology; VCH Publishers: New York, 1988.

- ²¹ Leibler, L.; Orland, H.; Wheeler, J. C. J. Chem. Phys. 1983, 79, 3550.
- 22 Nagarajan, R.; Ganesh, K. J. Chem. Phys. 1989, 90, 5843.
- 23 Marko, J. F.; Rabin, Y. Macromolecules 1992, 25, 1503.
- ²⁴ Gao, Z.; Eisenberg, A. *Macromolecules* **1993**, 26, 7353.
- ²⁵ Price, C. Pure Appl. Chem. 1983, 55, 1563.
- Hunter, R. J. Foundations of Colloid Science; Oxford: New York, 1991; Vol. 1.
- 27 Price, C.; Chan, E. K. M.; Stubbersfield, R. B. Eur. Polym. J. 1987, 23, 649.
- Astafieva, I.; Zhong, X. F.; Eisenberg, A. Macromolecules 1993, 26, 7339.
- ²⁹ Tuzar, Z.; Petrus, V.; Kratochvil, P. Makromol. Chem. 1974, 175, 3181.
- Prochazka, K.; Bednar, B.; Mukhtar, E.; Svoboda, P.; Trnena, J.; Almgren, M. J. Phys. Chem. 1991, 95, 4563.
- Wang, Y.; Kausch, C. M.; Chun, M.; Quirk, R. P.; Mattice, W. L. *Macromolecules* 1995, 28, 904.
- Tian, M.; Qin, A.; Ramireddy, C.; Webber, S. E.; Munk, P.; Tuzar, Z.; Prochazka,
 K. Langmuir 1993, 9, 1741.
- Pacovska, M.; Prochazka, K.; Tuzar, Z.; Munk, P. Polymer 1993, 34, 4585.
- ³⁴ Soen, T.; Inoue, T.; Miyoshi, K.; Kawai, H. J. Polym. Sci. Part A-2 1972, 10, 757.
- Nguyen, D. Ph.D. Thesis, McGill University, Montreal, Canada, 1994.
- ³⁶ Zhulina, E. B.; Birshtein, T. M. Vysokomol. Soedin. 1985, 27, 511.
- 37 Halperin, A. *Macromolecules* **1987**, 20, 2943.
- de Gennes, P.-G. Solid State Physics; Liebert, J., Ed.; Academic Press: New York, 1977; Suppl. 14, pp 1-18.
- ³⁹ Noolandi, J.; Hong, M. H. *Macromolecules* **1983**, *16*, 1443.
- Whitmore, M. D.; Noolandi, J. Macromolecules 1985, 18, 657.

- 41 Daoud, M.; Cotton, J. P. J. Phys. 1982, 43, 531.
- 42 Dan, N.; Tirrell, M. Macromolecules 1993, 26, 4310.
- Huglin M. B. In *Topics in Current Chemistry*; Springer-Verlag: Berlin, 1978; Vol.
 77, p. 141.
- 44 Light Scattering from Polymer Solutions; Huglin, M. B. Ed.; Academic Press:
 New York, 1972.
- Kratochvíl, P. Classical Light Scattering from Polymer Solutions; Jenkins, A. D.,
 Ed.; Elsevier Science Publishers: New York, 1987.
- 46 Wyatt, P. J. Anal. Chim. Acta 1993, 272, 1.
- 47 Hilfiker, R.; Chu, B.; Xu, Z. J. Colloid Interface Sci. 1989, 133, 176.
- ⁴⁸ Zimm B. H., J. Chem. Phys. 1948, 16, 1099.
- 49 Kim, S. H.; Cotts, P. M. J. Appl. Polym. Sci. 1991, 42, 217.
- Dynamic Light Scattering. Applications of Photon Correlation Spectroscopy;
 Pecora, R. Ed.; Plenum Press: N. Y., 1985.
- Chu, B. Laser Light Scattering. Basic Principles and Practice; Academic Press:Boston, 1991.
- 52 Brown, W. Dynamic Light Scattering: The Method and Some Applications;
 Oxford University Press: N. Y., 1993.
- Weiner, B. B. In Modern Methods of Particle Size Analysis; Barth, H. G.; Hays, J. J., Eds.; John Wiley and Sons: N. Y.1991; Chapter 3.
- 54 Finsy, R. Adv. Colloid Interface Sci. 1994, 52, 79.
- Billmeyer, F. W. Textbook of Polymer Science; John Wiley and Sons: New York, 1984.
- ⁵⁶ Grubisic, Z.; Rempp, P.; Benoit, H. J. Polym. Sci. Part B 1967, 5, 753.

Chapter 1. General Introduction

- 57 (a) Astafieva, I.; Zhong, X. F.; Eisenberg, A. Macromolecules 1993, 26, 7339.
 - (b) Astafieva, I.; Khougaz, K.; Eisenberg, A. Macromolecules in press
- 58 Gao, Z; Desjardins, A; Eisenberg, A. Macromolecules 1992, 25, 1300.

CHAPTER 2

Micellization of Ionic Block Copolymers

2.1. INTRODUCTION

The investigation of ion-containing block copolymers in solution has revealed that these materials form spherical aggregates, known as micelles, in both water and organic solvents. 1-4 Studies of the formation and characteristics of these aggregates have generated a great deal of interest, as micelles of ionic block copolymers provide an extremely versatile addition to the growing field of molecular self-assembly. Possible applications in the areas of advanced materials and drug delivery have spurred our own interest in this field.

For many years, the phenomenon of micellization has been known to occur in solutions of low-molecular weight amphiphiles (or surfactants) above a concentration known as the critical micelle concentration (cmc). The cmc is a function of both the amphiphile and the solvent environment, and also tends to vary with the method of detection. However, in general terms, we can state that, below the cmc, single amphiphiles exist in solution while, above the cmc, associates (or aggregates) tend to form. Due to differences in the kinetics of exchange between unimers and the self-assembled structures, the term "associate" is generally reserved for surfactant micelles,

while micelles of block copolymers are often referred to as "aggregates". This point will be further discussed later on.

To understand the formation of spherical micelles, it is important to realize that amphiphilic molecules consist of both an ionic or nonionic polar moiety, and at least one hydrocarbon chain. Since these two parts of the molecule have very different solubilities, amphiphiles in solution above the cmc will tend to undergo microphase separation. For example, in an aqueous environment, the hydrocarbon chains of a number of Aerosol OT (AOT) molecules will cluster together to form a liquid-like core, surrounded and protected by the solubilized ionic head groups.

The subject of the present article is the self-assembly of ionic block copolymers, which is in many ways analogous to the micellization of surfactants in solution. In our discussion, we hope to show that the combination of extremely high aggregate stability, low cmc's, and a wide range of aggregate sizes gives ionic block copolymers unprecedented versatility, and opens the door to many potential applications. Before embarking on a description of ion-containing block copolymers, however, a more general discussion of block copolymer micellization is required.

It has long been known that block copolymers in selective solvents will form spherical aggregates, with compact cores of insoluble blocks surrounded by a soluble corona composed of soluble blocks. Like their surfactant counterparts, micelles of block copolymers show an extremely narrow size distribution. The term micelle has been applied to these colloidal aggregates, due to the structural similarities with surfactant micelles; however, we shall see that micelles of block copolymers and low-molecular weight surfactants are quite different in terms of their lability and exchange kinetics. For a number of years, block copolymer micelles have been the subject of much interest, and some excellent reviews have been published in the field.⁵⁻⁷

Along with a number of experimental studies, block copolymer micelles have been the subject of considerable theoretical treatment in recent years.⁸⁻²¹ Of particular relevance

to the present review are theories proposed by Zhulina and Birshtein¹² and by Halperin¹⁶ for "star" micelles. These micelles are spherical with small cores and expanded coronae, which form when the length of soluble block is considerably longer than that of the insoluble block. Conversely, "crew-cut" micelles^{22,23} are structures with large cores and short coronal "hair", formed from asymmetric block copolymers with relatively long insoluble blocks. In the former case, theory predicts that the radius of the core (R_c) is independent of the soluble block length, and scales as N_B^{3/5}, where N_B is the number of units in the insoluble block.

At this point, it is important to mention that the theoretical treatment of block copolymer micelles, resulting in scaling relations such as the one given above, is generally based on thermodynamic considerations, and assumes an equilibrium between single chains and the micellar aggregates. Unlike associates of surfactants, which are extremely labile structures, the kinetics of exchange between block copolymer micelles and single chains in solution are slow, due to the high viscosity of the insoluble blocks within the micelle core. This is especially true in the case of the ionic block copolymer micelles which pertain to the present discussion; these have glassy polystyrene cores in an aqueous environment, or ionic cores with short-range electrostatic interactions in organic environments. In fact, on a reasonable time scale, the micelles of ionic block copolymers may be regarded as "frozen" structures, with no dynamic equilibrium between micelles and single chains. An application of theoretical models to such systems, therefore, requires us to assume that a dynamic equilibrium does exist at some stage of micelle formation, even though the final result is a frozen aggregate. These considerations should be kept in mind throughout the present review, as they serve to qualify our use of the term "micelle" in describing frozen aggregates of block copolymers.

Several theoretical treatments of block copolymers in selective solvents have addressed the phenomenon of the critical micelle concentration. 9,18-20 However, until very recently, the polydispersity of the insoluble blocks had not been properly considered. In a

new model for the micellization of block copolymers in solution, Gao and Eisenberg²¹ refined the treatment of Holland and Rubingh,^{24,25} in order to account for the polydispersity effect of the insoluble blocks on the cmc. The model describes the collapse of insoluble blocks into colloidal spheres below the cmc, such that the driving force for micellization is the van der Waals interaction between spherical particles.

We now turn our attention to the colloidal behavior of ionic block copolymers, which possess both hydrophilic blocks of ionic repeat units and hydrophobic blocks of nonionic units. In an AB diblock, for example, a block of nonionic A units is covalently linked to a block of ionic B units. Due to the high degree of incompatibilty between the ionic and nonionic blocks, ionic block copolymers in solution exhibit extremely low cmc's²⁶⁻²⁸ and high aggregate stability.^{3,4}

Ionic block copolymers in solution can be divided into two main categories: block polyelectrolytes and block ionomers. According to the definitions of polyelectrolytes and ionomers proposed by Eisenberg and Rinaudo,²⁹ the properties of block polyelectrolytes are governed by electrostatic interactions over the relatively large distances within the corona and between the micelles, while the properties of block ionomers are governed by short-range interactions within the micelle core.

The classification of ionic block copolymer as either block polyelectrolytes or block ionomers is determined by the nature of the solvent. Ionic block copolymers in water are block polyelectrolytes, forming micelles with nonionic cores and coronae made up of the soluble ionic blocks. In organic solvents, ionic block copolymers can be described as block ionomers, with ionic micelle cores surrounded by the nonionic soluble blocks. Following the terminology adopted for surfactants, ionic block copolymers in aqueous and nonaqueous solvents are sometimes referred to as regular and reverse micelles, respectively. In the "star micelle" regime, block ionomers generally have long nonionic blocks and short ionic blocks, whereas block polyelectrolytes have long ionic blocks and short nonionic blocks. The so-called "crew-cut" polyelectrolytes, on the other

hand, have relatively short ionic blocks, surrounding a large nonionic core. "Crew cut" micelles of block ionomers, to our knowledge, have not been investigated.

This paper will present an overview of the literature on ionic block copolymers in nonaqueous and aqueous solutions, with particular emphasis on work performed in this group. We will begin with a summary of the recent work on block ionomer micelles, followed by a discussion of block polyelectrolytes.

2.2. IONIC BLOCK COPOLYMERS IN ORGANIC SOLVENTS (BLOCK IONOMER MICELLES)

The ionic block copolymers which have been most extensively studied in organic solvents are the polystyrene-based diblock ionomers with long polystyrene blocks joined to relatively short ionic blocks. Diblock ionomers of this type, in which the ionic block is poly(metal acrylate), poly(metal methacrylate), or quaternized poly(4-vinylpyridine), will be the focus of the present discussion. However, it is worth mentioning that an investigation of quaternized polystyrene-b-poly(4-vinylpyridine)-b-polystyrene (PS-b-P4VP-b-PS) triblock ionomers in THF has also been reported. Another related system is sodium-neutralized poly(tert-butylstyrene)-b-lightly sulfonated polystyrene, which has recently been studied by light scattering in nonpolar solvents. 31

The following section on reverse micelles of ionic block copolymers will be divided into four parts. The first part will deal with the characterization of fundamental parameters of block ionomers using numerous techniques (size-exclusion chromatography, light scattering, small-angle X-ray scattering, etc.). The second part will discuss the problem of cmc determination of block ionomers. Next, nuclear magnetic resonance (NMR) investigations of the solubilization of water into the ionic cores and the dynamics of the soluble corona will be described. Lastly, an interesting application of block

ionomers will be presented: the size control of quantum-confined nanoparticles within a polymer host.

2.2.1. Characterization of Fundamental Parameters

Until quite recently, experimental work on the properties of ionic block copolymers in organic solvents was very limited. In the first detailed study of diblock ionomer reverse micelles,³ the aggregation behavior of polystyrene-b-poly(sodium methacrylate) (PS-b-PMANa) and polystyrene-b-poly(cesium methacrylate) (PS-b-PMACs) copolymers was investigated in solvents selectively good for the polystyrene block (e.g. dimethylformamide (DMF), tetrahydrofuran (THF)). Using size-exclusion chromatography (SEC) coupled with intrinsic viscosity measurements, micellar characteristics such as aggregation number and hydrodynamic radius were investigated systematically as a function of the ionic and polystyrene block lengths.

Typical size-exclusion chromatograms of block ionomers in selective solvents show up to three distinct peaks, attributable to micelles, single chains, and homopolystyrene.^{3,32} The micelle peak appears at the lowest elution volume, due to the large size of the micellar aggregates relative to that of the unimers. The relative area under the micelle and single chain peaks depends on the composition of the block ionomer, with longer ionic blocks resulting in a higher percentage of micellized material.

When a mixture of micelles with different molecular weights was injected repeatedly into the SEC column, the bimodal shape of the chromatogram was retained over 3 days, indicating the lack of a dynamic equilibrium between micelles and single chains.³ The existence of a single chain peak was attributed to a distribution in the length of the ionic block, with single chains having a lower ion content than aggregated chains. Infrared spectroscopy of micelle and single chain fractions supported this hypothesis. Despite the absence of a dynamic equilibrium, the term micelle is used for block ionomers,

on the basis of the structural and behavioral similarities with other block copolymer micelles.

A combination of SEC and viscometry was used to determine aggregation numbers and hydrodynamic radii (R_h) of polystyrene-b-poly(metal methacrylate) reverse micelles.⁴ Both the aggregation number and the hydrodynamic radius were found to increase as the length of the insoluble block increases. However, as the length of the soluble block increases, the aggregation number decreases and the hydrodynamic radius increases. The latter trend is understood on the basis of an increase in the corona thickness as the length of the polystyrene segment increases; thus the overall radius of the micelle increases, despite a lowering of the aggregation number.

The above trends were confirmed by dynamic light scattering (DLS) measurements.⁴ DLS was also used to test the stability of reverse micelles by the addition of polar solvents to different solutions of block ionomers. After an initial decrease in R_h upon addition of the polar solvent, the sizes of reverse micelles were found to remain constant over a period of several months.

One of the attractive features of block ionomer micelles is the wide range of aggregate sizes which is possible in these systems, as micellization is found to occur down to very short ionic block lengths. In fact, when the length of the ionic block is reduced to a single ionic unit, one obtains a useful conceptual bridge between micelles of block copolymers and those of surfactant amphiphiles, which generally possess a single ionic head group. Related to this discussion are the telechelic ion mers, 33 in which single ionic groups or zwitterions are fixed to both ends of the polymer chain, and the monochelic ionomers, 34-37 in which an ionic moiety is fixed to one end of the chain. In the case of monochelics, viscometry and static light scattering (SLS) have been used to determine cme's and aggregation numbers of carboxylate-terminated polystyrene chains in solvents of low dielectric constant. The aggregation behavior of 1,2-dicarboxyethyl-terminated polystyrene in cyclohexane has also been studied. 37

It has been found that small-angle X-ray scattering (SAXS) is a useful technique for obtaining structural information on block ionomer micelles. SAXS has been used to investigate micellar core sizes of polystyrene-b-poly(cesuim acrylate) (PS-b-PACs) and PS-b-PMACs in toluene for several ionic block lengths.³⁸ Typical SAXS profiles for block ionomer micelles (Figure 2.1) are a combination of a shape factor, which characterizes the size and shape of the scatterers (i.e., the ionic cores), and the structure factor, which characterizes distances between scatterers. The structure factor can also be related to order within the micelle solution.

From such scattering profiles, core sizes of the PS-b-PACs and PS-b-PMACs systems were found to obey the star model, scaling as N_B^{3/5}, independent of the PS block length. A proportionality constant of 6.5 Å was determined. The applicability of a thermodynamically-derived scaling relation is a good indication that block ionomer micelles, although undoubtedly frozen structures, approach equilibrium in the early stages of micelle formation. These micelles are formed by neutralization of single chains of acid-form block copolymers in organic solvent; before the core-forming blocks are 100% neutralized,³⁹ it is likely that micelles and single chains are in dynamic equilibrium. At some point, the equilibrium structures become frozen as solvent is excluded from an increasingly ionic core.

In further SAXS work, 40 the study of block length dependence was extended to include quaternized PS-b-P4VP. The same fit with the Halperin model was obtained, supporting the relationship $R_c = 6.5 N_B^{3/5}$ Å. High chain extension in the micelle core was observed for both ionic microdomains dispersed in a nonionic matrix and nonionic microdomains dispersed in an ionic matrix. This result proved that chain extension within the cores of block ionomers is due to the minimization of interfacial energy rather than to short-range ionic interactions. SAXS results, together with computer modelling of spherical shape factors, have been used to determine the radii polydispersity

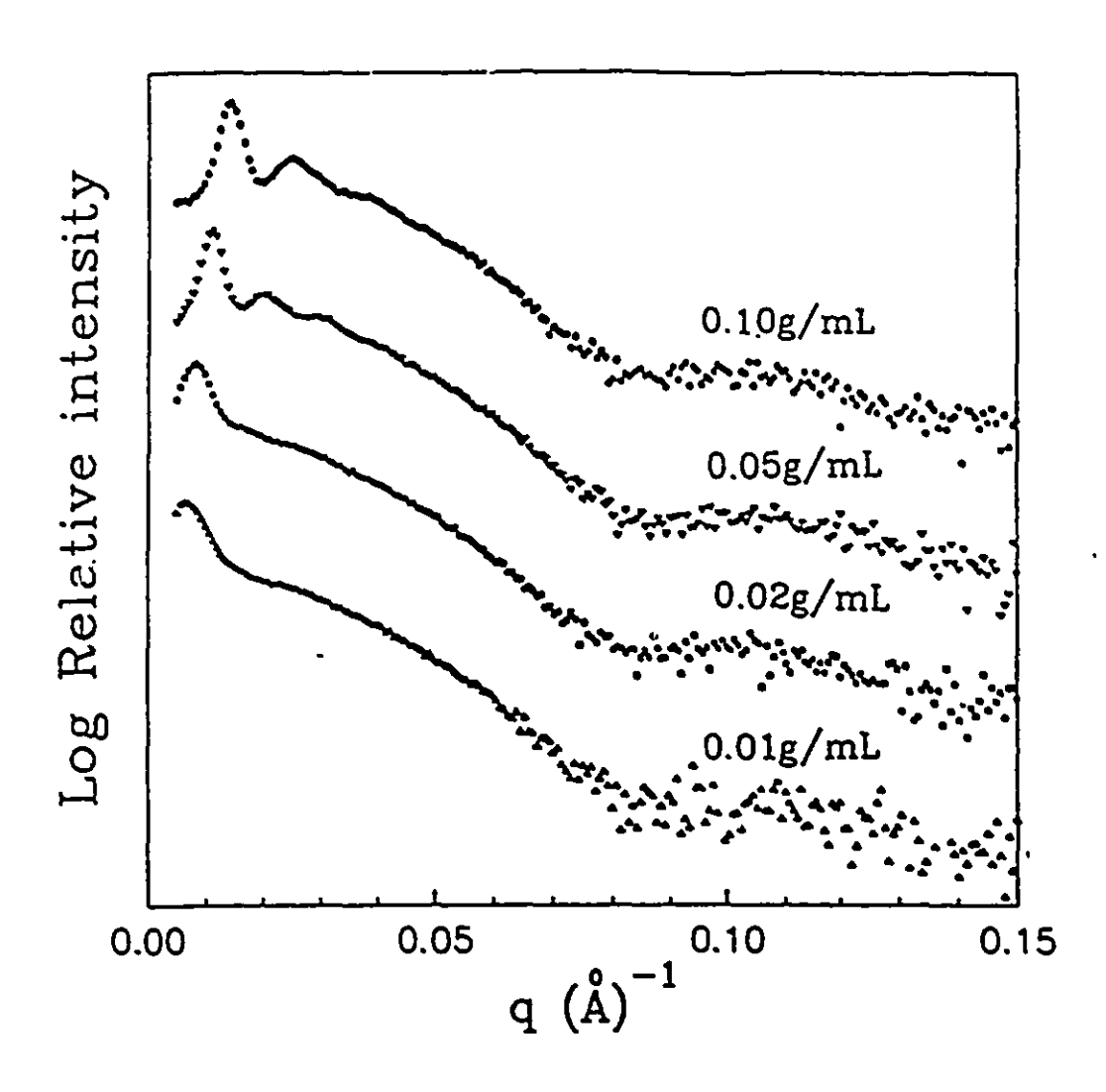


Figure 2.1. SAXS profiles of PS(600)-b-PACs(45) diblock ionomer in toluene in the concentration range from 0.01 g/mL to 0.10 g/mL.³⁸

indexes (RPI) of ionic cores.³⁸ These were found to be between 1.02 and 1.04, considerably smaller than the polydispersity indexes of the polymer chains.

2.2.2. Critical Micelle Concentrations of Block Ionomers

A wide range of techniques has been used to determine the critical micelle concentrations of block copolymers in selective solvent, such as fluorescence, osmometry, viscometry, and static light scattering. The latter method is sensitive to changes in the apparent weight-average molecular weight (M_w) of the solution, a quantity which includes contributions from both micelles and single chains. In a typical experiment, the quantity Kc/R(0) (where K is the optical constant and R(0) is the Rayleigh ratio extrapolated to 0 angle) is plotted as a function of concentration; since Kc/R(0) is inversely proportional to the apparent M_w, such a plot shows three distinct regions, corresponding to unimers in solution, a transition region, and micelles in solution.

The extremely low cmc's of block ionomer micelles make their determination by empirical methods difficult, as the unimer region is often at concentrations below the limit of detection. However, the cmc's can be evaluated by fitting the micelle and transition region according to an equation proposed by Debye.⁴² For systems with significant polydispersity in the insoluble block, a new method has been developed,²⁶ based on the micellization model of Gao and Eisenberg.²¹ Figure 2.2 shows plots of cmc vs. the insoluble block length for various systems,⁴³⁻⁴⁶ including AOT surfactant in benzene and nonionic block copolymers in selective solvents. From these plots, one can compare the extremely low cmc's of block ionomer micelles with the wide range of cmc's observed for other self-assembling species.

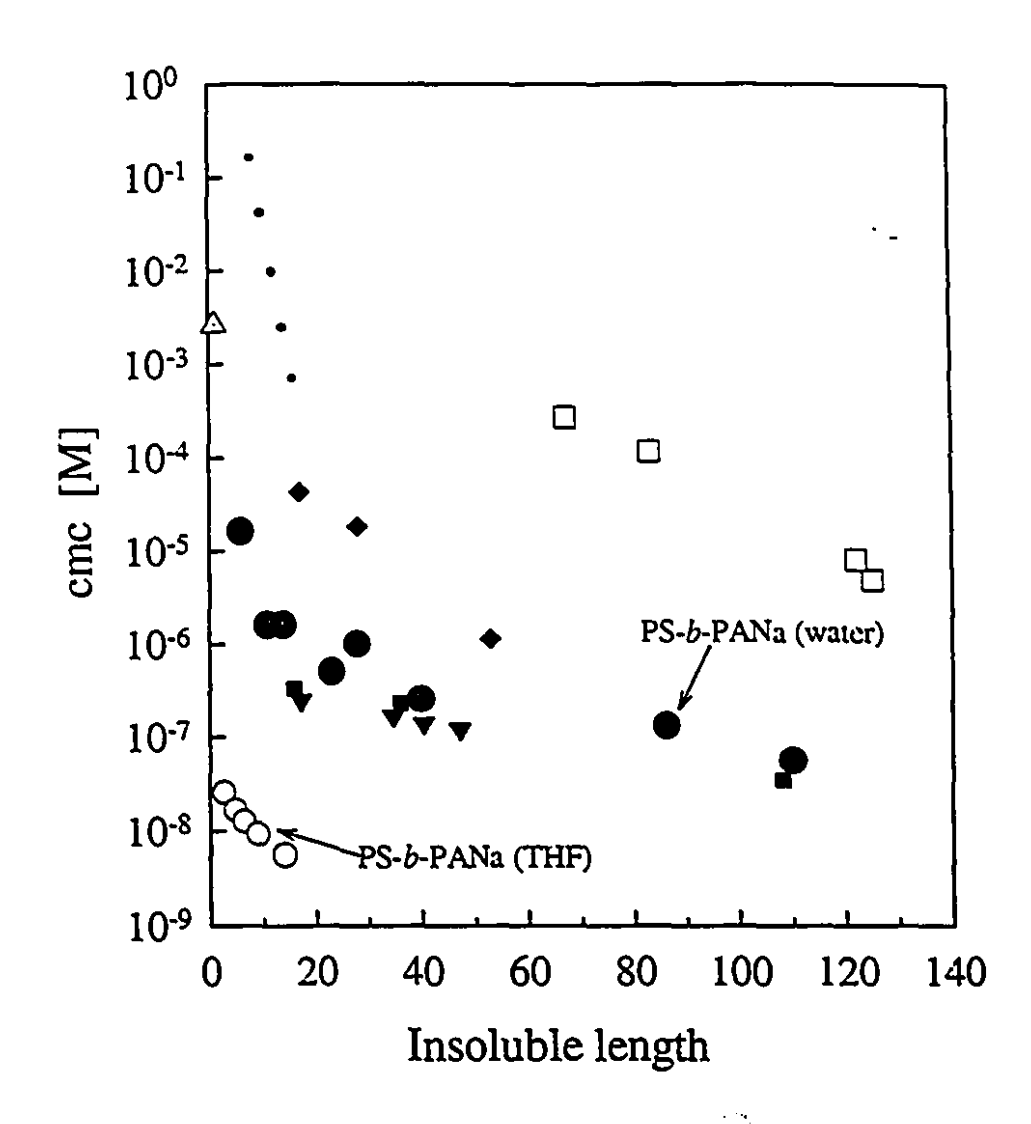


Figure 2.2. Typical cmc values for different micellar systems in aqueous media: sodium alkyl sulfonate surfactants (•),⁴⁴ poly(ethylene oxide)-*b*-poly(butylene oxide)-*b*-poly(ethylene oxide) (PEO-*b*-PBO-*b*-PEO) (\spadesuit),⁴⁶ PS-*b*-PANa (\spadesuit),²⁶ PS-*b*-PEO (\blacksquare) and PEO-*b*-PS-*b*-PEO (\blacktriangledown),⁴⁵ and in nonaqueous media: AOT (\triangle),⁴⁴ polystyrene-*b*-poly(isoprene) (PS-*b*-PI) (\square),⁴³ PS-*b*-PANa (\bigcirc).²⁷

2.2.3. Characterization of Water Solubilization and Chain Dynamics by NMR

An important feature of surfactant reverse micelles is their ability to solubilize water within the ionic core, creating water pools which can act as "microreactors" for hydrophilic reactants. Block ionomer micelles in nonpolar solvents are also able to solubilize small quantities of water, and the distribution coefficient of water between the ionic core and the solvent has been studied by proton NMR.^{47,48} A single chemical shift for the water protons is observed, which is a weighted average of the chemical shift of water in the reverse micelle and in the nonpolar solvent. The appearance of a single chemical shift indicates that the exchange of water between the ionic core and the solvent phase is very fast within the time scale of the NMR experiment. On these grounds, it seems that the ionic core is liquid-like in the presence of water.

From measurements of the observed chemical shift of the water protons,⁴⁷ the distribution coefficients in favour of water solubilization in different solvents were found to occur in the following order: cyclohexane > benzene - toluene > chloroform >> THF - DMF. Distribution coefficients were also investigated for ionic blocks with different functional groups,⁴⁸ and at 25°C they were found to decrease as follows: cesium carboxylate >> pyridinium methyl iodide.

NMR has also proven useful in the measurement of coronal chain dynamics at the segmental level. In systems of PS-b-PACs in carbon tetrachloride (CCl₄), the mobility of ²H-labeled polystyrene segments was probed at various distances from the ionic core. ⁴⁹ ²H relaxation times revealed that close to the ionic-nonionic junction there is a definite decrease in segmental mobility with respect to the "free" chain. Further from the ionic block, the segmental mobility is less restricted, and at a distance of ca. 40 units the mobility is close to that of the nonionic homopolymer. It was also found that segmental mobility decreased with increasing length of the ionic block. This result can be explained

on the basis of geometrical considerations; for star-like micelles, the segmental density at a particular distance from the core is higher when the ionic core is larger, resulting in a larger number of steric interactions.

2.2.4. Semiconductor Nanoparticles in Block Ionomer Micelles

The control of ionic core sizes through variations in the insoluble block length makes block ionomers attractive materials for the formation of polymer-nanoparticle composites. For example, the neutralization of polystyrene-b-poly(acrylic acid) (PS-b-PAA) block copolymers can introduce a wide range of metal ions into the core; the reduction of these ions, or treatment with H₂S, will effect the formation of ultra-small metal or metal sulfide particles within the cores, ⁵⁰ with sizes determined by the aggregation number of the block ionomer host. ⁵¹

One such application of block ionomers has been demonstrated by the precipitation of quantum-confined CdS nanoparticles within the cores of polystyrene-b-poly(cadmium acrylate) (PS-b-PACd).⁵¹ Quantum confinement arises from the extremely small sizes of these crystallites (< 60 Å), and results in excited states which are more energetic than those of bulk CdS. To prepare the composites, the ionic cores were placticized with water, after which the films were treated with H₂S for 8 hours. CdS particle sizes were determined from blue-shifts in the UV-vis spectrum, and these were plotted against the size of the original core ($R_c = 6.5 N_B^{3.5} Å$). A linear relationship was found between CdS particle sizes and ionic core sizes, up to a particle diameter of 50 Å, where the particle sizes level off (Figure 2.3). Below 50 Å, it appears that excellent size control of CdS particles can be achieved by selecting the appropriate ionic core size. Also shown in the plot are CdS nanoparticles synthesized in the multiplets of random ionomers (dotted circles), which allow for synthesis of particles down to 18 Å.⁵²

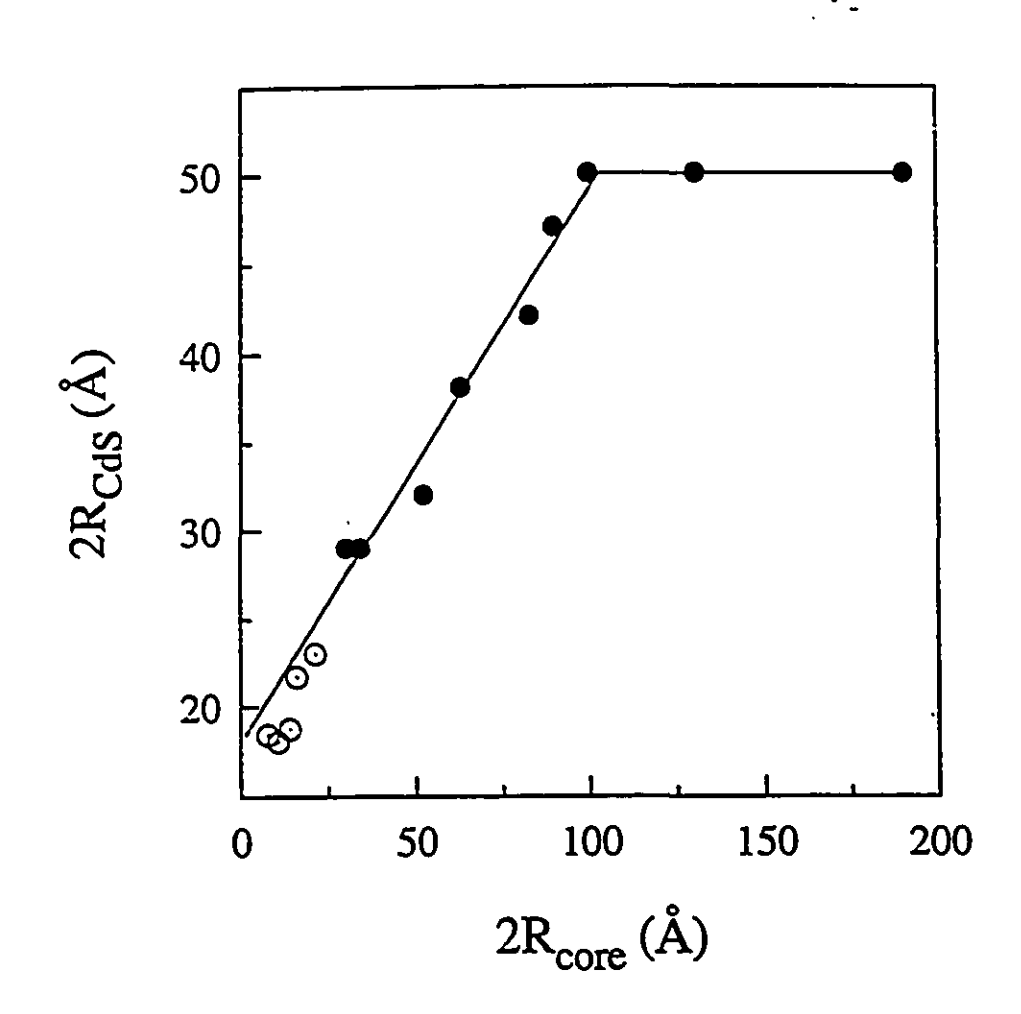


Figure 2.3. Plot of CdS particle diameter vs. diameter of original core (calculated from $R_c = 6.5 N_B^{3/5}$ Å). Dotted circles indicate CdS particles synthesized within the microdomains of random ionomers.⁵¹

The stability of the CdS-polymer composites was shown by dissolving the materials in organic solvents (e.g. toluene, THF) to form clear yellow solutions of CdS-containing reverse micelles.⁵¹ The micelles were stabilized by re-neutralizing the PAA block with NaOH. The yellow powders were then repeatedly precipitated into MeOH and redissolved, without significant changes in the UV-vis absorption spectrum of the composite.

2.3. IONIC BLOCK COPOLYMERS IN AQUEOUS MEDIA (BLOCK POLYELECTROLYTE MICELLES)

In this section, two types of block polyelectrolyte micelles will be discussed, star and crew cut micelles. One of the earliest studies of block polyelectrolytes was performed by Schindler and Williams, in which phase separation in films of polystyrene-b-poly(vinylpyridinium methyl bromide) was investigated.⁵³ Much of the pioneering studies of block polyelectrolyte star micelles in solution was performed by Selb and Gallot, and their work has been reviewed.^{1,2} It should be mentioned that the micellization of block polyelectrolytes on the surface of water has also been extensively studied.⁵⁴⁻⁵⁸ However, in general, studies of block polyelectrolyte micelles have been scarce. To date there are two theoretical models dealing with the micellization of block polyelectrolytes.^{19,59}

The following section will first focus on the characterization of aqueous star micelles by a variety of techniques. The effects of several factors, such as the solvent quality (i.e. salt concentration and temperature), block size, degree of neutralization, and solubilization on the micellization will be discussed. In the second part of this section, an overview of a aqueous crew cut micelles and a number of related morphologies, will be addressed.

2.3.1. Characterization of Star Micelles

The solvent quality has been found to influence the micellization of block copolymers. In general, when the solvent quality decreases, the solubility of the chains decreases, resulting in a lowering of the cmc and an increase in the aggregation number of the micelles. The quality of the solvent for block polyelectrolyte chains can be influenced, for example, by the addition of salt or by changing the temperature. The effects of solvent quality on the micellization of two block polyelectrolyte systems, polystyrene-b-poly(4-vinyl-N-ethylpyridinium bromide) (PS-b-P4VPEtBr) and PS-b-PANa, as well as the influence of block lengths, will now be discussed.

The solvent quality for PS(26)-b-P4VPEtBr(140) in a water (34 wt.%) /methanol mixture was explored as a function of LiBr concentration by SLS and sedimentation velocity. It was found that the weight fraction of the micelles and the apparent Mw increased at low salt content and remained essentially constant at and above 0.2 M LiBr concentration. At very low salt concentrations (0.01 M), no micelles were present. For some of the low salt concentrations, a cmc was observed which was found to decrease as the salt concentration increased. This observation corresponds to the transition from micelles to single chains, which occurred at lower concentration as the salt concentration increased. The effect of temperature on the cmc and the apparent Mw was studied for this sample at different salt concentrations. An increase in temperature resulted in an increase in the solvent quality and thus an increase in the cmc and a decrease in the aggregation number.

The effect of the solvent quality on micellization was found to depend on the length of the copolymer blocks. For instance, Selb and Gallot found that for short PS block lengths (< ca. 30 units), the cmc and molecular weight were strongly affected by the salt concentration. However, for larger PS block lengths, (> ca. 30 units), the effects of temperature and salt concentration were less important. Thus, it can be suggested that at

high PS block lengths, the micellization process is dominated primarily by the insoluble PS block.

Block polyelectrolytes formed from PS-b-PANa in aqueous solutions have also received considerable attention. ^{26,28,60} In this system, micelle formation occurred when single chains of PS-b-PAA were dissolved in methanol, due to microphase precipitation of the polystyrene blocks. The micelles were then neutralized by the addition of NaOH, and the subsequent ionic form precipitated from solution. It has been observed that block copolymers micelles consisting of hydrophobic-hydrophilic segments are difficult to dissolve directly in aqueous solvents. However, in the case of PS-b-PANa, heating the aqueous solutions at 100°C for a period of time rendered the copolymer micelles soluble. This heating process was followed by viscometry and SLS. ^{26,60} Due to their glassy cores, these aqueous micelles are most likely kinetically-frozen aggregates at normal concentrations, although we shall see that they do exhibit a cmc at very high degrees of dilution.

The cmc's of PS-b-PANa in water are shown in Figure 2.2.²⁶ These values were determined by fluorescence measurements using previously established methods.⁴⁵ It was found that the PS block length has a much greater effect on the cmc than the soluble PANa block length. For instance, an increase in the PS block length from 6 to 110 units, for a constant PANa block length of 1000 units, decreased the cmc by a factor of 320, while an increase in the PANa block length from 300 to 1400 lowered the cmc by less than a factor of 2.²⁶

A recent study explored more systematically the effects of the PANa block length and salt concentration on the cmc values.²⁸ A wide range of samples was investigated, with PS block lengths ranging from 6 to 110 units and PANa block length ranging from 44 to ca. 2400 units. For two series consisting of PS blocks of 11 and 23 units, it was observed that the cmc increased as a function of the PANa block length, passed through a maximum, then decreased as the PANa block length increased further. This maximum can

be explained by a balance of solubility effects. The change in the cmc values with increasing PANa block length was found to become less dramatic for longer PS block lengths (e.g. 110 units), in agreement with results of Selb and Gallot.

The effect of NaCl concentrations (C_s) (0.1 to 2.5 M) on the cmc was also investigated for the PS-b-PANa system.²⁸ The cmc values were found to decrease when the salt concentration increased, and log cmc versus $C_s^{1/2}$ was linear for most of the series investigated. The slope, d (log cmc) / d ($C_s^{1/2}$), was found to be a function of the PS block length. For three different series with PS block lengths of 6, 11 and 23 units, d (log cmc) / d ($C_s^{1/2}$) plotted against the PANa length exhibited sigmodal behavior. This relationship was related to conformational changes of of the polyelectrolyte chain as a function of the PANa block length.

SLS has also been used to characterize the PS-b-PANa system in 2.5 M NaCl. ⁶⁰ It was found that for short PS block lengths (i.e. 6 units) the micellization was strongly affected by the PANa block length. However, as the PS block length increased, the effect of the PANa block length on the aggregation numbers decreased. Aggregation numbers, calculated core radii, and radii of gyration (R_g) were compared with the scaling predictions of the star model. It was found that the scaling relations were a good representation of the R_c and R_g values. The calculated R_c values for this system in 2.5 M NaCl agreed with the values determined by SAXS for similar samples measured in the solid state. ⁴¹ This result implies that for the present system, the morphology of these micelles is the same in the solid state and in solution.

Micelles of polystyrene-b-poly(methacrylic acid) (PS-b-PMAA) have been extensively studied in mixed solvents of dioxane/water and water. $^{61-66}$ It has been pointed out that such micelles may be kinetically frozen when the solvent is very poor for the PS core (i.e. water rich solvents). The micellization process and coronal structure are influenced by the degree of neutralization (α) of the polyelectrolyte, as observed using DLS, viscosity and SLS by Kiserow et. al. 63 At low concentrations and ionic strengths,

the apparent hydrodynamic diameter increased gradually with α , due to the stretching of the ionized carboxylic groups. However, at higher concentrations, a maximum in R_h was observed, corresponding to α values of ca. 0.25-0.35. Similarly, at this α value, a maximum was observed in the viscosity and a minimum in the scattered light intensity. These results imply that a certain amount of ordering in the solutions exists as a result of repulsive interactions between highly charged micelles. Two well defined maxima were determined from DLS, corresponding to the collective mode and the diffusion of clusters of structurally organized micelles. Clusters of micelles have also been seen in such aqueous micellar systems as PS-b-PEO⁶⁷ and Triton X-100.⁶⁸

Solubilization of organic molecules into block polyelectrolytes is a subject of considerable interest due to numerous potential applications. Morishima et al. investigated the quenching of fluorescence probes in hydrophobic domains formed in poly(9-vinylphenanthrene)-b-poly(methacrylic acid) (PVPh-b-PMAA) in water.⁶⁹ The solubilization of organic molecules into aqueous solutions of PS-b-PMAA was also followed by fluorescence spectroscopy^{61,63} and DLS.⁶³ Valint and Bock solubilized toluene in block copolymers of poly(tert-butylstyrene)-b-poly(styrene sulfonate) (PTBS-b-PSS) in water and found an increase in the viscosity.⁷⁰

2.3.2. Characterization of Crew Cut Micelles

Crew cut micelles were prepared and characterized from polystyrene-b-poly(4-vinylpyrindinium iodide) (PS-b-P4VPMeI) in water.⁷¹ These micelles consisting of a large hydrophobic PS core and a relatively thin hydrophilic ionic corona (P4VPMeI) were found to form monodisperse stable micelles in water. Crew cut micelles were prepared by dissolving the polymer in DMF, then adding a selective non-solvent for the PS block. In order to determine the effect of different selective solvents, two procedures were used. In the first, water was added dropwise to the DMF solution; alternatively, methanol was first

added, followed by water. In both cases, the solutions were dialyzed against distilled water to remove DMF and methanol. The diameters of the micelle cores were measured by transmission electron microscopy (TEM), and were found to be smaller for the samples prepared by the addition of water, compared with those prepared from water and methanol. Also, the aggregation numbers and polydispersity indexes, calculated from TEM results, were found to be lower for the micelles prepared from the addition of water. The choice of selective solvent is therefore critical to the micellar properties. The higher aggregation number and broader distribution for micelles prepared using methanol and water was attributed to the different compatibility between styrene and water on one hand, and styrene and a methanol/water mixture on the other.

Recently, crew cut micelles were prepared from PS-b-PAA in water.^{72,73} Different micellar morphologies were observed by TEM depending on the relative block lengths.⁷³ Some of these morphologies consist of spheres, rods, lamellae, and vesicles. In addition, compound micelles were observed, in which reverse micelle-like aggregates are contained in up to micrometer-size spheres having hydrophilic surfaces. When the samples were dried, ordered needle-like solids formed spontaneously. After soaking in water, the separated needle-like solids showed birefringence under crossed polaroids. This phenomenon may suggest that the solids have crystal-like structure, in which the repeat unit is the micelle particle which is several tens of nanometers in diameter.

The PS-b-PAA spherical crew cut micelles were characterized in water by TEM and DLS for a wide range of block lengths. The R_c values scaled as $R_c \sim N_{PS}^{0.4}N_{PAA}^{-0.15}$ illustrating an influence of the soluble block length on the R_c values. From DLS measurements, the R_b values were determined, and the thickness and the degree of extension of the coronal chains were estimated from the R_c and R_b values. It was found that the ionized form of the PAA chains (at pH \sim 7) in the coronae had a highly extended conformation. This result was attributed to the charged nature of the PAA

chains, the low degree of curvature of the core and the relatively low concentration of micelles in the DLS experiment.

2.4. CONCLUSIONS

This review has attempted to summarize some recent findings in the field of ionic block copolymer micelles. Both block ionomer micelles and block polyelectrolyte micelles have been characterized extensively by a wide range of techniques. Low cmc's, high micelle stability, and control over aggregate sizes via copolymer composition make ionic block copolymers of interest for a number of possible applications, including drug delivery and material science. The solubilization of water into the cores of reverse micelles and the preparation of quantum-confined CdS nanoparticles of controlled sizes have illustrated the potential of these systems as microreactors in, for example, the controlled precipitation of metallic and semiconducting clusters. Crew-cut micelles have also been discussed as interesting new morphologies, providing further evidence of the versatility which is offered by solutions of ionic block copolymers.

2.5. ACKNOWLEDGMENT

This work was supported by the Natural Sciences and Engineering Research Council of Canada (NSERC) and Le Fonds pour La Formation de Chercheurs et L'Aide à la Recherche (FCAR, Quebec). M.M. and K.K. are grateful for scholarship funding provided from NSERC and FCAR.

2.6. REFERENCES

- Selb, J.; Gallot, Y. In *Polymeric Amines and Ammonium Salts*. Goethals, E. J. Ed.,
 Pergamon Press: New York, 1980, p 205.
- Selb, J and Gallot, Y. In *Development in Block Copolymers*; Goodman, I., Ed.; Elsevier Applied Science: London, U.K., 1985; Vol 2, pp 27-96.
- Desjardins, A.; Eisenberg, A. Macromolecules 1991, 24, 5779.
- Desjardins, A.; van de Ven, T. G. M., Eisenberg, A. Macromolecules 1992, 25, 2412.
- ⁵ Tuzar, Z.; Kratochvil, P. Adv. Colloid Interface Sci. 1976, 6, 201.
- Price, C. In *Developments in Block Copolymers*, Vol. 1; Goodman, I., Ed.; Applied Science Publishers: London, 1982, p.39.
- Tuzar, Z.; Kratochvil, P. In Surface and Colloid Science, Vol 15; Matijevic, E., Ed.; Plenum Press; New York, 1993, p.1.
- de Gennes, P.-G. In *Solid State Physics*; Leibert, L., Ed.; Academic Press: New York, 1978; Supplement 4.
- 9 Noolandi, J.; Hong, K. M. Macromolecules 1982, 15, 482.
- ¹⁰ Noolandi, J.; Hong, K. M. Macromolecules 1983, 16, 1443.
- Whitmore, M. D.; Noolandi, J. Macromolecules 1985, 18, 657.
- ¹² Zhulina, E. B.; Birshtein, T. M. Vysokomol. Soedin. 1985, 27, 511.
- ¹³ Fredrickson, G. H.; Helfand, E.; J. Chem. Phys. 1987, 87, 697.
- Bug, A. L. R.; Gates, M. E.; Safran, S. A.; Witten, T. A. J. Chem. Phys. 1987, 87,
 1824.
- Marques, C.; Joanny, J. F.; Leibler, L. Macromolecules 1988, 21, 1051.
- ¹⁶ Halperin, A. *Macromolecules* **1989**, 22, 3806.

- Halperin, A.; Alexander, S. Macromolecules 1989, 22, 2403.
- ¹⁸ Nagarajan, R.; Ganesh, K. J. Phys. Chem. 1989, 90, 5843.
- ¹⁹ Marko, J. F.; Rabin, Y. *Macromolecules* **1992**, 25, 1503.
- ²⁰ Yuan, X. F.; Masters, A. J.; Price, C. Macromolecules 1992, 25, 6876.
- ²¹ Gao, Z.; Eisenberg, A. Macromolecules 1993, 26, 7353.
- Nagarajan, R.; Barry, M.; Ruckenstein, Z. E. Langmuir 1986, 2, 210.
- Nagarajan, R.; Ganesh, C. Macromolecules 1989, 22, 4312.
- Holland, P. M.; Rubingh, D. N. J. Phys. Chem. 1983, 87, 1984.
- Holland, P. M. Adv. Colloid Interface Sci. 1986, 26, 111.
- Astafieva, I.; Zhong, X. F.; Eisenberg, A. Macromolecules 1993, 26, 7339.
- Khougaz, K.; Gao, Z.; Fisenberg, A. Macromolecules 1994, 27, 6341.
- Astafieva, I.; Khougaz, K.; Zhong, X.F.; Eisenberg, A. Macromolecules 1995, 28, 7127.
- ²⁹ Eisenberg, A.; Rinaudo, M. *Polymer Bull.* **1990**, 24, 671.
- Ishizu, K.; Kashi, Y.; Fukutomi, T.; Kakurai, T. Makromol. Chem. 1982, 183, 3099.
- ³¹ Zhou, Z.; Peiffer, D. J.; Chu, B. *Macromolecules* 1994, 27, 1428.
- Zhong, X. F.; Varshney, S. K.; Eisenberg, A. Macromolecules 1992, 25, 7160.
- Vanhoorne, P.; Jerome, R. In *Ionomers: Characterization, Theory, and Applications*; Schlick, S., Ed.; CRC Press: Boca Raton, Chapter 9, in press.
- Jalal, N.; Duplessix, R. J. Phys. (France) 1988, 49, 1775.
- (a) Davidson, N. S.; Fetters, L. J.; Funk, W. G.; Graessley, W. W.; Hadjichristidis
 Macromolecules 1988, 21, 112. (b) Pispas, S.; Hadjichristidis, N.

- Macromolecules 1994, 27, 1891. (c) Pispas, S.; Hadjichristidis, N.; Mays, J.M. Macromolecules 1994, 27, 6307.
- ³⁶ Zhong, X. F.; Eisenberg, A. *Macromolecules* **1994**, 27, 1751.
- ³⁷ Zhong, X. F.; Eisenberg, A. *Macromolecules* **1994**, 27, 4914.
- Nguyen, D.; Williams, C. E.; Eisenberg, A. Macromolecules 1994, 27, 5090.
- Khougaz, K.; Nguyen, D.; Williams, C. E.; Eisenberg, A. Can. J. Chem. In press.
- Nguyen, D.; Williams, C. E.; Eisenberg, A. To be published.
- Nguyen, D.; Varshney, S. K.; Williams, C. E.; Eisenberg, A. Macromolecules 1994, 27, 5086.
- Elias, H. G., In Light Scattering from Polymer Solutions; Huglin, M. B., Ed.;
 Academic Press: New York, 1972, Chapter 9.
- ⁴³ Price, C.; Chan, E. K. M.; Stubbersfield, R. B. Eur. Polym. J. 1987, 23, 649.
- Myers, D. Surfactant Science and Technology; VCH publishers; New York, 1988.
- Wilhelm, M.; Zhao, C. L.; Wang, Y.; Xu, R.; Winnik, M. A.; Mura, J. L.; Riess; G., Croucher, M. D. Macromolecules 1991, 24, 1033.
- Nicolas, C. V.; Luo, Y. Z.; Deng, N. J.; Attwood, D.; Collet, J. H.; Price, C.;
 Booth, C. *Polymer* 1993, 34, 138.
- Gao, Z.; Desjardins, A.; Eisenberg, A. Macromolecules 1992, 25, 1300.
- Khougaz, K.; Gao, Z.; Eisenberg, A., To be published.
- ⁴⁹ Gao, Z. Zhong, X. F.; Eisenberg, A. *Macromolecules* **1994**, 27, 794.
- Kunstle, H. PhD Thesis, Twente University, 1993.
- Moffitt, M.; McMahon, L.; Pessel, V.; Eisenberg, A., Chem. Mater. 1995, 7, 1185.
- 52 Moffitt, M.; Eisenberg, A., Chem. Mater. 1995, 7, 1178.

- Schindler, A.; Williams, J.L. Polym. Prepr. (Am. Chem. Soc., Polym. Chem. Div.)

 1968, 10, 832.
- ⁵⁴ Zhu, J.; Eisenberg, A.; Lennox, R. B. J. Am. Chem. Soc. 1991, 113, 5583.
- ⁵⁵ Zhu, J.; Eisenberg, A.; Lennox, R. B. Langmuir 1991, 7, 1579.
- ⁵⁶ Zhu, J.; Eisenberg, A.; Lennox, R. B. J. Phys. Chem. 1992, 96, 4727.
- ⁵⁷ Zhu, J.; Eisenberg, A.; Lennox, R. B. *Macromolecules* **1992**, *25*, 6547.
- ⁵⁸ Zhu, J.; Eisenberg, A.; Lennox, R. B. *Macromolecules* **1992**, *25*, 6556.
- ⁵⁹ Dan, N.; Tirrell, M. Macromolecules 1993, 26, 4310.
- Khougaz, K.; Astafieva, I.; Zhong, X. F.; Eisenberg, A. Macromolecules 1995, 28,
 7135.
- ⁶¹ Cao, T.; Munk, P.; Ramireddy, C.; Tuzar, Z.; Webber, S. E. *Macromolecules* 1991, 24, 6300.
- Prochazka, K.; Kiserow, D.; Ramireddy, C.; Tuzar, Z.; Munk, P.; Webber, S. E.

 Macromolecules 1992, 25, 454.
- Kiserow, D.; Prochazka, K.; Ramireddy, C.; Tuzar, Z.; Munk, P.; Webber, S. E. Macromolecules 1992, 25, 461.
- Tian, M.; Qin, A.; Ramireddy, C.; Webber, S. E.; Munk, P.; Tuzar, Z.; Procházka, K. Langmuir 1993, 9, 1741.
- Tuzar, Z.; Procházka, K.; Zuzková, I.; Munk, P. Polym. Prepr. (Am. Chem. Soc., Poly. Chem. Div.) 1993, 34, 1038.
- Qin, A.; Tian, M.; Ramireddy, C.; Webber, S. E.; Munk, P. Macromolecules 1994, 27, 120.
- Xu, R.; Winnik, M. A.; Hallett, F. R.; Riess, G.; Croucher, M. D. *Macromolecules* 1991, 24, 87.

- Brown, W.; Rymden, R.; Stam, J.; Almgren, M.; Svensk, G. J. Phys. Chem. 1989, 93, 2512.
- Morishima, Y.; Itoh, Y.; Hashimoto, T.; Nozakura, S.-I. J. Polym. Sci., Polym. Chem. Ed. 1982, 20, 2007.
- ⁷⁰ Valint, Jr., P. L.; Bock, J. *Macromolecules* 1988, 21, 175.
- Gao, Z.; Varshney, S. K.; Wong, S.; Eisenberg, A. Macromolecules 1994, 27, 7923.
- ⁷² Zhang, L.; Barlow, R. J.; Eisenberg, A. Macromolecules 1995, 28, 6055.
- ⁷³ Zhang, L.; Eisenberg, A. Science 1995, 268, 1728.

CHAPTER 3

Characterization of Polystyrene-b-Poly(sodium acrylate) Block Polyelectrolyte Micelles by Static Light Scattering

ABSTRACT

Block polyelectrolyte micelles formed by poly(styrene-b-sodium acrylate) in aqueous solutions were characterized by static light scattering (SLS). Initially, the solutions contained gel-like particles; the kinetics of disentanglement of these particles were measured from the intensity of the scattered light at different angles as a function of heating time at 100 °C. It was found that after ca. 50 hours of heating no further changes occurred in the scattered intensity. The effect of different sodium chloride concentrations on the aggregation numbers (Nagg), radii of gyration (Rg), and second virial coefficients (A2) of the resulting micellar solutions was determined for two block copolymers, PS(6)-b-PANa(180) and PS(23)-b-PANa(300). It was found that Nagg increased as a function of salt concentration at low salt contents, but the values remained constant above ca. 0.10 M NaCl. A range of samples with PS block lengths ranging from 6 to 71 units and PANa block lengths ranging from 44 to 780 units was measured in 2.5 M NaCl. As expected, the length of the insoluble block had a much greater effect on the aggregation numbers than that of the soluble block. The data were examined according to the scaling

predictions of the star model and several mean-field models. Comparison with several of the models showed good agreement with experimental values of N_{agg}, calculated core radius (R_c) and R_g as a function of block lengths. The core radii values of the micelles agreed very well with those determined independently for similar samples measured in the solid state by small-angle X-ray scattering (SAXS). From this result, it was concluded that the micelles in 2.5 M NaCl exist singly, i.e., that no supermicellar aggregates are present and that the core is solvent free.

3.1. INTRODUCTION

Considerable interest has recently focused on micelles formed by block copolymers. 1-5 With the advances made in the synthesis of block copolymers by anionic polymerization, specific tailored systems can be created for use in applications such as drug delivery 6 and catalysis. 7 An understanding of the relation between the physical properties of the block copolymer micelles, such as their critical micelle concentration (cmc), size, molecular weight and behavior in different media, and their structure not only is of academic interest but also is very important for such applications.

In the two previous publications, the micellization of a block polyelectrolyte system, poly(styrene-b-sodium acrylate) (PS-b-PANa), was investigated.^{8,9} The cmc values of this system were determined from fluorescence measurements for a range of block polyelectrolyte samples. The effects of block lengths and salt content on the cmc's were investigated. These results were summarized in Chapter 2.

In a previous publication,⁸ it was shown that the intrinsic viscosity of block polyelectrolyte solutions depends strongly on the thermal history of the samples, i.e., on the time and temperature of sample storage. It was found that heating a block polyelectrolyte solution of PS(40)-b-PANa(520) at 100 °C for ca. 80 hours yielded a

solution in which the viscosity was no longer dependent on further heating. The crnc values as determined by fluorescence spectroscopy showed no difference for samples which were heated or unheated. This latter result implies that micelle-like structures are present in both the unheated and heated solutions. The decrease in viscosity was attributed to the disruption of supermolecular aggregates which exist as a result of entanglements in the polyelectrolyte chains.

There are many theories dealing with the structure of polymeric micelles.⁵ A summary of some of these theories was given in Chapter 1. Several theories have been applied to polymeric micelles, and good agreement with experiments has been observed. 10-12 In general, the models can be categorized into two groups, the mean field models 13-18 and the star models. 19,20 The first describes micelles which are composed of a large core and a relatively thin and dense corona. The micellar corona is treated as having a uniform density. In the star models, on the other hand, the corona density decreases with increasing distance from the core. The star model was first proposed by Daoud and Cotton to describe the conformation of star shaped polymers.²¹ This model was later extended by Zhulina and Birshtein where scaling relations for the micellar characteristics were determined depending on the copolymer composition.¹⁹ In this model, four regions were distinguished, depending on the relative lengths of the block forming the core (N_B) and that forming the corona (N_A). Halperin²⁰ also extended the model of star shaped polymers and, for the case when N_B < < N_A, obtained scaling relations which agreed with those of Zhulina and Birshtein. 19 From a minimization of the free energy of the system, scaling predictions for the aggregation numbers and core and micelle radii were given as a function of the block lengths in these two theories.

There are two specific theories describing the micellization of block polyelectrolytes in solution, that of Marko and Rabin²² and that of Dan and Tirrell.²³ The first theory describes micelle formation in the weak and in the strong charge limit. The theory by Dan and Tirrell investigates the aggregation properties of these micelles in

aqueous salt solutions. For moderate salt concentrations, the scaling relations accounting for the polyelectrolyte nature of the corona were found to be the same as those predicted for micelles of neutral diblocks in a highly selective nonpolar solvent.^{20,24} Therefore, the aggregation number, cmc and chemical potential of block polyelectrolyte micelles are dominated by the core block. It should be noted that there are also several theories describing the properties of polyelectrolytes attached to surfaces.^{25,26} For example, Ronis describes the conformations of the polyelectrolyte block attached to a spherical surface as a function of several parameters, such as the screening length, the curvature of the colloid core, and the number of chains emanating from the core.²⁶

The purpose of the present chapter is to characterize the block polyelectrolyte micelle system, poly(styrene-b-sodium acrylate), by SLS. First, the kinetics of disentanglement of the block copolymers in aqueous solutions will be investigated as a function of different heating periods for several samples. Second, the effect of salt concentration on the micellar characteristics will be examined. Third, the micelles formed from a wide range of samples with PS lengths ranging from 6 to 71 units and PANa lengths ranging from 44 to 780 units will be characterized in 2.5 M NaCl. Theoretical scaling models will then be applied to investigate the agreement with the results obtained for these micelles which were formed most likely under nonequilibrium conditions. In the final section, comparisons to results obtained on similar samples from the solid state as well as to literature values for poly(styrene-b-ethylene oxide) (PS-b-PEO) micelles in water will be presented.

3.2. EXPERIMENTAL SECTION

3.2.1. Materials

The poly(styrene-b-sodium acrylate) block polyelectrolytes were prepared as described in a previous publication.⁸ First, the poly(styrene-b-tert-butylacrylate) block copolymers were synthesized by anionic block copolymerization in THF at -78°C in presence of LiCl. Sec-Butyllithium was used to initiate the styrene polymerization. After the end capping of the polystyrene blocks by α-methylstyrene, a certain amount of the tert-butylacrylate monomer was added to make the first block copolymer. The reaction mixture was partially withdrawn after 5 min and more tert-butylacrylate was added. This sequence of operations was repeated successively. This procedure allows the preparation of a series of copolymers with the same polystyrene block length and varying poly(tert-butylacrylate) block lengths. The polymers were precipitated into water and dried under vacuum at 80°C. The polymers were hydrolyzed for more than 10 hours in dioxane at 100°C in the presence of 1 M HCl. The poly(styrene-b-acrylic acid) copolymers were then obtained by freeze drying the reaction solution. The poly(styrene-b-sodium acrylate) copolymers were prepared by redissolving the acid form of the copolymers in methanol and neutralizing by adding the polymer solution to 0.2 M NaOH in isopropyl alcohol.

Three to four different copolymers were easily obtained for each series, which was the usual case of the present study. When more extensive studies were needed, eight different copolymers were made for each series. In these cases, special precautions had to be taken, especially in regard to the extremely high purity of the monomers and the strict prevention of the deactivation of the living polymer chains in the reactor during the repeated additions of the monomers and the withdrawals of polymer solution.

The molecular weight, composition and polydispersity index were determined by size exclusion chromatography (SEC) on the polystyrenes and the poly(styrene-b-tert-butylacrylate) copolymers. For one series of copolymers, the compositions were also

determined by ¹H NMR; the values were in good agreement with those obtained by SEC. The complete hydrolysis and neutralization of the polymers were confirmed by solid state ¹³C NMR. The abbreviations used indicate the copolymer composition; for example, PS(23)-b-PANa(44) represents a polystyrene chain of 23 units joined to a poly(sodium acrylate) chain of 44 units.

3.2.2. Sample Preparation for Static Light Scattering (SLS)

The polymer samples for the SLS measurement were dissolved in deionized water (Millipore MILLI-Q) and heated at 100 °C for 5 days in sealed glass ampoules. The concentration of the stock solutions was ca. 1-3 mg/mL. These solutions were diluted with the appropriate amount of sodium chloride (NaCl 99.999%, Aldrich) solutions to obtain polymer solutions of the required salt concentration and stirred overnight. The aqueous salt solutions were filtered through filters of 0,22 µm pore size, and the polymer solutions were filtered through filters of either 0.45 or 0.8 µm pore size, depending on the composition of the block copolymer. In general, for the block copolymers with polystyrene lengths ranging from 6 to 40 units, the 0.45 µm filter was used when the poly(sodium acrylate) chain length was below 300 units, and the 0.80 um filter was employed in all other cases. The filters used were always rinsed first with 10 mL of solvent prior to solvent and sample filtration in order to remove any possible contaminants. A common problem with the clarification of polyelectrolytes is polymer retention on the filters. Thus, as a precaution, the filter was rinsed with 4 mL of sample solution prior to sample filtration, which would saturate any possible adsorption sites on the filter. Also, the filter membrane was composed of cellulose acetate which showed negligible polymer retention.

The kinetics of micelle disentanglement was studied by dissolving the polymers in 0.10 M NaCl solutions and stirring overnight at room temperature. The solutions were then sealed, and the scattered intensity was measured at room temperature as a function of

heating time at 100 °C. Two different procedures were used for this measurement. In the first method, different solutions of approximately the same concentration were transferred into separate ampoules which were then sealed, heated, and opened after different heating times. The solutions were then filtered into the scintillation vials for the light scattering measurement once the solutions reached room temperature. The second method involved filtering the unheated solutions into scintillation vials which were then sealed and heated. The solutions were then removed, cooled, measured, and reheated without breaking the seal.

3.2.3. SLS Measurement

Light scattering experiments were performed using a DAWN-F multiangle laser photometer (Wyatt Technology, Santa Barbara, CA) at 25 °C, which operates at 15 angles, from 26 to 137°, and is equipped with a He-Ne laser (632.8 nm). Data acquisition and analysis utilized DawnF and SkorF software, respectively. The polymer solutions were filtered directly into scintillation vials, which were used for the light scattering measurements. The measurement was performed by dilution of a stock solution which had an approximate concentration in the range of 1 x 10⁻³ - 2 x 10⁻⁵ g/mL, depending on molecular weight of the sample; the concentrations were always larger than the cmc values as determined previously by fluorescence measurements.⁹ A minimum of four concentrations was used to determine the weight-average molecular weight, radius of gyration, and second virial coefficient with the aid of either a Zimm or a Debye plot, processed with the Aurora software.

3.2.4. Specific Refractive Index Increment Measurement (dn/dc)

The specific refractive index increment (dn/dc) was determined using the Wyatt/Optilab 903 interferometric refractometer and accompanying software (Dndc 2.01) at a wavelength of 630 nm. The cell constant was determined by calibration with different

concentrations of sodium chloride (99.999%, Aldrich) solutions. Eight to ten concentrations were measured for each dn/dc determination. For the polymers measured in salt solutions, the sample solutions were dialyzed exhaustively for one week in dialysis membranes with a molecular weight cutoff of either 8000 or 15 000 against the appropriate salt concentration. Prior to measurement, the dialysate was filtered and used in the reference cell. The dn/dc values were determined from the slope of a plot of refractive index versus polymer concentration. The polymer concentrations before and after dialysis were monitored by measuring the scattered intensity at 90°; the concentrations were found to deviate by as much as 10% for some samples.

3.3. RESULTS AND DISCUSSION

The Results and Discussion part is divided into six sections. In the first section, SLS theory and data manipulation will be described. The second section will address the kinetics of disentanglement of the micelles in solution for different heating times. The third and fourth sections will address the SLS results of the block polyelectrolyte micelles as a function of salt concentrations and, in more detail, at one constant salt concentration, i.e., 2.5 M NaCl, respectively. Applications of scaling theories will be given in section 5. In the final section, comparisons will be made with solid state results of the same system and with the aqueous nonionic micelle system PS-b-PEO.

3.3.1. Theory

Static light scattering is a convenient method of characterizing polymer solutions which gives the weight-average molecular weight, radius of gyration, and virial

coefficients. When the particle size is greater than approximately $\lambda/20$, it has been shown that 27

$$Kc/R(\theta) = \frac{1}{P(\theta)M_{W}} + 2A_{2}c + \dots$$
 (1)

where K is the optical constant $(2\pi^2(n_0 dn/dc)^2/\lambda_0^4N_{av})$, n_0 is the refractive index of the solvent, dn/dc is the specific refractive index increment, λ_0 is the wavelength in vacuum, N_{av} is Avogadro's number, c is the concentration, $R(\theta)$ is the Rayleigh ratio at the angle of measurement, $P(\theta)$ is the particle scattering function, M_w is the weight-average molecular weight, and A_2 is the second virial coefficient; since the solutions are dilute, the higher order virial coefficients have been neglected.

The particle scattering function describes the angular variation of the scattered intensity and accounts for the intraparticle interference. It can be expressed in the form of a power series in $\sin(\theta/2)$,

$$P(\theta) = 1 - \alpha_1 \sin^2(\theta/2) + \alpha_2 \sin^4(\theta/2) - \dots$$
 (2)

For small angles of observation, the reciprocal scattering function is given by

$$P(\theta)^{-1} = 1 + \frac{16\pi^2}{3\lambda^2} < R_g^2 >_z \sin^2(\theta/2),$$
 (3)

where $\langle R_g^2 \rangle_z$ is the square z-average radius of gyration. Therefore, from the initial slope of the inverse particle scattering function as a function of $\sin^2(\theta/2)$, the particle size can be evaluated independent of the particle shape.

A graphical method used to solve eq. 1, with the particle scattering function given by eq. 3, was developed by Zimm.²⁸ By plotting (Kc)/R(θ) for different angles and concentrations as a function of $\sin^2(\theta/2) + kc$, where k is a scaling factor, and extrapolating to zero concentration, information on the particle size can be obtained from the initial linear slope (eq.3). Similarly, in the limit of $\theta \to 0$, the particle scattering function is equal to unity and the slope of the line is proportional to the second virial coefficient. The intercepts from the zero concentration and zero angle lines yield the

inverse M_w . This graphical double linear extrapolation method is referred to as a Zimm plot.²⁸

For particles of very high molecular weight (e.g., > 10^6 g/mol), (Kc)/R(θ) exhibits significant curvature in the angular dependence. In these cases, special care must be taken when analyzing the data.²⁹ It should be noted that, for these high molecular weight cases, small errors in the extrapolations can result in a relatively large error when the reciprocal is computed in the Zimm plot for the evaluation of the molecular weight. Similarly, there would be a large error in the radius of gyration which depends on the M_W value. In these cases, the Debye plot, which is similar to the Zimm plot with the exception that the ordinate is plotted as $R(\theta)/(Kc)$, can be used. In the present study, both the Zimm and Debye plots were employed; their specific applications to the different block polyelectrolyte systems are discussed in section 3.3.2.

A second problem in the analysis of large particles is the evaluation of the radius of gyration from the angular dependence. The Zimm method is based on linear extrapolations of the concentrations and the angles. However, for large particles, the angular dependence is nonlinear at high angles. Thus, the data which depart significantly from linearity should be omitted in the analysis.²⁹ The advantage of the present instrument is the accessibility of a wide range of angles. Thus, it is possible to fit the angular dependence with a polynomial expansion of the particle scattering function in which the term linear in $\sin^2(\theta/2)$ would yield the radius of gyration (R_g) (eq. 2). The comparison of the R_g values determined by these two methods will be given in section 3.4.3.

The dissymmetry in the light scattered from large particles can be evaluated from the dissymmetry ratio, Z_d . This quantity is defined as the ratio of the scattered light of two angles which are symmetric about 90°. Most frequently, the angles used are 45° and 135°,

$$Z_{\rm d} = \frac{P(45)}{P(135)} = \frac{R(45)}{R(135)}$$
 (4)

This quantity is a measure of the particle size, since for large particles, the scattering at low angles will be larger due to constructive interference of the scattered light from different points in the particle. Also, the scattering at large angles will be reduced due to destructive interference of the scattered light. These dissymmetry ratios can also be correlated to various particle shapes.

Polyelectrolyte solutions with added salt are multicomponent systems consisting of polyions, co-ions, and counterions. The above theory can be used for these systems if the specific refractive index increment values are determined at constant chemical potential.³⁰ These values are determined after establishing Donnan equilibrium between the polyelectrolyte solution and the solvent by dialysis. Also, it should be noted that for block copolymers, due to the compositional heterogeneity of the systems, the M_w, R_g, and A₂ values refer to apparent values.²⁷

Micellar parameters can be calculated from the value of the apparent M_w . For instance, the aggregation numbers (N_{agg}) for block copolymer micelles are evaluated from the ratio of the apparent M_w of the micelles to that of the unassociated polymer. The core radius (R_c) can be calculated from N_{agg} using the following relation for the core volume, V_c ,

$$V_c = (4/3) \pi R_c^3 = N_{agg} N_B MW/(\rho N_{av}),$$
 (5)

where N_B, MW, and p are the number of repeat units, the repeat unit molecular weight, and the density $(1.05 \text{ g/mL})^{31}$ of the PS block, respectively. From the R_C values and N_{agg} it is possible to evaluate the surface area per chain (S/N_{agg}), given as

$$S/N_{agg} = 4 \pi R_c^2 / N_{agg}$$
 (6)

3.3.2. Time Dependence of SLS Data - Kinetics of Disentanglement

In a previous viscometric study, it was found that the PS-b-PANa samples in water form supermolecular aggregates which disaggregate upon heating.8 The present study by SLS was performed in order to supplement the previous results and to give further insight into this process. Initially, under the preparation conditions used here, the solid state morphology of PS-b-PANa samples consisted of a collapsed PS core surrounded by a matrix consisting of PANa chains. For the present block copolymer system, dissolution of the block copolymer may involve first the penetration of water into the continuous polyelectrolyte matrix, which, because of the slow dissolution of the PANa, would result in the formation of nonuniform gel-like particles. Indeed, it was observed that samples prepared at a concentration of, for example, 3 mg/mL formed initially a nonuniform gellike phase. These gel-like structures were more prevalent in block polyelectrolytes which had long PANa block lengths, e.g., 300 units. Upon heating, the interpenetrating ionic domains begin to dissociate, and the gel-like structures dissolve. It is interesting to note that the formation of a nonuniform gel phase was also apparent in poly(sodium acrylate) homopolymer prior to heating. Also, metastable structures have been found to exist in other micellar systems such as poly(styrene-b-ethylene-co-propylene) (PS-b-PEP) in decane, 32 It has been postulated that these structures arise from the solid state morphology.

In the present study of the disaggregation process, the solutions employed should be in the dilute concentration regime, whether the chains are present as single chains or as micelles. This regime has been defined^{33,34} as being below the overlap concentration, c*, where

$$c^* = M / (N_{av} R_g^3),$$
 (7)

where M is the molar mass. For example, for a typical block copolymer, PS(23)-b-PANa(300), with a number average molecular weight (M_n) of 3 x 10^4 g/mol and a radius

of gyration of ca. 30 nm, the overlap concentration is ca. 2 mg/mL. For the micelle of a molecular weight of 5 x 10⁶ g/mol and a R_g of 100 nm, the overlap concentration is ca. 8 mg/mL. These concentrations show that the SLS studies were performed in the dilute solution regime, and therefore the physical processes which occur at higher concentrations should not be operative. For instance, in the semidilute region, pseudogel domains are found: i.e., entangled polymer solutions behave as polymer networks swollen by the solvent. However, the gel-like phase, which could be present because of incomplete disentanglement of the ionic domains, as described earlier, may be present at a microscopic level in dilute solutions.

There has been some suggestion that aggregates may arise as a result of solubility problems of the block copolymer, due to the very low interaction parameter of the hydrophobic block and the aqueous solvent. Several workers have observed that block copolymers which consist of hydrophobic and hydrophilic components do not readily dissolve in water. In some cases, heating at high temperatures dissolved the polymer. S5,36 In other cases, the block copolymers were first dissolved in a small amount of a solvent which was selective for the hydrophobic block, and then diluted with water. S6-38

The nature of the block copolymer in the solid state structure can play an important role in the dissolution of the copolymer. For example, in a poly(styrene-b-4-vinylpyridinium ethyl bromide) (PS-b-P4VPEtBr) system, the P4VPEtBr blocks were found to precipitate upon quarternization of the P4VP blocks in dimethylformamide (DMF).³⁹ Thus, the morphology of these samples in the solid state consists of a continuous phase of PS and a discontinuous phase of P4VPEtBr. This morphology hinders the penetration of water into the polyelectrolyte domains since they are surrounded by a hydrophobic block. As mentioned previously, the solid state structure for the present system consists of collapsed PS blocks (discontinuous phase) surrounded by PANa blocks (continuous phase). The penetration of water into the polyelectrolyte domains is expected to be easier than into the discontinuous P4VPEtBr domains.

In order to determine meaningful aggregation numbers and micelle sizes by SLS, one should be sure that single micelles and not supermolecular aggregates are present in solution. Thus, a study of the kinetics of disentanglement was performed by SLS to supplement the previous viscosity study. SLS is a convenient method for this study, since information on the size and molecular weight of the particles in solution can be obtained from the angular dependence of the scattered light and from the magnitude of the scattered intensity, respectively.

Two methods of sample preparation for the study of disentanglement were described previously in section 3.2.2. The first method involved heating several separate solutions for different periods of time and filtering the solutions after a cooling period. The second method involved initial filtration of unheated solutions into vials, which were then sealed and subsequently used directly for the light scattering measurements. The disadvantage of the second method is that the solutions, prior to heating, were very difficult to filter; thus, it is likely that some of the supermicellar structures were removed by this process. In contrast, the solutions prepared by the first method were relatively easy to filter after a minimum amount of heating (1 hour), so it seems reasonable to expect that no significant amount of supermolecular aggregates was removed. Also, it should be noted that in both cases it was found that the scattered intensity as a function of angle was independent of the cooling times and cooling methods, i.e., gradual cooling or rapid quenching to room temperature.

Figure 3.1 shows the plots of the normalized Rayleigh ratio (R(θ)/c) as a function of angle, $\sin^2(\theta/2)$, for different heating periods at 100 °C for the PS(40)-b-PANa(520) system at a concentration of 6.8 x 10⁻⁵ g/mL. The solutions were prepared by the first method described, i.e., by heating, filtering, and measuring individual samples. It can be seen from this figure that the intensity of the scattered light at low angles decreases as a function of heating time, with the most significant changes occurring at low angles during the first 4 hours. For instance, the dissymmetry ratios as defined by eq. 4 for the unheated

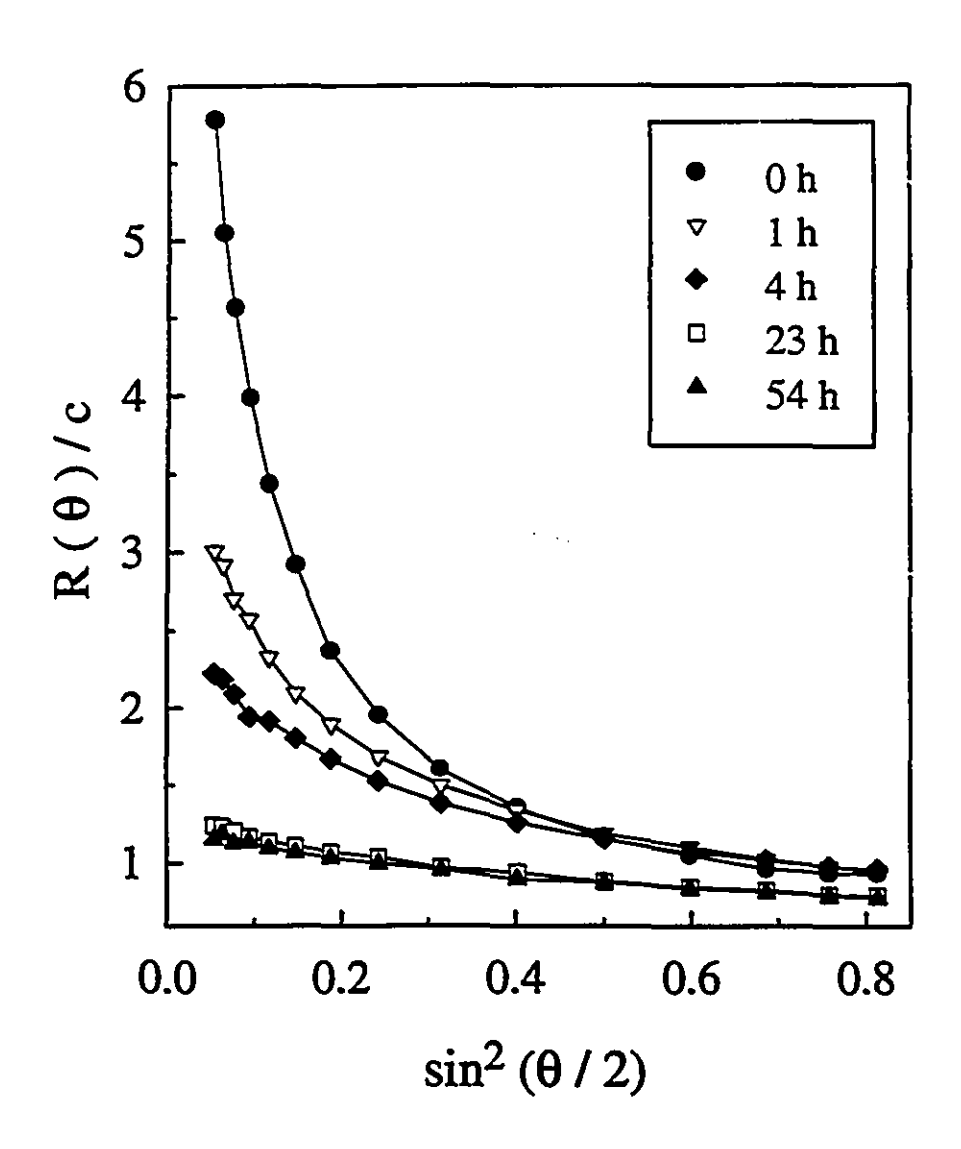


Figure 3.1. Effect of different heating times on the normalized plot of the Rayleigh ratio as a function of $\sin^2(\theta/2)$ for PS(40)-b-PANa(520).

sample and those heated for 1, 4, and 23 h. were 3.7, 2.4, 2.0, and 1.4, respectively. The decrease in the dissymmetry of scattered light with longer heating times shows the progressive disappearance of large particles which would scatter light considerably at low angles. For the longest heating period of 54 h., no significant further change in the Rayleigh ratios was observed. From this result, it can be concluded that most of the supermolecular aggregates have disentangled before ca. 50 h. of heating. The SLS results are in qualitative agreement with the viscosity results for the same polymer sample reported previously. For an incubation temperature of 100 °C, a plateau in the viscosity was attained after 80 h. of heating. Also, the viscosity of the sample was found to decrease rapidly in the first few hours of heating and to decrease more gradually with longer heating times.

In the present case, it is important to understand how the molecular parameters of block polyelectrolytes, i.e., the PS and PANa block lengths, influence the kinetics of disentanglements. These studies were performed on various block copolymers prepared by the second method, i.e., by heating and measuring the sample in one sealed ampoule. Certain trends for micelle disentanglement were observed. First, for block copolymers composed of a short PS block of 23 units and a PANa block of 81 units, the equilibrium was established after 30 minutes, as observed by no further change in the magnitude of the Rayleigh ratio at different angles. In contrast, for a sample with the same PS block length but a longer PANa block length of 330 units, equilibration took 24 hours. A similar trend was also observed for a PS block length (40 units), in that the samples with the longer PANa blocks reached equilibrium more slowly. This result is to be expected, since there would be more entanglements present with longer PANa units. The ratio of the Rayleigh ratio (90°) at t = 0 (no heating) and the Rayleigh ratio after a certain heating time, such as 20 hours, were compared. The samples, in order of increasing equilibration time, were found to be in the order of PS(23)-b-PANa(81) ~ PS(11)-b-PANa(160) < PS(40)-b-PANa(180) < PS(23)-b-PANa(330) < PS(40)-b-PANa(520). Thus, the PANa block size seems to be the determining factor in the disentanglement of the supermolecular aggregates.

In order to obtain a quantitative measure of the dissociation of supermicellar structures, aggregation numbers were evaluated for block polymers subjected to heating times of 1 and 5 days in a 0.10 M NaCl salt concentration. The aggregation numbers are given in Table 3.1 for two samples, PS(23)-b-PANa(160) and PS(86)-b-PANa(190). For instance, for PS(23)-b-PANa(160), the aggregation numbers were 530 and 140, and for PS(86)-b-PANa(190) they were 1100 and 550, for heating periods of 1 day and 5 days, respectively. Similarly, the apparent radii of gyration for the two samples decreased to ca. half their size after 5 days of heating: 93 and 45 nm for PS(23)-b-PANa(160) and 110 and 55 nm for PS(86)-b-PANa(190). Thus, all the samples in the present study were heated for 5 days prior to molecular weight determination by SLS, to ensure a high extent of disentanglement.

The question of dynamics in the cores of the present micelle system deserves some consideration. Initially, micelle formation occurred when the block copolymers were dissolved in methanol during the neutralization of the poly(acrylic acid) (PAA) blocks. Since methanol is a nonsolvent for PS, the micelle cores would be expected to be solvent-free and glassy. Thus, the exchange between single chains and micelles would be expected to be very slow. The micellar sample was then dried and dissolved in water, and the solutions were heated at 100°C. The glass transition temperatures (Tg) of the PS core for the molecular weight range investigated, i.e., between 6.2 x 10² and 9.0 x 10³ g/mol, were estimated to be below 100 °C. The PS cores at that temperature are thus not glassy, and the kinetics in the system is expected to increase, resulting in the possible exchange of single chains with micelles. Thus, in addition to dissociating the entanglements in the PANa chains, heating the solutions may also increase the mobility in the micelle system, resulting in equilibrium micelle structures. At room temperature, most of these structures would be expected to be "frozen"; this aspect will be discussed in section 3.3.3.3.

Table 3.1. Characterization of Poly(styrene-b-sodium acrylate) in 0.10 and 2.5 M NaCl by SLS for Different Heating Periods at 100°C.

PS(X)-b- PANa(Y)	C. (M)	M _w x 10 ⁻⁶	Nage	R _g (a) (nm)	R _g (b) (nm)	A ₂ x10 ⁴ (ml*mol /g ²)	R _c (nm)	S/N _{agg} (nm ² /chain)	Z,	
	1 day heating									
23- <i>b</i> -160	0.10	9.2	530	93		-0.060			1.6	
86- <i>b</i> -190	0.10	30	1100	110		-0.098			1.8	
		<u></u>		5 days	heating					
6- <i>b</i> -89	0.10	0.48	54	78	61	0.32	2.4	1.2	1.7	
l .	2.5	0.53	59	75	64	-1.2	2.4	1.2	1.7	
6- <i>b</i> -180	0.10	0.43	24	46	34	0.87	1.8	1.6	1.2	
	2.5	0.45	26	37	30	-0.20	1.8	1.6	1.2	
6- <i>b</i> -400	0.10	0.60	16	40	36	2.8	1.6	1.8	1.2	
	2.5	0.68	18	37	36	2.5	1.6	1.8	1.2	
11- <i>b</i> -69	2.5	0.49	65	91	72	-0.96	3.0	1.8	1.4	
11- <i>b</i> -160	2.5	1.0	63	64	55	0.27	3.0	1.8	1.3	
11- <i>b</i> -350	2.5	2.7	79	92	82	2.5	3.3	1.7	1.5	
23- <i>b</i> -44	2.5	0.92	140	30	30	-3.5	5.1	2.3	1.0	
23- <i>b</i> -81	2.5	1.6	160	44	40	1.4	5.2	2.2	1.1	
23- <i>b</i> -160	0.10	2.5	140	45	40	1.4	5.1	2.3	1.2	
	2.5	2.6	150	51	40	-0.034	5.4	2.1	1.2	
23- <i>b</i> -300	2.5	4.5	150	90	80	-0.36	5.1	2.2	1.7	
23- <i>b</i> -780	2.5	19	250	140	130	-0.13	6.1	1.9	6.1	
40- <i>b</i> -82	2.5	2.2	190	50	40	-0.69	6.7	3.0	1.1	
50- <i>b</i> -89	2.5	5.0	370	34	30	-1.2	9.0	2.8	1.1	
50- <i>b</i> -330	2.5	21	570	120	110	-0.46	10	2.4	3.0	
71- <i>b</i> -120	2.5	5.5	290	71	57	0.44	9.4	3.8	1.2	
86- <i>b</i> -190	0.10	18	550	55	50	-0.51	12	3.5	1.3	

The R_g values were evaluated in (a) from either a Debye or a Zimm plot and in (b) from linear extrapolations of Debye plots excluding higher angles. The calculations for N_{agg} were performed using three significant figures and subsequently rounded to two significant figures.

3.3.3. Aggregation Numbers and Micellar Sizes as a Function of Salt Concentration

3.3.3.1. Specific Refractive Index Increment

The specific refractive index increments (dn/dc) of some block polyelectrolytes were determined in water and in aqueous solutions of different NaCl concentrations. The values are given in Table 3.2. In deionized pure water, the dn/dc values were found to be independent of either the PS or the PANa block lengths for the range of block copolymers investigated, yielding the number 0.222 ± 0.003 mL/g. This value is similar to that given in the literature for poly(sodium acrylate), i.e., 0.231 mL/g, reported at a wavelength of 546 nm;⁴¹ the value for the present study is expected to be lower, in view of the wavelength of light used (630 nm).

The change in the dn/dc values with block length has been found to be negligible for block copolymers which have a small weight fraction of one of the blocks.³⁰ This situation should be valid in the present case, since the micelles consist of a highly expanded polyelectrolyte corona and a small compact core. The core is also expected to be solvent free, since the interactions between polystyrene and water are extremely unfavorable. A comparison of the R_g values with the calculated R_c values (eq. 5), shows that the core is, indeed, very small (Table 3.1). The micellar core is thus expected to be much smaller than the corona, and the dn/dc should not be affected by the composition of the micelles.

Because the dn/dc values were found to be independent of the polymer composition, the apparent molecular weight can be assumed to be close to the true molecular weight. This fact has been observed for several micellar systems, either because of the similarity in the refractive indices of the two blocks⁴² or because of the fact that the insoluble block consists of only a small fraction of the polymer and thus does not have a

Table 3.2. Specific Refractive Index of Poly(styrene-b-sodium acrylate) in Water and in NaCl Solutions at 25°C.

PS(X)-b-PANa(Y)	dn/dc [mL/g]	SOLVENT	
23- <i>b</i> -44	0.227 ± 0.004	water	
23- <i>b</i> -81	0.221 ± 0.002	water	
50- <i>b</i> -300	0.220 ± 0.007	water	
71- <i>b</i> -500	0.220 ± 0.004	water	
average	0.222 ± 0.003	water	
23- <i>b</i> -300	0.201 ± 0.004	0.025 M	
23- <i>b</i> -300	0.201 ± 0.003	0.050 M	
23- <i>b</i> -300	0.170 ± 0.002	0.10 M	
23- <i>b</i> -160			
	0.174 ± 0.004	0.10 M	
average	0.172 ± 0.002	0.10 M	
23- <i>b</i> -300	0.173 ± 0.007	1.0 M	
23- <i>b</i> -300	0.163 ± 0.005	2.5 M	

great effect on the dn/dc values.43

Since the change in the dn/dc values for different block lengths has been found to be negligible, the dn/dc values in different salt solutions were determined for only two block polyelectrolytes, PS(23)-b-PANa(300) and PS(23)-b-PANa(160). The dn/dc values of the dialyzed PS(23)-b-PANa(300) solutions were measured in different NaCl concentrations, ranging from 0.025 to 2.5 M. These results are also given in Table 3.2. For salt concentrations of 0.025 and 0.05 M, the dn/dc values remained constant at 0.201 mL/g. For 0.10 M, the dn/dc value was found to be 0.170 ± 0.002 mL/g. The dn/dc of PS(23)-b-PANa(160) measured in 0.10 M NaCl was 0.174 ± 0.004 mL/g, which was in agreement with the dn/dc value of PS(23)-b-PANa(300). For higher salt concentrations, i.e., 1.0 and 2.5 M, the dn/dc values were found to be 0.173 and 0.163 mL/g, respectively. A linear regression analysis was performed for the dn/dc values as a function of salt for the data at 0.10, 1.0, and 2.5 M NaCl. It was found that the intercept and slope of the line was 0.174 and -0.0040, respectively. Therefore, from the linear regression, the dn/dc values for salt concentrations ranging between 0.10 and 2.5 M, which were not directly measured, were calculated.

The dn/dc values of poly(sodium acrylate) determined at different wavelengths of measurement have been reported previously in the literature by different researchers. 41-46 They were found to depend both on the degree of neutralization and on the salt concentration. 44-46 It was found that the values were essentially constant below 0.10 M, but above 0.10 M, they decreased gradually with increasing salt content, due to the increasing refractive index of the solvent medium. 45,46 However, in the present system, a different trend of dn/dc with salt concentration was observed. For low salt concentrations (< 0.10 M), the dn/dc values decreased significantly but decreased only slightly for higher salt concentrations.

3.3.3.2. Typical Zimm Plots

Typical Zimm plots for polyelectrolyte micelles are given in Figure 3.2, plotted with a positive scaling factor. The graphs were chosen to illustrate a range of features typically found in such block copolymer micelles. The Zimm plots show the results for a constant PS block length of 23 units and different PANa block lengths of 44 (a) and 300 (b) units in 2.5 M NaCl. The effects of the PANa block length on the R_g, N_{agg}, and A₂ values as obtained for these two systems are given in Table 3.1.

First, it is interesting to compare the angular dependence of the Zimm plots for PS(23)-b-PANa(44) and PS(23)-b-PANa(300). The angular dependence of the sample with the longer PANa block (Figure 3.2b) exhibits more curvature than that with the shorter PANa block (Figure 3.2a). Consequently, the dissymmetry ratios for the PANa block lengths of 300 and 44 units were 1.7 and 1.0, respectively. The micelles formed from block copolymer containing 300 PANa units have a larger radius of gyration (90 nm) than that of the micelles with 44 PANa units (30 nm). This result is expected, since the size of the micelles is related to the dimensions of the block copolymer. The aggregation numbers of these two samples in 2.5 M salt are similar in magnitude, 140 and 150 for PS(23)-b-PANa(44) and PS(23)-b-PANa(300), respectively.

The second virial coefficient was evaluated from the concentration dependence of the light scattering data extrapolated to an angle of 0°. For the sample with the longer PANa block (300), the second virial coefficient in 2.5 M salt solution is greater than that of the sample with a shorter PANa block (44). The A₂ values for the 300 and 44 PANa unit lengths were -0.36 x 10⁻⁴ and -3.5 x 10⁻⁴ mL mol/g², respectively. These values suggest that the sample with the longer PANa chains is in a more favorable solvent than that with shorter PANa chains, perhaps because the longer PANa units solvate the micelle to a greater extent. As the soluble block length increases, it is expected that the solubility of the block copolymer will also increase. This result can be understood by considering

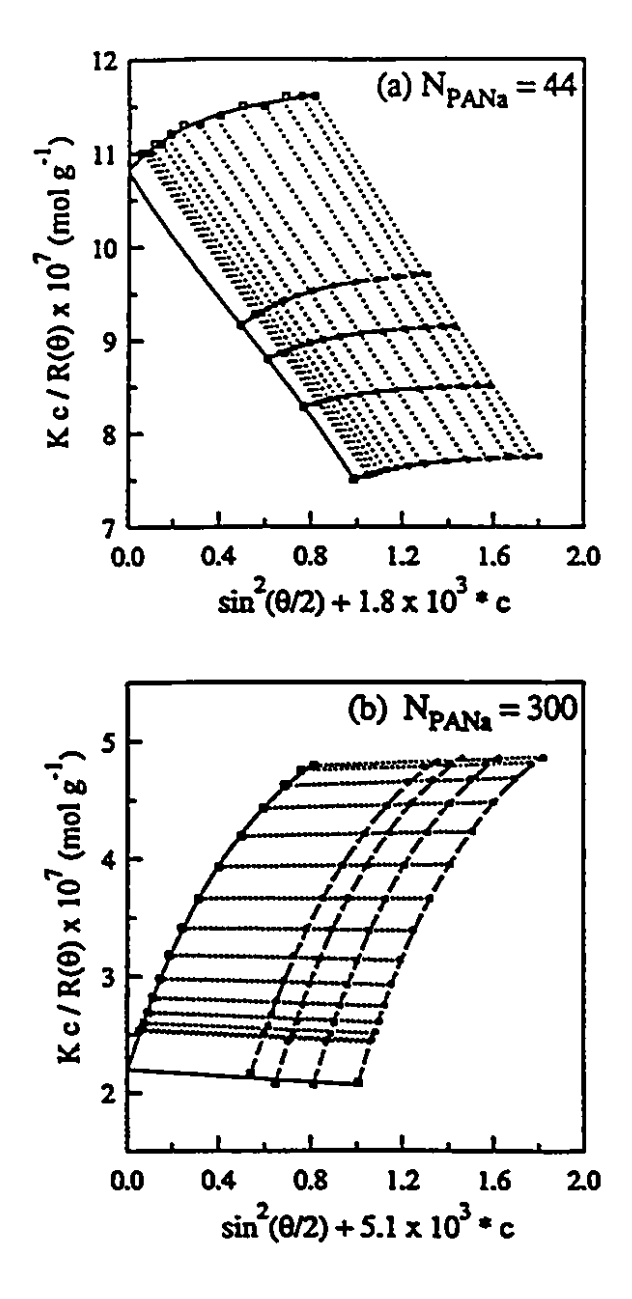


Figure 3.2. Typical Zimm plots for (a) PS(23)-b-PANa(44) and (b) PS(23)-b-PANa(300) in 2.5 M NaCl.

that an increase in the PANa length results in an increase in the corona density and hence a reduction in the unfavorable interactions between the hydrophobic core and the solvent. A similar trend in A_2 has been reported previously for PS-b-PEO in cyclopentane. ¹⁰

All the samples listed in Table 3.1 exhibited a linear dependence of $(Kc)/R(\theta)$ on the concentration. This result indicates that these micelles remain stable in the concentration range studied. Furthermore, the solutions can be seen to be in a dilute state, since the effects of the higher virial coefficients are negligible. In many block polyelectrolyte samples, the angular dependence of the $(Kc)/R(\theta)$ was nonlinear, which is expected for large particles. As mentioned previously in section 3.1, for large particles, the Debye plot gives a better estimate of M_W and R_g . In the present system, it was found that, for Z_d values below 1.7, the Debye and Zimm plots gave the same results. However, for particles which had Z_d values equal to and above 1.7, the Debye plot was used for a more accurate evaluation. In the present system, the R_g values were also determined from linear extrapolations of the $\theta=0^\circ$ line from the Debye plots, in which the values at high angles, where the points deviate significantly from linearity, were omitted. These results are summarized in Tables 3.1 and 3.3 and will be discussed in the subsequent sections.

3.3.3.3. Influence of Salt Concentration

The influence of a broad range of NaCl salt concentrations (C_S) on the micellar properties was explored for two block polyelectrolyte samples, PS(6)-b-PANa(180) and PS(23)-b-PANa(300). The results for the values of M_w, N_{agg}, R_g, A₂, and Z_d are given in Table 3.3. The aggregation numbers can be described by two regions, depending on the magnitude of C_S. For low salt concentrations, the aggregation numbers were found to increase with increasing salt concentration. For instance, the N_{agg} values for PS(6)-b-PANa(160) in 0.050 and 2.5 M NaCl increased from 11 to 26, respectively. Similarly, for PS(23)-b-PANa(300), the N_{agg} values in 0.050 and 2.5 M NaCl increased from 90 to 150,

Table 3.3. Micellar Properties of Some Poly(styrene-b-sodium acrylate) Block Polyelectrolytes Micelles in Different Salt Concentrations.

PS(X)-b- PANa(Y)	C. (M)	M _₩ × 10 ⁻⁶	Nagg	R _g ^(a) (nm)	R _g ^(a) (nm)	$A_2 \times 10^4$ (ml mol /g ²)	Z _d
		<u></u>					
6- <i>b</i> -180	0.025	0.19	12	87	7 5	3.25	2.1
	0.050	0.19	11	50	42	0.92	1.3
	0.10	0.43	24	46	34	0.87	1.2
	1.5	0.41	24	48	32	0.028	1.2
}	2.5	0.45	26	37	30	-0.20	1.2
		,	:			:	
23- <i>b</i> -300	0.050	2.7	87	90	80	2.13	1.7
	0.10	3.8	120	96	85	0.45	1.7
	0.25	4.6	150	93	82	-0.21	1.7
	0.50	4.4	150	93	82	-0.42	1.7
	1.0	4.6	150	95	85	-0.13	1.7
	1.5	4.6	150	95	85	-0.17	1.7
	2.5	4.5	150	90	80	-0.36	1.7

The R_g values were evaluated in (a) from either a Debye or a Zimm plot and in (b) from linear extrapolations of Debye plots excluding higher angles. The calculations for N_{agg} were done using three significant figures and subsequently rounded to two significant figures.

respectively. At higher salt concentrations (> ca. 0.10 M), the aggregation numbers were found to remain essentially constant. This result can also be seen in Table 3.1, which shows that the N_{agg} values for PS(6)-b-PANa(89) and PS(6)-b-PANa(400) were essentially the same in 0.10 and 2.5 M NaCl. Similar results for the dependence of N_{agg} on salt concentration have been obtained by Selb and Gallot in a mixed solvent system of water-methanol-LiBr.¹ For a typical polymer, e.g., PS(26)-b-P4VPEtBr(140), N_{agg} increased at low salt concentrations and remained essentially constant above 0.2 M LiBr. It should be noted that for a very low salt concentration (0.01 M), no micelles were seen for that sample.

It is interesting to note that micelles based on the block copolymer samples discussed above, i.e., PS(6)-b-PANa(180) and PS(23)-b-PANa(300), appear to have a structure which is not "frozen", since N_{agg} is a function of the salt concentration. In general, it has been found that if the solvent is extremely unfavorable for the block forming the core, the micelle structure can be frozen, ⁴⁷ especially if the T_g of the core is above room temperature. In the present case, the fact that N_{agg} changes with salt concentration might be due to the concentrations used in the study of these two samples, which were only ca. 2 - 6 times higher than the cmc values as determined previously. ⁹ Therefore, the system might still be in equilibrium since the concentrations are in the vicinity of the cmc. It would be expected that for longer PS block lengths, N_{agg} would be unaffected by the salt concentration since the micelles might already be frozen. It should also be borne in mind that for a PS block size of 6 units, the glass transition temperature is estimated to be ca. 260 K, ⁴⁰ i.e., below room temperature, which would contribute to the fluidity of the micelles.

The behavior of the aggregation numbers as a function of salt content can be explained by considering the behavior of block polyelectrolyte micelles in different salt concentrations. According the theory of Marko and Rabin,²² micelle formation in block polyelectrolytes is determined by a balance of the core-solvent interface energy and

Coulombic repulsions of the charged polyelectrolyte chains. In block polyelectrolyte micelles, electrostatic effects play a major role in micelle formation and predominate at low salt concentrations. According to this theory, micelle formation will not occur for highly charged diblock polyelectrolytes because of the strong electrostatic repulsive forces along the chain. At low salt concentrations, as described by Dan and Tirrell, ²³ electrostatic correlations dominate the chain conformations, and the aggregation behavior. As the salt concentration increases from very low concentrations, the electrostatic repulsions decrease and the aggregation number increases. At moderate salt concentrations, the aggregation numbers do not vary significantly with the addition of salt and the micellar properties are dominated by the core block properties. Therefore, Nagg, the cmc, and the chemical potential of the micelles are identical to those calculated for micelles of neutral diblock copolymers. However, the size of the corona is a function of the salt concentration.

Polyelectrolyte chains in water or in low salt concentrations expand due to electrostatic repulsions of the charges on the polymer backbone. This phenomenon is known as the polyelectrolyte effect. For the samples investigated, this effect was observed for only one sample, PS(6)-b-PANa(180) in 0.025 M NaCl. The Rg for this sample in 0.025 M NaCl is ca. 2 times larger than the value at higher salt concentrations. Table 3.3 shows the Rg values as a function of salt concentration; it is observed that, with that one exception, the Rg values do not vary significantly with the Cs. However, it should be noted that since SLS is more sensitive to larger particles in solution, the effects of salt on the single chains cannot be observed. It is conceivable that the dimensions of these chains are affected by the salt content to a greater extent than those of the micelles.

The dimension of the micelle with the polyelectrolyte chains in a fully extended conformation can be evaluated simply and is done here for the PS(6)-b-PANa(180) block polyelectrolyte. For instance, assuming a bond length of 0.25 nm per repeat unit and using the calculated value for the radius of the core, 2 nm (Table 3.1), the radius of the micelle

with fully extended polyelectrolyte arms is ca. 50 nm. A comparison of this value with the R_g values determined experimentally by the Debye plot using all angles in a nonlinear extrapolation ($R_g^{(a)}$) or using only the low angles in a linear extrapolation ($R_g^{(b)}$), 87 or 75 nm, respectively, suggests that the polyelectrolyte chain must be in a highly extended conformation. The experimental R_g values are larger than the calculated value. This difference is possibly due to the polydispersity of micelle sizes, 48 since the calculated value is based on a number average value, while the R_g values obtained from SLS measurements are z-average values.

The quality of the solvent for the block polyelectrolyte micelles as a function of salt concentration was evaluated from the A_2 values which are given in Table 3.3. These values were found to decrease with increasing salt concentration. This result is consistent with the trend observed for polyelectrolyte solutions.⁴⁹ The A_2 values were also found to have a linear dependence on the inverse salt concentration (C_s^{-1}). This relation is illustrated in Figure 3.3 on a semilog plot; in the inset, the C_s^{-1} axis is given as a linear scale. It should be noted that the A_2 values agree with those previously reported for poly(sodium acrylate) with molecular weights ranging from 3 x 10^4 to 6.4 x 10^5 g/mol.⁵⁰ These values are represented in Figure 3.3 as filled squares. Thus, within experimental error, the A_2 values do not differ significantly for the samples investigated in which the M_w of the PANa block ranged from 1.7 x 10^4 to 2.8 x 10^4 g/mol.

The theta point for these samples was evaluated to be at ca. 0.3 M NaCl, from Figure 3.3. It should be mentioned that, at salt concentrations above 2.5 M, the A₂ values appeared to increase, i.e., become positive. This phenomenon has been observed in other systems, such as cationic polyelectrolytes⁵¹ and polystyrene latexes stabilized by a graft copolymer of PAA.⁵² However, since the dn/dc values were not determined for salt concentrations above 2.5 M, the magnitude of A₂ values for higher salt concentrations cannot be quantified. The decrease in the solvent quality as a function of salt concentration for these block polyelectrolyte micelles will be addressed in a subsequent

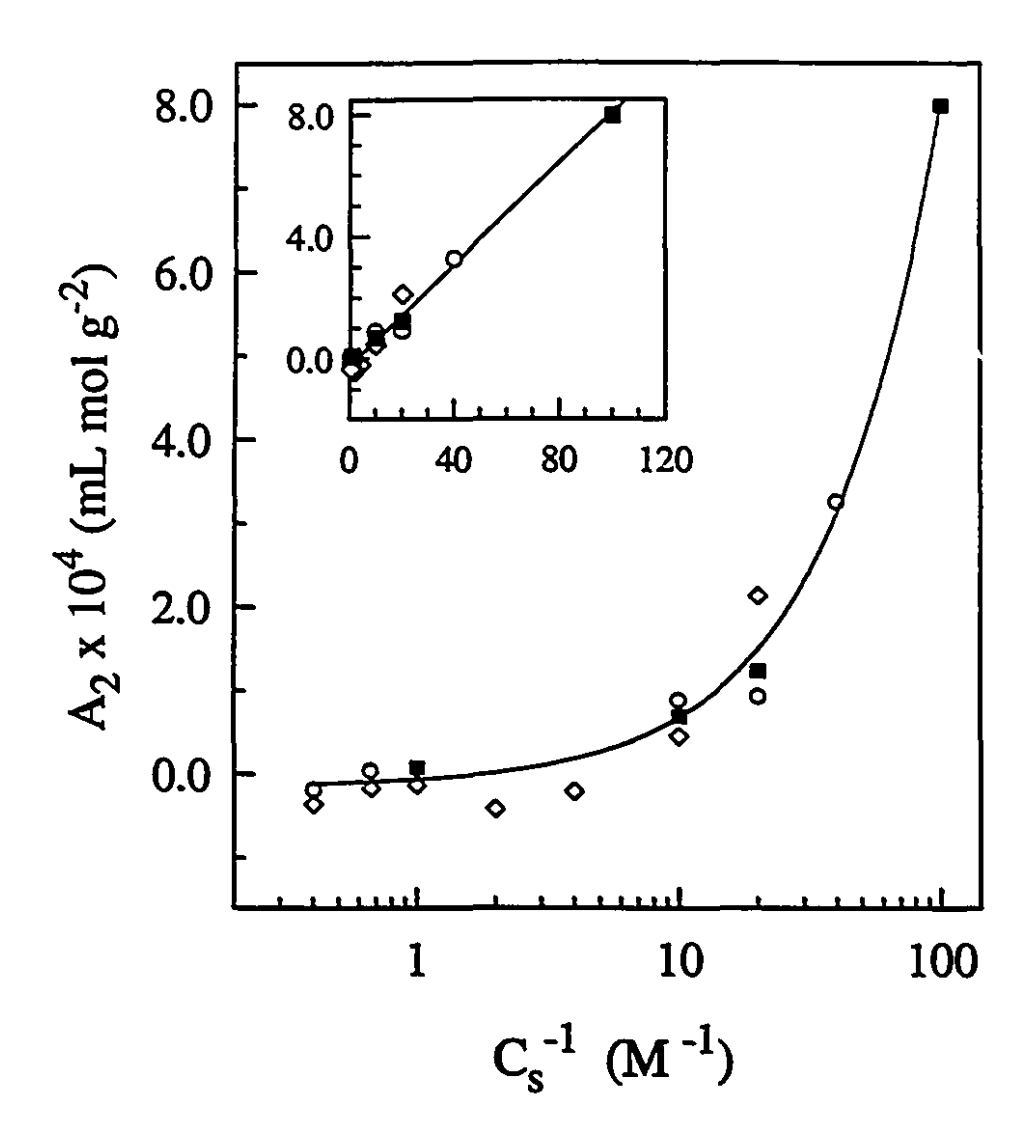


Figure 3.3. Second virial coefficient values for samples PS(6)-b-PANa(180)(\bigcirc), PS(23)-b-PANa(300) (\lozenge) and poly(sodium acrylate) (\blacksquare)⁵⁰ as a function of the inverse salt concentration on a semilog plot. The inset graph shows the relation on a linear plot.

paper dealing with the phase separation of these micelles at very low concentrations.⁵³

3.3.4. Characterization in 2.5 M NaCl

3.3.4.1. Aggregation Numbers and Calculated Core Radii

The results obtained from static light scattering for the weight-average molecular weights, aggregation numbers, and radii of gyration for the samples investigated are summarized in Table 3.1. The aggregation numbers and radii of gyration will also be discussed in some detail in the section dealing with the application of various micelle theories (section 3.3.5.). However, it is interesting at first to examine the effect of the soluble and insoluble block length on the aggregation numbers.

The inset of Figure 3.4 shows the aggregation numbers plotted as a function of the PANa block length for various PS block lengths. For the series consisting of PS block lengths of 6, 11, and 23 units, the Nagg values were found to show a slight dependence on the PANa block length. For the series consisting of a PS block length of 6 units, the aggregation numbers decreased as the soluble block length increased. For instance, as the PANa block length increased from 89 to 180 and to 400 units, the aggregation numbers decreased from 59 to 26 and to 18, respectively. This result agreed with previously reported results for different micellar systems, PS-b-P4VPEtBr¹ and PS-b-PEO,⁵⁴ for which it was observed that as the length of the soluble block increased, the aggregation number decreased.

For the PS(11) and PS(23) series, N_{agg} increased only slightly with increasing PANa block length. The mean N_{agg} values and their standard deviations for the PS(11) and PS(23) series [excluding the sample with the longest PANa block length, PS(23)-b-PANa(780)] were 69 ± 9 and 148 ± 6 , respectively. It has been previously reported by Selb and Gallot that once the block forming the micelle core exceeds a certain length,

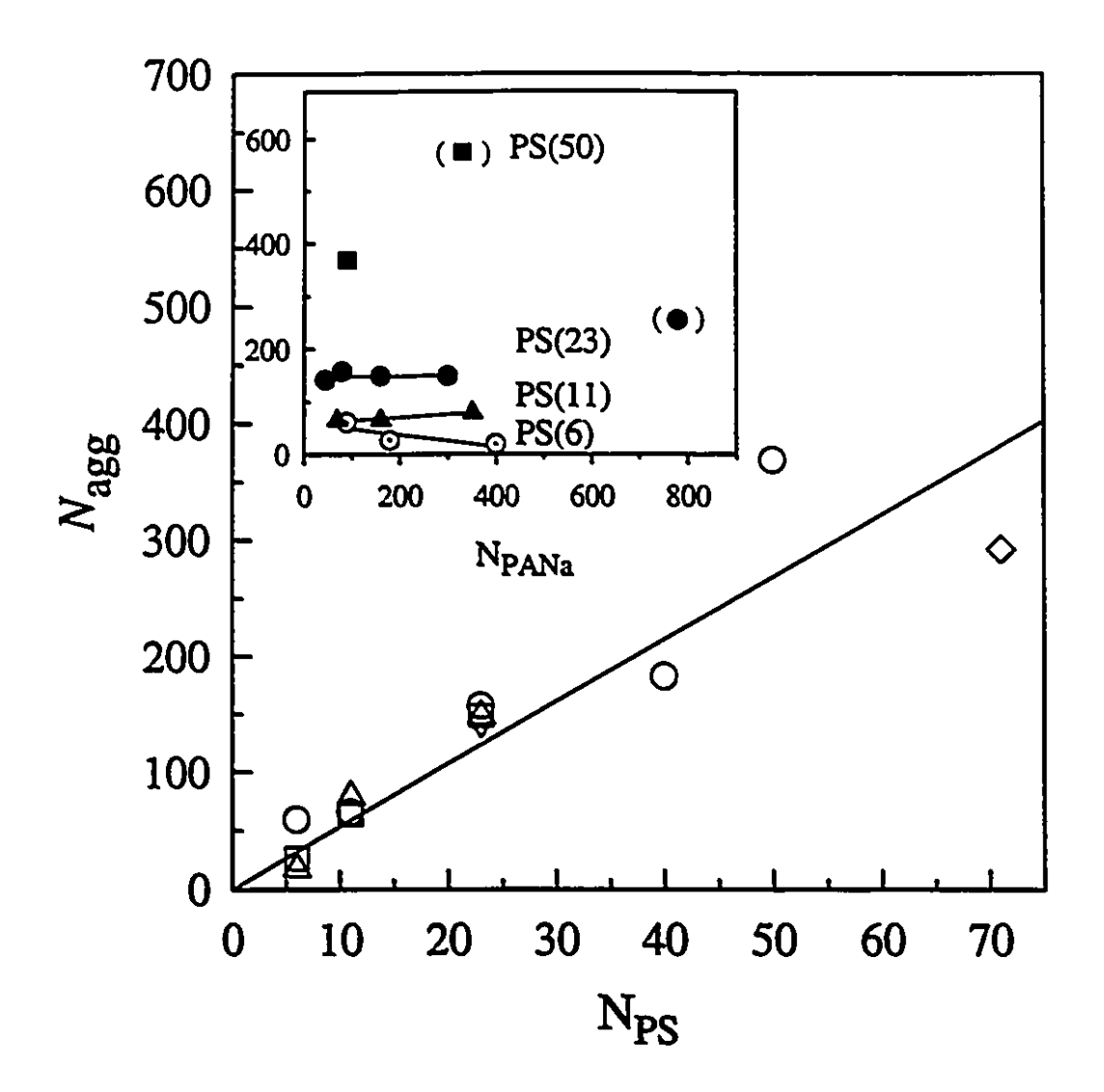


Figure 3.4. Aggregation number as a function of insoluble PS block length for almost constant PANa block lengths of 85 (\bigcirc), 170 (\square) and 350 (\triangle) units as well as the samples PS(23)-b-PANa(44) (∇) and PS(71)-b-PANa(120) (\Diamond). The inset graph shows the aggregation number as a function of PANa block length for constant PS block lengths. The points in parentheses represent the samples PS(50)-b-PANa(330) and PS(23)-b-PANa(780).

micellization is predominately determined by the core block properties and not those of the soluble block. This result was also seen in a previous publication on the PS-b-PANa block polyelectrolytes, where it was observed that the effect of the PANa block length on the cmc decreased with increasing PS block length. For the PS(50) series, it was found that N_{agg} increased considerably with increasing PANa block length. However, it should be noted that the PS(23)-b-PANa(780) and PS(50)-b-PANa(330) samples showed a much higher N_{agg} than the other samples in the series (shown in parentheses in the inset of Figure 3.4). These two samples also deviated from theoretical scaling predictions for N_{agg} and R_c, as will be seen in section 3.3.5. Therefore if the two samples [PS(23)-b-PANa(780) and PS(50)-b-PANa(330)] are omitted, there is not a significant dependence of the soluble block length on N_{agg}.

It is of interest to examine the dependence of the aggregation numbers on the insoluble block length. The plot of Nagg as a function of PS block length, for all the points given in Table 3.1, is shown in the main part of Figure 3.4. The only samples omitted were PS(23)-b-PANa(780) and PS(50)-b-PANa(330), for reasons discussed previously. For convenience, the symbols represent samples with different PS block lengths but approximately constant PANa block lengths selected from Table 3.1. The three different PANa block lengths were $85 \pm 4 \, (\bigcirc)$, $170 \pm 7 \, (\bigcirc)$, and $350 \pm 30 \, (\triangle)$ PANa units. For completeness, the results for samples PS(23)-b-PANa(44) and PS(71)-b-PANa(120), which had PANa block lengths different from those three block lengths, were also plotted. It was found that a common line could be drawn through all the points, regardless of the PANa block length. This fact confirms that there is not a significant dependence on the PANa block length on N_{agg}, as was discussed previously. From the slope of the line fitted through zero, the change in Nagg with PS block length was evaluated. For instance, when the PS block was varied from 10 and 50 units, the aggregation numbers increased from 54 to 270. Thus, it is seen again that the effect of the insoluble block length on N_{agg} is thus much greater than that of the soluble block length.

The values of the surface area per chain (S/N_{agg}), evaluated from eq. 6, are given in Table 3.1. These values were found to increase with increasing PS block length. A linear plot of the S/N_{agg} values as a function of the PS block length (graph not shown) was found to have the linear regression,

$$S/N_{agg} = 1.47 + 0.027 N_{PS},$$
 (8)

with a correlation coefficient of 0.87. It is interesting to note that the slope of this line is similar in magnitude to that obtained for micelles of PS-b-PAA in water (0.025).55 These latter samples resemble crew-cut micelles⁵⁶ since they are composed of long PS block, ca. 170 to 1400 units and relatively short PAA blocks. The S/Nagg values were also compared to those of the reverse micelle system, poly(styrene-b-cesium acrylate)12 (PS-b-PACs), poly(styrene-b-cesium methacrylate) (PS-b-PMACs), ¹² and poly(styrene-b-4vinylpyridinium methyl iodide) (PS-b-P4VPMeI)⁵⁷ in toluene. It was found that, for comparable core sizes, the dependence of S/Nagg on the insoluble block for the reverse micelle systems was larger than that found in the present system. For the samples with micelle cores composed of PACs and PMACs, the slope from a plot of S/Nagg as a function of core block length was 0.047 (nm² repeat unit)/chain, and for those composed of P4VPMeI the slope was 0.12 (nm² repeat unit)/chain. It should be mentioned that a second-order fit improved the regression coefficient for these two reverse micelle systems. Thus, the surface density of chains is larger in the present system, compared to that of the reverse micelle system. The differences in the S/N_{agg} values might be due to the preparation conditions of the micelles, i.e., whether micellization occurs under equilibrium or nonequilibrium conditions. The importance of sample preparation for reverse micelles was examined by Nguyen et al., 48 who investigated the core radii, aggregation numbers, and S/Nagg values as a function of the ionic chain polydispersity index and method of preparation.

3.3.4.2. Second Virial Coefficient Values.

The second virial coefficient for associating systems, such as block copolymers, can be quite complex to analyze. This fact is due to the dependence of A₂ on several parameters, such as the interaction of both blocks with the solvent, the molecular weight, and the configuration or size of the molecules in solution. Since the block copolymers form micellar structures, it is sometimes difficult to separate the dependence of the A₂ values on the different parameters. Some workers⁵ have found good agreement between experimental A₂ values and those calculated by using the hard sphere model.⁵⁸ However, in the present case, this model was not found to describe the system. In general, it was found that the block polyelectrolyte samples with the highest fraction of PS, such as PS(23)-b-PANa(44), had the lowest A₂ values. In general, as the fraction of PS decreased, the A₂ values increased. This result should be expected, as discussed in section 3.3.3.2., since the contribution of the unfavorable interactions between the PS core and aqueous solution would be minimized.

3.3.4.3. Radius of Gyration Values

As mentioned previously in section 3.3.3.2., for the present system the R_g values were evaluated by using all the data points either in a non linear expansion for $P(\theta)$ in a Zimm or a Debye plot $(R_g^{(a)})$ or from the slope of a linear extrapolation of a Debye plot, omitting the points at higher angles which deviate from linearity $(R_g^{(b)})$. The R_g values determined by these two methods are given in Table 3.1 for the samples in 0.1 and 2.5 M NaCl and in Table 3.3 for the samples in different NaCl concentrations. In general, the $R_g^{(b)}$ values were found to be smaller than the $R_g^{(a)}$ values. Also, it should be noted that the radii of gyration of some samples were found to be larger than the calculated radius of a micelle having a fully stretched corona block. In particular, this result was found for PS(6)-b-PANa(89), PS(11)-b-PANa(69), and for block polyelectrolyte samples which

were symmetric in the PS and PANa block lengths. This result may be due to polydispersity effects of the micelles, as discussed in section 3.3.3.3. Also, it has been found by Cogan et al.⁵⁹ that, for small symmetric copolymers of PS-b-PEO in cyclohexane with traces of water in the core, the coronal chains were found to be severely stretched as compared to asymmetric copolymers. This result is consistent with the present observations for the micelles formed from symmetric copolymers, which were found to be in a more stretched configuration relative to those formed from asymmetric copolymers.

3.3.5. Applications of Scaling Theories

Since data have been obtained for a wide range of block polyelectrolytes in aqueous solutions, it was of interest to interpret the results for the present block polyelectrolytes according to the various models which are available. In this section, scaling theories for the star model and the mean-field models will be applied to the PS-b-PANa system in 2.5 M NaCl. It should be recalled that the block copolymers may have been in a mobile state when heated at 100 °C. However, at room temperature most of these micelles, especially those with very long PS block lengths, are in a frozen state,

3.3.5.1. Star Model

One scaling model which is relevant to the present study is that of Dan and Tirrell, ²³ which suggests that, at intermediate salt concentrations, the micellar parameters scale according to Halperin's star model. ²⁰ In this section, the scaling relations of the star model for N_{agg}, calculated R_C, and R_g will be investigated for block polyelectrolyte micelles in 2.5 M NaCl according to the scaling relations of the star model.

The model predicts that the aggregation number of the micelles is proportional to $aN_{\rm B}^{4/5}$, where a is the monomer size and $N_{\rm B}$ is the number of monomeric units in the

insoluble block. This scaling relation was found to give a satisfactory description of the micelles in 2.5 M NaCl (graph not shown). The linear regression was N_{agg} = -5.9 + 12 N_B^{4/5}, with a correlation coefficient of 0.86. This result shows that the aggregation numbers of the block polyelectrolyte micelles are independent of the ionic block length within the confidence intervals of the linear regression. However, it should be recalled that some effects of the soluble block on N_{agg} or R_C were observed (Figure 3.4). The intercept of the line (-5.9) can also be taken as being essentially zero, since typical values of N_{agg} range from 20 to 400. It should be noted that the block copolymers of composition PS(50)-b-PANa(330) and PS(23)-b-PANa(780) were omitted from the analysis of the linear regression. These two block copolymers form micelles which have the highest molecular weight of all the samples investigated and do not fit the scaling relation. It might be possible that the scaling relations fail for these high aggregation numbers or that since these samples contain the longest soluble block for the two series, they might contain some supermicellar structures.

The Halperin star model also suggests that the scaling relation between the core radius and the length of the insoluble block is $R_c \propto aN_B^{3/5}$. Figure 3.5 shows the calculated core radii plotted according to the above relation for the block polyelectrolyte micelles (filled circles). The solid line represents the linear regression through the points, and the dotted line represents the 95% confidence limit intervals, excluding the two block copolymer samples PS(50)-b-PANa(330) and PS(23)-b-PANa(780) (shown in parentheses), as was previously mentioned. The slope of the line is 0.79 nm/(PS repeat unit)^{3/5}, with an intercept of essentially zero (-0.16) and a correlation coefficient of 0.98.

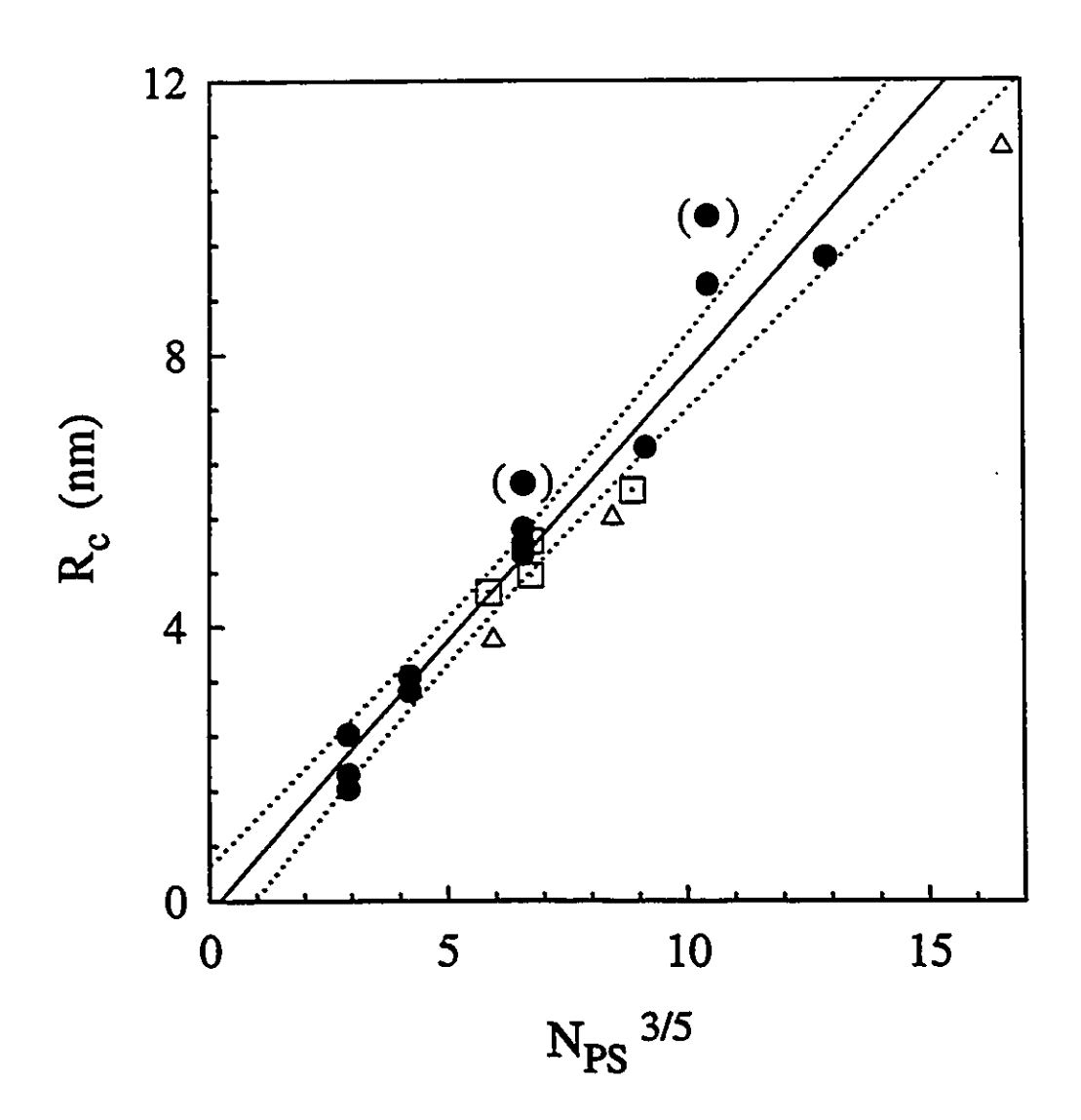


Figure 3.5. Radius of the core as a function of the PS block length to the power of 3/5, according to the star model for PS-b-PANa in 2.5 M NaCl (\bullet), PS-b-PMACs and PS-b-P4VPMeI in the solid state (\square), 60 and PS-b-PEO in water (\triangle). 54 The solid line represents the linear regression through the data, and the dashed line represents the 95% confidence limits.

This result shows that within the 95% confidence interval, R_C is independent of the ionic block length, as was also seen in the scaling behavior for aggregation numbers.

The same scaling behavior for R_C has also been found to apply to reverse micelles as investigated recently by small-angle X-ray scattering (SAXS), ^{12,57} which allows the measurement of the core radius directly. The reverse micellar systems investigated consisted of a soluble polystyrene corona attached to an insoluble ionic block composed of either PACs, ¹² PMACs, ¹² or P4VPMeI in toluene. ⁵⁷ The mirror system, forming regular micelles consisting of a PS core and a PACs corona, was also studied in the solid state by SAXS. ⁶⁰ The prefactors, which are proportional to the typical monomer size, a, for the reverse and regular micelles, were found to be 0.91 and 0.72 nm/(repeat unit) ^{3/5}, respectively, which seemed reasonable in view of the differences in the monomer volumes. ⁶⁰

According to the star model, the radius of the micelle is proportional to $N_B^{4/25}N_A^{3/5}$. This scaling relation was investigated using the two series of R_g values evaluated (Table 3.1). The linear relation for both R_g values as plotted according to the star model for the 2.5 M salt solution had a correlation coefficient of 0.69. The relation using $R_g^{(a)}$ was found to have a higher slope; however, the line was within the confidence limit intervals of that using $R_g^{(b)}$. Figure 3.6 shows the relationship of $R_g^{(b)}$ to the block lengths according to the above scaling relation; the dotted line represents the linear regression through the data, and the solid line represents a linear regression which was forced through the origin.

3.3.5.2. Mean-Field Models

In addition to the star model, there are mean-field theories which give scaling relations for several micellar parameters. In general, these theories describe micelles formed from relatively large cores and small coronas. These models therefore do not

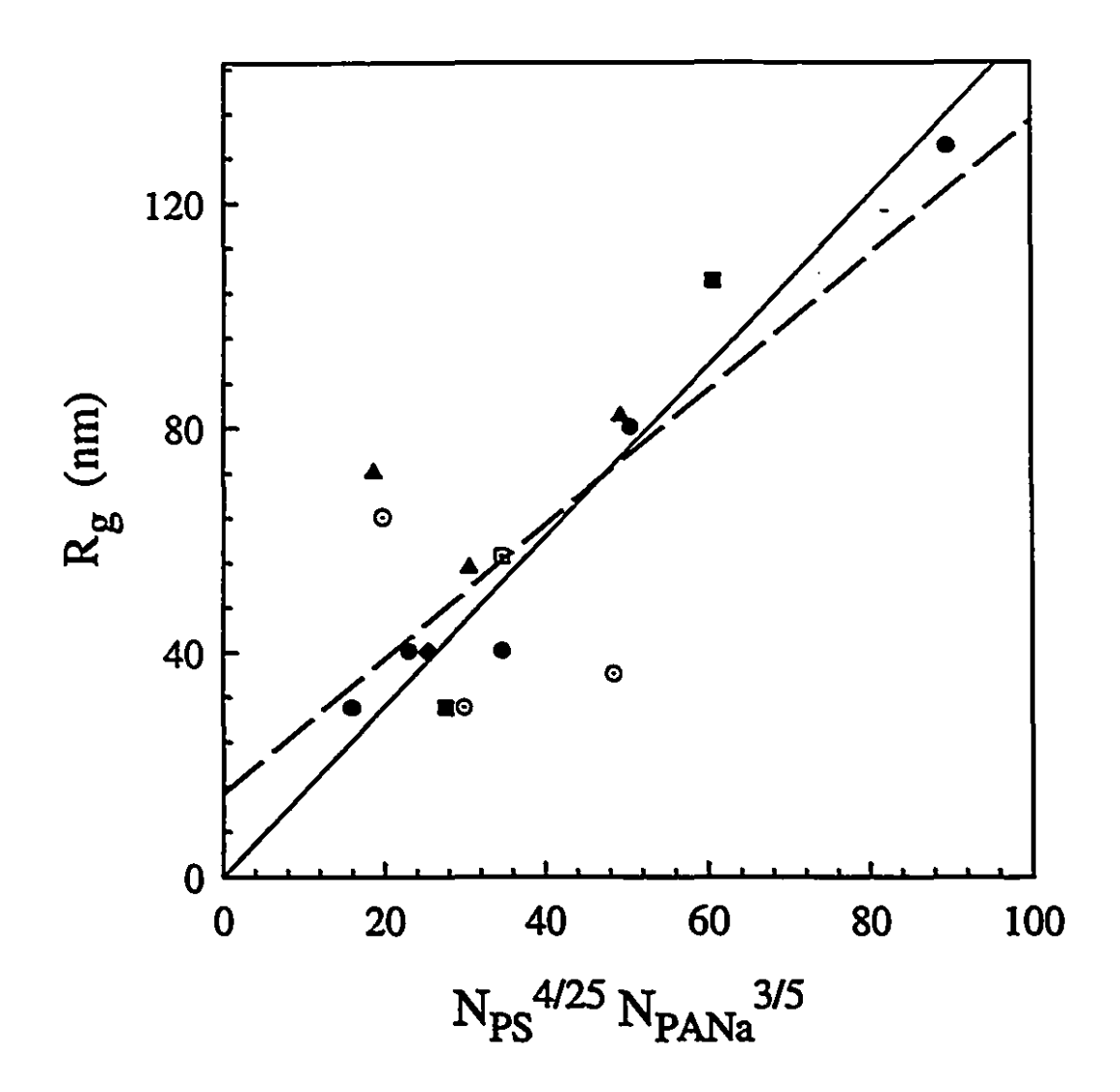


Figure 3.6. Radius of gyration ($R_g^{(b)}$) according to the scaling predictions of the star model for PS-b-PANa in 2.5 M NaCl for different PS block lengths of 6 (O), $11(\triangle)$, 23 (\bullet), 40 (\bullet), 50 (\blacksquare), and 71 (\square) units. The lines represent linear regressions through the data; the dashed line is the best fit, and the solid line is forced through the origin.

describe star type micelles; however, it was still of interest to apply these models to the present system. In this section, the results of the SLS measurements will be compared with four mean-field theories, those of de Gennes, ¹³ Leibler et al., ¹⁵ Whitmore and Noolandi, ¹⁶ and Nagarajan and Ganesh. ¹⁸

The theories by de Gennes¹³ and Leibler et al., ¹⁵ describe the micelle properties as being dominated by the insoluble block. The scaling relations given by de Gennes are $R_c \approx N_B^{2/3}$ and $N_{agg} \approx N_B$. Similarly, the scaling relations obtained by Leibler et al. were $R_c \approx N_B^{0.53}$ and $N_{agg} \approx N_B^{0.6}$. The correlation coefficients for the line using these scaling relations are given in Table 3.4. It can be seen that good agreement is obtained.

The theories by Whitmore and Noolandi 16 and by Nagarajan and Ganesh 18 suggest scaling relations for the micellar parameters which are proportional to $N_A{}^{\alpha}N_B{}^{\beta}$. In the theory by Whitmore and Noolandi, the structural parameters were determined for block copolymers in a homopolymer of $A.^{16}$. The exponents of the scaling relation for the R_c values were found to fall within a range; for example, for α the range was from -0.1 to 0 and for β it was from 0.67 to 0.76.

The α exponent for the present system was determined by plotting the log of the micellar parameter as a function of log N_A for a constant N_B . Similarly, for the evaluation of β , the log of the micellar parameters were plotted as a function of log N_B for a constant N_A . It should be mentioned that the two samples having the highest aggregation numbers are omitted for the present discussion. The values of the β exponents for R_C and N_{agg} were found to be 0.67 and 1, respectively. It is interesting to note that these exponents are the same as those proposed by de Gennes. The evaluation of the α exponent was not quite as clear, since, as shown in Figure 3.4, the dependence of N_{agg} on the soluble block length varied as a function of the PS block in some cases. The values of α for R_C and N_{agg} were found to be (-0.3, 0.05, and 0.006) and (-0.8, 0.2, and 0.01), respectively, for PS block lengths of 6, 11, and 23 units. In view of the large standard deviation for these values, the exponents were taken as being essentially zero.

Table 3.4. Summary of Results Obtained for Different Theoretical Scaling Relations.

Theory	R _c	r ^{2(a)}	Nage	r ²⁽ⁿ⁾	R _s	r²
Star Model ^{19,20}	N _B 3/5	0.98	N _B 4/5	0.86	N _A 3/5N _B 4/25	0.69
de Gennes ¹³	N _B 2/3	0.97	N _B	0.83		
Leibler ¹⁵	N _B 0.53	0.98	N _B 0.6	0.87		
Whitmore- Noolandi ¹⁶ or Nagarajan- Ganesh ¹⁸	N _B ^{0.67} N _A ⁰	0.97	N _B N _A ⁰	0.83		

⁽a) Correlation coefficient evaluated omitting samples PS(23)-b-PANa(780) and PS(50)-b-PANa(330) (see text).

The correlation coefficients for the lines $R_c \propto N_B^{0.67} N_A^{0}$ and $N_{agg} \propto N_B N_A^{0}$ were 0.97 and 0.83, respectively, and were thus found to agree with the relations of de Gennes. The scaling relations according to these two theories are summarized in Table 3.4. It was found that the mean-field theories mentioned above describe to the present system.

3.3.6. Comparison with Solid State Results and with those for PS-b-PEO in Water

In Figure 3.5, the core radii for the 2.5 M salt concentration were compared with the values obtained from the solid state, represented as dotted squares. The solid state results were determined in an independent study of block polyelectrolytes by SAXS.⁶⁰ In that study, the core radii were measured for three PS-b-PMACs and one PS-b-P4VPMeI sample which were cast from tetrahydrofuran-methanol (70:30 v/v) or DMF-water (95:5 v/v) mixtures, respectively. The solvent was evaporated slowly, and the films were subsequently dried. The resulting morphology consists of a collapsed PS block surrounded by either a soluble PMACs or P4VPMeI block. In the solid state, the styrene core is embedded in a continuum of PMACs or P4VPMeI. The agreement of the R_c values for the samples in solution and those in the solid state was within the 95% confidence limits. Agreements between solid and solution results have been observed previously, for example, in block ionomer reverse micelles.⁵⁷ Agreement would be expected, since the micelle morphology is expected to be retained during solvent evaporation, once micelle formation has occurred.⁶¹

Two conclusions can be made based on the agreement of the core radii in the 2.5 M salt solution and in the solid state. First, for the 2.5 M salt concentration, the core radii were determined from calculations based on the aggregation numbers. Therefore, it can be assumed that, in the 2.5 M salt concentration, the polyelectrolyte corona does not form supermicellar structures. Clearly, if some supermicellar structures were present in the

solution, then the calculated $R_{\rm C}$ values would be significantly larger than those obtained from the solid state. Second, the agreement also shows that the core in the 2.5 M salt concentration is solvent free, since the two values agree. This result is expected because of the extremely unfavorable interaction between PS and water.

It is also of interest to compare the results of the present system with those of a nonionic hydrophilic system, PS-b-PEO in water, 54 In that study, it was found that two populations of particles are present in solution, regular micelles and loose micellar clusters consisting of tens of micelles. The presence of clusters is not surprising since it has been observed by SLS that poly(ethylene oxide) forms intermolecular associations due to hydrophobic interactions.62 Also, a recent study investigated the formation of these PEO clusters, which co-exist with molecularly dissolved PEO, by a variety of techniques, including DLS, SLS, and size exclusion chromatography (SEC). The Rc values for the regular micelles formed from three samples, PS(108)-b-PEO(400), PS(35)-b-PEO(450), and PEO(102)-b-PS(39)-b-PEO(102), were calculated from the aggregation numbers (eq. 5).⁵⁴ These values are represented in Figure 3.5 as hollow triangles; for the triblock sample, half of the PS block length was used in the calculation for the plot. A comparison of these two systems illustrates the effect on the micellization behavior of block copolymers having an insoluble PS block attached to either an ionic (PANa) or nonionic (PEO) block. It can be seen that the values for the core radii of the PS-b-PEO in water are very similar in magnitude to those of the present block polyelectrolyte system. This result is to be expected, since the nature of the core is the dominant factor in micellization.

3.4. CONCLUSIONS

The block polyelectrolyte micellar system of poly(styrene-b-sodium acrylate) was investigated in aqueous media. First, it was found that heating the solutions for 5 days at

100 °C resulted in the dissociation of supermicellar aggregates, which are encountered upon sample dissolution. These supermicellar structures were postulated to exist as a result of the ionic interactions in the block polyelectrolytes in the phase separated solid state morphology. As was observed by studying the disentanglement process for different block polyelectrolytes, the samples which had shorter PANa lengths dissociated faster. To a first approximation, this process was found to be independent of the PS block length.

Two block polyelectrolyte samples were investigated as a function of NaCl concentration. It was found that at low salt concentrations, the aggregation numbers initially increased with increasing salt concentration, and then eventually leveled off. The R_g values were independent of C_S, except for PS(6)-b-PANa(180) in 0.025 M NaCl. The second virial coefficient values decreased linearly with the inverse salt concentration, and the values agreed with literature values for PANa.⁵⁰

For the block polyelectrolyte system in 2.5 M NaCl, good agreement was obtained between the micellar parameters and the scaling relations of the star and some mean-field models. In general, it was found that for the present system the aggregation numbers and the calculated core radii were essentially independent of the length of the soluble block within the confidence intervals of the linear regression. The calculated core radii values for samples in 2.5 M NaCl were found to be in good agreement with those determined previously in the solid state by SAXS. The R_C values were also found to be similar to those of PS-b-PEO in water.

3.5. ACKNOWLEDGMENT

We thank Dr. Xing Fu Zhong, who synthesized the block copolymers in connection with another project. We also thank Dr. Raymond J. Barlow for useful discussions and Dr. Joon S. Kim and Matthew Moffitt for helpful suggestions. This work

Chapter 3: Characterization of PS-b-PANa Block Polyelectrolyte Micelles by Static Light Scattering

was supported by the Natural Science and Engineering Research Council of Canada (NSERC). K. Khougaz also thanks FCAR (Le Fonds pour La Formation de Chercheurs et L'Aide à la Recherche) and NSERC for scholarship funding.

3.6. REFERENCES

- Selb, J.; Gallot, Y. In *Polymeric Amines and Ammonium Salts*; Goethals, E. J., Ed.; Pergamon Press: New York, 1980; pp 205-218.
- Price, C. In Development in Block Copolymers; Goodman, I., Ed.; Elsevier Applied Science: London, 1982; Vol. 1, pp 39-80.
- Riess, G.; Hurtrez, G.; Bahadur, P. Encyclopedia of Polymer Science and Engineering; Kroschwitz, J., Mark, H. F., Bikales, N. M., Overberger, C. G., Menges, G., Eds., Wiley: New York, 1985; Vol. 2, pp 324-434.
- Selb, J.; Gallot, Y. In *Development in Block Copolymers*; Goodman, I., Ed.; Elsevier Applied Science: London, 1985; Vol. 2, pp 27-96.
- Tuzar, Z.; Kratochvíl, P. In Surface and Colloid Science; Matijevic, E., Ed.; Plenum Press: New York, 1993; Vol. 1, pp 1-83.
- (a) Rolland, A.; O'Mullane, J.; Goddard, J.; Brookman, L.; Petrak, K. J. Appl. Polym. Sci. 1992, 44, 1195.
 (b) El-Nokaly, M. A., Piatt, D. M., Charpentier, B. A., Eds. Polymeric Delivery Systems: Properties and Applications; ACS Symposium Series 520; American Chemical Society: Washington, DC, 1993.
 (c) Kwon, G.; Suwa, S.; Yokoyama, M.; Okano, T.; Sakurai, Y.; Kataoka, K. J. Controlled Release 1994, 29, 17.
- (a) Fendler, J. H.; Fendler, E. J. Catalysis in Micellar and Macromolecular Systems; Academic Press: New York, 1975. (b) Kitahara, A. Adv. Colloid Interface Sci. 1980, 12, 109.
- Astafieva, L, Zhong, X. F., Eisenberg, A. Macromolecules 1993, 26, 7339.
- 9 Astafieva, I., Khougaz, K.; Eisenberg, A. Macromolecules 1995, 28, 7135.
- ¹⁰ Vagberg, L. J. M.; Cogan, K. A.; Gast, A. P. *Macromolecules* 1991, 24, 1670.

- 11 Xu, R.; Winnik, M.; Riess, G.; Chu, B.; Croucher, M. D. *Macromolecules* 1992, 25, 644.
- Nguyen, D.; Williams, C. E.; Eisenberg, A. Macromolecules 1994, 27, 5090.
- de Gennes, P.-G. Solid State Physics; Liebert, J., Ed.; Academic Press: New York, 1977; Suppl. 14, pp 1-18.
- 14 Noolandi, J.: Hong, M. H. Macromolecules 1983, 16, 1443.
- 15 Leibler, L.; Orland, H.; Wheeler, J. C. J. Chem. Phys. 1983, 79, 3550.
- Whitmore, M. D.; Noolandi, J. Macromolecules 1985, 18, 657.
- 17 Munch, M. R.; Gast, A. P. Macromolecules 1988, 21, 1360.
- 18 Nagarajan, R.; Ganesh, K. J. Chem. Phys. 1989, 90, 5843.
- ¹⁹ Zhulina, E. B.; Birshtein, T. M. Vysokomol. Soedin. 1985, 27, 511.
- 20 Halperin, A. *Macromolecules* **1987**, 20, 2943.

Macromolecules 1994, 27, 7090.

- 21 Daoud, M.; Cotton, J. P. J. Phys. 1982, 43, 531.
- 22 Marko, J. F.; Rabin, Y. Macromolecules 1992, 25, 1503.
- 23 Dan, N.; Tirrell, M. Macromolecules 1993, 26, 4310.
- ²⁴ Marques, C.; Joanny, J. F.; Leibler, L. *Macromolecules*, 1988, 21, 1051.
- (a) Miklavic, S. J.; Marcelja, S. J. Phys. Chem. 1988, 92, 6718. (b) Mirsa, S.;
 Varanasi, S.; Varanasi, P. P. Macromolecules 1989, 22, 5173. (c) Pincus, P. Macromolecules 1991, 24, 2912. (d) Ross, R. S.; Pincus, P. Macromolecules 1992, 25, 2177. (e) Wittmer, J.; Joanny, J. F. Macromolecules 1993, 26, 2691.
 (f) Zhulina, E. B. Macromolecules 1993, 26, 6273. (g) Seidel, C. Macromolecules 1994, 27, 7085. (h) Misra, S.; Mattice, W. L.; Napper, D. H.
- (a) Ronis, D. Macromolecules 1993, 26, 2016. (b) Ronis, D. Phys. Rev. E 1994,
 49, 5438.

- 27 Huglin, M. B. Ed. Light Scattering from Polymer Solutions; Academic Press: New York, 1972.
- 28 Zimm B. H., J. Chem. Phys. 1948, 16, 1099.
- ²⁹ Wyatt, P. J. Anal. Chim. Acta, 1993, 272, 1.
- Kratochvíl, P. Classical Light Scattering from Polymer Solutions; Jenkins, A. D., Ed.; Elsevier Science Publishers: New York, 1987.
- Brandup, J., Immergut, E.H., Eds. Polymer Handbook, 3rd ed.; John Wiley and Sons: New York, 1989.
- Stejskal, J.; Konák, C.; Helmstedt, M.; Kratochvíl, P. Collect, Czech. Chem. Commun. 1993, 58, 2282.
- 33 Adam, M. Macromolecules 1977, 10, 1229.
- 34 de Gennes, P.-G. Scaling Concepts in Polymer Physics; Cornell University Press: Ithaca, NY, 1979.
- ³⁵ Danicher, L.; Banderet, A. Colloid Polym. Sci. **1981**, 259, 701.
- Wilhelm, M.; Zhao, C.-L.; Wang, Y.; Xu, R.; Winnik, M.; Mura, J.-L.; Reiss, G.; Croucher, M. D. Macromolecules 1991, 24, 1033.
- Morishima, Y.; Itoh, Y.; Hashimoto, T.; Nozakura, S.-I. J. Polym. Sci., Polym. Chem. Ed. 1982, 20, 2007.
- Kiserow, D.; Prochazka, K.; Ramireddy, C.; Tuzar, Z.; Munk, P.; Webber, S. E. Macromolecules 1992, 25, 461.
- ³⁹ Selb, J.; Gallot, Y. Makromol. Chem. 1980, 181, 809.
- 40 O'Driscoll, K.; Sanayei, R. A. Macromolecules 1991, 24, 4479.
- ⁴¹ Morcellet, M.; Louceux, C. Makromol. Chem. 1978, 179, 2439.
- 42 Zhou, Z.; Chu, B. J. Colloid Interface Sci. 1988, 126, 171.
- ⁴³ Price, C.; McAdam, J. D. G.; Lally, T. P.; Woods, D. Polymer 1974, 15, 228.

- 44 Orofino, T. A.; Flory, P. J. J. Phys. Chem. 1959, 63, 283.
- Kitano, T.; Taguchi, A.; Noda, I.; Nagasawa, M. Macromolecules 1980, 13, 57.
- 46 Kato, T.; Tokuya, T.; Nozaki, T.; Takahashi, A. Polymer 1984, 25, 218.
- 47 (a) Tian, M.; Qin, A.; Ramireddy, C.; Webber S.E.; Munk, P.; Tuzar, Z.; Prochazka, K. Langmuir 1993, 9, 1741. (b) Tuzar, Z.; Kratochvil, P.; Prochazka, K.; Munk, P. Collect. Czech. Chem. Commun. 1993, 58, 2362.
- Nguyen, D.; Zhong, X.-F.; Williams, C. E.; Eisenberg, A. Macromolecules 1994, 27, 5173.
- Nagasawa, M.; Takahashi, A. In Light Scattering from Polymer Solutions; Huglin,
 M. B., Ed.; Academic Press: New York, 1972; Chapter 16.
- Takahashi, A.; Hayashi, J.; Kagawa, I. Kogyo Kagaku Zasshi, 1957, 60, 1059.
- 51 Stejskal, J.; Benes, M. J.; Kratochvíl, P.; Peska, J. J. Polym. Sci. 1973, 11, 1803.
- 52 Buscall, R. J. Chem. Soc., Faraday Trans. 1, 1981, 77, 909.
- Barlow, R. J.; Zimmerman, S.: Khougaz, K.; Eisenberg, A. Submitted for publication in J. Polym. Sci., Polym. Phys. Ed.
- Xu, R.; Winnik, M. A.; Hallett, F. R.; Riess, G.; Croucher, M. D. *Macromolecules* 1991, 24, 87.
- Zhang, L.; Barlow, R. J.; Eisenberg, A. Macromolecules in press.
- Gao, Z.; Varshney, S. K.; Wong, S.; Eisenberg, A. *Macromolecules* 1994, 26,
 7923.
- Nguyen, D.; Williams, C. E.; Eisenberg, A. Submitted for Publication in Macromolecules.
- Flory, P. J. *Principles of Polymer Chemistry*; Cornell University Press: New York, 1953; Chapter 12, p 530.
- ⁻⁵⁹ Cogan, K. A.; Gast, A. P.; Capel, M. Macromolecules 1991, 24, 6512.

- Nguyen, D.; Varshney, S. K.; Williams, C. E.; Eisenberg, A. Macromolecules 1994, 27, 5086.
- Soen, T.; Inoue, T.; Miyoshi, K.; Kawai, H. J. Polym. Sci. Polym. Phys. Ed. 1972, 10, 757.
- 62 Polik, W. F.; Burchard, W. Macromolecules 1983, 16, 978.
- Polverari, M.; van de Ven, T. G. M. To be published in J. Solution Chem.

CHAPTER 4

Determination of the Critical Micelle Concentration of Block Copolymer Micelles by Static Light Scattering

ABSTRACT

A method is proposed for the determination of the critical micelle concentration (cmc) of block copolymer micelles from static light scattering measurements, which is based on a recent model of micellization of block copolymers. The method considers the polydispersity of the block copolymers, the variation of the total single chain concentration with total concentration, and the relationship between the cmc and the length of the insoluble block. One family of block ionomers, polystyrene(660)-b-poly(sodium acrylate) with a low polydispersity index and ionic block lengths varying from 2.6 to 14 units, was investigated by light scattering near the cmc in THF. For this system, which had a relatively narrow molecular weight distribution and which showed a weak dependence of the cmc on the insoluble block length, it was found that the cmc values could be evaluated both by the present proposed extrapolation method and by the Debye equation. However, for polystyrene(470)-b-poly(4-vinylpyridine)(52) in toluene, where the dependence of the cmc on the block length is stronger, the Debye equation was not an adequate representation of the system while the proposed method was. Simulated light scattering

curves for polystyrene-b-polyisoprene in n-hexadecane were calculated for various distributions for the insoluble block length. It was found that for monodisperse samples the Debye equation gave a good fit, while for broad distributions the Debye equation did not describe the Kc/R(0) versus concentration curves and the cmc values were found to depend on the range of points used in the cmc evaluation.

4.1. INTRODUCTION

In recent years, there has been increasing interest in the formation and the properties of block copolymer micelles. 1-4 These micelles are formed when the polymer concentration exceeds the critical micelle concentration (cmc), below which only single chains are present. The evaluation of this quantity can give considerable insight into the thermodynamics of micelle formation. Extensive data have been accumulated for micelles formed from low molecular weight surfactants, 5 but data for block copolymer micelles are still limited.

In the case of block copolymers, the cmc values are frequently lower than those in surfactants; in some polymer systems it is not even possible to observe the cmc under isothermal conditions. In some of these cases, the critical micelle temperature (CMT) has been evaluated.^{3,6-10} The CMT as a function of solvent concentration in binary mixtures has also been studied.¹¹ A recent study bridges surfactants and polymers by investigating the cmc of monochelic polymers consisting of one ionic group attached to a polystyrene chain and reports the cmc under isothermal conditions.¹² The differences between the properties of monomeric and polymeric surfactants in both aqueous and nonaqueous solutions have also been studied.¹³

Micelle formation in block copolymers differs from that in surfactants because of differences in the formation process. Below the cmc, monomolecular micelles 1,14 are

postulated to exist in block copolymers, where the soluble block surrounds the insoluble block copolymer, keeping the insoluble block in solution. The insoluble block in this unfavorable solvent is in a collapsed conformation and, as the polymer concentration increases, the insoluble blocks are attracted to each other and begin to associate. During this process, the solvent is progressively driven out of the micelle core, which would explain the swelling of the micelle near the cmc that has been observed on dilution in some systems. 15-18 Also, stopped flow experiments have found that the first step for the dissociation of triblock copolymer micelles is an influx of solvent molecules into the core. 19

An important factor in the cmc properties of block copolymer micelles is the polydispersity of the polymer chains. A recent micellization model²⁰ accounts for this effect by using an extension of a mixed micelle model developed by Holland and Rubingh^{21,22} for low molecular weight surfactants. It was found that the concentration of single chains increases as a function of total polymer concentration. This effect becomes more important as the polydispersity increases. Thus, a sharp cmc cannot be observed for block copolymer micelles formed from polydisperse blocks. Therefore, techniques which monitor micelles rather than the change in single chains are preferable for the cmc determination of block copolymer micelles.²⁰ Many such techniques have been used to determine the cmc, including fluorescence,²³⁻²⁵, light scattering,^{15,26-28} osmometry,^{3,29} and viscosity.²⁹

Static light scattering (SLS) is a technique sensitive to the weight-average molecular weight (M_w) of the species in solution. As a solution composed primarily of micelles is diluted, the solution composition changes to a system which contains comparable amounts of micelles and unimers. Upon further dilution, the cmc is reached and the solution contains only unimers. This transition can be followed from the behavior of the inverse molecular weight as a function of concentration. This quantity can be monitored, for example, from the ratio of the concentration to scattered intensity, as in the

case of light scattering, or from the behavior of the reduced osmotic pressure, as in the case of osmometry. Several workers have found these trends, and the cmc was taken as the point below which the inverse molecular weight remained constant, i.e., where only unimers were present.^{3,30-32} This point is shown schematically in Figure 4.1, in a plot of the reciprocal apparent weight-average molecular weight, $(M_{w,app})^{-1}$, as a function of concentration. In this figure, $(M_{w,app})^{-1}$ is depicted as Kc/R(0) as in the case for SLS, where K is the optical constant, c is the concentration, and R(0) is the Rayleigh ratio extrapolated to zero angle. Three regions are represented in this figure: (a) unimer region, (b) coexistence of unimers and micelles and (c) predominantly micellar region. Some polymeric micelles have extremely low cmc values, and the unimer region cannot be observed by the above methods. In these cases, cmc determination is difficult, and the Debye equation³³ has been used as an approximation for the cmc evaluation.³⁴⁻³⁶ Other extrapolations of the scattered intensity from the lower micelle region to the value for the unassociated polymer have also been employed to determine the cmc.³⁷

This chapter introduces a method of evaluating the cmc for systems where only the micelle region and a part of the transition region of micelles to unimers is observed in the absence of the single chain region. A method was designed to evaluate the cmc from static light scattering measurements using a recent micellization model for block copolymers in solution which takes the polydispersity of the block copolymer into consideration.²⁰ The increase of the inverse apparent molecular weight was analyzed as a function of decreasing concentration, but the present method does not address the anomalous micellization phenomena which have been observed in some systems.^{29,38-41} The purpose of this chapter is to illustrate the cmc determination by SLS using this method for reverse micelles formed by two block copolymer systems. The first is a block ionomer, poly(styrene-b-sodium acrylate) (PS-b-PANa), having a polystyrene block of a constant length attached a sodium acrylate block of varying length; the second is a

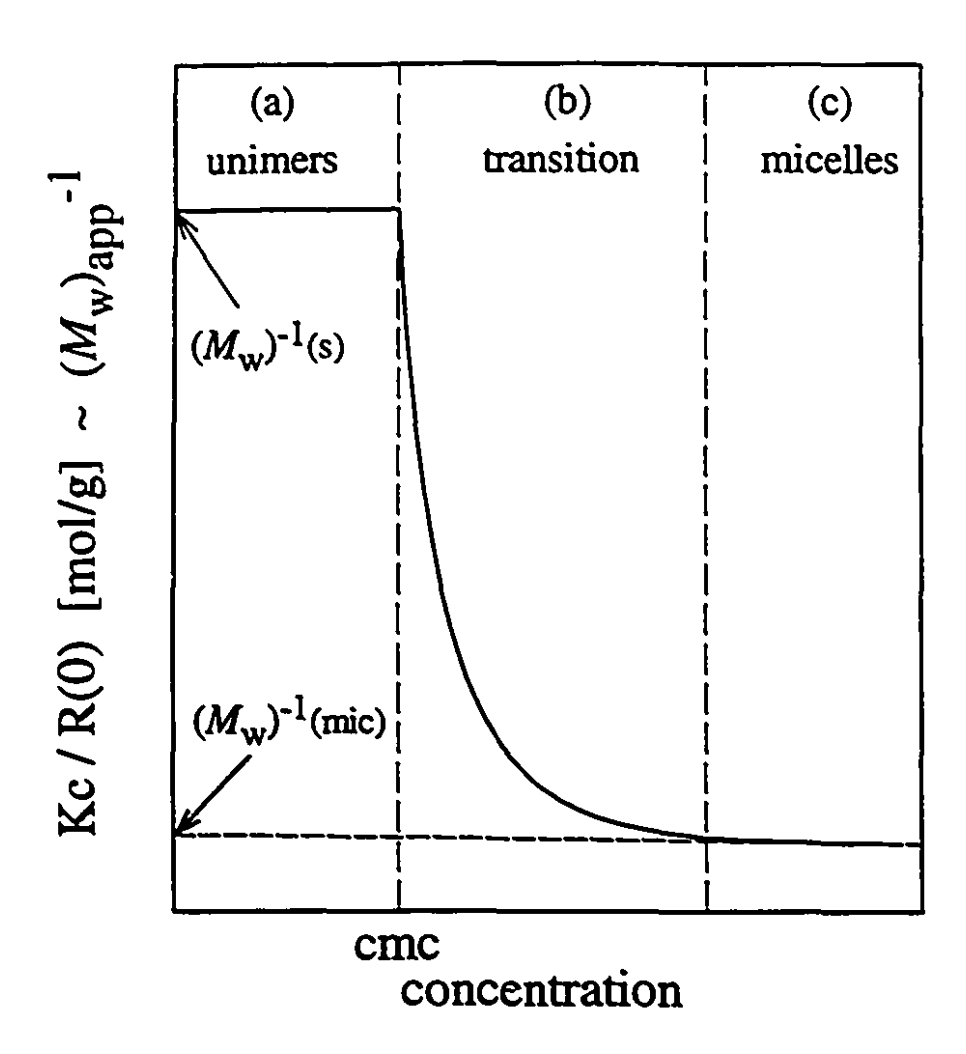


Figure 4.1. Range of existence of different species in solution as a function of concentration according to the closed association model.³³

nonionic block copolymer, poly(styrene-b-4-vinylpyridine) (PS-b-P4VP). An extensive study of the PS-b-PANa block ionomer system will be subject of the next chapter. The present chapter consists of a brief description of the theory and of the method, followed by results for the two systems. The effect of the polydispersity on the cmc is shown by generating Kc/R(0) versus concentration curves for the poly(styrene-b-isoprene) (PS-b-PI) system. The discussion addresses the results of the cmc determination as well as the effect of polydispersity.

4.2. THEORY

Static light scattering is a convenient method for the characterization of micelles. When the particle size is not small compared to the wavelength of vertically polarized light, then the following relation applies:⁴³

$$Kc/R(\theta) = \frac{1}{P(\theta)M_w} + 2A_2c+...$$
 (1)

where K is the optical constant $(2\pi^2(n \, dn/dc)^2/\lambda_0^4N_{av})$, n is the refractive index, dn/dc is the specific refractive index increment at constant chemical potential, λ_0 is the wavelength in vacuum, N_{av} is Avogadro's number, c is the concentration, $R(\theta)$ is the Rayleigh ratio at the angle of measurement, $P(\theta)$ is the particle scattering function, and A_2 is the second virial coefficient; the higher order virial coefficients have been neglected, which is valid for sufficiently dilute solutions. The particle scattering function describes the angular variation of the intensity and takes into account the intraparticle interference. When the data are extrapolated to zero degrees, this term becomes equal to one. In the case of block copolymers, the weight-average molecular weight is an apparent one due to the chemical heterogeneity of the copolymer. 44,45

The micellization model developed recently for block copolymers²⁰ addresses some of the differences between the micellization of block copolymers and of surfactants by accounting for the polydispersity of the block copolymer and the dependence of the cmc on the length of the insoluble block. In the case of low molecular weight surfactants, the static light scattering data can be evaluated in terms of the Debye equation³³

$$K(c - cmc)/(R(0) - R_{cmc}) = 1/(M_N)_w + 2A_2(c - cmc) + ...$$
 (2)

where R(0) is the Rayleigh ratio extrapolated to the zero degree angle, $R_{\rm cmc}$ is the Rayleigh ratio at the cmc, $(M_N)_w$ refers to the apparent weight-average molecular weight of the aggregate, and A_2 is the second virial coefficient; the higher order virial terms are neglected. This model can be applied only to micelles formed by monodisperse block copolymers.

For polydisperse block copolymers, the single chain concentration is not constant at different total polymer concentrations. In the case of a polydisperse system, eq. 2 is modified by replacing the cmc with the total single chain concentration (S) and the apparent weight-average molecular weight is given in terms of the sum of the weighted fraction of the apparent weight-average molecular weight of the species in solution, i.e., $M_w = (\sum c_i M_i)/c$. This yields

$$Kc/R(0) = 1/[M_w(s) \times S/c + M_w(mic) \times (1-S/c)] + 2A_2c$$
 (3)

where $M_W(s)$ and $M_W(mic)$ are the apparent weight-average molecular weights of the single chain and the micelle, respectively. Equation 3 is equivalent to equation 2 when the second virial coefficient is zero.

Theoretically the molecular weight distribution of living polymers is expected to be a Poisson distribution.⁴⁶ However, experimentally, distributions have been found to be broader, and the Gaussian distribution has been suggested as a reasonable representation of the system.⁴⁷ In this model, the polydispersity of the insoluble block, which has a

greater effect on the cmc than that of the soluble block, is described by a Gaussian distribution, and the mole fraction of the *i*th component in the mixture (α_i) is given by

$$\alpha_i = (2\pi)^{-1/2} \sigma^{(-1)} \exp[-(N_i - N)^2/2\sigma^2]$$
 (4)

where $\sigma = DP_n$ (P.I. - 1)^{1/2}, P.I. = DP_w/DP_n and $N = DP_n$. Here P.I., DP_n and DP_w refer to the polydispersity index, the number-average degree of polymerization, and the weight-average degree of polymerization, respectively.

It should be noted that for broader distributions, i.e., when the polydispersity index is high, the Gaussian distribution may no longer be applicable due to the truncation of the distribution function for chain lengths at zero. In these cases, other distribution functions such as the Schulz-Flory distribution⁴⁶ should be employed. The amount of truncation which occurs for the polydispersity indices used in the present case (1.1 and 1.2) is not significant. For example, for polydispersity indices of 1.1 and 1.2, more than 99.9 % and 98.8 % of the area under the curve, respectively, is used in the calculation for the mole fraction. The truncation would naturally be larger for higher polydispersity indices. The area which is covered in the Gaussian distribution can be evaluated for different polydispersity indices from the definition of σ , and for a range of 3σ , more than 99.7 % of the area is used.

The sum of the mole fraction of the *i*th component in the micellar phase (x_i) is given as

$$\sum_{i=1}^{n} x_{i} = \sum_{i=1}^{n} \frac{(\alpha_{i}c)}{(c + f_{i}C_{i} - S)} = 1$$
 (5)

where c is the total concentration of the mixture, f_i is the activity coefficient, which can be assumed to be unity for ideal mixing and C_i is the cmc for a monodisperse polymer. If the C_i and α_i are known, then the S can be obtained from eq. 5 as a function of the total concentration, c. Once S is known, the single chain concentration of the *i*th component (C_i^s) and its mole fraction in the micelle can be calculated using the following equations

$$C_{i}^{s} = \frac{\alpha_{i}f_{i}C_{i}c}{c + f_{i}C_{i} - S}$$
 (6)

$$x_{i} = \frac{\alpha_{i}c}{c + f_{i}C_{i} - S}$$
 (7)

This model predicts the dependence of the free energy of micellization on the length of the insoluble block for block copolymer micelles. It has been suggested that the insoluble block collapses to form a ball when the polymer is in the single chain state. The free energy of interaction for the collapsed blocks can be accounted for by the Hamaker equation, in which the free energy is proportional to the sphere radius. Since the collapsed blocks interact only with those found in their proximity, the free energy of micellization is proportional to the radius of the collapsed insoluble block. Since the volume of the micellar core is proportional to N_B, the number of repeat units in the insoluble block, the radius of the sphere is related linearly to N_B^{1/3}. Thus, the cmc for a monodisperse polymer is given by

$$\log C_i = aN_B^{1/3} + b \tag{8}$$

where a and b are constants. This equation is valid only for a collapsed block and differs from that for surfactants where the cmc is found to be proportional to the number of methylene groups.⁴⁸⁻⁵¹ The cmc for a polydisperse system, cmc(mix), is evaluated from the following

$$\operatorname{cmc}(\min) = \{\sum_{i}^{n} (\alpha_{i} / f_{i}C_{i})\}^{-1}$$
(9)

In this chapter, the theory described above is used to determine the cmc by fitting the light scattering data, Kc/R(0), as a function of concentration. The a and b constants are determined from a minimization of χ , which is defined by the following equation

$$\chi^{2} = \Sigma [(Kc/R(0))_{expt} - (Kc/R(0))_{cal}]^{2} / (Kc/R(0)_{expt})^{2}$$
(10)

Chapter 4. Determination of the cmc of Block Copolymer Micelles by Static Light Scattering

where the calculated ratio of Kc/R(0) is obtained using eq. 3.

The parameters used for the calculation are the concentration (molar), Kc/R(0) (mol/g), the number of repeat units in the insoluble block, the polydispersity of the insoluble block, which is assumed to be similar to that of the soluble block (1.10), and the apparent weight-average molecular weights of the micelles and single chains. Since the cmc value is very low, no correction is needed for the single chain content, and the micelle apparent molecular weight used is determined from a Zimm plot in the high concentration region. For the block copolymer series, the data for each copolymer mentioned above are combined for the calculations. The calculations are performed first for a constant value of b and varying a, and when the iterations are complete for the range of a values, the b value is changed and the process is repeated. A common step size used in the final determination of the a and b values is 0.01. For each point on the Gaussian distribution, C; is evaluated from eq. 8, and x; is summed (eq. 5). The total single chain concentration is varied and the process is repeated until the Σx_i is equal to unity or for a maximum of 15,000 iterations. This calculation is repeated for the required range of a and b values, and the minimum values as determined by eq. 10 are obtained. The light scattering curves of Kc/R(0) versus concentration can be generated for a given polymer once the a and b values have been determined.

4.3. EXPERIMENTAL

4.3.1. Sample Preparation.

The block copolymers, poly(styrene-b-sodium acrylate) and poly(styrene-b-4-vinylpyridine) were prepared by sequential anionic polymerization; the details are given in

Chapter 5 and 7, respectively. The polydispersity of the homopolystyrene block was determined from size exclusion chromatography (SEC) in tetrahydrofuran before the addition of the second block. For the light scattering measurements, the polymer samples were dried for 4 days at 60 °C in a vacuum oven. The PS-b-PANa and the PS-b-P4VP block copolymers were dissolved in dry tetrahydrofuran (distilled over a sodium benzophenone complex) and in dry toluene (distilled over calcium hydride), respectively. The solvent and polymer solutions were filtered through 0.2 and 0.45 µm PTFE filters, respectively, into scintillation vials which were used for the light scattering measurements. A minimum of four concentrations was used to determine the weight-average molecular weight, radius of gyration, and second virial coefficient by constructing a Zimm plot. The cmc measurement was performed by successive dilutions of the samples. The intensity values for each concentration were extrapolated to zero angle, and these values were used in the cmc determination.

4.3.2. Static Light Scattering.

Light scattering experiments were performed using a DAWN-F multiangle laser photometer (Wyatt Technology, Santa Barbara, CA) equipped with a He-Ne laser (632.8 nm). Data acquisition and analysis utilized the DawnF and SkorF software, respectively. Zimm plots were processed with Aurora software. The specific refractive index increment was determined using the Wyatt/Optilab 903 interferometric refractometer and accompanying software (Dndc 2.01) at a 630 nm wavelength. Five to eight concentrations were measured for each specific refractive index increment determination.

4.4. RESULTS AND DISCUSSION

4.4.1. PS-b-PANa System.

A typical plot of Kc/R(0) versus concentration for the fitted experimental points for one of the block ionomers, polystyrene(660)-b-poly(sodium acrylate)(8.9), is given in Figure 4.2. As previously discussed, the light scattering curve does not show the unimer region, which could not be attained by this method because the value of the scattered intensity was far too low to be determined by the light scattering measurement. The Kc/R(0) value for the unimer region was estimated from the weight-average molecular weight of the homopolystyrene with 660 units and was found to be approximately 13 x 10^{-6} mol/g, thus making the extrapolation of the present curve unfeasible. However, the micelle region and the beginning of the transition region of the micelles to the unimers was observed and used in the cmc determination by the program. The a and b values, evaluated according to the calculation program, were found to be -0.64 and -6.71, respectively. Once these constants are known, the relation between the cmc of the monodisperse block copolymer and the insoluble block length as well as the effect of polydispersity can be evaluated.

Theoretical Kc/R(0) values were generated for different cmc values to determine the sensitivity of the calculated cmc value. This was accomplished by varying either the a or the b constant determined in the fitting procedure. The percent deviation from the determined cmc value (9.2 x 10⁻⁹ M) and the corresponding cmc values were: \pm 20 % (1.1 x 10⁻⁸ and 7.4 x 10⁻⁹ M) and \pm 50 % (1.4 x 10⁻⁸ and 4.6 x 10⁻⁹ M). These curves are plotted in Figure 4.2 as a solid line for the cmc value, dashed lines for the 20 % difference, and dotted lines for the 50 % difference. The sensitivity of the cmc determination for this method falls approximately within the 20 % limit. It is also interesting to note that a 20 % and a 50 % error in the cmc value corresponds approximately to a 1 % and 5 % error in

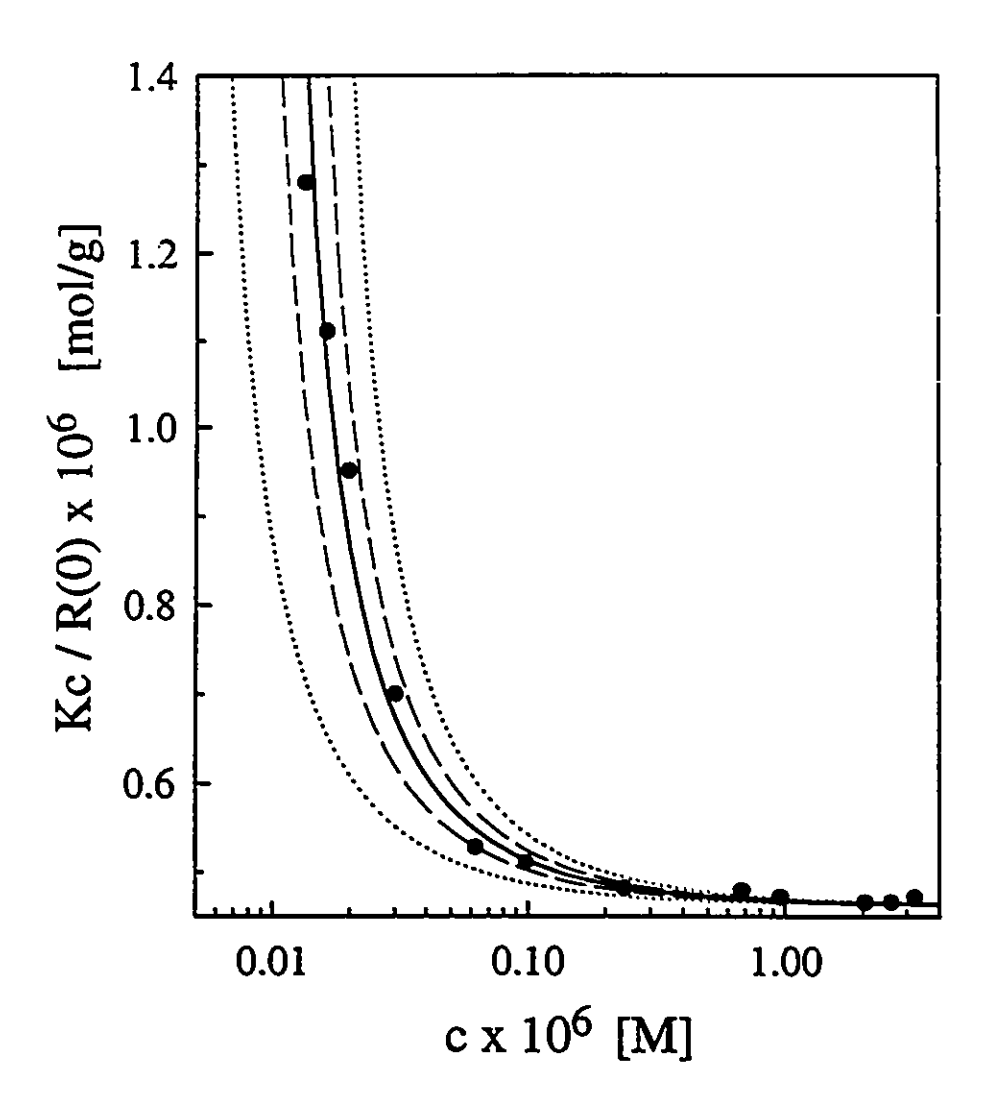


Figure 4.2. Typical cmc determination for PS(660)-b-PANa(8.9) in THF from the program calculations (—) and with intentional deviations of 20 % (-----) and 50 % (......).

Table 4.1. Critical Micelle Concentration for the Poly(styrene-b-sodium acrylate) Series in THF

PS(x)-b-PANa(y)	cm	e (M)	Percent Difference
	Polydisperse (eq. 9)	Debye Equation (eq. 2)	
660- <i>b</i> -2.6 660- <i>b</i> -4.7 660- <i>b</i> -6.4 660- <i>b</i> -8.9 660- <i>b</i> -14	2.5 x 10 ⁻⁸ 1.6 x 10 ⁻⁸ 1.2 x 10 ⁻⁸ 9.0 x 10 ⁻⁹ 5.4 x 10 ⁻⁹	2.1 x 10 ⁻⁸ 1.3 x 10 ⁻⁸ 1.5 x 10 ⁻⁸ 9.2 x 10 ⁻⁹ 5.0 x 10 ⁻⁹	16 19 25 2.2 7.4

Chapter 4. Determination of the cmc of Block Copolymer Micelles by Static Light Scattering

the b value and similarly an 8 % and 20 % error in the a value, respectively. The a and b values must therefore be evaluated precisely.

The cmc values determined by using a curve fitting program involving the Debye equation (eq. 2) for the cmc were found to be within experimental error of the values using the present program (Table 4.1). This result is not surprising since the polydispersity of the block was estimated to be less than 1.1.47 Also, the low magnitude of the a constant (-0.64) in eq. 8 shows that there is a relatively weak dependence of the cmc on the length of the insoluble block; furthermore, the insoluble block length is relatively short. The polydispersity should therefore not have a great effect on the fit of the Debye equation. To see the effect of the polydispersity, Kc/R(0) values as a function of concentration were calculated assuming different polydispersity indices. These values are represented by lines in Figure 4.3, where the symbols represent the measured data. The cmc values from the different polydispersity indices of 1.0, 1.1, and 1.2 were 9.2×10^{-9} , 9.0×10^{-9} , and 8.7×10^{-9} M, respectively. The percent deviation for the polydispersity indices of 1.1 and 1.2 from the 1.0 value were 2 % and 5 %, respectively. These values indicate that in the present system the effect of polydispersity on the cmc values is not very large as could be predicted from the small value of the a constant.

4.4.2. PS-b-P4VP System.

2504

The cmc of the second system, polystyrene(470)-b-poly(4-vinylpyridine)(52), was measured in toluene and the data are shown in Figure 4.4. The a and b constants determined using the current method were -1.66 and -0.90, respectively. The solid and dashed lines represent the fit of the experimental data obtained from the program and from the Debye equation, respectively. The current method is able to describe the points in the transition region very well in contrast to the Debye equation. The cmc values determined from these two methods differ by a factor of ca. 3; the cmc values were 3.5×10^{-8} M and

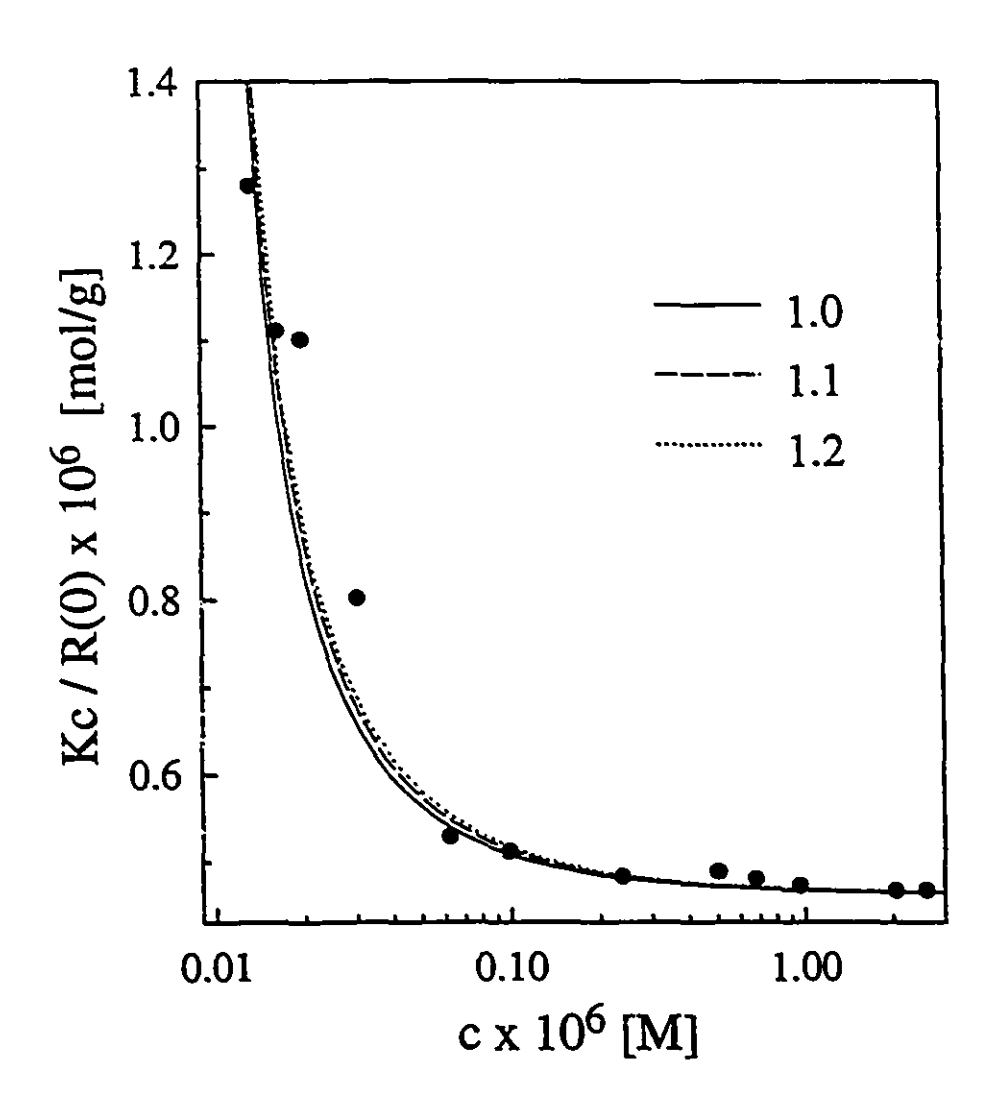


Figure 4.3. Effect of the polydispersity index on the cmc determination of PS(660)-b-PANa(8.9) in THF.

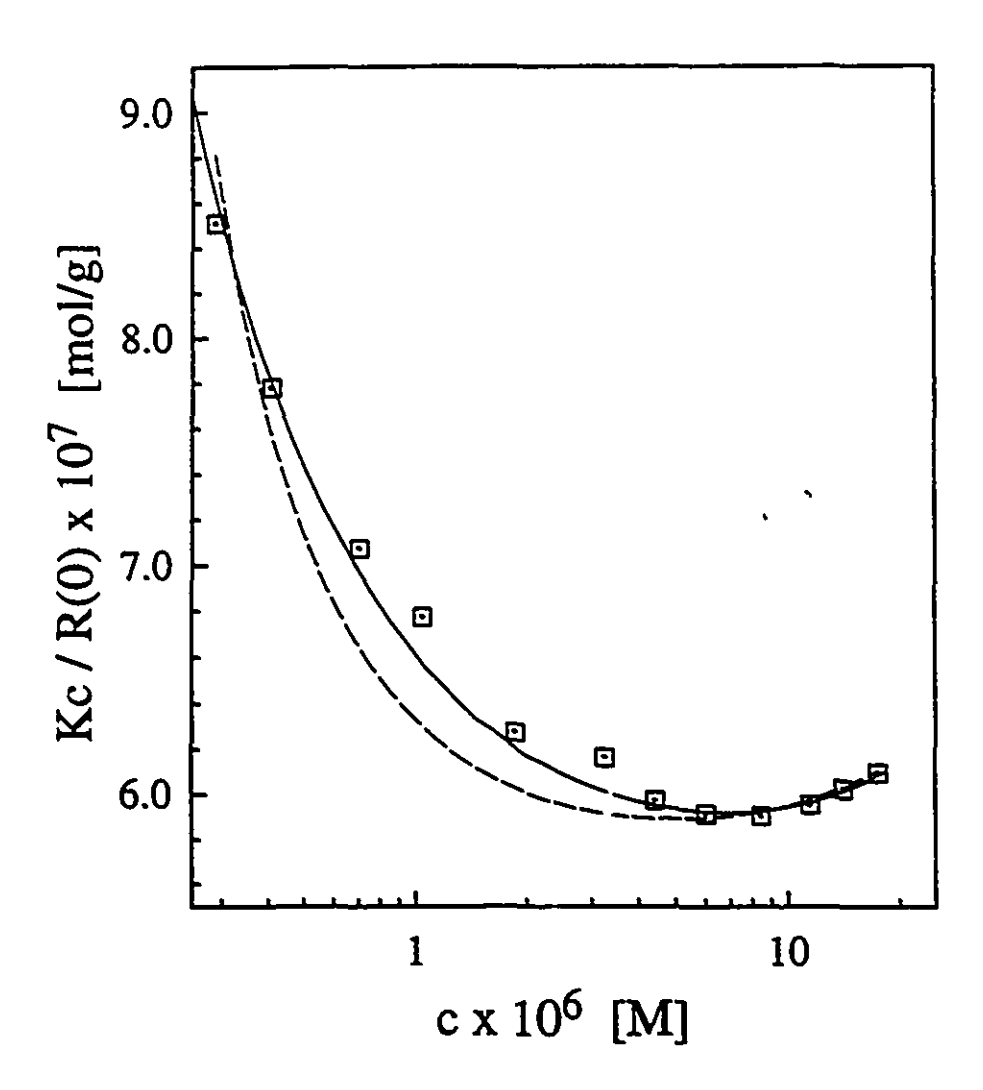


Figure 4.4. Cmc determination for PS(470)-b-P4VP(52) in toluene; the lines (—) and (— —) represent the fits obtained from the current method and the Debye equation, respectively.

 1.1×10^{-7} M, as obtained by the current method and by the Debye equation, respectively. For this system, the Debye equation does not describe the light scattering curves and the cmc value. This result is due to the greater dependence of the cmc value on the length of the insoluble block, as determined by the value of the a constant; also the length of the insoluble block was greater as compared to that of the PS-b-PANa block ionomer series.

The larger effect of the polydispersity on the cmc's for PS-b-P4VP compared to PS-b-PANa can be observed from plots of the total single chain concentration as a function of concentration. These plots are given in Figure 4.5 for different polydispersity indices. In contrast to the PS-b-PANa system, the cmc values (denoted by arrows) for PS-b-P4VP are significantly influenced by the polydispersity. It should also be noted that for the PS-b-P4VP block copolymer, discontinuity in the total single chain concentration at the cmc becomes less sharp as the polydispersity increases.

4.4.3. PS-*b*-PI System.

To illustrate the effect of polydispersity on the cmc values, the polystyrene-b-polyisoprene system was modeled by assuming different polydispersity indices for the insoluble block. The a and b constants for this system in n-hexadecane, from the results of Price et al., were previously determined to be -1.65 and 3.55, respectively. The higher magnitude of the a constant shows a stronger dependence of the cmc values on the insoluble block length as compared to the block ionomer system. The Kc/R(0) values as a function of concentration were calculated as described previously for different polydispersity indices. The parameters used for the generation of these values were the a and b constants, an insoluble block length of 67, a second virial coefficient value of zero and a single chain and micellar apparent weight-average molecular weight of 2.4 x 10^4 and 5.4×10^5 g/mol, respectively. The results are represented by symbols in Figure 4.6 for the polydispersity indices of 1.0, 1.1, and 1.2, respectively. It can be seen from these points

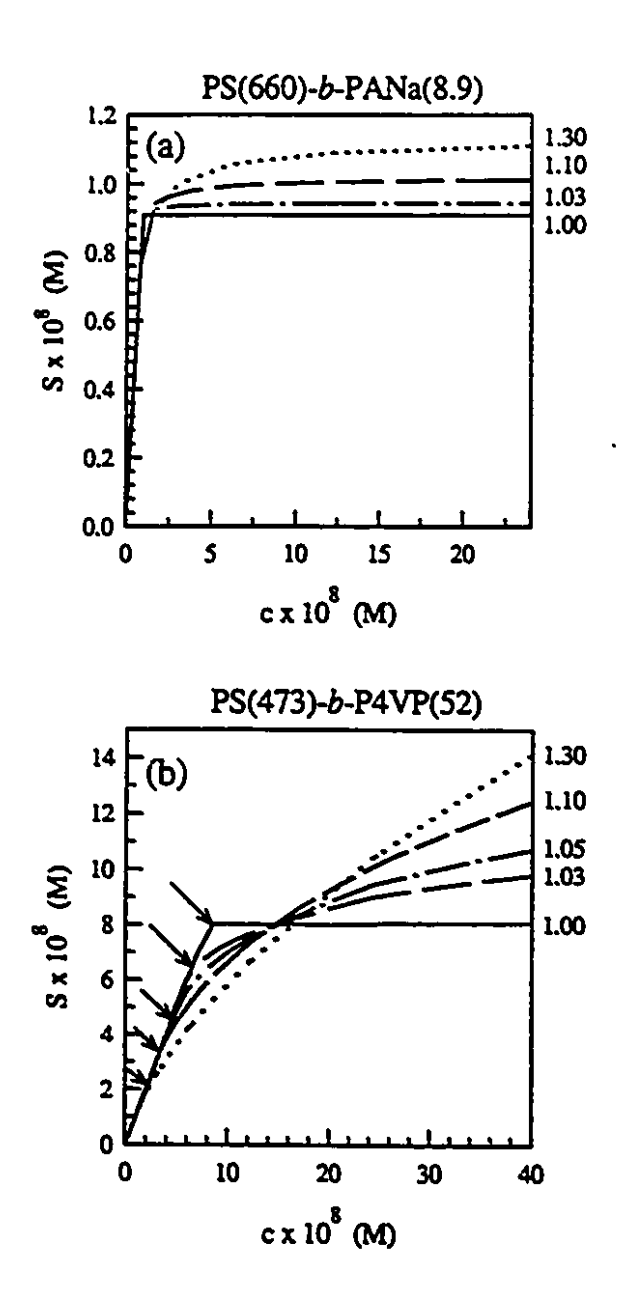


Figure 4.5. Single chain concentrations as a function of total concentration at different polydispersity indices for (a) PS-b-PANa in THF and (b) PS-b-4VP in toluene.

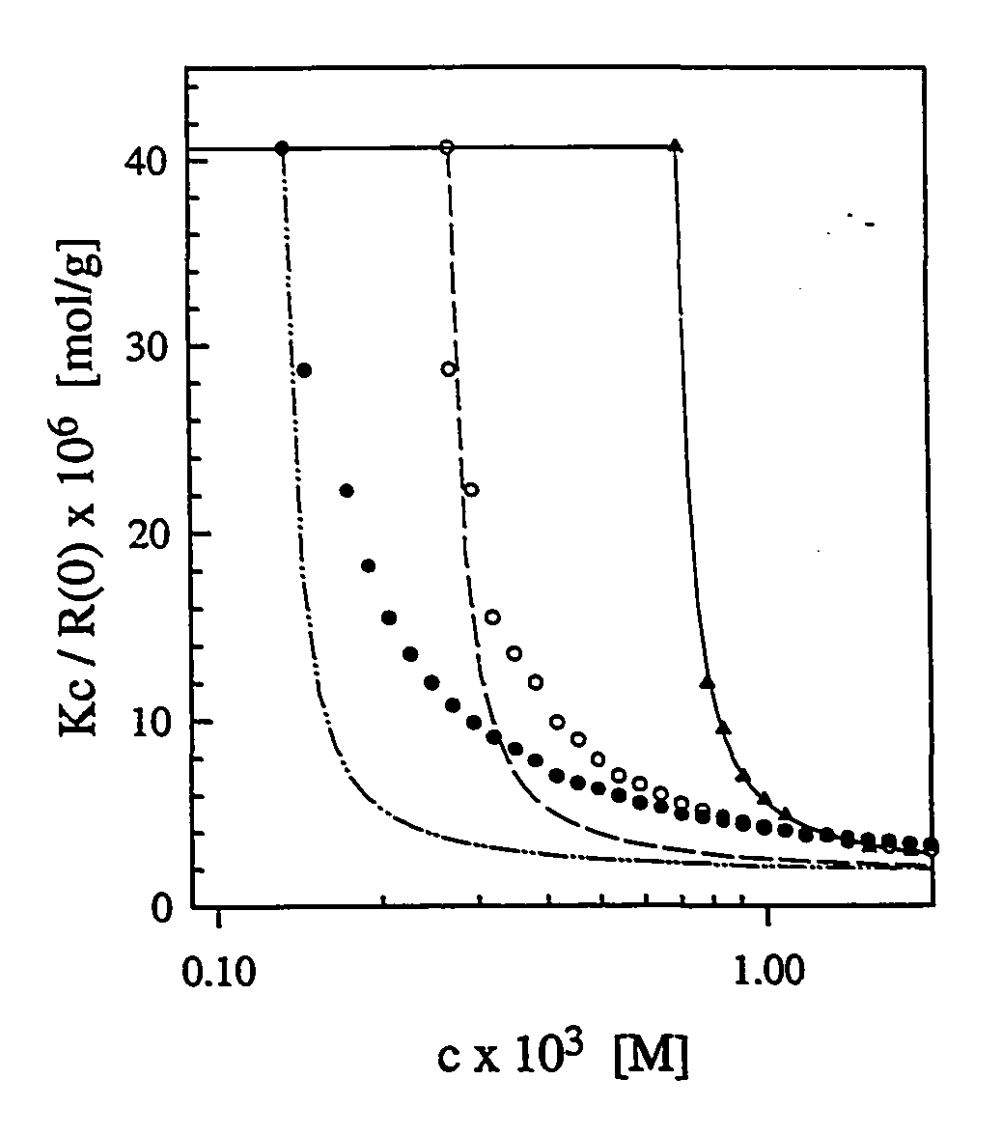


Figure 4.6. Effect of polydispersity index on the cmc values for simulated data of a PS-b-PI system. The symbols represent the data generated for different polydispersities: (A) 1.0, (O) 1.1 and (O) 1.2. The lines represent the fit from the Debye equation through the simulated data for the different polydispersity indices (——) 1.0, (——) 1.1, (———) 1.2, respectively.

that there is a large effect of the polydispersity index on the cmc values. For instance, the cmc value for a polydispersity index of 1.0 (7.0 x 10^{-4} M) decreases approximately 2.6 times and 5.4 times for a polydispersity index of 1.1 (2.7 x 10^{-4} M) and 1.2 (1.3 x 10^{-4} M), respectively.

The applicability of the Debye equation to this system at various polydispersities was investigated by fitting the generated points according to eq. 2. For the polydispersity index of 1.0, the Debye equation fits the generated points very well. However, for the higher polydispersity indices, the Debye equation clearly cannot account for the behavior of the Kc/R(0) values as a function of concentration. However, the cmc values for the higher polydispersity indices agree with the real cmc values even though the fit does not pass through all or even most of the points in the transition region. It should be noted that these cmc values were determined from the generated points, including the first point of the unimer region.

In general, for low cmc values the unimer region may not be attainable. Therefore, it is of interest to compare the results of the fit when the highest value of the inverse apparent molecular weight is less than that at the unimer line. In this case, the cmc values as obtained from eq. 2 deviate progressively from the real cmc value as the polydispersity increases. For instance, when the Kc/R(0) value or the inverse $(M_{w,app})$ is 3 times less than the inverse unimer molecular weight, the cmc values for the polydispersity indices of 1.1 and 1.2 were 3.8 x 10^{-4} M (41 %), and 2.3 x 10^{-4} M (77 %), respectively, where the number in parenthesis denotes the percent error from the generated cmc value.

The cmc values as evaluated by the Debye equation were found to depend on the range of data values used in the fit. Figure 4.7 illustrates this effect for the polydispersity index of 1.2. For example, when the inverse $(M_{w,app})$ is ca. 5, 7 times, or 10 times lower than that in the unimer region, then the corresponding cmc values as evaluated from the Debye equation were: 3.0×10^{-4} (2.3), 4.2×10^{-4} (3.2), and 6.1×10^{-4} (4.7), respectively.

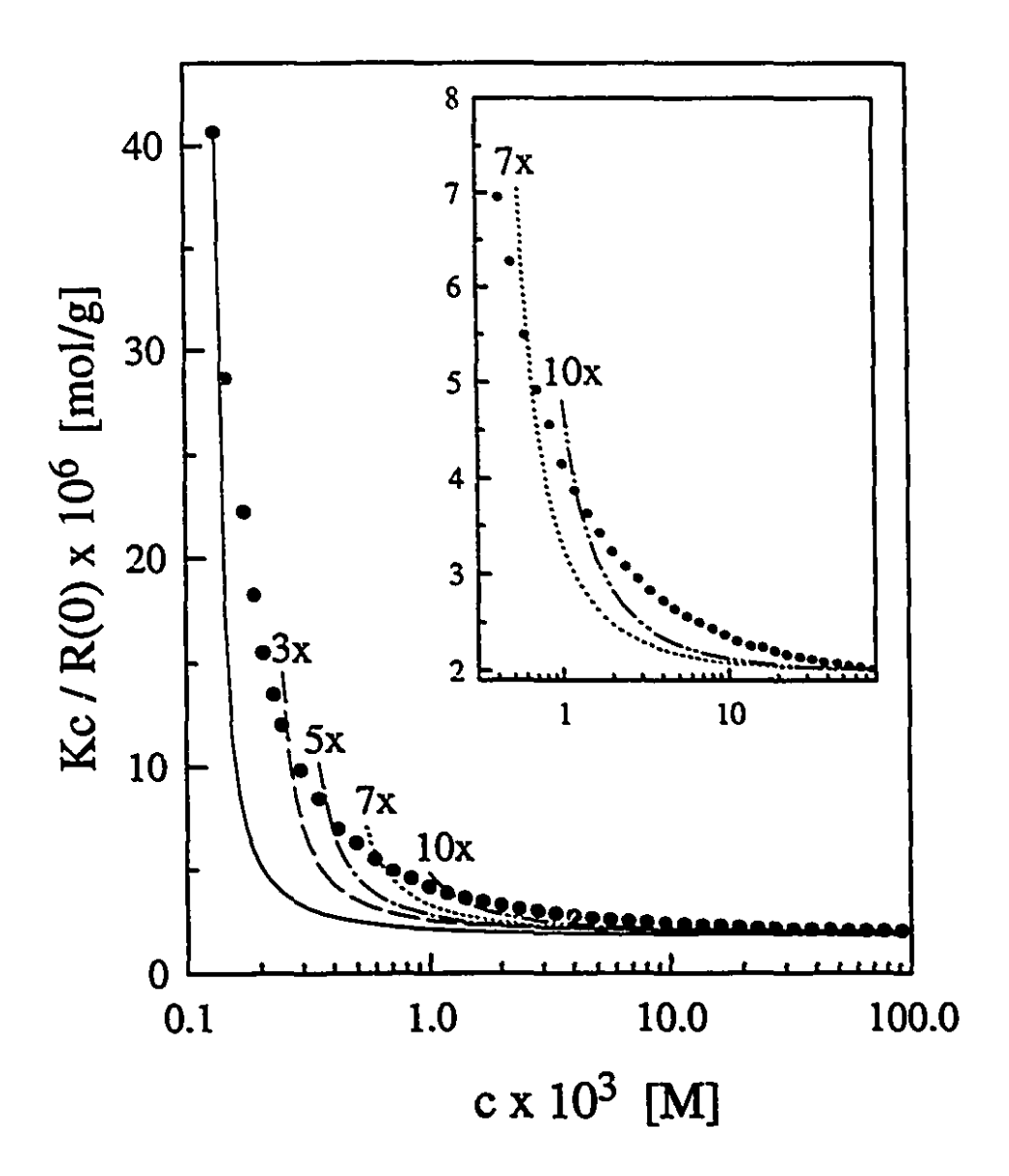


Figure 4.7. Debye equation fit for the simulated data of the PS-b-PI sytem with a polydispersity index of 1.2. The solid line indicates the fit when the first point on the unimer line is included. The other lines represent the fits for different ranges of Kc/R(0) values used. These ranges are indicated by numbers which refer to the ratio of the Kc/R(0) value for the unimer to the cutoff value. The inset graph is a magnification of the 7 and 10 times ratio, respectively.

where the numbers in parenthesis denote the ratio of the cmc value to the real cmc value. Figure 4.7 also illustrates that when the range used is 7 and 10 times lower than the unimer line, the points still show the transition region of micelles to unimers. Thus for polydisperse block copolymer systems which have significant dependence of the cmc on the insoluble block length, the Debye equation is no longer applicable and the cmc values must be accounted for by the present approach.

4.5. CONCLUSIONS

The present method, which uses a fitting procedure based on a micellization model for block copolymers in solution, was able to evaluate the cmc for block copolymer micelles from SLS data, for cases where scattering from the unimer region was not measurable. Certain characteristic features of the micellization of block copolymers, such as the change of the total single chain concentration with the total polymer concentration and the polydispersity of the insoluble chain, were accounted for by this method. The values of the a and b constants, which describe the dependence of the log(cmc) on $N_B^{1/3}$, were evaluated. These values are constant for a series of block copolymers consisting of a constant block length for the soluble block and different lengths for the insoluble block. These constants allow the prediction of the cmc values for different insoluble block lengths as well as of the effect of the polydispersity index of the insoluble block on the cmc values. It was found that the cmc values as evaluated from this program are accurate within approximately 20 %.

The effect of the polydispersity on the cmc depends on the size of the a constant, which characterizes the insoluble block length dependence. For the block ionomer series, it was found that this dependence was weak and the cmc values generated by assuming different polydispersity indices did not change significantly. In the case of the PS-b-P4VP

system, the dependence of the cmc on the insoluble block length was stronger, and the cmc could only be evaluated by the present approach. The PS-b-PI system was modeled to show the effects of the polydispersity on a system which has a significant dependence of the cmc on the insoluble block length. It was found that the Debye equation was able to evaluate the cmc values only when the first point of the unimer line was used in the determination, even though the fit did not pass through the data points in the transition region. However, the unimer region is often impossible to measure, and for these cases the Debye equation is not able to describe the cmc values. In general, for block copolymer systems which have a low value of a, as well as monodisperse block copolymers, the Debye equation and the present approach are both able to represent the cmc values. However, for systems with higher a values and larger polydispersities, only the present approach is able to evaluate the cmc values.

4.6. ACKNOWLEDGMENT.

The authors would like to thank Dr. Francis Bossé for help in composition of the program and Dr. Xing Fu Zhong, who synthesized the block copolymers in connection with another project. The authors would also like to thank one of the reviewers for valuable comments regarding molecular weight distributions of polymers. This work was supported by the Natural Sciences and Engineering Research Council of Canada (NSERC). K.K. is grateful for scholarship funding provided from NSERC and Le Fonds pour La Formation de Chercheurs et L'Aide à la Recherche (FCAR).

4.7. REFERENCES

- Selb, J.; Gallot, Y. In *Polymeric Amines and Ammonium Salts:* Goethals, E.J. Ed., Pergamon Press: New York, 1980, p.205.
- Price, C. In *Development in Block Copolymers*: Goodman, I., Ed.; Elsevier Applied Science: London, U.K., 1982; Vol. 1, p. 39
- ³ Price, C. Pure and Appl. Chem. 1983, 55, 1563.
- Riess, G.; Hurtrez, G.; Bahadur, P. Encyclopedia of Polymer Science and Engineering, 2nd ed., Wiley: New York, 1985; Vol 2, p. 324.
- Mukerjee, P.; Mysels, K. J., "Critical Micelle Concentrations of Aqueous Surfactant Systems", NSRDS-NBS 36. Government Printing Office: Washington, DC, 1971.
- 6 Price, C.; Chan, E. K. M.; Stubbersfield, R. B. Eur. Polym. J. 1987, 23, 649.
- 7 Zhou, Z.; Chu, B. J. Colloid Interface Sci. 1988,126, 171.
- Price, C.; Stubbersfield, R. B.; El-Kafrawy, S.; Kendall, K. D. Bri. Polym J. 1989, 21, 391.
- Quintana, J. R.; Villacampa, M.; Munoz, M.; Andrio, A.; Katime, I. A.
 Macromolecules, 1992, 25, 3125.
- 10 Linse, P.; Malmstem, M. Macromolecules 1992, 25, 5434.
- 11 Quintana, J. R.; Villacampa, M.; Katime, I. A. Macromolecules 1993, 26, 601.
- ¹² Zhong, X.F.; Eisenberg, A. Macromolecules 1994, 27, 1751.
- Richtering, W.; Loffler, R.; Burchard, W., Macromolecules 1992, 25, 3642.
- Sadron, C. Angew. Chem. Internat. Edn. Engl. 1963, 2, 248. (b) Sadron, C. Angew. Chem. 1963, 75, 472.
- Tuzar, Z.; Stepanek, P.; Konak, C.; Kratochvil, P. J. Colloid and Interface Sci. 1985, 105, 372.

- 16 Yeung, A. S.; Frank, C. W. Polymer 1990, 31, 2089.
- 17 Yeung, A. S.; Frank, C. W. Polymer 1990, 31, 2101.
- ¹⁸ Tuzar, Z. Macromol. Rep. 1992, A29 (Suppl. 2), 173.
- Bednar, B.; Edwards, K.; Almgren, M.; Tormod, S.: Tuzar Z. Makromol. Chem., Rapid Commun. 1988, 9, 785.
- ²⁰ Gao, Z.; Eisenberg, A. *Macromolecules* **1993**, 26,7353
- 21 Holland, P. M. and Rubingh, D. N. J. Phys. Chem. 1983, 87, 1984.
- Holland, P. M. Adv. Colloid Interface Sci. 1986, 23, 111.
- ²³ Zhao, C. L.; Winnik, M. A.; Reiss, G.; Croucher, M. D. Langmiur 1990, 6, 514.
- Wilhelm, M.; Zhao, C. L.; Wang, Y.; Xu, R.; Winnik, M. A.; Mura, J. L.; Riess,
 G.; Croucher, M. D. Macromolecules 1991, 24, 1033
- Astafieva, I.; Zhong, X. F.; Eisenberg, A. Macromolecules 1993, 26, 7339.
- ²⁶ Cogan, K. A.; Gast, A. *Macromolecules* **1990**, 23, 745.
- Tuzar, Z.; Konak, C.; Stepanek, P.; Kratochvil, P.; Prochazka, K. Polymer, 1990,31, 2118.
- Ouintana, J. R.; Villacampa, M.; Katime, I. A. Macromolecules 1993, 26, 606.
- ²⁹ Sikora, A.; Tuzar, Z. Makromol. Chem. 1983, 184, 2049.
- ³⁰ Price, C.; McAdam, J. D. G.; Lally, T. P.; Woods, D. *Polymer* **1974**, *15*, 228.
- Booth, C.; Naylor, de V.T., Price, C.; Rajab, N.S.; Stubbersfield, R.B. J. Chem. Soc. Faraday Trans. 1 1978, 74, 2352.
- ³² Prochazka, K.; Delcros, H.; Deimas, G. Can. J. Chem. 1988, 66, 915.
- Elias, H. G., in *Light Scattering from Polymer Solutions*; Huglin, M. B., Ed.; Academic Press: New York, 1972, Chapter 9.
- 34 Anacker, E.W.; Rush, R.M.; Johnson, J.S. J. Phys. Chem. 1964, 68, 81.
- ³⁵ Selb, J.; Gallot, Y. Makromol. Chem. 1981, 182, 1491.
- Hilfiker, R.; Chu, B.; Zhongde, X. J. Colloid Interface Sci. 1989, 133, 176.

- Nicholas, C. V.; Luo, Y. Z., Deng, N. J.; Atwood, D.; Collett, J. H.; Price, C.; Booth, C., *Polymer* 1993, 34, 138.
- 38 Lally, T. P.; Price, C. Polymer 1974, 15, 325.
- 39 Mandema, W.; Zeldenrust, H.; Emeis, C. A. Makromol. Chem. 1979, 180, 1521.
- 40 Canham, P. A.; Lally, T. P.; Price, C.; Stubbersfield, R. B. J. Chem. Soc. Faraday

 Trans. I 1980, 76, 1857,
- ⁴¹ Zhou, Z.; Chu, B. Macromolecules 1988, 21, 2548.
- 42 Khougaz, K.; Zhong, X. F.; Eisenberg A., in preparation.
- 43 Zimm, B.H. J. Chem. Phys., 1948, 16, 1093.
- Benoit, H.; Froelich, D. In Light Scattering from Polymer Solutions, Huglin, M.
 B., Ed.; Academic Press: New York, 1972, Chapter 11.
- Renliang, X.; Winnik, M. A.; Hallett, F.R.; Riess, G.; Croucher, M.D.

 Macromolecules 1991, 24, 87.
- Elias, H.G. *Macromolecules*. *Structure & Properties*, Plenum Press: New York, 1977; Vol 1, p. 287.
- Nguyen, D.; Zhong, X. F.; Williams, C. E.; Eisenberg, A., Submitted to Macromoiecules.
- 48 Lindman, B.; Wennerstrom, H. Top. Curr. Chem. 1980, 87, 1.
- Tanford, C. The Hydrophobic Effect: Formation of Micelles and Biological Membranes; John Wiley & Sons: New York, 1980.
- Mayers, D. Surfactant Science and Technology; VCH Publishers, Inc.: New York, 1988.
- Rosen, M.J. Surfactants and Interfacial Phenomena 2nd ed.; John Wiley & Sons:
 New York, 1989.
- ⁵² Zhong, X. F.; Varshney, S. K.; Eisenberg, A. Macromolecules 1992, 25, 7160.
- Gauthier, S.; Eisenberg, A. Macromolecules 1987, 20, 760.

CHAPTER 5

Aggregation and Critical Micelle Concentrations of Polystyrene-*b*-Poly(sodium acrylate) and Polystyrene-*b*-Poly(acrylic acid) Micelles in Organic Media

ABSTRACT

Block copolymer micelles formed from polystyrene-b-poly(sodium acrylate) (PS-b-PANa) and polystyrene-b-poly(acrylic acid) (PS-b-PAA) were characterized in organic solvents. The critical micelle concentrations (cmc's) were determined for one block copolymer series in which PS blocks of 660 units were attached to either relatively short PANa or PAA blocks ranging in lengths from 2.6 to 18 units. The cmc's for these block copolymers in toluene, tetrahydrofuran (THF), and chloroform were found to range from ca. 1×10^{-7} to 5×10^{-9} M. The a and b constants in the relation log cmc = $a \times 10^{-1}$ N_B is the insoluble block length were evaluated and correlated to the polymer-solvent interaction parameters for the present systems as well as for several other block copolymer micelles. The PS(660)-b-PANa(x) series was also investigated by size exclusion chromatography (SEC) in tetrahydrofuran (THF). Two peaks in the SEC chromatograms could be distinguished, one corresponding to micellized block copolymers and the other to unassociated chains. The position of the latter peak was the same as that

of the PS homopolymer, which was also present. These micelles were also characterized by static and dynamic light scattering (SLS and DLS). The effect of the soluble (PS) block length on the aggregation was investigated by SLS in THF. For this study, three PS-b-PANa series containing PS block lengths of 190, 630 and 2300 units attached to PANa blocks ranging in lengths from 4.2 to 69 units were characterized. The aggregation numbers (N_{agg}) were found to be influenced significantly by the soluble PS block length (N_{PS}). The N_{agg} and the calculated core radii (R_c) were found to scale with the block lengths as $N_{agg} \propto N_{PANa}^{0.5} N_{PS}^{0.5} = 0.6$ and $R_c \propto N_{PANa}^{0.5} N_{PS}^{0.5} = 0.2$.

5.1. INTRODUCTION

Micelles formed from amphiphilic low molecular weight surfactants and block copolymers have vast application in areas such as detergency, 1 oil recovery, 2 drug delivery systems, 3 and catalysis, 4 among others. For such applications, an understanding of certain parameters such as the critical micelle concentration (cmc), the aggregation number, the size and the stability is first required. The use of block copolymers is advantageous in many cases since micelle systems can be created to achieve the desired properties by changing the nature and/or the length of the blocks. Thus, in recent years, considerable effort has been devoted to the characterization of block copolymer micelles, and the subject has been reviewed. 5-8

The cmc is an important thermodynamic parameter describing the concentration above which micelles form. Cmc values have been determined for several nonionic block copolymers in aqueous⁹⁻¹² and in organic media.^{13,14} The thermodynamics of micelle formation have been obtained from the temperature dependence of the cmc^{15,16} or from

the concentration dependence of the critical micelle temperature (CMT) which is the temperature below which micelles form. 17-24

Cmc values have also been determined for ionic block copolymer micelles. Two types of micelles can be distinguished depending on the solvent nature in which micellization occurs, block polyelectrolyte and block ionomer micelles. In aqueous media, one obtains block polyelectrolyte micelles in which a nonionic core is surrounded by an ionic corona. These systems have been characterized by several techniques.^{7,25-29} The cmc values have been determined for some of these systems such as polystyrene-*b*-poly(4-vinylpyridinium ethyl bromide) (PS-*b*-P4VPEtBr)²⁵ and polystyrene-*b*-poly(sodium acrylate) (PS-*b*-PANa).^{29,30} In organic solvents, one obtains block ionomer micelles in which the micelle core is ionic and is surrounded by a nonionic corona.

Investigations of the cmc's of block ionomers are scarce. These systems are of interest because of their stability³¹ and their possible applications in areas such as the preparation of semiconductor particles³² and as microreactors.⁴ A recent preliminary study has shown that for a block ionomer series, PS(660)-b-PANa(x) in THF, the cmc values decreased from 2.5 x 10⁻⁸ to 5.4 x 10⁻⁹ M when the insoluble (PANa) block length increased from 2.6 to 14 units.³³ The present study further explores the effects of several parameters on these low cmc values as well as their effects on certain micellar characteristics such as the aggregation numbers and micelle sizes.

There are several methods which have been used to evaluate the cmc's of block copolymer micelles. These methods include fluorescence spectroscopy, 9,12,29,30 osmometry, 13,17 viscosity 13 and light scattering, 10,15,16,33 Recently, a method was developed to determine the cmc's of polydisperse block copolymer micelles of low cmc by static light scattering (SLS). 34 The details of this method were given in Chapter 4. This method is based on the theory of Gao and Eisenberg 35 which accounts for the effects of

polydispersity in block copolymers. It should be mentioned that, more recently, the influence of polydispersity on the micellization of triblock copolymers of PEO-b-PPO-b-PEO and PPO-b-PEO-b-PPO in aqueous solutions have been theoretically examined by Linse. ³⁶ In the theory of Gao and Eisenberg, the cmc was found to depend on the length and polydispersity of the insoluble block. ³⁵ For instance, an increase in the polydispersity index results in a decrease in the cmc. The single chain concentration was also found to increase with the total polymer concentration, in contrast to monodisperse systems in which the single chain concentration remains constant above the cmc. The effect of polydispersity on the cmc was found to decrease as the dependence of the cmc on the insoluble block length (N_B) decreased. This dependence could be evaluated from the value of the constant a in the equation $\log cmc \propto a N_B^{1/3}$.

The SLS method which has been proposed takes into account these effects of polydispersity on the cmc, i.e. the change in the single chain concentration with total concentration and the polydispersity of the insoluble block. SLS is a convenient technique for the evaluation of the cmc, since it is sensitive to the apparent weight average molecular weight ($M_{w,app}$) of the particles in solution. The proposed measuring the $M_{w,app}$ for block copolymer micelles as a function of concentration (c), three different regions can be distinguished, the micelle region (c > cmc), the transition region of micelles to single chains (c ~ cmc), and the single chain region (c \leq cmc). In general, the cmc can be evaluated from the onset of the single chain region. Unfortunately, in many block copolymer systems, the single chain region can not be measured due to the low value of the cmc. For such cases, an extrapolation method using an equation developed by Debye can be used. This equation, as well as the method mentioned above, describe the cmc values for block copolymers which have a weak dependence of the cmc on the insoluble block length as well as for monodisperse block copolymers. However, for block

copolymers which have a strong dependence of the cmc on the insoluble block length and which are polydisperse, only the proposed method was able to evaluate the cmc.³⁴

Since the present chapter focuses on the association of block ionomer micelles, the following sections will briefly describe some of the relevant results pertaining to these Micellization of block ionomers has been studied extensively in this systems. laboratory^{31,38-44} as well as in others.⁴⁵⁻⁴⁸ Block ionomer micelles have been shown to possess several characteristic features. For instance, they have been found to be extremely stable.31,38 This stability allows for the characterization of the micelles by SEC.31,39 In general, two peaks could be identified from the SEC chromatograms, one corresponding to the micellized block copolymer and the other due to block copolymers present as single chains. In addition, in some cases, polystyrene homopolymer was eluted as a separate peak. The peak containing a lower ionic content arises from the polydispersity in the lengths of the ionic blocks, which, for narrow molecular weight distributions, such as 1.10, are broad compared to truly monodisperse chains. This result can be understood from the concept of a threshold length for micellization, i.e. a critical micelle length (CML) which was proposed.³⁹ For instance, very short ionic block lengths, below the CML, remain soluble and unassociated while longer ionic block lengths, above the CML, prefer micellization at concentrations typical of SEC measurements (i.e. ca. 2 mg/mL). The CML was found by computer modeling of SEC chromatograms to vary between 2 to 3 ionic block units, independent of the PS block length which ranged from 190 to 2300 units.

Additional studies have concentrated on the characterization of block ionomer micelles by still other techniques. The dependence of the micellar characteristics on the block copolymer composition of polystyrene-b-poly(metal methacrylate) and polystyrene-

b-poly(methacrylic acid) was systematically investigated by SEC, DLS, and viscometry.^{31,38} Small-angle X-ray scattering (SAXS) studies also probed the dependence of the core radius on the insoluble and soluble block lengths in the solid state and in solution for block ionomers with a nonionic PS block attached to an ionic block consisting of either poly(cesium acrylate),⁴² poly(cesium methacrylate)⁴² or poly(quarternized 4-vinyl pyridine).⁴³ The scaling relations of the star model⁴⁹ were found to describe the systems.^{41,42} A ²H NMR study investigated the dynamics of PS segments in the corona.⁴⁰ It was found that segments near the core had a restricted mobility compared to those further from the core or to single chains in solution.

The purpose of the present chapter is to characterize block copolymer micelles formed from polystyrene-b-poly(sodium acrylate) and polystyrene-b-poly(acrylic acid) in organic solvents. The chapter is divided into three parts. The first two parts focus on the aggregation of two block copolymer series in which a PS block of constant length (660 units) is attached to either PANa or to PAA blocks of relatively short lengths, ranging from 2.6 to 21 units. In the first part, the cmc values for these block copolymer micelles are reported as a function of the nature of the solvent and the core block, i.e. salt versus acid forms. The second part concentrates on the characterization of the block copolymer micelles by SEC in tetrahydrofuran (THF) and by SLS and DLS in different solvents. In the third part of this chapter, the aggregation behavior of three different block copolymer series consisting of 190, 630 and 2300 PS units attached to various PANa blocks ranging in length from 4 to 67 units are examined by SLS in THF. This latter part extends the results obtained from a previous SEC study³⁹ on these samples.

5.2. EXPERIMENTAL

5.2.1. Synthesis

The block copolymers were prepared by sequential anionic polymerization; the details are given in ref 39. For convenience, only a brief summary is given here. The copolymers were synthesized by polymerizing the styrene monomer, followed by addition of tert-butyl acrylate. The initiator was the reaction product of sec-butyllithium with a few drops of α-methylstyrene. The polymerization was carried out in tetrahydrofuran (THF) at -78°C under an attaosphere of nitrogen. The apparatus employed for the polymerization allowed the withdrawal of the reaction mixture during the course of the synthesis. Therefore, for a given constant polystyrene block length, a series of diblocks was obtained with poly(tert-butyl acrylate) segments of different lengths. Aliquots of the reaction mixtures were withdrawn for characterization after the polystyrene block was formed and every time following addition of the second monomer. Polystyrene-bpoly(acrylic acid) (PS-b-PAA) was obtained by acid-catalyzed hydrolysis of the tert-butyl acrylate segments in toluene at 110°C using p-toluenesulfonic acid as the catalyst. The PS-b-PAA was recovered and purified by repeated precipitations into cold methanol. The samples were then dried in a vacuum oven at 50°C for 48 h. The composition of the copolymers was determined by either FT-IR using copolymers in the ester form or by titration of the acid. Table 5.1 summarizes the composition of the block copolymers and the polydispersity indices (P.L) of the PS homopolymer and the ester form of the block copolymer. The molecular weight of the polystyrene block was determined with a precision of ± 5% by size exclusion chromatography in THF using narrow molecular weight polystyrene standards.

For neutralization of the PS-b-PAA, a known amount of the dry copolymer was dissolved in benzene/methanol (90/10 (v/v)) at a concentration of 2% (w/w). The acid samples were neutralized by the addition of a stoichiometric amount of NaOCH₃, which

Table 5.1. Composition and Polydispersity Index of the PS Homopolymers and the Block

Copolymers

PS(x)-b-PANa(y)	P.L.ª	PS(x)-b-PANa(y)	P.Lª
190- <i>b</i> -0	1.12	630- <i>b</i> -0	1.10
190- <i>b</i> -10	1.10	630- <i>b</i> -4.2	
190- <i>b</i> -24	1.13	630- <i>b</i> -18	1.12
		630- <i>b</i> -31	1.12
660- <i>b</i> -0	1.05		
660- <i>b</i> -2.6		2300- <i>b</i> -0	1.12
660- <i>b</i> -4.7		2300- <i>b</i> -4.6	
660- <i>b</i> -8.9		2300- <i>b</i> -31	
660- <i>b</i> -14		2300- <i>b</i> -69	1.12
660- <i>b</i> -18			
660- <i>b</i> -21	1.05		

^a The P.I. for samples with very short ester blocks were not measured.

was prepared by reacting Na with methanol in THF. The solutions were stirred for 30 minutes, and the diblock ionomers were recovered by freeze drying. The samples were then further dried at 60°C for 48 h. under vacuum. Abbreviations are used to indicate the copolymer composition; for example, PS(660)-b-PANa(8.9) represents a polystyrene chain of 660 units joined to a poly(sodium acrylate) chain of 8.9 units; PAA denotes poly(acrylic acid).

5.2.2. Size Exclusion Chromatography

The SEC measurements were performed in THF and at room temperature on a Varian 5010 liquid chromatography apparatus equipped with a refractive index detector. The molecular weights and polydispersity indices of the PS and the PS-b-poly(tert-butyl acrylate) were evaluated using a Varian DS-604 computer with SEC application software. The flow rate was 1.0 mL/min. Two columns were used in series, Progel -TSK G2000-HXL and G4000 HXL (Supelco Inc.) with effective molecular weight ranges from 10² to 10⁴ g/mol and from 10² to 8 x 10⁶ g/mol, respectively. The columns were calibrated using five polystyrene standards of narrow molecular weight distributions. The concentrations of the polymer solutions were ca. 2 mg/mL and they were filtered (0.45 μm pore size) prior to injection. To determine the percent of micelles for the PS(660)-b-PANa block ionomers, the samples were injected in triplicate.

5.2.3. Sample Preparation for Light Scattering

For the light scattering experiments, toluene and THF were distilled over calcium hydride and sodium benzophenone complex, respectively, while chloroform (spectrograc'e) was dried with molecular sieves. The polymer solutions were prepared by dissolving the dried block copolymer in the distilled or filtered solvent (0.2 µm PTFE filters, Chromatographic Specialties) and the solutions were stirred. Prior to the measurements,

the polymer solutions were filtered through 0.45 μ m PTFE filters directly into dust free scintillation vials or into test tubes for the SLS and DLS measurements, respectively. Measurements at different concentrations were performed by diluting the filtered polymer solution with filtered solvent. The dilutions were followed by the weighing of the solutions with an analytical balance having a precision of \pm 0.001 g. Typical initial polymer solvent concentrations for the SLS measurements were in the range of 2 x 10⁻³ - 2 x 10⁻⁵ g/mL, depending on molecular weight of the sample. For the DLS measurements the concentration range used was ca. 2 - 5 x 10⁻³ g/mL.

5.2.4. Static Light Scattering Measurements

Light scattering experiments were performed using a DAWN-F multiangle laser photometer (Wyatt Technology, Santa Barbara, CA) at 25°C, which operates at 15 angles, from 26 to 137°, and is equipped with a He-Ne laser (632.8 nm). The data were acquired and processed with the accompanying software. A minimum of four concentrations was used to determine the weight average molecular weight, radius of gyration and second virial coefficient with the aid of a Zimm plot. The measurements were performed at least in duplicate for each sample; the average value is reported. The error in the weight average molecular weight was estimated to be less than 10%.

The specific refractive index increment (dn/dc) was determined using the Wyatt/Optilab 903 interferometric refractometer and accompanying software at a wavelength of 630 nm. The cell constant was determined by calibration with different concentrations of sodium chloride (99.999%, Aldrich) solutions. Eight to ten concentrations were measured for each dn/dc determination. These values are given in Table 5.2. It was found that these values were the same as those of PS; the literature values for toluene, THF and chloroform are 0.110, 0.194, and 0.170 mL/g, respectively, 50

Table 5.2. Specific Refractive Index Increments of PS(660)-b-PANa(x) in Different Solvents at 630 nm and 25°C.

PS(660)-b-PANa(x)	Solvent	dn/dc (mL/g)	
4.7	toluene	0.105 ± 0.007	
21	toluene	0.111 ± 0.006	
·			
14	chloroform	0.174 ± 0.01	
21	chloroform	0.167 ± 0.01	

Light scattering from a dilute polymer solution, when the particle size is greater than approximately $\lambda/20$, has been described by 51

$$Kc/R(\theta) = \frac{1}{P(\theta)M_W} + 2A_2c+... \tag{1}$$

where K is the optical constant, $(2\pi^2 (n_0 dn/dc)^2/\lambda_0^4 N_{av})$, n_0 is the refractive index of the solvent, λ_0 is the wavelength in vacuum, N_{av} is Avogadro's number, c is the concentration, $R(\theta)$ is the Rayleigh ratio at the angle of measurement, $P(\theta)$ is the particle scattering function, M_w is the weight average molecular weight, and A_2 is the second virial coefficient. This equation can be solved graphically with a Zimm plot, S_2 in which S_2 is plotted as a function of S_2 (S_2) + kc, where k is a scaling factor. By

extrapolating to zero concentration as well as zero angle, the intercept gives the inverse M_w and the corresponding slopes of these two lines yield A_2 and R_g .

For block copolymers, M_w refers to an apparent weight average molecular weight $(M_{w, app})$ because of the chemical heterogeneity of the copolymer.⁵³ However, since dn/dc values for the block copolymer were found to be the same as literature values for polystrene (Table 5.2), $M_{w,app}$ is close to the true M_w . The constancy of the dn/dc is most likely due to the small weight fraction of the insoluble block.⁵⁴

Certain micellar parameters, such as the aggregation numbers (N_{agg}) , core radii (R_c) and surface area per chain (S/N_{agg}) , can be calculated from the value of the M_w . For instance, the aggregation numbers were evaluated from the ratio of the weight-average molecular weight of the micelles $(M_w(\text{mic}))$ to that of the unassociated block copolymer. The core radii were determined from N_{agg} using the following relation for the core volume, V_c ,

$$V_c = (4/3) \pi R_c^3 = N_{agg} N_B MW/(\rho N_{av}),$$
 (2)

where N_B, MW and p are the number of repeat units, the repeat unit molecular weight and the density of the PANa block, respectively. The density of the PANa block was determined from pycnometric measurements to be 2.05 g/mL. From the R_C and N_{agg} values, the surface area per chain (S/N_{agg}), given as

$$S/N_{agg} = 4 \pi R_c^2 / N_{agg}$$
 (3)

can be calculated.

The cmc values were determined from the Debye equation³⁷ which was developed for monodisperse surfactants and has been previously used in the determination of cmc's for block copolymer micelles.^{34,55} It can be described as,

$$K c / R(0) = c / [M_w(s) \times cmc + M_w(mic) \times (c-cmc)] + 2 A_2 (c-cmc)$$
 (4)

where R(0) is the Rayleigh ratio extrapolated to zero angle, $M_w(s)$ and $M_w(mic)$ are the weight average molecular weights of the single chains and the micelles, respectively. The Kc/R(0) values were plotted as a function of concentration and the cmc was evaluated from fitting the resulting curve using the program Peak Fit (Jandel Scientific). It should be noted that when the cmc is evaluated for polydisperse block copolymer micelles, the cmc in eq. 4 should be replaced by the concentration of single chains which has been found to change with total polymer concentration. The reader is referred to Chapter 4 for details concerning this procedure.

5.2.5. Dynamic Light Scattering Measurements

Dynamic light scattering studies were performed on a Brookhaven Instruments Corp. photon correlation spectrometer with a BI-2030 digital correlator and a Spectra Physics 120 helium/neon laser with a wavelength of 632.8 nm. The scattering angle used was 90°. A refractive index matching bath of filtered decalin (0.2 µm) surrounded the scattering cell, and the temperature was controlled to 25°C.

The correlation function $(G_2(t))$ for a single exponential decay can be given as a function of time (t) by 56

$$G_2(t) = B (1+\beta \exp(-2\Gamma t))$$
 (5)

where B is the baseline, β is an optical constant which depends on the instrument, and Γ is the decay rate for the process. This rate is given by

$$\Gamma = Dq^2 \tag{6}$$

where D is the translation diffusion coefficient and q is the absolute value of the scattering vector,

$$q = 4 \pi n / (\lambda_0 \sin (\theta/2)) \tag{7}$$

The diffusion coefficient for spherical particles is related to the hydrodynamic radius (R_h) by the Stokes-Einstein equation,

$$D = k_B T / (6 \pi \eta R_b)$$
 (8)

where $k_{\rm B}$ is the Boltzmann constant, T is the absolute temperature and η is the viscosity of the solvent medium. In general, the diffusion coefficients should be extrapolated to zero concentration. However, for the present system, the DLS results were found to be independent of concentration, probably due to the relatively small particle radius (< 30 nm).³⁸

5.3. RESULTS AND DISCUSSION

This section is divided into three parts. The first part concentrates on the cmc's of two series of block copolymers, PS(660)-b-PANa(x) and PS(660)-b-PAA(x). The effects of the solvent and the insoluble block (length and nature) on the cmc's are investigated. As an application of the mixed micelle model, the distributions of the block copolymers present as single chains and in the micellar fractions are evaluated. Correlations of the constants describing the dependence of the log cmc on the N_B^{1/3} are made with the polymer-solvent interaction parameter for the present system as well as for other block copolymer micelle systems previously investigated. The second part addresses other aspects of aggregation. The percent of micelles in solution for the PS(660)-b-PANa(x) block ionomer series are evaluated in THF by SEC. Also, the aggregation numbers, second virial coefficients, and micelle radii, for the PS(660)-b-PANa(x) and PS(660)-b-PAA(x) series as a function of the insoluble block length for different solvents are investigated. The third part deals with the effect of the soluble PS block length on the

micellization of PS(x)-b-PANa(y) block ionomers in THF for three series consisting of PS blocks of lengths of 190, 630 and 2300 units, attached to PANa blocks of various lengths. The scaling relation between the aggregation number and the PS and PANa block lengths is explored.

5.3.1. cmc's for PS(660)-b-PANa(x) and PS(660)-b-PAA(x) Block Copolymer Micelles

5.3.1.1. Solvent and Insoluble Block Effects

The cmc values for PS(660)-b-PANa(x) and PS(660)-b-PAA(x) were evaluated for different PANa and PAA block lengths ranging from 2.6 to 18 units. Typical data obtained from SLS for the PS-b-PANa series in THF are presented in Figure 5.1. The lines are the fits used to determine the cmc values; this will be discussed in more detail in the subsequent paragraph. From the behavior of the Kc/R(0) values as a function of concentration, two regions can be distinguished. At high concentrations, the scattered intensity is predominantly due to the presence of micelles. In this region, extrapolation of the Kc/R(0) values to zero concentration gives the inverse weight average molecular weight of all the particles in solution $(M_{w,total}^{-1})$ and the slope of this line is proportional to the second virial coefficient. At intermediate concentrations, the transition region is observed in which micelles dissociate to single chains. In this region, the Kc/R(0) values increase with decreasing total concentration; this trend represents a decrease in $M_{w,total}$. For instance, for the PS(660)-b-PANa(8.9) block ionomer (Figure 5.1), the micelle region occurs at > ca. 1 x 10⁻⁷ M and the transition region occurs at ca. < 1 x 10⁻⁷ M. It should be noted that the region which corresponds to the existence of predominantly single

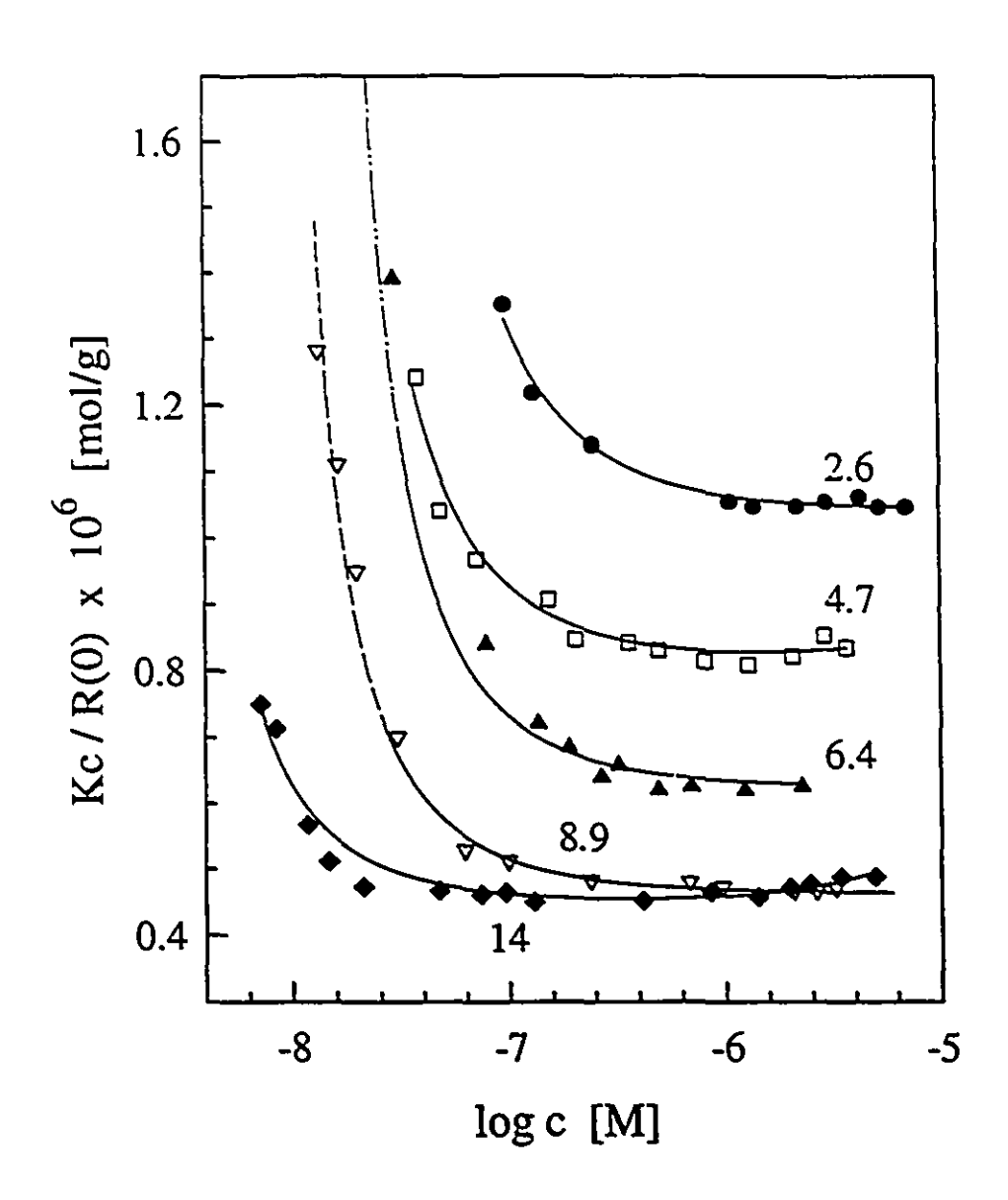


Figure 5.1. Plots of Kc/R(0) used in cmc determinations for PS(660)-b-PANa(x) for different PANa block lengths in THF.

chains, i.e. c < cmc, was not attained in these measurements because the sensitivity of the instrument did not allow measurement at such low concentrations.

The cmc values for the PS(660)-b-PANa(x) and PS(660)-b-PAA(x) block copolymers were evaluated by fitting the Kc/R(0) values as 2 function of concentration using the Debye equation (eq. 4). The details of this procedure were given in the Experimental section. Typical fits obtained for these block copolymers are depicted in Figure 5.1 as solid lines. As discussed Chapter 4, the sensitivity of the cmc's evaluated by this method falls within a 20% error limit.³⁴ The agreement of the lines with the data points shows that the Debye equation gives a good representation of the micelle and transition regions. A similar procedure was also followed for the acid block copolymers in toluene and good agreement was also observed. Previously, the cmc's for this PS-b-PANa block ionomer series were investigated by SLS in THF.³⁴ The Debye equation was found to fit the light scattering curves because of relatively weak dependence of the cmc on the insoluble block length, and also because of the low polydispersity of the PANa blocks. Therefore, for the present system, the effects of polydispersity on the cmc are not significant.

Figure 5.2 summarizes the cmc values determined for PS(660)-b-PANa(x) and PS(660)-b-PAA(x) as a function of the insoluble block length, i.e. N_{PANa} or N_{PAA}. It should be noted that the cmc's could not be evaluated for PANa block lengths higher than 14 units in THF and toluene or 18 units in chloroform because of their low values. In general, it was found that as the length of the insoluble block increased, the cmc values decreased. This result is expected, since the solubility of the single chains decreases with increasing insoluble block length; thus, micellization occurs at lower concentrations. It is interesting to examine the effect of solvent on the cmc values for the PS(660)-b-PANa(x) block ionomers. The cmc's were found to decrease in the order chloroform > THF ~

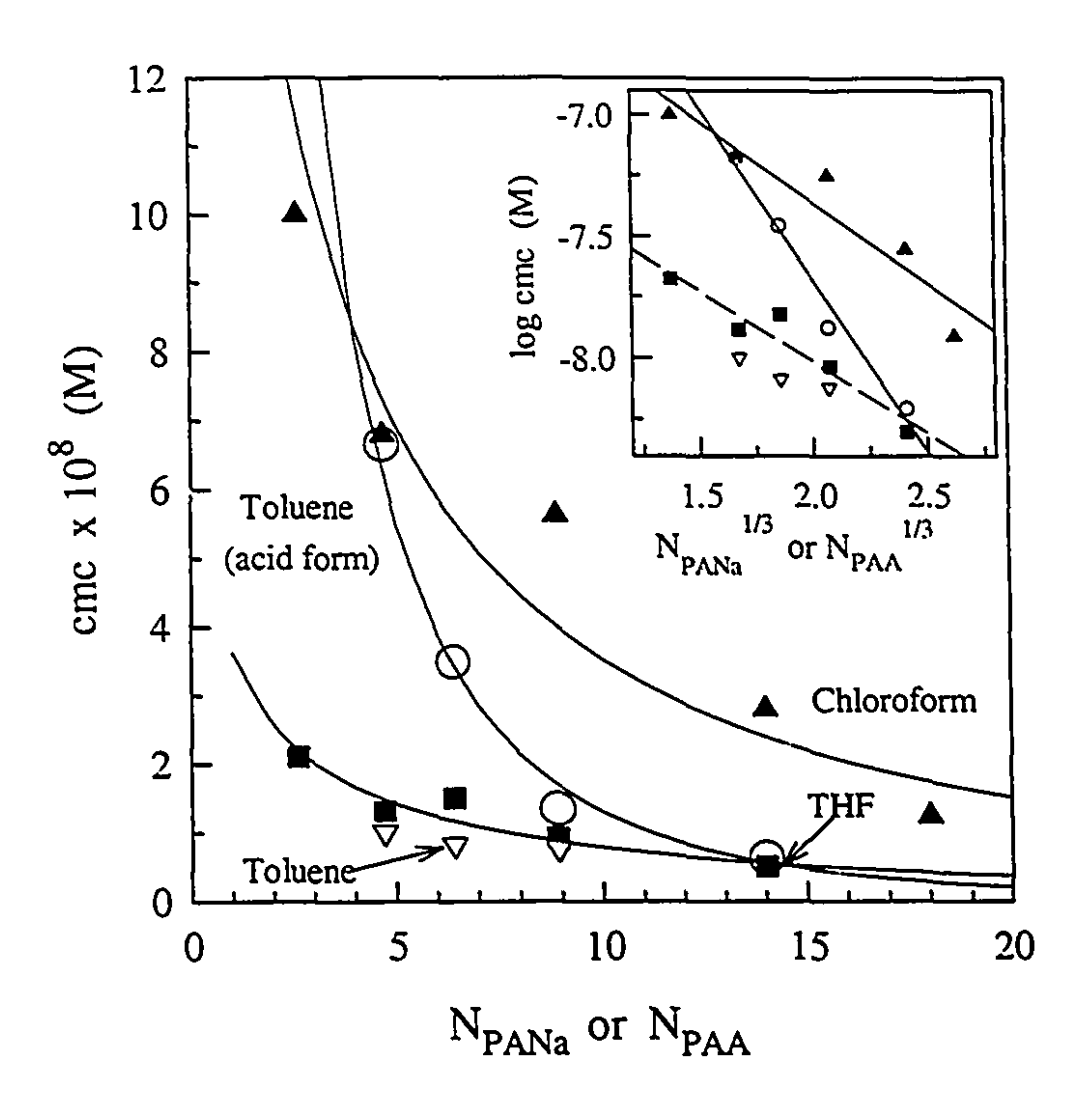


Figure 5.2. Cmc values of PS(660)-b-PANa(x) in chloroform, THF and toluene, and of PS(660)-b-PAA(x) in toluene, as a function of the insoluble block length. The inset represents the data plotted as the log of the cmc as a function of $N_{PANa}^{1/3}$.

toluene. It should be noted that the difference (on a linear scale) between the cmc's in chloroform and those in THF or toluene decreased as the insoluble block length increased.

The cmc's for PS(660)-b-PAA(x) were investigated only in toluene (Figure 5.2). The cmc values for PS(660)-b-PAA(x) show an interesting trend. First, for insoluble block lengths of ca. 5 units, the cmc values for the acid form are similar to those of the salt form in chloroform, while at ca. 14 units, the cmc values are similar to those of the salt form in THF. From the trend of the dashed line, it is expected that for PANa block lengths lower than 4.6 units, the cmc values for the acid form might be larger than those for the salt form in chloroform; for block lengths greater than 14 units, the cmc values apparently converge with those for the salt form in THF.

It is interesting to compare the magnitude of the present cmc values with those previously measured for other block copolymer systems. First, it should be recognized that the cmc's depend on both the soluble and insoluble block lengths. However, cmc's for different systems can be characterized by certain typical cmc ranges. The cmc's for some block copolymer systems will be given here for illustrative purposes. For instance, if one considers the mirror image system of the present block ionomer, i.e. PS(x)-b-PANa(1000) block polyelectrolytes in water, the cmc's have been found to range from ca. 2 x 10⁻⁵ to 6 x 10⁻⁸ M for insoluble PS block lengths ranging from 6 to 110 units.²⁹ The cmc values for PS-b-PEO and PEO-b-PS-b-PEO in water for approximately this PS block length range were found to be slightly lower.⁵⁷ The cmc values for PS-b-PI in n-hexadecane for various PI block lengths were found to range from ca. 3 x 10⁻⁴ to 8 x 10⁻⁶ M for PS block lengths ranging from 67 to 120 units.¹⁸ Thus, for comparable insoluble block lengths, the cmc's for the present systems represent the lowest values which have yet been reported. There are clearly systems with lower cmc values for comparable block lengths; however, we have not found any reports describing a systematic study.

5.3.1,2. Theoretical applications of the Mixed Micelle Model

In the mixed micelle model developed for block copolymer micelles, it was suggested that the cmc for a monodisperse block copolymer (C_i) is given as,³⁵

$$\log C_i = a N_B^{1/3} + b \tag{9}$$

where a and b are constants and N_B is the insoluble block length. This relation was found to describe the cmc values of PS-b-PI in n-hexadecane and those of PS-b-PANa in water.³⁵ The effect of the polydispersity on the cmc depends on the magnitude of the a constant, which is a measure of the dependence of the log cmc on the insoluble block length. In the present system, since the effect of polydispersity has been found not to be significant,³⁴ the cmc evaluated by the Debye equation is close to C_i and the relation can be investigated directly.

The inset of Figure 5.2 shows the data plotted according to eq. 9; the resulting linear regressions are also presented as curves in the main plot of the cmc versus N_{PANa} in Figure 5.2. The agreement with this relation was found to be satisfactory for PS-b-PANa in THF and for PS-b-PAA in toluene. For the neutralized copolymer in chloroform the data showed more scatter in the linear regression. Also, it should be noted that for PS-b-PANa in toluene, not enough cmc values were determined to obtain a meaningful regression. The values for the a and b constants are given in Table 5.3. It should be noted that plots of log cmc versus N_{PANa} also gave satisfactory linear regressions; this fact may be due to the weak dependence of the cmc on N_{PANa} . Thus, the dependence of the log cmc on $N_{PANa}^{1/3}$ for the present systems is not very sensitive; however, the $N_{PANa}^{1/3}$ dependence is consistent with the theory.

The molecular weight distribution of the block copolymer molecules present as single chains (S) and present in the micelle fraction (M) can be calculated from the mixed

Table 5.3. Summary of the *a* and *b* Constants for Different Block Copolymer Systems and the Hildebrand Solubility Parameters⁵⁰ used in the Evaluation of Core-Solvent Interactions.

Block Copolymer		Solvent	а	ь	δ (cal/cm ³) ^{1/2}		<i>.</i> 12
Core	Corona				core corona		solvent
PANa	PS	Chloroform	-0.66	-6.03	ca. 16 ^f	9.1	9.3
PANa	PS	THF	-0.58	-6.86	ca. 16 ^f	9.1	
PAA	PS	Toluene	-1.42	-4.83	ca. 11 ^f	9.1	8.9
PVP	PS ^a	Toluene	-1.66ª	-0.90a	ca. 10 ^f	9.1	8.9
PS	PANab	Water	-0.68e	-4.02e	9.1		24
PS	Ыс	n-Hexadecane	-1.65e	3.55e	9.1	8.0	7.7
PS	PEO d	Water	-0.45	-5.26	9.1	10.5	24

a, b, c, d evaluated from data given in reference 34, 18, 29, and 57, respectively. a = a and b constants determined in ref 34 and 35, respectively. f calculated values based on ref 60 (see text).

micelle model³⁵ using equations 6 and 7, given in Chapter 4. Figure 5.3 gives such a plot for PS(660)-b-PANa(8.9) in THF. The total molecular weight distribution of all the polymer chains is given as a solid curve (total). The distributions of the single chains and micelle fraction are given as a percentage of the total distribution for a concentration of 5 times the cmc (denoted by subscripts in the figure). The distributions of the single chains and micelle fractions were found to overlap extensively for the block ionomer. It should be noted that the N_{PANa} value for the peak maxima are somewhat lower for the single chain fraction than the micelle fraction. The lack of segregation between the single chain and micelle fractions is due to the relatively weak dependence of the cmc on the insoluble block length as expressed in the low value of the constant a in eq. 9. For the acid form at these concentrations, the distributions for the single chains and micelle fractions were found to be slightly more segregated at low PAA block length compared to the salt form (graph not shown). This fact was due to larger dependence of the log cmc on the insoluble block length.

5.3.1.3. Correlations of the a and b Constants with Interaction Parameters

In general, micellization theories have considered three contributions to the total free energy of a micelle, that of the core, the shell and the core/shell interface.⁸ It is of interest to correlate these contributions to the quality of the solvent for the core and for the shell blocks using the Flory-Huggins interaction parameter (χ). This section describes the results of such a correlation. Table 5.3 summarizes the a and b values determined for the present system as well as those previously determined for other systems.^{34,35} It

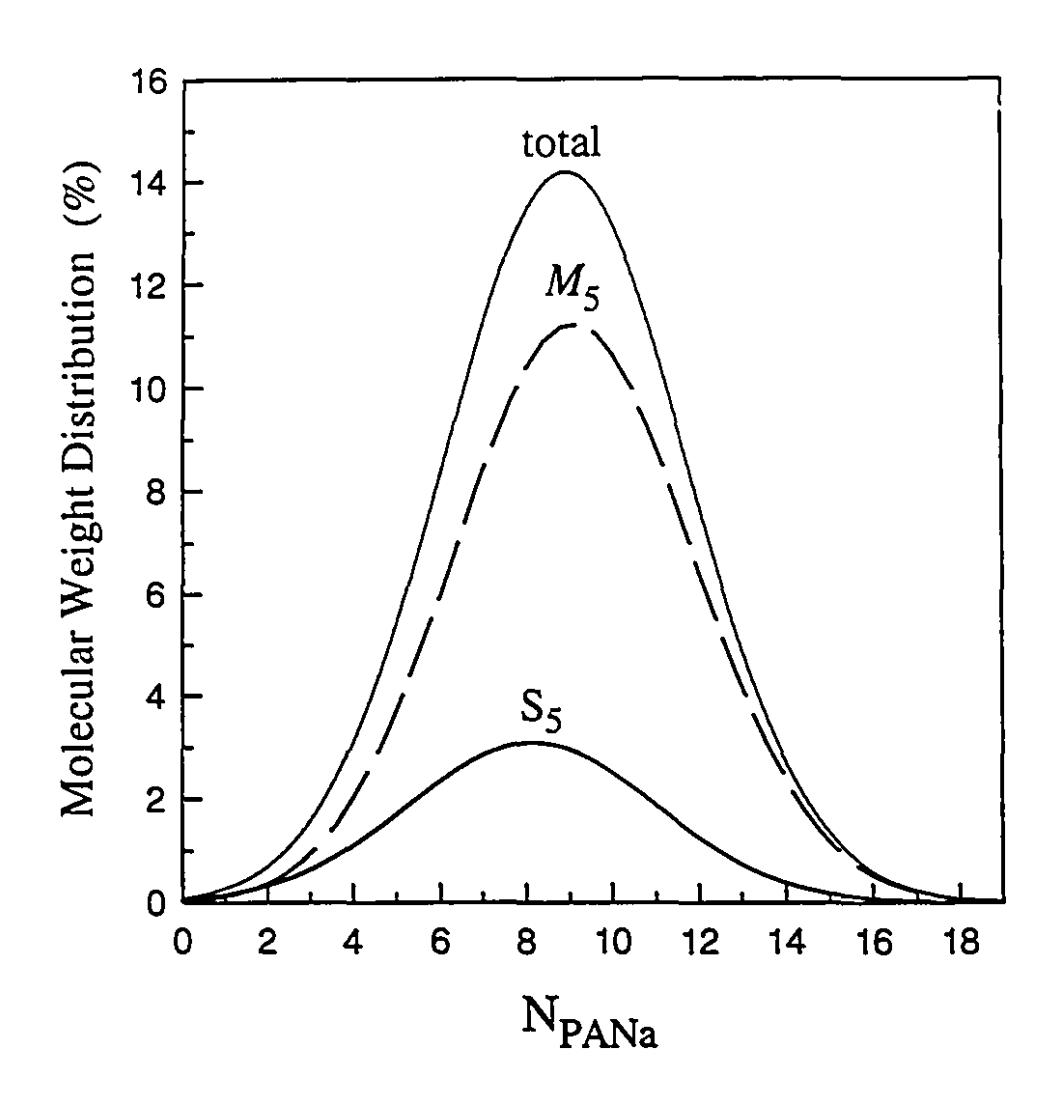


Figure 5.3. Molecular weight distribution of the single chains (S) and the micelle fraction (M) at 5 times the cmc for PS(660)-b-PANa(8.9) in THF.

should be noted that certain theories, such as that of Nagarajan and Ganesh, 58 allow the calculation of the interaction parameters from the micellar parameters such as aggregation numbers, core radii etc. We have tried to extract the χ values for PS(660)-b-PANa(x) in THF by these approaches; however, the interaction parameter between the polymer forming the core and the solvent ($\chi_{core-sol}$) was found to decrease progressively as the insoluble PANa block length increased. The PS-THF interaction parameter was nearly constant, with a value of 0.5.

Since not all χ values are known for the different systems listed in Table 5.3, it is necessary to estimate these values. The polymer-solvent in eraction parameter (χ_{ps}) can be described as a sum of entropic and enthalpic contributions. The entropic contribution for nonpolar systems and polar systems in the absence of specific polymer-solvent interactions is given as a constant, ca. 0.34. The enthalpic contribution can be estimated from the values of the Hildebrand-Scatchard solubility parameters (δ); the χ_{ps} is thus given by, δ 0

$$\chi_{ps} = (\delta_s - \delta_p)^2 V_s / R T + 0.34$$
 (10)

where δ_s and δ_p are the solubility parameters for the solvent and polymer, respectively, V_s is the molar volume of the solvent and R is the gas constant. This equation provides a qualitative indication of the interaction parameters. It should be noted that for polar systems with specific interactions between the components, the intermolecular forces between molecules should also be taken into account.⁵⁰

In order to evaluate the quality of the estimate of the χ values calculated from eq. 10, comparison can be made with χ values which are available in the literature. For instance, the calculated and the literature χ values for PS in different solvents are given below.⁵⁰

Chapter 5. Aggregation and cmc's of PS-b-PANa and PS-b-PAA Micelles in Organic Media

Solvent	T (°C)	χ _{exp}	χ _{cal}
water	162	4.4	5.0
formamide	162	4.1	5.0
ethylene glycol	162	3.8	4.4
methanol	162	2.2	1.7
n-hexadecane	183	1.2	0.73
toluene	27	0.43	0.35

The average difference between the experimental and estimated χ values was 22%. From this comparison, the χ values evaluated from eq. 10 can be used qualitatively to illustrate the general trends in the χ values, but not for quantitative predictions. It should also be noted that for this illustration, the δ values at 25°C were employed. In general the δ values change with temperature; however, this dependence is not known for many systems.

The literature values for the solubility parameters for the solvents and polymers are given in Table 5.3.⁵⁹ It should be noted that these values are not available for PAA, PVP and PANa. However, they can be evaluated from group contributions of the cohesive energy (E_{coh}) and the molar volume (V) from

$$\delta = (E_{coh} / V)^{0.5} \tag{11}$$

The $E_{\rm cch}$ were evaluated from the tables of van Krevelen or Fedors.⁶¹ For PANa, the value of Na was not known; thus, as an approximation, the value for Cd was used. The values are also given in Table 5.3.

In the following paragraphs, the correlations of the a and b are discussed first for block copolymers having a soluble PS block (PS-b-PANa, PS-b-PAA and PS-b-P4VP) followed by block copolymers having the same insoluble block, i.e., PANa (PS-b-PANa in

chloroform and THF) and PS (PS-b-PI, PS-b-PANa, and PS-b-PEO). The trends of the a and b constants with the estimated $\chi_{core-sol}$ values are illustrated in Figure 5.4a and b respectively. The a and b values plotted are for polymer/solvent systems having a PS corona and a PS core. The line shown in Figure 5.4a is a linear regression through all the points.

The correlation between the a constants and the $\chi_{core-sol}$ values was considered for block copolymer micelles having a soluble PS block in a good solvent, i.e. PS-b-PANa in THF and in chloroform, PS-b-PAA in toluene, and PS-b-P4VP in toluene (Table 5.3). For these block copolymers, the estimated $\chi_{core-sol}$ values were found to decrease according to the nature of the insoluble block in the following order, PANa (in THF) (9.4) > PANa (in chloroform) (6.4) > PAA (3.4) > P4VP (0.74), where the numbers in parentheses are the estimated $\chi_{core-sol}$ values. The absolute magnitude of the a constants was found to increase in the following order; PANa (0.58) < PAA (1.42) < P4VP (1.66). This trend is opposite to that of the $\chi_{core-sol}$ values, i.e. the polymers with the largest $\chi_{core-sol}$ have the smallest dependence (i.e., the smallest absolute value of a) of the log cmc on $N_{\rm B}^{1/3}$. This qualitative trend is shown in Figure 5.4a.

The magnitude of the b constants for the block copolymers having a constant soluble PS block can also be correlated to the polymer-solvent interaction parameters (Figure 5.4b). The b constants are expected to reflect the interaction between the soluble block and the solvent as well as the free energy of the core/shell interface. The free energy of the interface arises from the interactions between the core and the shell region which consists of the soluble block and the solvent. Therefore, $\chi_{core-sol}$ also contributes to the magnitude of the b constant. The absolute magnitude of the b values were found to change in the following order: PANa (6.86) > PAA (4.83) > P4VP (0.90). For these

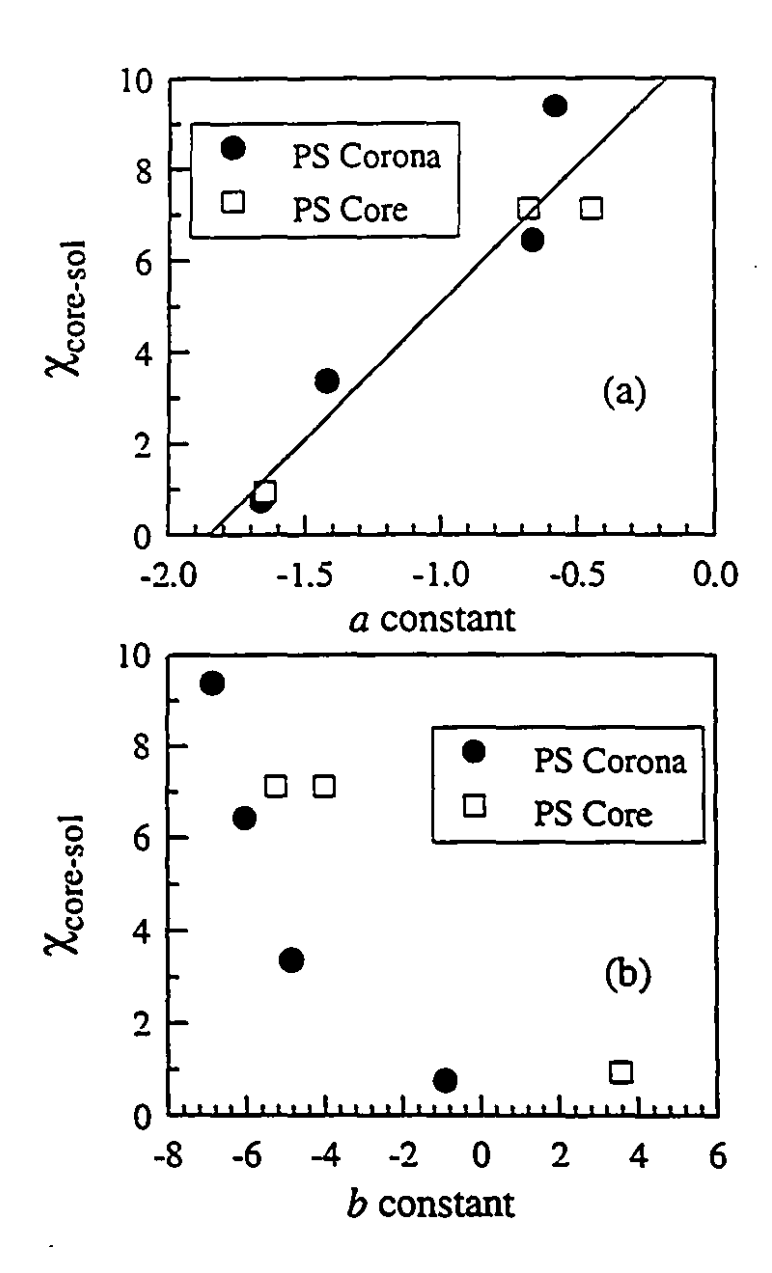


Figure 5.4. Correlations of the a and b constants with the interaction parameters of the polymer forming the core and the solvent.

samples, the values for the interaction parameter between the polymer forming the corona and the solvent ($\chi_{corona-sol}$) are expected to be similar in magnitude since they reflect the interaction between PS and either THF or toluene. Therefore, the $\chi_{core-sol}$ values must contribute significantly to the values of the b constants. The observed trends in b are opposite to those observed for $\chi_{core-sol}$ given above. Thus, the polymers with the largest $\chi_{core-sol}$ values have the smallest b values, as is in the case of the block ionomer micelles. As a result, micellization for these samples occurs at lower concentrations.

The a and b constants for the other block copolymers systems (Table 5.3) having the same insoluble block can also be correlated to the polymer-solvent interaction parameters. For instance, if the block copolymers with PANa cores are considered, it was found that the a constants for PS-b-PANa in chloroform (-0.66) and THF (-0.58) were essentially the same. This result was due to the similarity in the interaction parameter between PANa and the solvents. Similarly, the constants for the block copolymers having a PS core can be considered. The three systems are PS-b-PANa and PS-b-PEO in water, and PS-b-PI in n-hexadecane. The a values for the block copolymers in water, PS-b-PANa (-0.68) and PS-b-PEO (-0.45), were found to be similar in magnitude. The PS-b-PI in the n-hexadecane system, in comparison to PS-b-PANa and PS-b-PEO in water, had a larger dependence of the log cmc on the insoluble block length (a = -1.65) and a larger b value (3.55), thus a higher cmc than the block copolymers in water. These values reflect the weaker interaction between the PS core with n-hexadecane.

5.3.2. Aggregation of PS(660)-b-PANa(x) and PS(660)-b-PAA(x) Block Copolymer Micelles

5.3.2.1. Size Exclusion Chromatography

In the course of the SEC characterization of the PS(660)-b-PANa(x) block ionomer micelles in THF, two peaks with different elution volumes were observed in the chromatograms. Two peaks have been observed in previous SEC studies of block ionomer micelles, 31,39 which, as was discussed in the introduction, are due to micellized and unassociated polymer chains. In the present study, the position of the unassociated polymer chains was the same as that of the corresponding polystyrene homopolymer, PS(660). It has been found in a previous study that the unassociated polymer arises from some PS homopolymer as well as from the presence of block ionomer chains containing a lower ion content than those in the micelles. The presence of the latter species has been postulated to arise from the polydispersity of the ionic block, with the block ionomers of very short ionic block lengths being preferentially soluble as single chains. Above the CML, which has been evaluated to be ca. 2 to 3 units, 39 the block ionomers favor micellization for concentrations used in the SEC experiments.

The percent of micellized chains in the block ionomers was determined from the relative areas of the micellized and the unassociated chains in the chromatograms. These values were determined in triplicate and the average and the standard error values are given in Table 5.4. It is important to establish that no significant adsorption of the PS(660)-b-PANa(x) block ionomers occurred on the SEC columns. The amount of adsorption was evaluated from the percent difference in the ratio of the peak areas to the concentration of injected polymer for the PS(660) and the block ionomers. It was found that the percent difference was below 10 %, with the exception of PS(660)-b-PANa(2.6)

Table 5.4. Summary of the Weight Average Molecular Weights and Aggregation

Numbers for PS(660)-b-PANa(x) and PS(660)-b-PAA(x) as Determined by SLS in

Different Solvents

PS(660)-	micellized	Toluene		THF		Chloroform	
b-X	chains	M _w x 10 ⁻⁶		M _w x 10 ⁻⁶ g/mol		M _w x 10 ⁻⁶ g/mol	
		g/	mol			1	
	(%)	total	micelle	total	micelle	total	micelle
PANa(x)					ł	ı	
2.6	21 ± 1	1.1	5.0	0.76	3.4	0.30	1.4
4.7	65 ± 4	1.4	2.2	1.2	1.9	0.60	1.0
6.4	79 ± 3	1.8	2.2	1.6	2.0	0.66	0.92
8.9	84 ± 1	2.1	2.4	2.2	2.6	1.1	1.4
14	82 ± 2	2.2	2.7	2.2	2.7	1.6	2.2
18	87 ± 1	2.5	2.9	2.8	3.2	2.2	2.9
21	88 ± 2	2.8	3.2	2.9	3.3	l	
PAA(x)				i	!	l	
4.7		0.46	0.66			İ	
6.4		0.61	0.76				
8.9		1.4	1.6				
14		2.2	2.7				

in which the difference was 15%.

The percent of micellized chains was found to increase as the length of the insoluble block increased. Unfortunately, in the present chromatograms, the relative contributions of the PS homopolymer and of the block ionomer containing low ionic content to the area of unassociated chains can not be distinguished. However, in view of the synthesis procedure, the PS content is expected to be constant for the block ionomer series; thus, the observed changes in the percent of micellized chains are due to the decrease in the amount of the block ionomers of low ion content. For PANa block lengths above ca. 8.9 units, the percent of micellized chains seems to be constant at ca. 88 %. From this value, the amount of PS homopolymer is estimated to be ca. 12 %.

5.3.2.1.1. Comparison of the cmc and the CML concept

In view of the SEC results, it is useful to discuss the cmc results previously obtained (section 5.3.1.2) in light of the CML concept. Previously, it was established by using the mixed micelle model, that there was very little segregation in the molecular weight distribution of the single chain and micelle fractions (Figure 5.3). Thus, at concentrations of the SEC experiment, no fractionation is to be expected. However, the SEC chromatograms show that as the insoluble block length increases for short ionic block lengths, the percentage of chains which micellize increases. The phenomenon can be understood by recalling that the mixed micelle model is valid only for collapsed insoluble blocks. Thus, deviations are expected for block lengths which are shorter than the minimum length required for collapse. In these cases, the CML concept is operative: it was previously found that at the concentrations used in SEC, very little micellization occurs for insoluble block lengths less than 2 to 3 units.³⁹ Support for this view comes

from a consideration of monochelics, i.e. polymer chains containing one ionic unit at the end, such as carboxylate-terminated polystyrene (PS(100)-COONa), studied in THF.⁶² For this system, it has been found that the cmc was ca. 1 x 10⁻⁴ M, or 1 mg/mL, which was similar to the concentrations used in SEC measurements (2 mg/mL). Therefore, the present findings are consistent with the notion that in the SEC experiments, the concentrations used were above the cmc values for collapsed blocks, but below those for very short uncollapsed blocks.

5.3.2.2. Static Light Scattering

The PS(660)-b-PANa(x) and PS(660)-b-PAA(x) reverse micelles were characterized by SLS in order to determine the aggregation numbers and second virial coefficient values. The light scattering data were analyzed from Zimm plots obtained in the micelle region, i.e. at high concentrations (see Figure 5.1). In general, from these plots, information can be obtained on the weight-average molecular weight (M_w), the second virial coefficient (A_2) and the radius of gyration (R_g) of the particles in solution. In the present case, the R_g values could not be evaluated since the particles were found to scatter light isotropically. Thus, the particle sizes were < λ /20, i.e., < ca. 32 nm. This section will present the results obtained by SLS on the reverse micelles by first discussing the M_w and the aggregation numbers and second the A_2 values.

The weight average molecular weight which was obtained by SLS is an average value for the solutes present in solution. As was previously discussed, the SEC chromatograms of these block copolymer solutions show peaks for both micellized and unmicellized block copolymer chains. The total weight average molecular weight $(M_{w,total})$ can thus be described as

$$M_{w,total} = f_{mic} \times M_{w}(mic) + (1 - f_{mic}) \times M_{w}(s)$$
 (12)

where $f_{\rm mic}$ is the percent of micellized chains. For the molecular weight of the single chains, the value for PS(660) was used. Since the cmc was much lower than the concentrations used, the $M_{\rm w}$ (mic) required no correction for the cmc values. The $M_{\rm w,total}$ and $M_{\rm w}$ (mic) values and the calculated aggregation numbers are given in Tables 5.4 and 5.5, respectively.

The aggregation numbers (N_{agg}) of the micelles were investigated in different solvents. Figure 5.5 shows the N_{agg} values plotted for PS(660)-b-PANa(x) in toluene, THF and chloroform, and for PS(660)-b-PAA(x) in toluene, as a function of the insoluble block length, i.e. either N_{PANa} or N_{PAA}. The lines represent linear regressions through the data, shown to illustrate the general trends observed. It should be noted that the N_{agg} values for the sample with the shortest insoluble block length, PS(660)-b-PANa(2.6), are not represented on the graph. The N_{agg} values for this sample were found to be much larger than those of the other samples. For instance, the N_{agg} values for PS(660)-b-PANa(2.6) in toluene, THF and chloroform were 72, 49, and 20, respectively (Table 5.5). These large values may result from the adsorption of some of the polymer on the SEC columns (section 5.3.2.1) which would lead to a smaller percent of micelles and therefore larger N_{agg} values.

The N_{agg} values for PS(660)-b-PANa(x) in toluene were found to be very similar to those in THF, and a single line represented the increase of N_{agg} with N_{PANa} for these two solvents; the dotted lines shown in the plot represent the 95% confidence limits. The N_{agg} values in chloroform were found to be lower than those in toluene or THF for low ionic block lengths; however, at higher ionic block lengths, the N_{agg} values approached

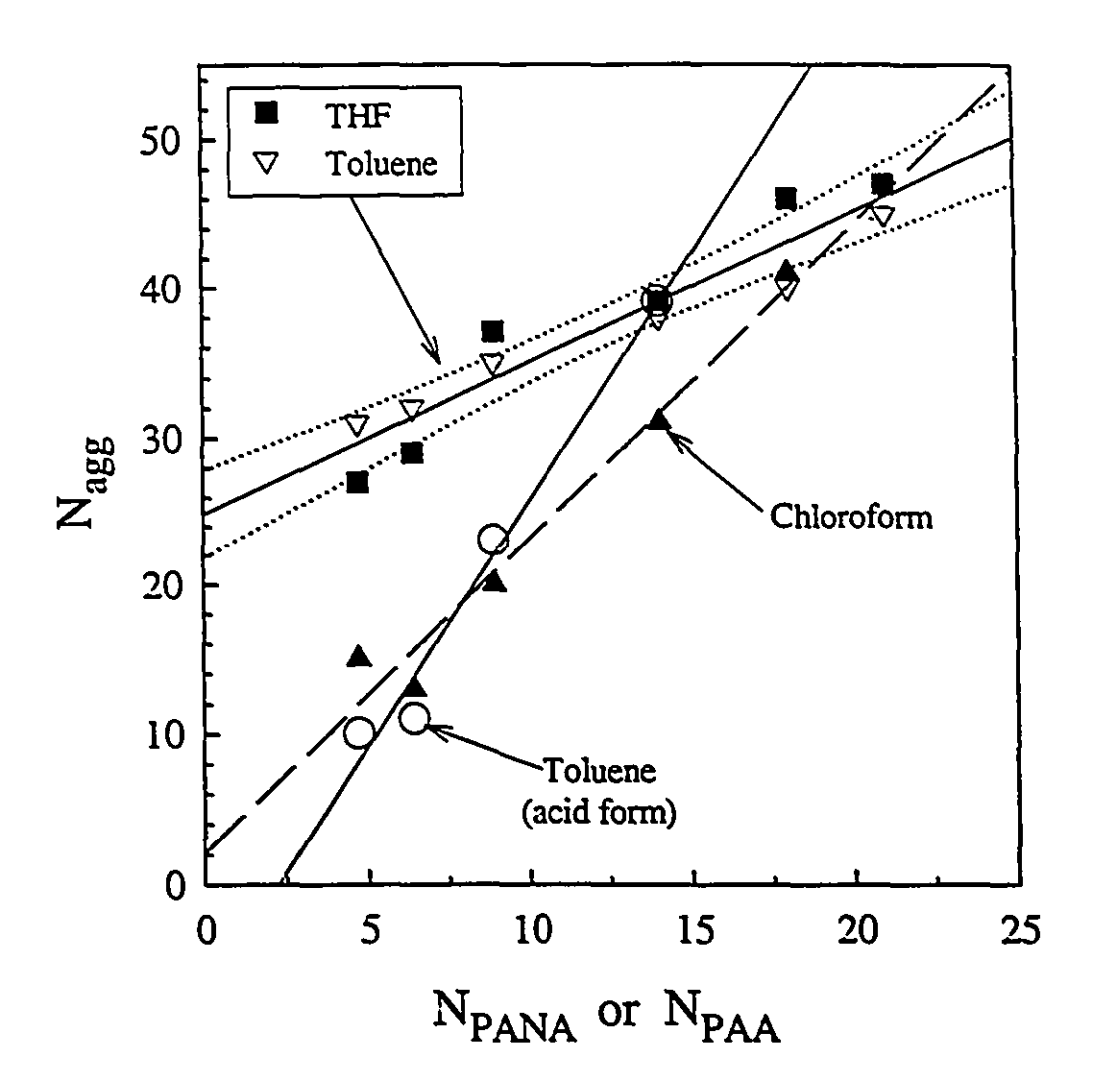


Figure 5.5. Aggregation numbers for PS(660)-b-PANa(x) and PS(660)-b-PAA(x) in different solvents plotted as a function of the insoluble block length. The solid and the dashed lines represent linear regressions and 95 % confidence intervals.

those of toluene or THF. For PS(660)-b-PAA(x) in toluene, the N_{agg} values were found to be equal to those in chloroform at ca. 4.7 units and to those in toluene or THF at 14 units. These PANa block lengths also correspond to those at which the cmc values were observed to be the same (Figure 5.2). A comparison of Figures 5.2 and 5.5 suggests that the trends in the N_{agg} values for these systems were found to be essentially opposite to those previously observed in the log cmc values, which seems reasonable.

It is of interest to investigate the trends in Figure 5.5 and the points at which the lines cross. For instance, at an insoluble block length of 5 units, the N_{agg} values decrease in the order PANa in toluene ~ PANa in THF > PAA in toluene ~ PANa in chloroform. On the other hand, if the trends are extrapolated to higher insoluble block lengths, such as 25 units, the N_{agg} values decrease in a different order, PAA in toluene > PANa in chloroform ~ PANa in toluene ~ PANa in THF. It should be noted that the trends which are observed in the aggregation numbers for these samples which have relatively short insoluble block lengths (0.4 to 3 mol %) may not necessarily be indicative of the behavior for higher ionic block lengths. For instance, a study given in Chapter 6, probed the effect of different degrees of neutralization on the micellization of two block copolymer samples, PS(600)-b-PAA(34) and PS(600)-b-PAA(45). In that study, the aggregation numbers in toluene for the acid block copolymers were found to be lower than those of the Na neutralized samples. Therefore, caution should be exercised when extending the present trends to longer insoluble block lengths.

The quality of the solvent for the block copolymer can be determined from the second virial coefficient values. These values represent an average quantity over all the particles in solution, and are given in Table 5.5. In general, it was found that the A₂ values decreased as the total molecular weight of the particles in solution increased. This trend is expected since, in general, the solvent quality decreases as M_w increases. However

Table 5.5. Summary of the Results Obtained for PS(660)-b-PANa(x) and PS(660)-b-PAA(x) by SLS and DLS in Different Solvents

Composition	Toluene			THF			Chloroform		
PS(660)-b-X	N _{agg}	A ₂ x 10 ⁴	D _h	Nagg	A ₂ x 10 ⁴	D _h	Nagg	A ₂ x 10 ⁴	D _h
		(mL mol/g ²)	(nm)		(mL mol/g ²)	(nm)	<u> </u>	(mL mol/g ²)	(nm)
PANa(x)				1					
2.6	72	0.56	46	49	0.70	49	20	0.70	48
4.7	31	0.65	46	27	0.75	47	15	0.77	44
6.4	32	0.58	47	29	0.50	50	13	0.58	50
8.9	35	0.52	53	37	0.56	53	20	0.79	53
14	38	0.64	54	39	0.38	52	31	0.68	50
18	40	0.37	57	46	0.40	56	41	0.65	55
21	45	0.36	59	47	0.31	52			57
PAA(x)				1					
4.7	9.6	0.69		ł			1		
6.4	11	0.75		1					
8.9	23	0.28							
14	39	0.39		1			l		

the error in the A_2 values can be significant for such low values, i.e. in the 10^{-5} mL mol/ g^2 range. The average values and standard deviations in the different solvents were found to be similar in toluene (0.5 ± 0.1) , in THF (0.5 ± 0.2) , and in chloroform (0.7 ± 0.1) (values given as x 10^{-4} mL mol/ g^2). Similarly, the average A_2 value for PS(660)-b-PAA(x) in toluene was (0.5 ± 0.2) x 10^{-4} mL mol/ g^2 . These A_2 values were found to be significantly lower than those for linear PS of the same weight average molecular weight. For instance, A_2 for PS in toluene⁶³ at a M_w of 2 x 10^6 g/mol is 2.5 x 10^{-4} mL mol/ g^2 , which is higher by a factor of five than those determined for the reverse micelles.

5.3.2.3. Dynamic Light Scattering

The hydrodynamic diameters (D_h) for PS(660)-b-PANa(x) were determined from DLS data using eq. 8. These values are summarized in Table 5.5 for the block ionomers in toluene, THF and chloroform. The D_h values were found to be very similar in these three solvents. The D_h for block copolymer micelles are expected to depend on the aggregation number as well as on the length of the soluble block and the quality of the solvent. The former parameter affects the core size, while the latter two parameters effect the sizes of the PS coronal chains. The size of the polymer chains can be described by the empirical Mark-Houwink parameter, which, for theta solvents, has a value of 0.50. The values for this coefficient for PS in toluene, THF and chloroform are ca. 0.74, 0.72 and 0.75.50 Thus, the expansion of the PS corona in these solvents is expected to be very similar.

The R_h values of the block copolymer micelles have been described by the star model, ⁴⁹ which addresses block copolymer micelles which have a small core and a relatively large corona. Several scaling relations have been developed to describe the micelle characteristics. The R_h scales as,

$$R_h \sim a N_A^{3/5} N_B^{4/25} \tag{13}$$

where a is the length of a monomer unit, N_A and N_B are the number of monomer units in the soluble and insoluble blocks, respectively. The R_h values plotted according to this relation are given in Figure 5.6. The solid and the dashed lines represent the linear regression through the data for the three solvents and the 95% confidence limits, respectively. The slope and intercept of the line was 0.68 and 0.35, respectively, with a correlation coefficient of 0.94. This scaling prediction thus adequately describes the R_h values, with the exception of those for the PS(660)-b-PANa(2.6) block copolymers, which were omitted in the linear regression analysis. It is possible that for these samples, the PANa block is not sufficiently long to adopt a collapsed conformation. Consequently, the insoluble block would exist in an extended conformation, which might result in larger micelle size.

The R_h values can be used to calculate the A_2 values for hard spheres. These A_2 values are given as 64

$$A_2 = 16 / 3 \pi N_{av} R_t^3 / M_w(mic)^2$$
 (14)

where R_t is the equivalent thermodynamic radius. It was found that the A_2 values were in the same range as those measured by SLS (Table 5.5). For instance, for PS(660)-b-PANa(x) in toluene, the average of the measured and the calculated values were (0.5 \pm 0.2)x 10⁻⁴ and (0.23 \pm 0.09) x 10⁻⁴ mL mol/g², respectively. The thermodynamic intermicellar interactions are thus close to those for hard spheres.

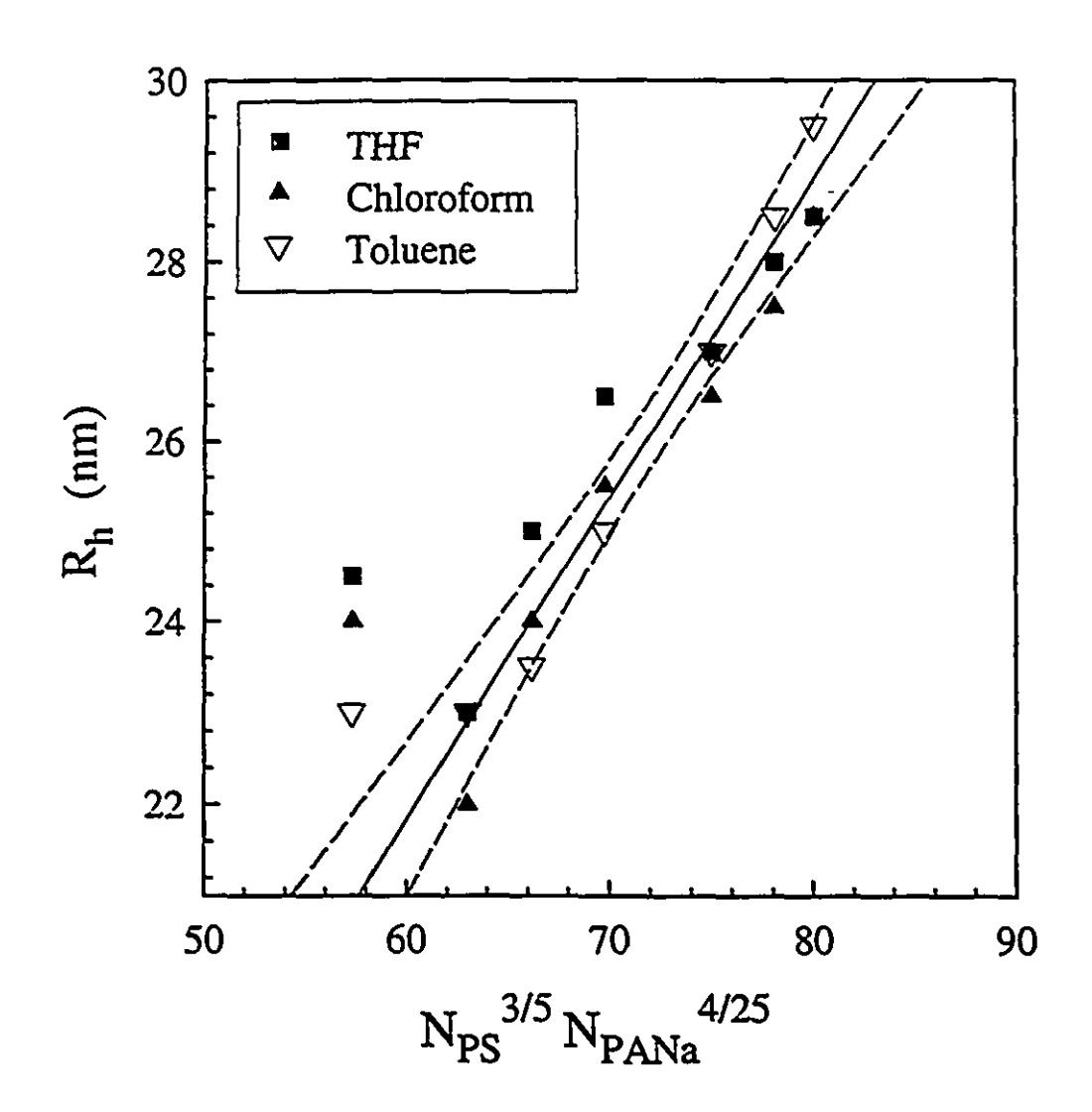


Figure 5.6. Hydrodynamic radii for PS(660)-b-PANa(x) in different solvents plotted according to the scaling relation of the star model.

5.3.3. Effect of PS block lengths on the aggregation of PS-b-PANa block ionomers

In this part of the chapter, a description is given of the effects of the soluble block lengths on the aggregation of PS-b-PANa block copolymers in THF as investigated by SLS. The composition and polydispersity indices of the block copolymers are given in Table 5.1. The PS block lengths investigated had 190, 630 and 2300 units, attached to PANa blocks ranging in length from 4.2 to 69 units. The results obtained on the block ionomers are given in Table 5.6. The percent of micellized chains given in this table was determined by SEC in a previous study.³⁹ From these values, the weight average molecular weight of the micelles and the aggregation numbers were evaluated as described in the previous section (5.3.2.2).

Figure 5.7 illustrates a plot of the N_{agg} values as a function of the PANa block length for different PS block lengths. Included in this figure are the values for the PS(660)-b-PANa(x) block ionomers discussed in the previous section. From the trends, it can be concluded that for a constant PANa block length, the N_{agg} values decrease as the length of the PS block increases. This decrease in the N_{agg} values was more pronounced for longer PANa block lengths. Thus, the soluble block length was found to influence the aggregation numbers significantly.

The PS(190)-b-PANa(24) sample had a much higher aggregation number (590) than the other samples investigated. The mole percent of the ionic block for this sample was 11 %, much higher than that of the other samples investigated, which ranged from 0.20 to 5 %. It is possible that this sample forms aggregates having a nonspherical morphology. For polymers containing an ionic phase such as the segmented ionene systems⁶⁵ and block ionomers of poly(n-hexyl methacrylate)-b-poly(cesium methacrylate),⁶⁶

Table 5.6. Summary of SLS Results for PS(x)-b-PANa(y) in THF.

PS(x)-b- PANa(y)	micellized chains (%) ³⁹	M _w x 10 ⁻⁶ g/mol total micelle		N _{agg}	R _g (total)	$A_2 \times 10^4$ (mL mol/g ²)
190- <i>b</i> -10	96	2.55	2.64	130	42	0.35
190- <i>b</i> -24	97	12.6	13.0	590	85	1.1
630- <i>b</i> -4.2	77	1.03	1.32	20	54	0.42
630- <i>b</i> -18	95	5.05	5.31	79	50	0.50
630- <i>b</i> -31	98	6.92	7.04	100	50	0.56
2300- <i>b</i> -4.6	68	3.84	5.54	23	58	
2300- <i>b</i> -31	83	8.23	9.89	41	65	0.40
2300- <i>b</i> -69	84	12.5	14.8	60	68	0.54

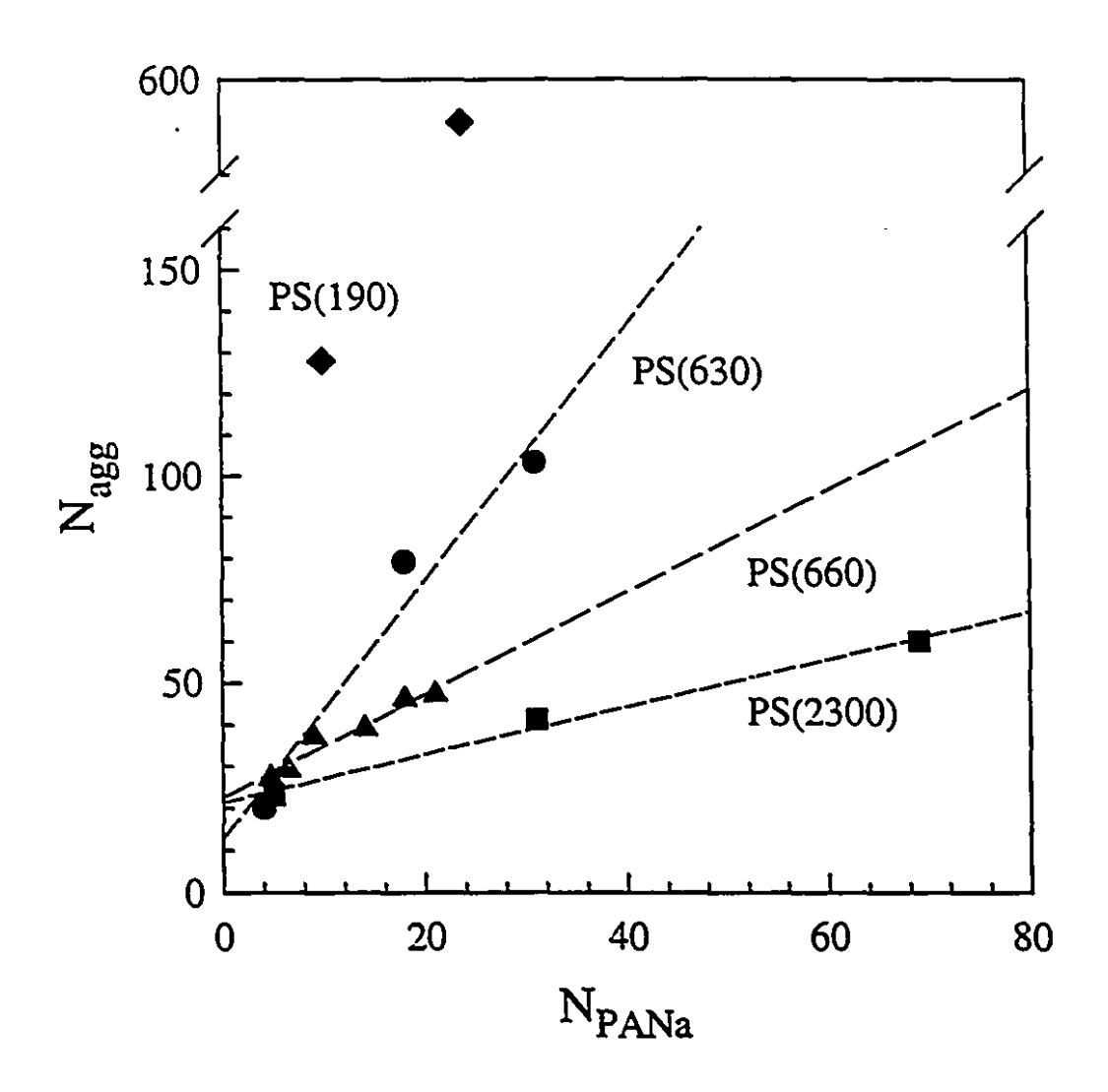


Figure 5.7. Aggregation numbers of PS(x)-b-PANa(y) in THF plotted as a function of the PANa block length for different PS block lengths.

the cylindrical or lamellar morphology has been observed in bulk at an ionic content of ca. 10 %. In nonionic block copolymers such as PS-b-PI, the transition from spherical to cylindrical morphology has been observed at a higher mole percent (ca. 17 mol %).67,68 The morphological change occurs at lower mole fraction for the ionic system compared to the nonionic system due to the larger interaction parameter between the two blocks.69

It was of interest to determine the scaling relation between the aggregation numbers and the PS and PANa block lengths. The PS(190)-b-PANa(24) block copolymer sample is omitted from the present discussion, for reasons discussed above. Since the PS block length was found to influence the N_{agg} values, theories such as the star model⁴⁹ could not be employed. The effect of the soluble and insoluble blocks on N_{agg} are considered in the mean field theories of Whitmore and Noolandi,⁷⁰ and that of Nagaragan and Ganesh.⁵⁸ The N_{agg} values can be described by

$$N_{agg} \propto N_{PANa}^{\alpha} N_{PS}^{\beta} \tag{15}$$

where α and β are constants. The β constant was determined from a plot of log N_{agg} versus log PS for a constant PANa block length of 10 units. The β constant was evaluated to be -0.64. Similarly, the α constant was determined from the slope of a plot of log N_{agg} versus log N_{PANa} for constant PS block lengths. Since the α values were found to vary with the PS length, for instance they were 0.82, 0.38, 0.36 for PS block lengths of 630, 660 and 2300 units, respectively, the average value was employed (0.52). A linear relationship between the N_{agg} values and $N_{PANa}{}^{0.5}N_{PS}{}^{-0.6}$ was found with a correlation coefficient of 0.83 (graph not shown).

The dependence of the core radii (R_c) (calculated from eq. 2), on the PS and PANa block lengths was also investigated. The R_c values are expected to obey the same scaling relation given in eq. 15 with different α and β values. The values for the α and β

constants were determined in the same manner as those for the N_{agg} scaling relation. The β constant was evaluated from a log-log plot of R_c versus N_{PS} for a N_{PANa} value of 10 units and was found to be -0.22. The α constant was a function of the PS block length; they were 0.45, 0.46, and 0.45 for PS block lengths of 630, 660, and 2300 units. The average value (0.45) was used to evaluate the scaling relation. The main part of Figure 5.8 shows the plot of R_c as a function of $N_{PANa}^{0.5}N_{PS}^{-0.2}$. The solid and dotted lines correspond to the linear regression having a correlation coefficient of 0.95 and the 95% confidence limits, respectively. The intercept and slope of the line were -0.03 and 2.4, respectively. It is to be expected that the correlation coefficient for scaling relations involving the radius are better than those involving N_{agg} , since the calculation of R_c involves the cube root of N_{agg} (eq.2).

For the present block ionomer system, the scaling relations of N_{agg} and R_c were found to depend significantly on the length of the PS block length. The theory of Nagarajan and Ganesh⁵⁸ has predicted a significant dependence on the micellar parameters on the soluble block for systems in which the solvent is very good for the soluble block. This appears to be applicable to the present case, where THF is a good solvent for PS. The micellar parameters for PEO-b-PPO block copolymers in water were modeled in that theory.⁵⁸ It was found that N_{agg} and R_c scaled as $N_{agg} \propto N_{PPO}^{0.73}N_{PEO}^{-0.51}$ and $R_c \propto N_{PPO}^{0.73}N_{PEO}^{-0.17}$. The magnitude of the dependence on the length of the soluble block (PEO) was found to be similar to the present system ($N_{agg} \propto N_{PANa}^{0.5} N_{PS}^{-0.6}$ and $R_c \propto N_{PANa}^{0.5} N_{PS}^{-0.6}$).

The scaling relation of another micellar parameter, the surface area per chain (S/N_{agg}), calculated from eq. 3 was also investigated. It was found that S/N_{agg} was

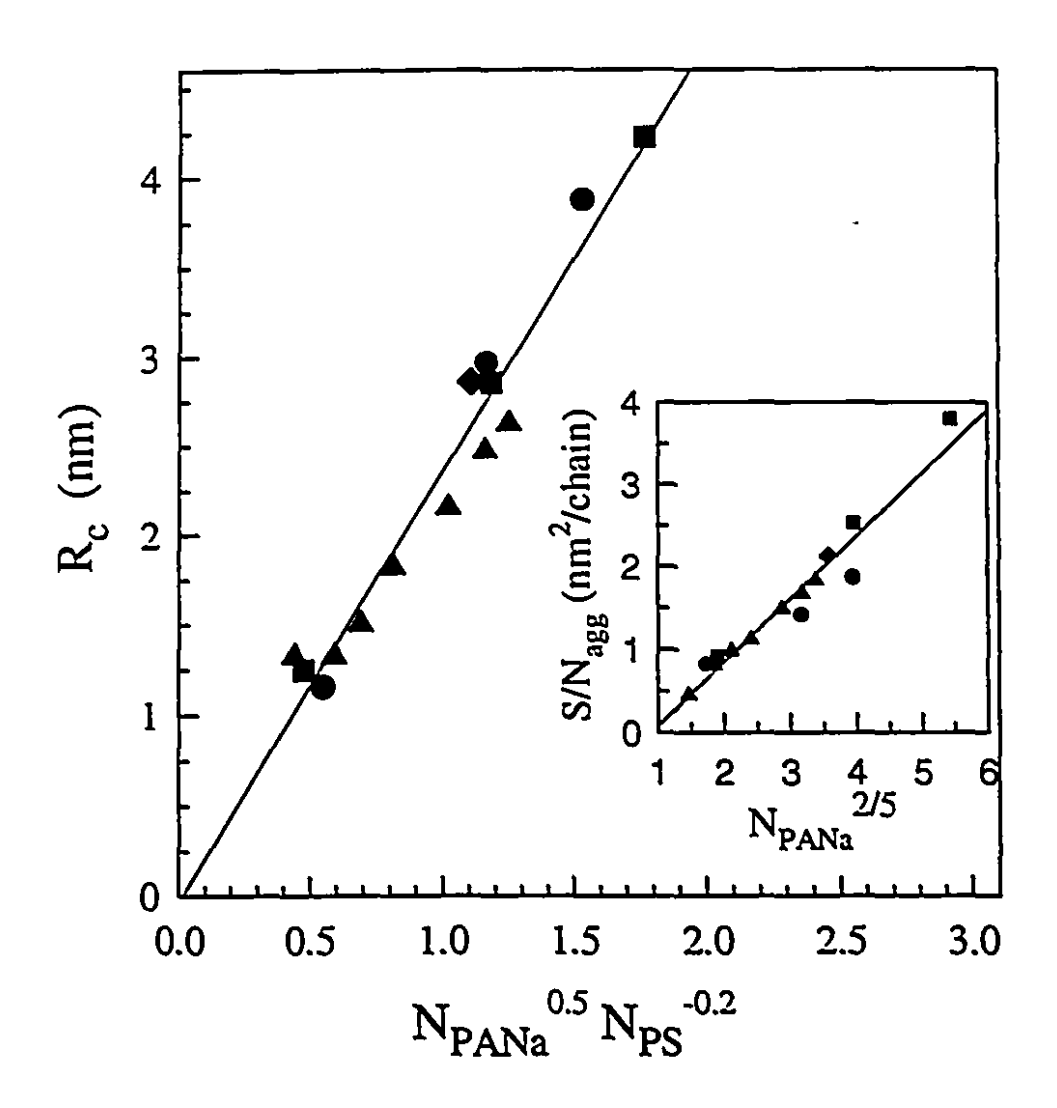


Figure 5.8. Calculated core radii for the PS(x)-b-PANa(y) samples investigated in THF plotted as a function of the PS and PANa block lengths for the series with PS block lengths of 190 (\spadesuit), 630 (\spadesuit), 660 (\spadesuit) and 2300 (\blacksquare) units. The inset is a plot of the surface area per chain as a function of N_{PANa}^{2/5}.

proportional to N_{PANa}^{2/5}, as predicted by the star model.⁴⁹ The inset of Figure 5.8, shows this scaling relation, in which the regression coefficient was 0.94. The intercept and slope of the line were -0.68 and 0.76, respectively. From this result, it can be seen that the soluble (PS) block length has no effect on the surface area per chain values.

The micellization of similar block ionomers has been investigated in a previous SAXS study.⁴¹ The block ionomers were composed of PS blocks attached to either poly(cesium acrylate) (PACs) or poly(cesium methacrylate) (PMACs). The samples were measured in toluene at a concentration of ca. 0.05 g/mL which was much higher than those used in the present SLS study (ca. 2 - 0.02 mg/mL). The composition of several of these block ionomers was identical to those given in Table 5.6, with the exception that a Cs counterion was used in the samples studied by SAXS.

The N_{agg} values for the block ionomers as determined by both SLS and SAXS are given in Table 5.7. In general, satisfactory agreement was obtained between the two methods with the exception of two samples. For instance, the N_{agg} value for PS(190)-b-PACs(24) was found to be significantly smaller by SAXS than by SLS. The lower value by SAXS is probably due to the fact that a spherical morphology was assumed in the calculations, whereas by SLS it was suggested that the sample most likely has a nonspherical morphology. The PS(2300)-b-PANa(69) sample was found to be significantly larger by SAXS compared to that evaluated by SLS. This difference is not fully understood at this time but may be related to sample preparation conditions. It should also be noted that the present study found a strong influence of the soluble block length on N_{agg}, while by SAXS the N_{agg} were found to be independent of the PS block length. Excluding these two samples, a plot of N_{agg} values determined by SLS versus those determined by SAXS had a slope close to unity (1.1) when the linear regression was passed through the origin (graph not shown).

Table 5.7. Comparison of Aggregation Numbers Determined by SLS and SAXS⁴¹

Composition	SLS	SAXS	
	(Na, THF)	(Cs, Toluene)	
PS(190)-b-PA(10)-Na or Cs	130	120	
PS(190)-b-PA(24)-Na or Cs	590	88	
PS(630)-b-PA(4.2)-Na or Cs	20	34	
PS(630)-b-PA(18)-Na or Cs	79	86	
PS(630)-b-PA(31)-Na or Cs	100	140	
PS(2300)-b-PA(69)-Na or Cs	41	110	

5.4. CONCLUSIONS.

The aggregation of two block copolymer series, PS(660)-b-PANa(x) and PS(660)-b-PAA(x), was investigated by SLS, SEC and DLS. The cmc's were determined for the salt form in toluene, THF and chloroform and for the acid form in toluene. These values were found to decrease as the insoluble block length increased. In general, the cmc values ranged from 1×10^{-7} to 5×10^{-9} M. The a and b constants in the relation log cmc = a $N_{PANa}^{1/3} + b$, were determined for these systems. The value of the a constant for the block ionomer system was relatively small (ca. -0.6) which is reflected in a weak dependence of the cmc on the PANa block length. As a consequence, very little

segregation was found in the molecular weight distributions of the block copolymers present as single chains in solution and those in the micelle fraction.

For the present systems as well as for several other block copolymer micelles, the a and b constants were correlated to the estimated interaction parameters between the polymer forming the core and the solvent, $\chi_{core-sol}$. It was found that the magnitudes of the a values were proportional to the $\chi_{core-sol}$ values, while the b values were inversely proportional to the $\chi_{core-sol}$ values. This result shows that when the interaction between the polymer forming the micelle core and the solvent is strong (large incompatibility), the dependence of the cmc on the insoluble block length is weak (small absolute value of a) and the cmc values are low (small b value).

The mixed micelle model describes the cmc values for block copolymers which have collapsed insoluble blocks. For insoluble blocks which have lengths less than the minimum length required for collapse, the CML concept seems valid. These chains, which are ca. 2 to 3 units long, are expected to have cmc's which are larger than those assuming collapsed insoluble blocks.

Other aspects of aggregation such as the aggregation numbers, second virial coefficient values and the hydrodynamic radii were also investigated. The trends in the aggregation numbers with increasing insoluble block lengths were found to opposite to observed for the cmc values. The hydrodynamic radii for PS(660)-b-PANa(x) in toluene, THF and chloroform were found essentially to be the same, since the expansion of PS in these solvents is expected to be similar.

The effect of the soluble block on the aggregation of three PS(x)-b-PANa(y) block ionomer series was investigated in THF. For these block ionomers, the PS block lengths were either 190, 630, 660 or 2300 units, attached to PANa blocks of various lengths, ranging from ca. 2.6 to 69 units. The aggregation numbers increased as the PANa block

length increased and decreased as the length of the soluble block increased. The aggregation numbers and core radii for these four series could be described by $N_{agg} \propto N_{PANa}^{0.5}N_{PS}^{-0.6}$ and $R_c \propto N_{PANa}^{0.5}N_{PS}^{-0.2}$, respectively. The surface area per chain was found to be proportional to $N_{PANa}^{2/5}$ as has been predicted by the star model.

5.5. ACKNOWLEDGMENTS.

We would like to thank Dr. Sunil Varshney who synthesized some of the block copolymers in connection with another project. This work was supported by the Natural Science and Engineering Research Council of Canada (NSERC). K. K. would also like to thank FCAR (Le Fonds pour La Formation de Chercheurs et L'Aide à la Recherche) and NSERC for scholarship funding.

5.6. REFERENCES

Myers, D. Surfaces, Interfaces, and Colloids. Principles and Applications; VCH Publishers: New York, 1991.

- Langevin, D. In Reverse Micelles Biological and Technological Revelance of Amphiphilic Structures in Apolar Media; Luisi, P. L.; Straub, B. E., Eds. Plenim Press: New York, 1982, p. 287.
- (a) Petrak, K. British Polymer Journal 1990, 22, 213. (b) Kataoka, K.; Kwon,
 G. S.; Yokoyama, M.; Okano, T.; Sakurai, Y. J. of Controlled Release 1993, 24,
 119.
- (a) Fendler, J. H.; Fendler, E. J., Catalysis in Micellar and Macromolecular Systems; Academic Press: New York, 1975.
 (b) Khmelnitsky, Y. L.; Levashov, A. V.; Klyachko, N. L.; Martinek, K. Russian Chemical Reviews 1984, 53, 319.
 (c) Luisi, P. L.; Giomini, M.; Pileni, M. P.; Robinson, B. H., Biochim. Biophys. Acta 1988, 947, 209.
- Price, C. In Development in Block Copolymers: Goodman, I., Ed.; Elsevier Applied Science: London, U.K., 1982; Vol 1, pp 39-80.
- Riess, G.; Hurtrez, G.; Bahadur, P. Encyclopedia of Polymer Science and Engineering, 2nd ed., Wiley: New York, 1985; Vol 2, pp 324-434.
- Selb, J.; Gallot, Y. In *Development in Block Copolymers*; Goodman, I., Ed.; Elsevier Applied Science: London, U.K., 1985; Vol 2, pp 27-96.
- Tuzar, Z.; Kratochvil, P. Surface and Colloid. Sci. Series, Matijevic Ed.; Plenum Press: New York, 1993; Vol 1, pp.1-83.

- Wilhelm, M.; Zhao, C. L.; Wang, Y.; Xu, R.; Winnik, M. A.; Mura, J. L.; Riess,
 G.; Croucher, M. D. Macromolecules 1991, 24, 1033.
- Nicholas, C. V.; Luo, Y-Z.; Deng, N.-J.; Attwood, D.; Collett, J. H.; Price, C.; Booth, C. Polymer 1993, 34, 138.
- Wanka, G.; Hoffmann, H.; Ulbricht W. Macromolecules 1994, 27, 4145.
- 12 Nakashima, K.; Anzai, T.; Fujimoto, Y. Langmuir 1994, 10, 658.
- 13 Sikora, A.; Tuzar, Z. Makromol. Chem. 1983, 184, 2049.
- ¹⁴ Vagberg, L.J. M.; Cogan, K. A.; Gast, A. P. *Macromolecules* 1991, 24, 1670.
- Quintana, J. R.; Villacampa, M.; Munoz, M.; Andrio, A.; Katime, I. A. Macromolecules 1992, 25, 3125.
- Quintana, J. R.; Villacampa, M.; Katime, I. A. Macromolecules 1993, 26, 601.
- 17 Price, C. Pure and Appl. Chem. 1983, 55, 1563.
- 18 Price, C.; Chan, E. K. M.; Stubbersfield, R. B. Eur. Polym. J. 1987, 23, 649.
- 19 Price, C.; Chan, E. K. M.; Stubbersfield, R. B. Eur. Polym. J. 1987, 23, 649.
- ²⁰ Zhou, Z.; Chu, B. J. Colloid Interface Sci. 1988, 126, 171.
- Price, C.; Stubbersfield, R. B.; El-Kafrawy, S.; Kendall, K. D. Bri. Polym J. 1989,
 21, 391.
- Quintana, J. R.; Villacampa, M.; Munoz, M.; Andrio, A.; Katime, I. A. Macromolecules 1992, 25, 3125.
- 23 Linse, P.; Malmstem, M. *Macromolecules* **1992**, 25, 5434.
- Zhou, Z.; Chu, B.; Peiffer, D. G. Macromolecules 1993, 26, 1876.
- Selb, J.; Gallot, Y. In *Polymeric Amines and Ammonium Salts*; Goethals, E. J. Ed.;
 Pergamon Press: New York, 1980; p. 205.

- Morishima, Y.; Itoh, Y.; Hashimoto, T.; Nozakura. S.-I. J. Polym. Sci., Polym. Chem. Ed. 1982, 20, 2007.
- (a) Cao, T.; Munk, P.; Ramireddy, C.; Tuzar, Z.; Webber, S. E. Macromolecules
 1991, 24, 6300. (b) Kiserov, D.; Prochazka, K.; Ramireddy, C.; Tuzar, Z.; Munk,
 P.; Webber, S. E. Macromolecules 1992, 25, 461.
- 28 Khougaz, K.; Astafieva, I.; Eisenberg, A. Macromolecules in press.
- 29 Astafieva, I.; Zhong, X. F.; Eisenberg, A. Macromolecules 1993, 26, 7339.
- Astafieva, I.; Khougaz, K.; Eisenberg, A. Macromolecules in press.
- Desjardins, A.; Eisenberg, A. Macromolecules 1991, 24, 5779.
- (a) Möller, M. Synth. Met. 1991, 41-43, 1159.
 (b) Ng Cheong Chan, Y.;
 Schrock, R. R.; Cohen, R. E. J. Am. Chem. Soc. 1992, 114, 7295.
 (c) Moffitt,
 M.; McMahon, L.; Pessel, V.; Eisenberg, A. Chem. Mater. 1995, 7, 1185.
- Tuzar, Z.; Konak, C.; Stepanek, P.; Kratochvil, P.; Prochazka, K. Polymer 1990, 31, 2118.
- Khougaz, K.; Gao, Z.; Eisenberg, A. Macromolecules 1994, 27, 6341.
- 35 Gao, Z.; Eisenberg, A. *Macromolecules* **1993**, *26*, 7353.
- 36 Linse, P. Macromolecules 1994, 27, 6404.
- Elias, H. G., In Light Scattering from Polymer Solutions; Huglin, M. B., Ed.;
 Academic Press: New York, 1972, Chapter 9.
- Desjardins, A.; van de Ven, T. G. M.; Eisenberg, A. *Macromolecules* 1992, 25, 2412.
- Zhong, X. F.; Varshney, S. K; Eisenberg, A. Macromolecules 1992, 25, 7160.
- 40 Gao, Z.; Zhong, X. F.; Eisenberg, A. Macromolecules 1994, 27, 794.

- Nguyen, D.; Varshney, S. K.; Williams, C. E.; Eisenberg, A. Macromolecules 1994, 27, 5086.
- Nguyen, D.; Williams, C. E.; Eisenberg, A.; Macromolecules 1994, 27, 5090.
- Nguyen, D.; Zhong, X. F.; Williams, C. E; Eisenberg A. Macromolecules 1994, 27, 5173.
- Khougaz, K.; Nguyen, D.; Williams, C. E.; Eisenberg, A. J. of Can. Chem in press.
- 45 Schwab, F. C.; Hellwell, L. J. Ind. Eng. Chem. Prod. Res. Dev. 1984, 23, 435.
- Phoon, C. L.; Higgins, J. S.; Burchard, W.; Peiffer, D. G. Makromol. Rep. 1992,A29, 179.
- ⁴⁷ Zhou, Z.; Chu, B.; G. Wu; Peiffer, D. G. Macromolecules 1993, 26, 2968.
- ⁴⁸ Zhou, Z.; Peiffer, D. G.; Chu, B. *Macromolecules* **1994**, 27, 1428.
- (a) Zhulina, E. B.; Birshtein, T. M. Polymer Science USSR 1985, 27, 570.
 (b) Halperin, A. Macromolecules 1987, 20, 2943.
- Brandup, J., Immergut, E.H., Eds. *Polymer Handbook*; 3rd ed., John Wiley and Sons: New York, 1989.
- Huglin, M. B. Ed. Light Scattering from Polymer Solutions; Academic Press: New York, 1972.
- 52 Zimm B. H., J. Chem. Phys. 1948, 16, 1099.
- Benoit, H.; Froelich, D. In Light Scattering from Polymer Solutions; Huglin, M.
 B., Ed.; Academic Press: New York, 1972; Chapter 11.
- Kratochvíl, P. Classical Light Scattering from Polymer Solutions; Jenkins, A. D.,
 Ed.; Elsevier Science Publishers: New York, 1987.
- (a) Selb, J.; Gallot, Y. Makromol. Chem. 1981, 182, 1491. (b) Hilfiker, R.; Chu,
 B.; Zhongde, X. J. Colloid Interface Sci. 1989, 133, 176.

- Brown, W. Dynamic Light Scattering: The Method and Some Applications;
 Oxford University Press: N. Y., 1993.
- Wilhelm, M.; Zhao, C. L.; Wang, Y.; Xu, R.; Winnik, M. A.; Mura, J. L.; Riess;
 G., Croucher, M. D. *Macromolecules* 1991, 24, 1033.
- 58 Nagarajan, R.; Ganesh, K. J. Chem. Phys. 1989, 90, 5843.
- Barton, A. F. M. Handbook of Solubility Parameters and other Cohesion Parameters; CRC Press: Boca Raton, Florida, 1983.
- Prausnitz, J. M.; Lichtenthaler, R. N.; Gomes de Azevedo, E. Molecular

 Thermodynamics of Fluid-Phase Equilibria; Prentice-Hall Inc: Englewood Cliffs,

 1986.
- Bicerano, J. *Prediction of Polymer Properties*; Marcel Dekker: New York, 1993, Chapter 5.
- 62 Zhong, X. F.; Eisenberg, A. Macromolecules 1994, 27, 1751.
- Appelt, B.; Meyerhoff, G. Macromolecules 1980, 13, 657.
- Flory, P. J. *Principles of Polymer Chemistry*; Cornell University Press: Ithaca, New York, 1953.
- Feng, D.; Wilkes, G. L.; Stark, J.E.; Lier, C. M. J. Macromol. Sci. Chem. 1989, A26, 1151.
- Venkateshwaran, L. N.; York, G. A.; DePorter, C. D.; McGrath, J. E.; Wilkes,G.L. Polymer 1992, 33, 2277.
- 67 Bates, F.S.; Fredrickson, G. H. Annu. Rev. Phys. Chem. 1990, 41, 525.
- Hashimoto, T.; Fujimura, M.; Kawai, H. Macromolecules 1980, 13, 1660.
- (a) Leibler, L. Macromolecules 1980, 13, 1602. (b) Fredrickson, G. H.; Helfand,
 E. J. Chem. Phys. 1987, 87, 697.

Whitmore, M. D.; Noolandi, J. Macromolecules 1985, 18, 657.

Effect of the Degree of Neutralization on the Micellization of Block Ionomers

ABSTRACT

The effect of neutralization on the micellization of polystyrene-b-poly(acrylic acid) (PS-b-PAA) was investigated by static light scattering (SLS) and small-angle X-ray scattering (SAXS). The block copolymers, present initially in single chain form in either dioxane or benzene/methanol (90/10 (v/v)), were neutralized to different degrees by the addition of cesium hydroxide dissolved in methanol. The solutions were simultaneously monitored by SLS. It was found that micelle formation began near 5% neutralization. The normalized scattered light intensity at 90° (I₉₀/c) increased dramatically in the neutralization range between ca. 10 and 60%. For neutralization degrees between 60 and ca. 100%, I₀₀/c did not change significantly with a further increase in the percent of neutralization. In the second part of the study, two block copolymers, PS(600)-b-PAA(34) and PS(600)-b-PAA(45) were prepared from benzene/methanol (90/10 (v/v)) with different degrees of neutralization: 5, 25, 60, 100 and 150%. The resulting solutions were freeze dried and the dried samples were redissolved in toluene. These samples were investigated by SLS and SAXS. By SLS, the aggregation numbers (Nagg) were found to be the same between 5 and 60% neutralization. An increase in Nagg was observed in going from 60 to 100%; i.e., Nagg increased from 82 to 92 for PS(600)-b-PAA(34), and from 79 to 110 for PS(600)-b-PAA(45). The N_{agg} values for the two block copolymers at 150% neutralization were found to be the same as those for 100% neutralization. The core radii values (R_c) were measured for the neutralized PS(600)-b-PAA(45) samples at 0.05 g/mL in toluene by SAXS. The R_c values increased from 5 to 60% neutralization, remained constant from 60 to 100%, and increased again in the range from 100 to 150 %. The results are explained by dynamic considerations. For low percent neutralization, between 5 and 60%, the micelles and single chains are proposed to be in a dynamic equilibrium state. For higher percent neutralization, between 60 and 100 %, the dynamics are probably much slower.

6.1. INTRODUCTION

Block copolymers tend to form micellar structures when dissolved in a solvent which is selective for one of the blocks. Increasing interest has focused on the formation and characterization of these micelles, and the phenomenon has been reviewed. 1-5 Recently, considerable research has been performed on nonionic block copolymers which micellize in aqueous media 6-12 or in organic solvents. 13-17 Research on the micellization of ionic block copolymers, as compared to that on nonionic block copolymers, is more scarce. Ionic block copolymers, due to their amphiphilic nature, are able to form either polyelectrolyte or ionomer micelles, depending on the nature of the solvent. For instance, in an aqueous environment, polyelectrolyte micelles are formed with a hydrophobic core and a charged ionic corona. Several studies have focused on the characterization of these micelles. 4,18-20 In organic solvents, ionomer micelles are formed with an ionic core and a nonionic corona. The latter micelle structure will be the focus of the present chapter.

Block ionomer micelles which are composed of a nonionic corona of polystyrene and an ionic core of either neutralized poly(methacrylic acid) or poly(acrylic acid), or

quarternized poly(4-vinylpyridine), have been extensively studied in this laboratory by several techniques. ²¹⁻³⁰ The results of some of these studies were given in chapter 2. It was shown that block ionomer micelles composed of polystyrene-b-poly(metal methacrylate) form very stable micelles. ²¹ A systematic study investigated the dependence of the block copolymer composition on the micellar characteristics by size exclusion chromatography (SEC), ²¹ DLS, ²² and viscometry. ²¹ The method of micelle preparation was found to influence significantly the micelle characteristics. For instance, the neutralization medium had an effect on the hydrodynamic radius (R_h) of the micelles. The block copolymer neutralized in benzene/methanol was found to have a larger R_h than that in dioxane. It should be noted that both solvents dissolved the acid copolymer as single chains. Also, it was found that neutralized samples which were recovered by freeze drying and redissolved had a larger aggregation number (N_{agg}) and R_h compared to those which were formed directly upon neutralization. ²²

One parameter which has not yet been investigated is the effect of different degrees of neutralization on the micellar properties of block ionomers. This study is the focus of the present chapter in which polystyrene-b-poly(acrylic acid) is neutralized to different amounts. The samples were measured by using two complementary scattering techniques, static light scattering and small-angle X-ray scattering. Information on the weight-average molecular weight, radius of gyration, second virial coefficient, and core radius was obtained by these two methods in combination. This chapter will first discuss the neutralization of the acid copolymer with cesium hydroxide as a function of the solvent and the ionic block length. The results on samples prepared with different degrees of neutralization as investigated by SLS and SAXS will then be presented and discussed.

6.2. EXPERIMENTAL

6.2.1. Materials

The block copolymers, polystyrene-b-poly(acrylic acid), were prepared by sequential anionic polymerization; the details are given in ref (21). For convenience, a summary of the synthesis will be given here. The copolymers were synthesized by sequential anionic copolymerization of the styrene monomer followed by tert-butyl acrylate. The initiator was the reaction product of sec-butyllithium with a few drops of α methylstyrene. The polymerization was carried out in tetrahydrofuran (THF) at -78°C under an atmosphere of nitrogen. The apparatus employed for the polymerization allowed the withdrawal of the reaction mixture in the course of the synthesis. Therefore, for a given constant polystyrene block length, a series of diblocks was obtained with poly(tertbutyl acrylate) segments of different lengths. Aliquots of the reaction mixtures were withdrawn for characterization after the polystyrene block was formed and every time following addition of the second monomer. Polystyrene-b-poly(acrylic acid) (PS-b-PAA) was obtained by acid-catalyzed hydrolysis of the tert-butyl acrylate segments in toluene at 80°C using p-toluenesulfonic acid as the catalyst. The PS-b-PAA was recovered and purified by repeated precipitation in cold methanol. The samples were then dried in a vacuum oven at 50°C for 48 h. The composition of the copolymers was determined by either FT-IR using copolymers in the ester form or by titration of the acid. The molecular weight of the polystyrene block was determined with a precision of \pm 5% by size exclusion chromatography in THF using narrow molecular weight polystyrene standards. The polydispersity index of the PS block was 1.10.

For neutralization of PS-b-PAA, a known amount of the dried copolymer was dissolved in benzene/methanol (90/10 (v/v)) at a concentration of 2% (w/w). The acid samples were neutralized by dropwise addition of CsOH in methanol to the solutions. For two block copolymers; PS(600)-b-PAA(34) and PS(600)-b-PAA(45), samples with

different degrees of neutralization were prepared, i.e. 5, 25, 60, 100 and 150 %, by addition of different amounts of CsOH/methanol. The solutions were stirred for 1 to 2 hours, and the diblock ionomers were recovered by freeze drying. The samples were then further dried at 60°C for 48 h. under vacuum. Abbreviations are used to indicate the copolymer composition; for example, PS(600)-b-PACs(34) represents a polystyrene chain of 600 units joined to a poly(cesium acrylate) chain of 34 units; PAA denotes poly(acrylic acid).

6.2.2. Sample Preparation for SLS

Three PS-b-PAA block copolymers, PS(600)-b-PAA(45), PS(600)-b-PAA(34) and PS(600)-b- PAA(13), were prepared by dissolving the copolymer either in dioxane or in a benzene/methanol mixture (90/10 (v/v)). The initial concentrations of the solutions depended on the block copolymer composition, and they ranged from ca. 2.5×10^{-3} to 6×10^{-3} 10⁻³ g/g. The solvent and polymer solutions were filtered through 0.2 and 0.45 µm PTFE filters, respectively, into scintillation vials which were used for the light scattering measurements. Titration curves were obtained by adding dropwise a predetermined amount of CsOH/methanol to the PS-b-PAA block copolymer solutions. concentration of CsOH used was 1.0, 0.44 M and 0.18 M for PAA block lengths of 45, 34 and 13 units, respectively. The amounts of CsOH/methanol added did not represent a significant volume as compared to the total volume of the solution. For instance, to achieve 100% degree of neutralization of PS(600)-b-PAA(45) in dioxane (10 mL), 144 μL of CsOH/methanol was required. This amount of CsOH/methanol represents ca. 1.4 % of the total volume. It should be noted that these values are given for illustrative purposes only, since the actual solution volume is changing during the course of the measurement, as will be explained below. After each addition of CsOH/methanol, the solutions were stirred for ca. 10 min. and the scattered light intensity was measured five times; the average value was used. Typical average percent error in the scattered intensity at 90° was ca. 3 %. For higher degrees of neutralization, the scattered intensity increased above the detection limit of the detectors, and thus the polymer solutions were diluted by the addition of solvent. For the two samples PS(600)-b-PAA(45) and PS(600)-b-PAA(34), which were prepared with specific degrees of neutralization (5, 25, 60, 100, 150%), the weight-average molecular weight (M_w), radius of gyration (R_g), and second virial coefficient (A₂) were determined by constructing a Zimm plot. A minimum of four concentrations was used for each Zimm plot analysis.

6.2.3. Static Light Scattering and Specific Refractive Index Increment (dn/dc) Measurement

Light scattering experiments were performed using a DAWN-F multiangle laser photometer (Wyatt Technology, Santa Barbara, CA) at 25°C, which operates at 15 angles, from 26 to 137°, and is equipped with a He-Ne laser (632.8 nm). Data acquisition and analysis utilized the DawnF and SkorF software, respectively. Zimm plots were processed with Aurora software. The specific refractive index increments (dn/dc) were determined using the Wyatt/Optilab 903 interferometric refractometer and accompanying software (Dndc 2.01) at a wavelength of 630 nm. The cell constant was determined by calibration with different concentrations of sodium chloride (99.999%, Aldrich) solutions. Eight to ten concentrations were measured for each dn/dc determination. The dn/dc values were obtained from the slope of a plot of refractive index versus polymer concentration. The dn/dc values for PS-b-PAA and PS-b-PACs were found to be 0.110 mL/g, which is the same as the literature values for polystyrene in toluene.31 It should be noted that, in general, for block copolymers with different refractive indices, an apparent weight-average molecular weight (Mwapp) is obtained by SLS.32 However, in the present case, M_{w.app} is close to the true M_w values since the refractive index increments of the block copolymers and of the soluble block in toluene were the same. This result is probably due to the small weight fraction of the insoluble block.

6.2.4. Sample Preparation for SAXS

Micellar solutions were obtained by dissolving the freeze-dried powder in toluene at a concentration of 5% (0.05 g/mL). For the SAXS experiment, the solution was enclosed in a 1.5 mm thick cell with Kapton® windows. The SAXS measurements were carried out at room temperature.

6.2.5. SAXS Measurement

The small-angle X-ray scattering experiments were performed at the D22 station of the LURE-DCI synchrotron radiation source (Orsay, France). A description of the spectrometer has been published elsewhere.³³ It is a specialized spectrometer equipped with double crystal, fixed exit monochromator providing a beam of a narrow energy range tunable from 4 to 15 KeV (0.3 to 0.08 nm). The size of the beam at the sample was about 1 mm². The scattered X-rays were detected with a Xe-CO₂ gas filled, one dimensional position sensitive detector with a resolution of 217 μ m. Samples were studied in the angular q range from 0.06 nm⁻¹ to 3.0 nm⁻¹ (q = 4 π sinθ / λ , where θ is one half the scattering angle, and λ is the X-ray wavelength). The resulting scattering intensities were corrected for the incident beam decay, sample thickness and transmission. The background scattering from the solvent was also subtracted. The q resolution is of the order of 0.003Å⁻¹.

6.3. RESULTS AND DISCUSSION

The Results and Discussion section is divided into three parts. In the first part, the effect of neutralization on the micellization of PS-b-PAA is discussed qualitatively. Neutralization was followed in two different solvents, dioxane and a benzene/methanol mixture for three different block copolymers. The aim was to examine the effect that

increasing degree of neutralization has on the solvent quality for the block copolymer, in particular for the block forming the micelle core. In the second and third parts, more quantitative results are presented which were obtained by SLS and SAXS, respectively. The samples investigated were prepared with specific degrees of neutralization and measured in toluene which is a non-solvent for PAA and PACs.

6.3.1. Titration of PS-b-PAA with CsOH/MeOH

Figure 6.1 summarizes some of the results obtained in this study for the titration of PS(600)-b-PAA(45) as well as the results for this sample with different degrees of neutralization. The aggregation numbers (N_{agg}) (Figure 6.1a) and core radii (R_c) (Figure 6.1b) will be discussed in sections 6.3.2 and 6.3.3. First, a typical titration curve obtained for PS(600)-b-PAA(45) dissolved in dioxane, which is given in Figure 6.1b, will be addressed. For this sample, the scattered intensity at 90° was normalized to the polymer concentration and measured as a function of the percent neutralization of the PAA chains with CsOH/methanol. It should be noted that PS-b-PAA in dioxane is present as single chains, since the solvent is good for both blocks. However, upon neutralization, the solubility of the partially neutralized PAA block decreases, and thus the chains associate to form the micelle core.

It is interesting to establish at which percent neutralization of the PAA chains micellization starts from a solution of single chains. This value can be determined by examining the inset of Figure 6.1b, which shows the normalized scattered intensity (I₉₀/c) as a function of the percent neutralization near the origin of the plot. It was found that I₉₀/c was constant below ca. 5% neutralization, after which the value began to increase. Thus, micellization occurred in the block copolymer when ca. 2 of the 45 PAA units per chain (i.e. ca. 5%) were converted to the salt form.

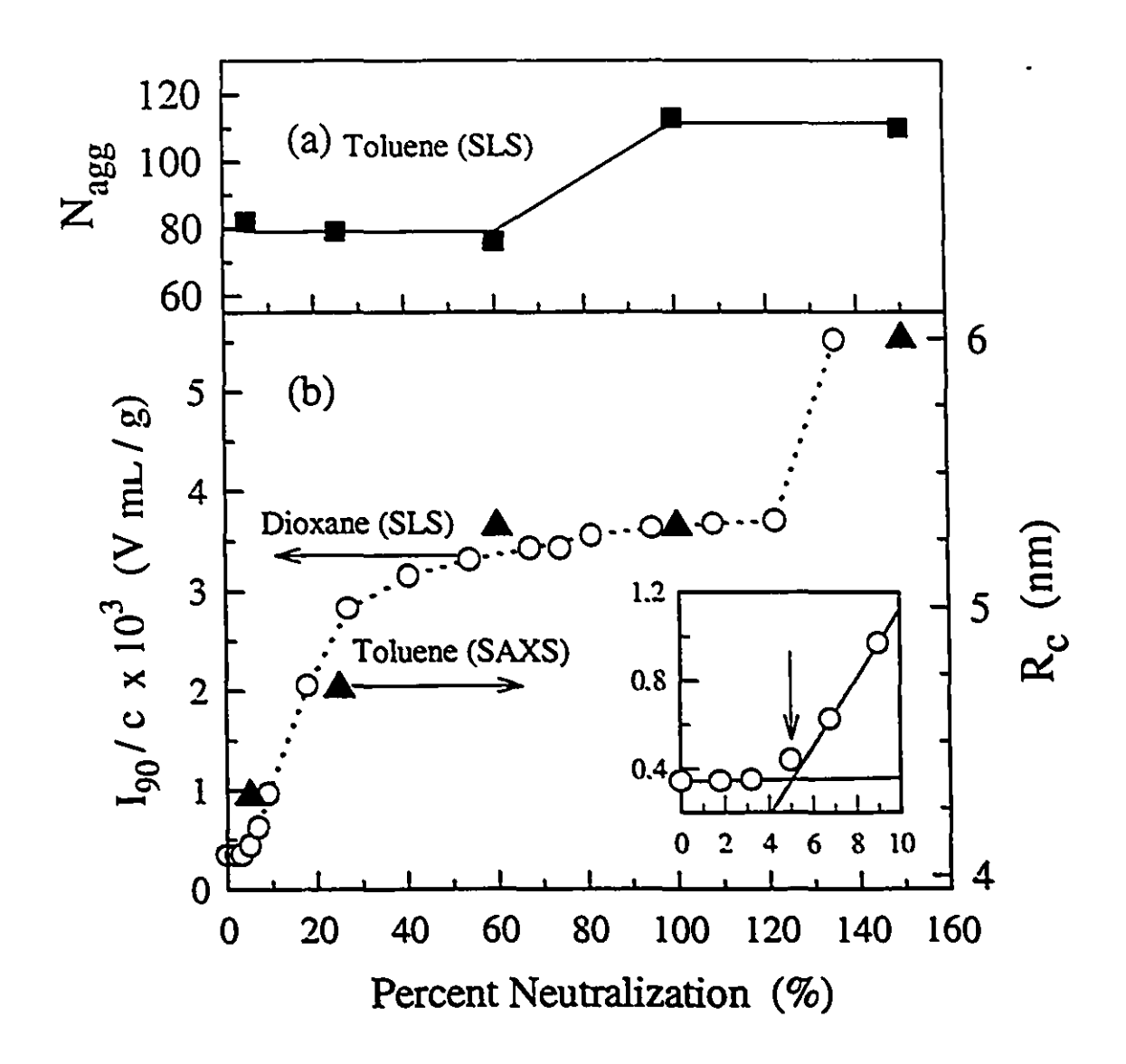


Figure 6.1. Summary of results for PS(600)-b-PAA(45) as a function of percent neutralization; (a) aggregation numbers (N_{agg}) for freeze dried samples measured in toluene; (b) core radii (R_c) for freeze dried samples measured in toluene (Δ) and scattered light intensity at 90° normalized to polymer concentration (I_{90}/c) as a function of the percent neutralization with CsOH/methanol measured in dioxane (O). The inset shows I_{90}/c for low percent of neutralization. The lines are shown as a guide for the eye.

A similar titration was performed for PS(600)-b-PAA(13) and PS(600)-b-PAA(34) in benzene/methanol (90/10 (v/v)), with the results shown in Figure 6.2. In this solvent mixture, the block copolymers are also initially present as single chains. The titration curve will be discussed in greater detail later in this section. It should be noted that the first increase in I₉₀/c also occurred at low degrees of neutralization for both block copolymers, specifically at ca. 7% (see inset of Figure 6.2). This value was found to be independent of the PAA block length.

Once micellization has begun, it is of interest to examine the effects of further addition of CsOH/methanol on I₉₀/c. For PS(600)-b-PAA(45) in dioxane (Figure 6.1b), it was observed that above 5%, I₉₀/c increased rapidly with increasing degree of neutralization. For instance, between 10 and 60% neutralization, the normalized scattered intensity increased by a factor of ca. 6. A further increase in the degree of neutralization resulted in a less dramatic increase in the scattered intensity. For instance, from 60 to 100% neutralization, the scattered intensity increased by only 10 %. However, at 135% neutralization, I₉₀/c increased significantly. This latter increase may arise from the solubilization of the excess neutralizing agent, CsOH, in the micelle core, and will be discussed in section 6.3.3.

The shape of the titration curve can give information on the solvent environment for the block copolymer with increasing degree of neutralization. First, it should be noted that for low degrees of neutralization, the micelle cores are expected to be swollen with dioxane and methanol. This occurs because the core is composed of PAA chains which are only partially neutralized. The dioxane and methanol would preferentially solvate the unneutralized sections of the PAA block while the block copolymer is in the micellar form. However, as the percent neutralization increases, the high ionic content of the core is expected to create an unfavorable environment for dioxane and methanol. As a result, these solvents would be expelled progressively from the micelle core. Consequently, it can be suggested that the micelle cores are more swollen at low degrees of neutralization

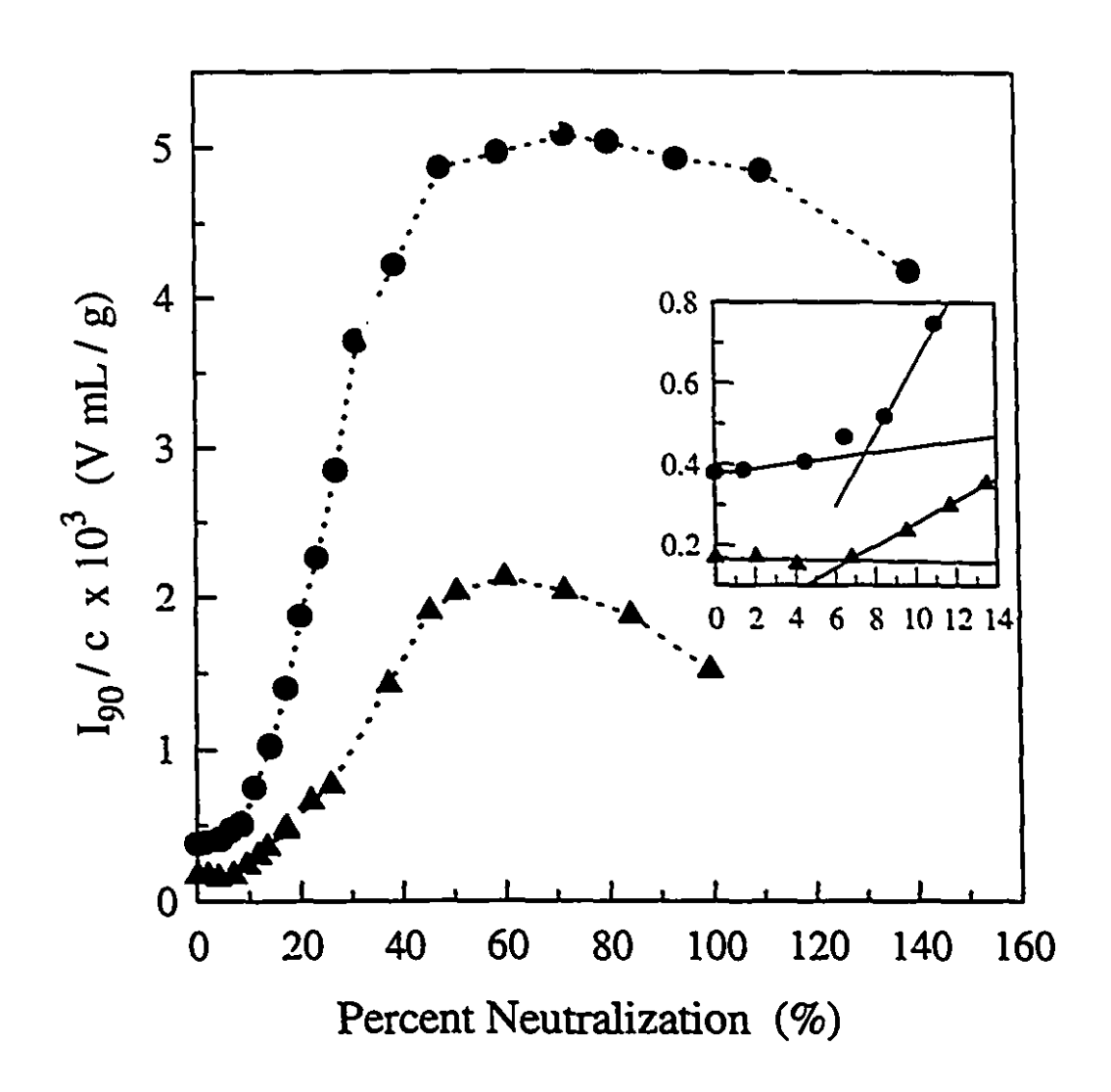


Figure 6.2. Scattered light intensity at 90° normalized to polymer concentration (I_{90}/c) as a function of the percent neutralization with CsOH/methanol in benzene/methanol (90/10 (v/v)) for PS(600)-b-PAA(34) (\bullet) and PS(600)-b-PAA(13) (\triangle). The lines are shown as a guide for the eye.

than those at higher degrees.

For low degrees of neutralization, the cmc values would be expected to decrease with increasing neutralization. This aspect can be understood because increasing the degree of neutralization results in the increase in the number of ionic groups per chain, and the association of ionic chains would be expected to be stronger than that of acid chains. Also, as a result of the increase in the number or concentration of ionic groups, the solvent quality for the core decreases. Therefore, micelles would form at a lower concentration. Since the cmc decreases, the increase in I₉₀/c at low degrees of neutralization can be attributed, in part, to an increase in the number of the micelles.

To relate I_{90}/c to the weight-average molecular weight (M_w) of the particles, M_w was evaluated for PS(600)-b-PAA(45) in dioxane for two degrees of neutralization, 7 and 50%. These measurements were performed by taking the samples which had been measured for the titration curve (Figure 6.1b) and diluting them with dioxane to obtain different concentrations. The results for these samples at different concentrations were represented as Zimm plots. The M_w values for the 7% and 50% neutralized samples were determined to be 1.6 x 10^5 and 9.3 x 10^5 g/mol, respectively. Thus, M_w increases by a factor of ca. 6 in this neutralization range.

The effect of using benzene/methanol (90/10 (v/v)) as the solvent medium for the neutralization process was investigated. As noted previously, for this solvent composition, the acid block copolymer is present as single chains, since benzene and methanol are good solvents for the PS and the PAA blocks, respectively. Thus, at low degrees of neutralization it would be expected that the methanol would solvate the unneutralized sections of the PAA block, in the same manner as dioxane and methanol discussed previously. Figure 6.2 illustrates the results obtained for two block copolymers, PS(600)-b-PAA(34) and PS(600)-b-PAA(13). The shape of the titration curve was similar to that of PS(600)-b-PAA(45) dissolved in dioxane (Figure 6.1b). However, for higher degrees of neutralization, i.e. above ca. 100% for PS(600)-b-PAA(34) and above

ca. 80% for PS(600)-b-PAA(13), further increase in the percent neutralization resulted in a slight decrease of I₉₀/c. At this point, the reason for the slight decrease is not fully understood.

6.3.2. SLS Results on Freeze Dried Samples

In order to relate the normalized scattered intensities as a function of the percent neutralization to the actual changes in the micelle aggregation numbers and sizes, samples for PS(600)-b-PAA(34) and PS(600)-b-PAA(45) with different degrees of neutralization, i.e. 5, 25, 60, 100, and 150 %, were prepared and investigated. The PS-b-PAA copolymers were dissolved in benzene/methanol (90/10 (v/v)) and CsOH/methanol was added dropwise in order to obtain micelles that have a low polydispersity in core sizes. The neutralized samples, which were recovered by freeze drying, consisted of micellar structures which were simply redissolved in toluene, a selective solvent for PS, and then characterized by SLS and SAXS. Thus, complications arising from the penetration of solvent in the micelle core are avoided.

The results for the SLS measurements of the copolymers dissolved in toluene are given in Table 6.1. The aggregation numbers (N_{agg}) were determined from the ratio of $M_{\rm w}$ of the micelles to that of a single chain. It should be recalled that the acid form of the block copolymer aggregates in toluene. It was found for PS(600)-b-PAA(34) that the aggregation numbers (N_{agg}) increased from 63 to 80, in going from 0% to 5% neutralization. Thus, the incorporation of just a few ionic groups along the PAA chain affects the micellization significantly. The aggregation numbers for 5, 25 and 60% neutralization were essentially constant at a value of ca. 82 ± 3 . A significant increase in N_{agg} was observed between 60 and 100% neutralization, i.e. from 81 to 92. The same trends in N_{agg} were observed for PS(600)-b-PAA(45). For instance, N_{agg} was ca. 79 ± 2 for the samples at 5, 25 and 60%, and N_{agg} increased from 76 to 110 between 60 and

Table 6.1. Results for Different Percent Neutralization for PS-b-PAA in Toluene.

Percent Neutralization (%)	M _w x 10 ⁻⁶ (g/mol)	N _{neg}	R _g (nm)	A_2 $\times 10^5$ mL mol $/ g^2$	R _c (nm)		
PS(600)-b-PAA(34)							
0	4.1	63	27	1.4			
5	5.1	80	26	1.0			
25	5.6	85	25	1.8			
60	5.5	81	26	1.4			
100	6.4	92	34	1.8			
150	6.5	93	29	1.3			
<u> </u>	PS(600)-b-PAA(45)						
5	5.4	82	24	0.67	4.3		
25	5.3	79	24	0.35	4.7		
60	5.3	76	24	0.94	5.3		
100	8.1	110	31	0.68	5.3		
150	7.9	110	29	0.42	6.0		

100%. Also, the N_{agg} values for both copolymers were measured for 150% neutralization and were found to be the same as those for 100% neutralization. This result shows that there is no effect c.: N_{agg} for neutralization levels above the stoichiometric amount. The results for PS(600)-b-PAA(45) are illustrated in Figure 6.1a.

The trends in the aggregation numbers with increasing percent neutralization can be examined by speculating on the dynamics of the block copolymer in the neutralization medium. The aggregation numbers fall into three regions, depending on the percent neutralization, i.e. between 5 and 60%, between 60 and 100%, and between 100 and 150% (Figure 6.1a). The region between 5 and 60% will be considered first. In the previous section, it was suggested that for low degrees of neutralization, the single chains and micelles were in a dynamic equilibrium state due to the solubilization of solvent in the micelle cores. As a result, micelle formation was expected to occur under equilibrium conditions. In this study, the aggregation numbers of the micelles recovered by freeze drying from this dynamic state were found to be independent of the degree of neutralization. The freeze dried samples, which were redissolved in toluene, would be expected to exist in a much less mobile state than those in benzene/methanol. This can be anticipated, since toluene is a non-solvent for the PAA block, and thus the micelle cores would not be swollen with solvent in contrast to the situation with methanol. Therefore, significant rearrangement of the micelles in the toluene solutions would not occur.

The dynamics of the system for the second region, ranging from 60 to 100% are believed to be considerably reduced compared to those for the lower degrees of neutralization. This can be understood by considering that an increase in the degree of neutralization of the core forming block reduces its solubility, resulting in micelle formation. As a result of the decreased solubility, the unfavorable solvent is progressively expelled from the core. This process increases the glass transition temperature (T_g) of the core, resulting in a decreased mobility in the core. In fact, when the temperature of measurement is below the T_g , the micelle core can be considered as "frozen". As a result

of some or all of these factors, the aggregation numbers for the redissolved freeze dried samples were found to increase with increasing percent neutralization between 60 and 100%.

In the third region, for degrees of neutralization between 100 and 150%, the aggregation numbers were the same as those at 100%. This result was expected, since a further increase in the neutralization above 100% would not change the ionic nature of the block copolymers appreciably.

The radius of gyration (R_g) and second virial coefficient (A_2) values determined by SLS for PS(600)-b-PAA(34) and PS(600)-b-PAA(45) are given in Table 6.1. For both block copolymers, it was found that the R_g values were essentially constant for the neutralization range of 0 to 60 %, and increased slightly for the samples at 100 and 150% neutralization. For instance, for PS(600)-b-PAA(34), the average R_g value for the samples at 0 to 60% neutralization was 26 ± 1 nm, and that for PS(600)-b-PAA(45) for the samples at 5 to 60% was 24 nm. For 100 and 150% neutralization, the R_g values for both samples were only slightly higher than those at lower degrees of neutralization, with a value of ca. 30 nm. The A_2 values did not exhibit any specific trends with the percent neutralization.

6.3.3. SAXS Results on Freeze Dried Samples

The core sizes for the neutralized PS(600)-b-PAA(45) samples were measured by SAXS. In general, for an assembly of scattering particles, the scattered intensity (I(q)) is the product of the particle shape factor (P(q)) and the structure factor (S(q)), which characterizes the spatial correlation of the scatterers. Since it is a product of two functions, it is often difficult to separate one from the other experimentally. In the present system, since the sizes of the spheres are so much smaller than the characteristic distances

between them, and since the contrast between the two media is substantial, the attribution is unambiguous.

The SAXS profiles showed a pronounced shape factor peak for samples at and above 5% neutralization. However, for the acid diblock, PS(600)-b-PAA(45), no shape factor features were observed due to the low contrast between the PAA and PS blocks. From the position of the minima of the shape factor, one can calculate the radius of the cores (R_c). A detailed description of the data analysis has been published elsewhere.²⁸

The core radii were found to increase with increasing percent neutralization from 5% to 60%; they remained constant from 60% to 100% neutralization and increased at 150% neutralization. The R_c values are summarized in Table 6.1. The trends in R_c with increasing degree of neutralization were similar to those of the I₉₀/c values for PS(600)-b-PAA(45) in dioxane. The results are compared in Figure 6.1b. From the R_c values, it can be suggested, that micelles begin to form between 0 and 5% neutralization, and that the cores continue to grow in size until 60% of the acid is neutralized. The initial growth in R_c accompanies the replacement of the protons in the acid diblock by the Cs⁺ ions, which are larger in size than the protons. The fact that R_c remained constant between 60 and 100% neutralization suggests that a preferred core size for the micelle has been attained. At 150% neutralization, the extra neutralizing agent enters the core in which the medium is already highly polar, thus increasing the core size. The solubilization of the excess cesium hydroxide in the micelle cores was also found to occur in PS(600)-b-PAA(45) neutralized in dioxane (Figure 6.1b). The solubilization of excess neutralizing agent in or near the ionic cores has also been suggested for many random³⁶ and telechelics ionomers.37

6.4. CONCLUSIONS

It was found that when single chains of PS-b-PAA were neutralized, they started to form micelles near 5% neutralization. The onset of micellization was almost identical for samples having a PS length of 600 units and PAA lengths of 45, 34 and 13 units. It was found that I₉₀/c increased for the block copolymers significantly in the range of 10 to 60% neutralization. For neutralization levels above 60%, the normalized scattered intensity did not change significantly with a further increase in the degree of neutralization. For certain degrees of neutralization above ca. 100% the solvent media were found to affect the I₉₀/c values, with an increase for dioxane, but a decrease for benzene/methanol solvents.

The block copolymers PS(600)-b-PAA(34) and PS(600)-b-PAA(45) neutralized with different degrees in benzene/methanol (90/10 (v/v)), freeze dried and redissolved in toluene were studied by SLS and SAXS. The results fell into three regions, depending on the percent neutralization. In the first region, for degrees of neutralization between 5 and 60%, the micelle cores were expected to be swollen with solvent, during the neutralization in benzene/methanol and the association which occurs would likely be dynamic. It was found that the Nagg values were constant, and the aggregation numbers did not depend on the percent of neutralization. The R_c values in this range increased due to the replacement of the protons with the Cs⁺ ions, which are larger in size. In the second region, for degrees of neutralization between 60 to 100%, dynamics are expected to be much slower. In that range, the Nagg values were found to increase with increasing percent neutralization and the R_c was found to be constant. The two results would suggest that the density of the micelle core increases in this range. Finally, at degrees of neutralization between 100 and 150%, the Nagg values were constant, showing no further dependence of the aggregation on the percent of neutralization. On the other hand, Rc increased due to the solubilization of the excess neutralizing agent into the ionic cores.

6.5. ACKNOWLEDGMENT

The authors would like to thank Dr. Sunil K. Varshney who synthesized the block copolymers in connection with another project as well as Dr. Joon-Seop Kim and Mr. Matthew Moffitt for very useful discussions. This work was supported by the Natural Sciences and Engineering Research Council of Canada (NSERC) and Le Fonds pour La Formation de Chercheurs et L'Aide à la Recherche (FCAR). K.K. and D.N. are grateful for scholarship funding provided from NSERC and FCAR.

6.6. DEDICATION

We would like to dedicate this work to professor Jim Guillet on the occasion of his seventieth birthday.

6.7. REFERENCES

- Selb, J.; Gallot. Y. In *Polymeric Amines and Ammonium Salts*; Goethals, E. J., Ed.; Pergamon Press: New York, 1980; pp. 205-21.
- Price, C. In *Development in Block Copolymers-I*; Goodman, I., Ed.; Elsevier Applied Science: London, 1982; pp. 39-80.
- Riess, G.; Hurtrez, G.; Bahadur, P. Encyclopedia of Polymer Science and Engineering; Kroschwitz, J.; Mark, H. F.; Bikales, N. M.; Overberger, C. G.; Menges, G., Eds.; Wiley: New York, 1985; Vol 2., pp. 324-434.
- Selb, J.; Gallot, Y. In *Development in Block Copolymers-II*; Goodman, I., Ed.; Elsevier Applied Science: London, 1985; pp. 27-96.
- Tuzar, Z.; Kratochvíl, P. In Surface and Colloid Science; Matijevic, E., Ed.; Plenum Press: New York, 1993; Vol 1, pp. 1-83.
- Kwon, G.; Naito, M.; Yokoyama, M.; Okano, T.; Sakurai, Y.; Kataoka, K.
 Langmuir 1993, 9, 945.
- Nicholas, C. V.; Luo, Y.-Z.; Deng, N.-J.; Attwood, D.; Collett, J. H.; Price, C.; Booth, C. Polymer 1993, 34, 138.
- 8 Caldérara, F.; Hruska, Z.; Hurtrez, G.; Lerch, J.-P.; Nugay, T.; Riess, G.
 Macromolecules 1994, 27, 1210.
- ⁹ Zhou, Z.; Chu, B. *Macromolecules* 1994, 27, 2025.
- Yang, Z.; Pickard, S.; Deng, N.-J.; Barlow, R. J.; Attwood, D.; Booth, C.
 Macromolecules 1994, 27, 2371.
- Kabanov, A. V.; Nazarova, I. R.; Astafieva, I.; Batrakova, E. V.; Alakhov, V. Y.;
 Yaroslavov, A. A.; Kabanov, V. A. Macromolecules 1995, 28, 2303.

- Nivaggioli, T.; Alexandridis, P.; Hatton, T. A.; Yekta, A.; Winnik, M. A. Langmuir 1995, 11, 730.
- Kiserow, D.; Chan, J.; Ramireddy, C.; Munk, P.; Webber, S. E. Macromolecules 1992, 25, 5338.
- Antonietti, M.; Heinz, S.; Schmidt, M.; Rosenauer, C. Macromolecules 1994, 27, 3276.
- 15 Siqueira, D. F.; Nunes, S. P.; Wolf, B. A. Macromolecules 1994, 27, 4561.
- Unal, H. I.; Price, C.; Budd, P. M.; Mobbs, R. H. Eur. Polym. J. 1994, 30, 1037,
- Villacampa, M.; Quintana, J. R.; Salazar, R.; Katime, I. Macromolecules 1995, 28, 1025.
- Morishima, Y.; Itoh, Y.; Hashimoto, T.; Nozakura, S.-I. J. Polym. Sci., Polym. Chem. Ed. 1982, 20, 2007.
- (a) Cao, T.; Munk, P.; Ramireddy, C.; Tuzar, Z.; Webber, S. E. Macromolecules
 1991, 24, 6300. (b) Kiserov, D.; Prochazka, K.; Ramireddy, C.; Tuzar, Z.; Munk,
 P.; Webber, S. E. Macromolecules 1992, 25, 461.
- Astafieva, I.; Zhong, X. F.; Eisenberg, A. Macromolecules 1993, 26, 7339.
- Desjardins, A.; Eisenberg, A. Macromolecules 1991, 24, 5779.
- Desjardins, A.; van de Ven, T. G. M.; Eisenberg, A. Macromolecules 1992, 25, 2412.
- Zhong, X. F.; Varshney, S. K; Eisenberg, A. Macromolecules 1992, 25, 7160.
- Khougaz, K.; Gao, Z.; Eisenberg, A. Macromolecules 1994, 27, 6341.
- ²⁵ Gao, Z.; Eisenberg, A. *Macromolecules* **1993**, 26, 7353.
- 26 Gao, Z.; Zhong, X. F.; Eisenberg, A. Macromolecules 1994, 27, 794.

- Nguyen, D.; Varshney, S. K.; Williams, C. E.; Eisenberg, A. Macromolecules 1994, 27, 5086.
- Nguyen, D.; Williams, C. E.; Eisenberg, A. Macromolecules 1994, 27, 5090.
- Nguyen, D.; Zhong, X. F.; Williams, C. E.; Eisenberg, A. Macromolecules 1994, 27, 5173.
- Nguyen, D.; Williams, C. E.; Eisenberg, A. To be Published.
- Brandup, J.; Immergut, E. H., Eds. *Polymer Handbook*; 3rd edition, John Wiley and Sons; New York, 1989.
- Benoit, H.; Froelich, D. In Light Scattering from Polymer Solutions; Huglin, M. B., Ed.; Academic Press: New York, 1972; Chapter 11.
- Dubuisson, J. M.; Dauvergne, J. M.; Depautex, C.; Vachette, P.; Williams, C. E.
 Nucl. Instr. Meth. Phys. Res. 1986, A246, 636.
- Williams, C. E. In Neutron, X-Ray and Light Scattering: Introduction to an Investigative Tool for Colloidal and Polymeric Systems; Lindner, P., Zemb, Th., Eds.; North-Holland: Amsterdam, 1991; p. 101.
- Williams, C. E. In Neutron and Synchrotron Radiation for Condensed Matter Studies I.; Baruchel, J., Hodeau, J.-L., Lehmann, M. S., Regnard, J.-R., Schlenker, C., Eds.; Springer-Verlag: Berlin, 1993; Chapter 10.
- Kim, J.-S.; Eisenberg, A. J. Polym. Sci.: Part B: Polym. Phys. 1995, 33, 197 and references therin.
- 37 Bagrodia, S.; Tant, M. R.; Wilkes, G. L.; Kennedy, J. P. *Polymer* 1987, 28, 2207.

CHAPTER 7

Distribution of Water in Solutions of Reverse Micelles of AOT and Block Ionomers in Toluene

ABSTRACT

The distribution of water between toluene and the ionic cores of sodium bis [2ethylhexyl]sulfosuccinate (AOT) and block ionomer reverse micelles was evaluated by ¹H chemical shift measurements of water at different temperatures. The block ionomer reverse micelles investigated were composed of a nonionic polystyrene (PS) block attached to an ionic block consisting of either poly (sodium methacrylate) (PMANa), poly(sodium acrylate) (PANa), poly(cesium acrylate) (PACs), or poly(4-vinylpyridinium methyl iodide) (P4VPMeI). The water content was described by the ratio R, defined as the molar ratio of the total amount of water to either the number of moles of surfactant for AOT, or to the number of moles of ionic repeat units for the block ionomers. It was found that for R = 6, the distribution coefficient of water (K) decreased in the following order for the different ionic groups: $COO^-Cs^+ > SO_3^-Na^+ \sim COO^-Na^+ >> N_{py}^+(Me)I^-$, where N_{py}^+ (Me)I- represents pyridine quarternized with methyl iodide. This trend is explained by the stronger interaction of water with the anionic reverse micelle systems compared to that with the cationic reverse micelle system. The distribution of water is therefore governed not only by the interactions between water and the solvent but the interactions between water and the micelle core are also a major contributing factor. The thermodynamics for the transfer process were determined from the temperature dependence of K. An entropy-enthalpy compensation appeared to exist in the water transfer process. For AOT and PS-b-PACs, the enthalpy (ΔH_t^0) and entropy (ΔS_t^0) of transfer were similar to those calculated for the transfer of water from a toluene phase to a bulk water phase. For PS-b-PANa, PS-b-PMANa and PS-b-P4VPMeI, ΔH_t^0 and ΔS_t^0 were found to be more negative. This result was attributed to the stronger interaction energy and greater amount of ordering of water. The mobility of different nuclei in the block ionomer micelles was probed by multinuclei relaxation measurements. It was found that the mobility of the water nuclei (1H , 2H , and ^{17}O) and the ^{23}Na counterion increased with R.

7.1. INTRODUCTION

Amphiphilic molecules such as low molecular weight surfactants or block copolymers can associate in aqueous or in organic solvents to form regular and reverse micelles, respectively. These micelles can serve as unique carrier vehicles due to their ability to solubilize compounds in their core. Regular micelles consist of a hydrophobic core and a hydrophilic corona, while reverse micelles consists of a hydrophilic core and a hydrophobic corona. Due to the polar nature of the core in reverse micelles, water can be easily solubilized into these micellar solutions. The solubilized water is distinct from bulk water in properties such as microviscosity, acidity, and polarity.^{1,2} Reverse micelles containing water are very important in areas such as the catalysis of small molecules^{2,4} and biopolymers, ^{1,5} as delivery systems, ⁶ and as models for the study of hydration in membranes and cells.⁴

A very well characterized surfactant forming reverse micelles is sodium bis(2-ethylhexyl)sulfosuccinate (AOT). This anionic surfactant consists of a double tailed alkyl

chain and a polar head group composed of a sulfonate ion, sodium counterion and two ether groups. The structure is given in Figure 7.1. The solubilized water in this reverse micelle system has been studied extensively by a variety of techniques such as calorimetry, 7.8 nuclear magnetic resonance (NMR), 9-12 Fourier-transform infrared spectroscopy (FT-IR), 13 fluorescence spectroscopy, 14 electron spin resonance (ESR), 15 and various scattering methods, including light scattering, 16 small angle X-ray (SAXS), 17 and small angle neutron scattering (SANS), 18

Figure 7.1. Structure of AOT

The size and physical properties of the hydrated reverse micelle depend specifically on the molar ratio of water to surfactant (R). For the AOT reverse micelles, it was found by several studies 10,15 that at low values of R, water is bound to the surfactant layer and is thus immobilized. As the amount of water is increased, i.e. when the hydration requirements of the surfactant head group are exceeded, water begins to form a water pool in the cores of the reverse micelles. The first appearance of free water in the micelle cores indicates the transition into the water in oil (W/O) microemulsion regime. The different types of water which are present are able to exchange quite rapidly with one another. The amounts of water solubilized by the AOT reverse micelles depend on the

solvent used. For instance, amounts up to R = 40 can be solubilized in AOT reverse micelles in isooctane without the addition of a cosurfactant.¹⁹

Block copolymers possess the unique feature of forming micelles of well defined size, since tailor-made systems can be synthesized with varying lengths and chemical composition of the blocks. Several studies have probed the solubilization of hydrophobic²⁰⁻²⁵ compounds into block copolymer micelles, as well as into hydrogels²⁶ containing block copolymer micelles.²⁷ Also, there have been several theories pertaining to the solubilization of compounds in polymeric micelles.²⁸⁻³⁰ The solubilization of water into graft³¹⁻³⁵ and block copolymers³⁶⁻⁴¹ has also been investigated and will be reviewed briefly.

Polymeric microemulsion systems composed of an amphiphilic polymer of polystyrene with polyethylene oxide (PEO) grafts have received considerable attention. This polymer system was examined as a function of the solvent composition for a toluene/water/2-propanol mixture by electron microscopy (EM),³² SANS,³³ dynamic light scattering (DLS),^{31,34} viscosity measurements,³⁴ and NMR.³⁵ Above a certain water concentration (ca. 4 wt. %), swollen reverse micelles were formed, and up to ca. 13 wt. % of water could be stabilized by the polymer.³⁵ This result was the first evidence of the formation of a large water pool stabilized by polymeric surfactants. Other morphologies, e.g. those in which the core consisted of PS surrounded by PEO, were also achieved, depending on the relative solvent composition.³³ The role of the cosurfactant was also investigated; it was found that the only critical parameter for the formation of a translucent system is the existence of mutual solubility for the ternary system.³¹

The emulsifying properties of PS-b-PEO were investigated in a toluene-water mixture as a function of the copolymer composition, molecular weight, and polymer structure, i.e. diblock and triblock forms.³⁶ It was found that oil/water and water/oil emulsions could be formed depending on the relative solvent composition. The formation of microemulsions in the presence of cosurfactants such as 2-propanol or butylamine was

also investigated. The poly(styrene-b-2-vinylpyridine) (PS-b-P2VP)³⁷ and poly(2-vinylpyridine-b-ethylene oxide) (P2VP-b-PEO)³⁸ block copolymer systems were also studied in a ternary solvent mixture composed of water, toluene and alcohol.

The effects of water on poly(styrene-b-ethylene oxide) (PS-b-PEO) in cyclopentane were investigated by DLS³⁹ and by static light scattering (SLS).⁴⁰ The addition of water had substantial effects on the aggregation behavior of these chains. It was observed that upon saturation with water, the hydrodynamic radii and aggregation numbers increased markedly for samples at high dilution. The addition of water was also found to decrease the critical micelle concentration (cmc) values. A self-consistent field theory was applied to describe the micelle behavior in the presence of two immiscible solvents, each selective for one of the blocks.³⁰

In this laboratory, considerable effort has concentrated on the characterization of reverse micelles formed from block ionomers in organic solvents. 41-45 The partition of water in one such block ionomer micelle system, poly(styrene-b-sodium methacrylate) (PS-b-PMANa), was investigated by measuring the proton chemical shift of water and interpreting it using a mass action model. The partition of water was found to favor the reverse micelle as the polarity of the solvent decreased. For instance, the increase in partition followed the trend cyclohexane > toluene - benzene > chloroform >> tetrahydrofuran - dimethylformamide. The order of this trend reflects an increase in the polarity of the solvents and thus an increase in the water solubility in these solvents.

This previous study⁴¹ also established a direct correlation between the free energy of transfer of water from the solvent phase to the reverse micelle phase and the free energy of transfer of water from the solvent phase to water, the latter determined from solubility data. This result allows the prediction of the free energy of transfer of water into reverse micelles in any solvent, once the solubility of water in the solvent is known. Because of this linear relation, it can be concluded that the transfer of water into the micelle core is similar in all solvents and is governed by the nature of the interactions between the water

and the solvents. A correlation between the free energy of water transfer with the solvatochromic parameters of several solvents was also observed in AOT reverse micelles.⁴⁷

The present chapter focuses on the thermodynamics of water transfer in various reverse micelle systems by determining the partition of water from ¹H chemical shift measurements at different temperatures. The reverse micelle systems investigated are the AOT surfactant and the diblock ionomers composed of a nonionic polystyrene block (PS) attached to an ionic block consisting of either poly(sodium methacrylate) (PMANa), poly (sodium acrylate) (PANa), poly (cesium acrylate) (PACs), or poly (4-vinylpyridinium methyl iodide) (PVPMeI). The purpose of the study is to examine the dependence of the thermodynamic parameters of water solubilization in the reverse micelles on the chemical nature of the ionic core and the block lengths of the block ionomers. This chapter is divided into three parts. The first part addresses the theoretical aspects of water transfer. In the second part, the thermodynamic results for the different reverse micelle systems having a constant water ratio of 6 are considered. In the third part, NMR relaxation studies of different nuclei in the water core are discussed.

7.2. EXPERIMENTAL

7.2.1. Polymer Synthesis

The block copolymers, poly(styrene-b-sodium methacrylate), poly(styrene-b-sodium acrylate), and poly(styrene-b-4-vinylpyridinium methyl iodide) were prepared by sequential anionic polymerization; the details are given in refs 48, 49 and 50, respectively. For convenience, only a summary of the procedure will be given here. The copolymers were synthesized by sequential anionic copolymerization of the styrene monomer followed

by either *tert*-butyl methacrylate (*t*-BuMA), *tert*-butyl acrylate (*t*-BuA) or 4-vinylpyridine (4VP) monomer. The initiator used for *t*-BuMA was *n*-butyllithium and that for t-BuA and 4VP was the reaction product of *sec*-butyllithium with a few drops of α-methylstyrene. The polymerization was carried out in tetrahydrofuran (THF) at -78°C under an atmosphere of nitrogen. The apparatus employed for the polymerization allowed the withdrawal of the reaction mixture in the course of the synthesis. Therefore, for a given constant polystyrene block length, a series of diblocks was obtained with poly (*tert*-butyl methacrylate), poly (*tert*-butyl acrylate) or poly(4-vinylpyridine) segments of different lengths. Aliquots of the reaction mixtures were also withdrawn for characterization after the polystyrene block was formed and every time following addition of the second monomer.

Polystyrene-b-poly(methacrylic acid) (PS-b-PMA) and polystyrene-b-poly(acrylic acid) (PS-b-PAA) were obtained by acid-catalyzed hydrolysis of the *tert*-butyl methacrylate or the *tert*-butyl acrylate segments in toluene at 80°C using p-toluenesulfonic acid as the catalyst. The PS-b-PMA and PS-b-PAA were recovered and purified by repeated precipitation in methanol, methanol/water mixtures, or water depending on the composition of the diblocks. The polystyrene-b-poly(4-vinylpyridine) (PS-b-P4VP) was recovered and purified by repeated precipitation in hexanes.

The acid contents of the PS-b-PMA and PS-b-PAA copolymers were determined in THF/H₂O mixtures using aqueous NaOH as titrant and phenolphthalein as the indicator. The 4-vinylpyridine content was determined by nonaqueous titration of the vinylpyridine segments with perchloric acid.

For the quarternization of the P4VP blocks, the PS-b-P4VP block copolymers were dissolved in dried THF (5% solution), and freshly distilled methyl iodide was added in 10-fold excess. The reaction solution was refluxed under nitrogen for 3-4 hours to achieve full quarternization. The disappearance of the 1414 cm⁻¹ 4VP IR band was taken

as evidence of complete quarternization. The copolymers were recovered by precipitation in 2-propanol (10-fold volume excess) and were dried in a vacuum oven at 60°C.

The molecular weight of the polystyrene block was determined with a precision of ± 5% by size exclusion chromatography in THF using narrow molecular weight polystyrene standards. The polydispersity indices of the PS blocks varied from 1.05 to 1.20. The polymer samples were dried in a vacuum oven at 60°C before use. The sample notation used indicates the copolymer composition; for example, PS(440)-b-PMANa(18) represents a polystyrene chain of 440 units joined to a poly(sodium methacrylate) chain of 18 units.

7.2.2. Sample Preparation

The sodium bis(2-ethylhexyl)sulfosuccinate, aerosol OT (AOT), was purchased from Aldrich and used without further purification. NMR solutions were prepared by dissolution of the AOT or the polymer samples in toluene-d₈ (C₇D₈, 99.6%, Cambridge Isotope Laboratories). Deionized water (MILLI-Q, Millipore) was added to the solutions with a microsyringe to obtain a specified value of R; for the surfactant experiments, R refers to the molar ratio of water to surfactant concentration; for the block copolymers, R refers to the molar ratio of water to the ionic repeat units, i.e. COONa or NCH₃I. For the first part of this study, this ratio was kept constant at a value of 6; for the second part it was varied from 2 to 10.

Four or five different concentrations were measured for each distribution coefficient determination by dilution of a stock solution. The total weight of each sample in the NMR tube was constant at 1.00 ± 0.05 g. Typical concentration ranges of AOT and polymer solutions were 0.015 - 0.002 g/g and 0.04 -0.01 g/g, with water additions of 4-0.5 μ L and 3-1 μ L, respectively. The concentrations of the polymer samples were higher than those of AOT in order to shift the water peak upfield from the protons on the PS backbone, which otherwise would obscure the water proton resonance. After water

addition, the samples were shaken vigorously. It should be noted that some polymer samples, in particular those of high polymer concentration, were found to be viscous; these samples were immersed in a sonicator for a maximum period of one hour to aid in the solubilization of water. It was found that sonication did not affect the position or shape of the water peak even if the samples were sonicated for as long as 12 hours.

7.2.3. NMR Measurement

NMR spectra were recorded using Varian 200 (4.70 T) and 300 (7.05 T) MHz spectrometers. For the variable temperature experiments, the probe was calibrated using the chemical shift difference of two ethylene glycol peaks. 1 H chemical shifts were recorded at variable temperatures between 25 and 54 \pm 1°C, with a minimum sample equilibration time of ten minutes at each temperature. All spectra were referenced to the deuterated toluene solvent peak (2.09 ppm). Relaxation measurements were performed at 25°C for 1 H, 2 H, 23 Na, and 17 O nuclei. The spin-lattice or longitudinal relaxation rates (R₁) were measured using an inverse-recovery pulse sequence. The spin-spin or transverse relaxation rates (R₂) were determined from the line width at half height ($\Delta v_{1/2}$), i.e. R₂ = $\pi \Delta v_{1/2}$.

7.3. THEORETICAL ASPECTS OF WATER TRANSFER

The solubilization of water in the cores of the reverse micelles was treated by a mass action model.⁴⁶ This model regards the solubilization process in terms of stepwise incorporation of solute molecules into micelles. The equilibrium constant for the distribution of the solute is described on the basis of an exchange between two phases, the reverse micelle phase and the organic phase. The distribution coefficient (K) is given by, 51, 52

$$K = [S_{mic}] / ([S_{sol}] [D_T])$$
 (1)

where $[S_{mic}]$ and $[S_{sol}]$ are the concentration of solute in the micelle and in the solvent phase, respectively, and $[D_T]$ refers to the total surfactant concentration; for the block ionomers, it signifies the concentration of the ionic block on a repeat unit basis, i.e. moles of repeat unit per kilogram of solvent. Conventionally, the term $[D_T]$ is replaced by the concentration of micellized surfactant $([D_M])$, which is related to the total surfactant concentration by the critical micelle concentration (cmc) as,

$$[D_T] = [D_M] + cmc$$
 (2)

However, for $[D_T] > >$ cmc, eq. 1 would be expected to be valid. The applicability of this assumption to the present study will be discussed in section 7.4.1.1.

In the previous paper, this model was applied to the study by NMR of the solubilization of water in reverse micelles.⁴¹ If the exchange of solute is fast as compared to the time scale of the NMR experiment, the observed chemical shift of the solute (δ_{obs}) is an average over all possible solute locations. The δ_{obs} is given as

$$\delta_{obs} = p \, \delta_{mic} + (1-p) \, \delta_{sol} \tag{3}$$

where p refers to the fraction of solute in the micelle phase and δ_{mic} and δ_{sol} are the chemical shifts of the solute in the micelle and in the solvent phase, respectively. δ_{sol} can be determined by measuring the chemical shift of the solute in the absence of micelles. Figure 7.2 illustrates typical NMR spectra in which the chemical shift of water is determined in the solvent phase and in a solution of the block ionomer reverse micelles. Since the fraction of solute in the micelle phase to solvent phase is given as $[S_{mic}]/[S_{sol}] = p/(1-p)$, the fraction of solute in the micelle can be related to K,

$$p = K[D_T] / (1 + K[D_T])$$
 (4)

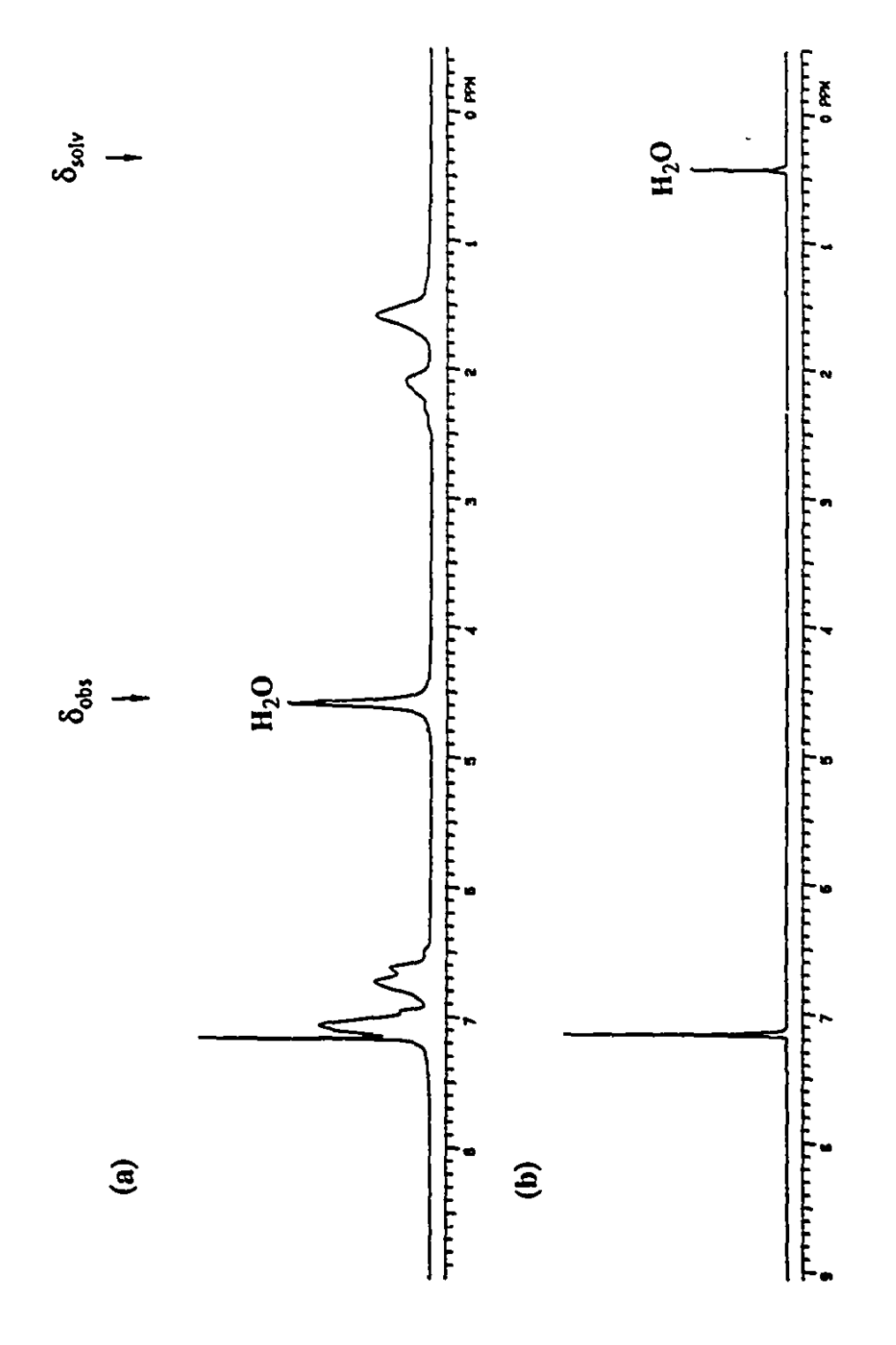


Figure 7.2. Typical NMR Spectra of (a) PS-b-PMANa in benzene- d_6 and (b) water in benzene- d_6 at 25°C.

By substituting eq. 4 into eq. 3 we obtain,

$$(\delta_{\text{obs}} - \delta_{\text{sol}}) / [D_{\text{T}}] = -K (\delta_{\text{obs}} - \delta_{\text{mic}})$$
 (5)

The distribution coefficient can thus be obtained from the slope of a plot of $(\delta_{obs} - \delta_{sol})$ / $[D_T]$ as a function of δ_{obs} . By measuring K at different temperatures, the thermodynamic parameters for the transfer process can be evaluated according to the equation,

$$\Delta G_{t} = -RT \ln K = \Delta H_{t} - T \Delta S_{t}$$
 (6)

It should be emphasized that these thermodynamic parameters refer only to the transfer process of the solute from the solvent phase to the micelle phase. Therefore, the thermodynamic changes which occur with respect to the micelles when the solute is solubilized are not determined.

7.4. RESULTS AND DISCUSSION

7.4.1. Thermodynamic Parameters at R = 6

In this section, the distribution coefficients and thermodynamic parameters of water transfer from the toluene phase to the reverse micelle phase of AOT and the block ionomers, PS-b-PMANa, PS-b-PANa, and PS-b-P4VPMeI will be discussed. Comparison of the results will be made between the different reverse micelle systems and between the micelle systems and the transfer of water from a toluene phase to a bulk water phase. The effect of having a different counterion on the transfer of water will be investigated for one block ionomer sample, PS-b-PACs. The possibility of forming a water pool in block ionomer reverse micelles will also be addressed.

7.4.1.1. AOT

The distribution coefficients of water in the reverse micelle solutions of AOT were determined from the observed proton chemical shift of water (δ_{obs}) for a broad concentration range, from ca. the cmc to ca. 40 times greater than the cmc. The data, plotted according to eq. 5 for four temperatures of measurement ranging from 25 to 46°C, are shown in Figure 7.3. From the slope of these lines, the distribution coefficients were evaluated. It is clear that at low AOT concentrations (which give low values of δ_{obs}), i.e. near the cmc, the data deviate substantially from linearity. Since for these concentrations, $[D_T] \sim$ cmc, then $[D_M]$ should be used for the evaluation of K (eq. 5).

[D_M] was evaluated from the difference of the total surfactant concentration, [D_T], and the cmc, as described in eq. 2. The cmc values were determined under the present experimental conditions by measuring the ¹H chemical shift of water for different surfactant concentrations. Figure 7.4 illustrates a typical cmc evaluation depicted on a semilog plot at 46°C, in which the ¹H chemical shifts of water were plotted as a function of the inverse total surfactant concentration. The cmc was evaluated from the point of intersection of the single chain region at low concentrations and the transition region from single chains to micelles at intermediate concentrations. In Figure 7.4, the linear regressions through these two regions are represented by dashed lines, and the cmc is taken as the point of intersection. The cmc values for the different temperatures are summarized in Table 7.1 along with those determined by another method to be discussed later. The cmc's were found to decrease linearly with temperature; the correlation coefficient for the plot was 0.997 (plot not shown). The cmc value at 25°C, 2.4 ± 0.5 mM, compares well with that reported for AOT in benzene-d₆, 2.8 ± 0.5 mM.⁵³ The latter cmc value was evaluated by similar ¹H chemical shift measurements of solubilized water at an R value of 6.5.

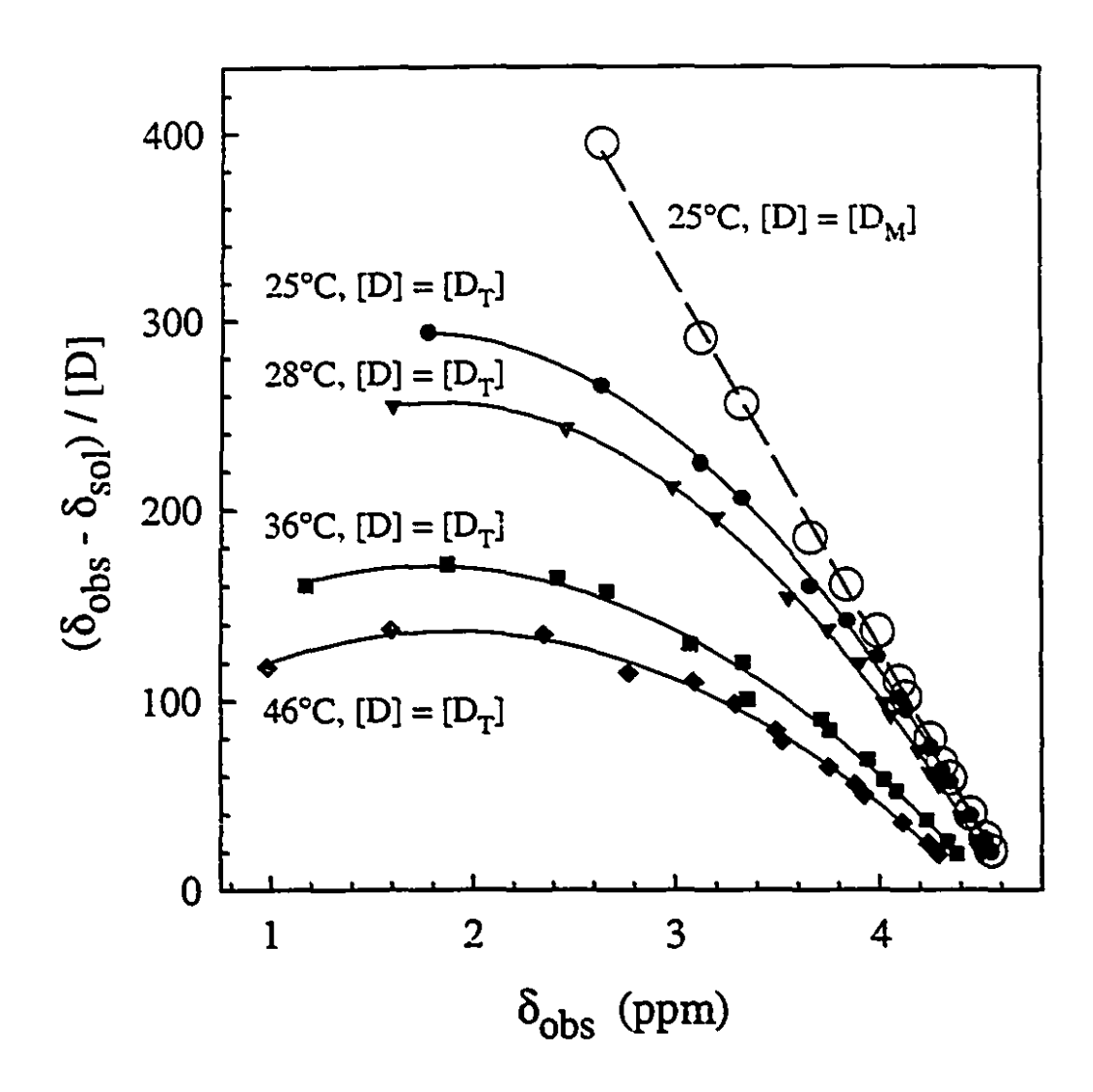


Figure 7.3. Plots for the evalutation of the distribution coefficients using $[D_T]$ (see text) for AOT in toluene_{d8} at different temperatures and using $[D_M]$ at 25°C (O). The solid and dashed lines represent second order and first order regressions through the points, respectively.

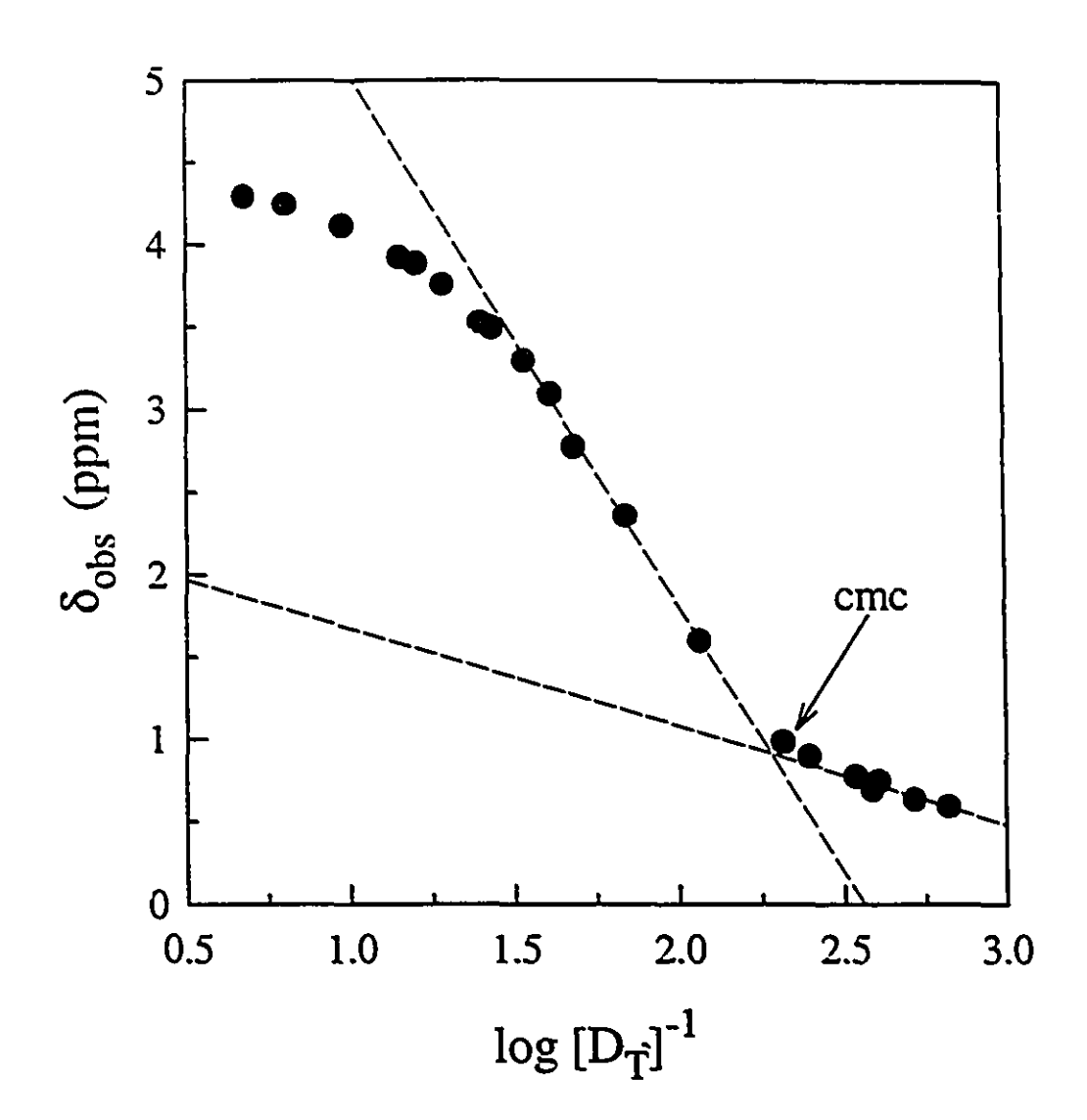


Figure 7.4. Semilog Plot of observed ¹H chemical shift of water as a function the inverse total surfactant concentration.

Table 7.1. Summary of Cmc and K Values for AOT Reverse Micelles in Toluene for R=6 at Different Temperatures.

Temperature	cmc (± 0.5) × 10 ³ (mM)		K (m ⁻¹)		
(°C) (±1°C)	δ _{obs} vs [D _T] ⁻¹	Fit of eq. 7	eq. 5 using [D _M]	eq. 5 using $[D_T]$ (initial slope)	Fit of eq. 7
25	2.4	2.3	190	180	190
28	2.7	2.7	170	160	174
39	3.9	3.7	120	100	120
46	4.6	4.3	90	78	95

Figure 7.4 also illustrates the effects of increasing AOT concentration on the magnitude of the 1 H chemical shift of water. At low AOT concentrations, below the cmc, the observed chemical shift was similar to the value of water in the toluene phase (0.41 ppm for 46°C). As the surfactant concentration increased, the chemical shift moved further downfield due to the association of water with the AOT headgroups during the formation of the reverse micelles. As the concentration was increased further, the water began to associate in the core forming hydrogen bonds with other water molecules. Thus, at higher concentrations, the $\delta_{\rm obs}$ approached the value of bulk water (ca. 4.5 ppm). This observation is due to the emergence of free or unbound water in the micelle core, which dominates the value of $\delta_{\rm obs}$ as the fraction of free water increases.

From the determined cmc values, the distribution coefficients were evaluated by replacing $[D_T]$ with $[D_M]$ in eq. 5. The resulting plots were observed to be linear for all the temperatures investigated. A typical plot using $[D_M]$ is represented using hollow circles in Figure 7.3 for the data at 25°C. The plots for the other temperatures have been omitted for clarity, but are just as linear. The slopes from these lines were used to evaluate K, and these results are summarized in Table 7.1. It was found that all the data could be linearized in this fashion with the exception of samples at very low concentrations, i.e. ca. less than 1.7 times the cmc.

In Figure 7.3, it can be seen that for large values of $\delta_{\rm obs}$, which correspond to high concentrations, i.e. ca. 10 times above the cmc, the points which were corrected for the cmc using $[D_{\rm M}]$ in eq. 5 corresponded closely to those using $[D_{\rm T}]$. Therefore, it was of interest to determine the distribution coefficient values using the initial slopes (at high values of $\delta_{\rm obs}$) of these uncorrected lines. This analysis would also be expected to be valid according to the assumption given in eq. 2, i.e. that when $[D_{\rm T}] >>$ cmc, then $[D_{\rm M}]$ can be approximated by $[D_{\rm T}]$. The values for K using $[D_{\rm M}]$ and those using the initial slope of the relation employing $[D_{\rm T}]$ are also given in Table 7.1. The K values evaluated from the initial slopes were found to deviate from those using $[D_{\rm M}]$; the percent difference was 5,

6, 17 and 13% for temperatures of 25, 28, 36 and 46°C, respectively. In order to see whether this difference was significant, the experimental error in the distribution coefficient values for the present experiment was evaluated. The error was estimated from the difference of two independent measurements for K; this difference was found to be less than 8%. Since this number is comparable to the differences mentioned above, with the exception of the data at 39°C, the K values as determined using [D_M] or the initial slopes of [D_T] in eq. 5, are believed to be the same within experimental error.

The thermodynamic parameters for the AOT reverse micelles were evaluated using the two different values for K as a function of temperature (Table 7.1) according to eq. 6. The values for the enthalpies of transfer were -28 and -32 kJ/mol, and the entropies of transfer were -0.051 and -0.063 kJ/(mol K), for the K values determined by using $[D_M]$ and $[D_T]$, respectively. Again, these values agree within experimental error. Thus, the thermodynamic parameters of water transfer can be evaluated using either the data at high surfactant concentrations, i.e. $[D_T] > 10$ x cmc, or using a broader concentration range, including concentrations near the cmc, and correcting for the cmc values.

Since the shape of the plots of $(\delta_{obs} - \delta_{sol})/[D_T]$ versus δ_{obs} plots were found to be influenced by concentrations near the cmc, an attempt was made to extract the cmc values from the data. By combining equations 2 and 5, where $[D_M]$ was replaced by $([D_T] - cmc)$, and rearranging, the observed chemical shift is given by the following,

$$\delta_{\text{obs}} = \frac{\delta_{\text{sol}} + K\delta_{\text{mic}}([D_{\text{T}}] - \text{cmc})}{1 + K([D_{\text{T}}] - \text{cmc})}$$
(7)

By plotting δ_{obs} versus $[D_T]$ and fitting the resulting curve, the values for K, δ_{mic} , and the cmc were determined. It should be noted that when concentrations less than the cmc were plotted the shape of this curve was the mirror image of the plot given in Figure 7.4. However, the curve fitting procedure was performed for concentrations which were above the cmc, specifically for concentrations ca. 2 times higher than the cmc. The data points used in the evaluation were those shown in Figure 7.3, in which the lowest concentration

was omitted (4.7 x 10^{-3} mol/kg). The results for the cmc and K are given in Table 7.1. The cmc values were found to be the same within experimental error as those determined from the intersection of the δ_{obs} versus $[D_T]^{-1}$ plots (Figure 7.4). Similarly, the values for K were found to agree with those evaluated using $[D_M]$ in eq. 5. Evaluation of eq. 7 may thus serve as an alternative method of determining the cmc and K. This method has the advantage that concentrations below the cmc are not needed for the evaluation of the cmc. However, it should be noted that a large range of data points, in particular at concentrations near the cmc, is required to obtain accurate results.

7.4.1.2. Block Ionomers

The distribution coefficients of water were evaluated for block ionomer micelles composed of a nonionic block of polystyrene and ionic blocks composed of either poly(sodium methylacrylate), poly (sodium acrylate) or poly (4-vinylpyridinium methyl iodide). The composition of the samples, the polydispersity indices of the PS block, and the mole percentages of ionic block in the copolymers are given in Table 7.2. The lengths of both blocks were varied; they ranged from 310 to 660, and from 17 to 42 units for the polystyrene and for the ionic blocks, respectively. The mole percentage of the ionic blocks ranged from 3 to 12%.

It was found that for the block ionomers, in contrast to the AOT reverse micelles, the data as plotted according to eq. 5 using [D_T] were linear. A typical plot is given in Figure 7.5. It should be noted that a narrower concentration range was used here compared to that for the AOT reverse micelles (see Figure 7.3). Lower concentrations could not be employed because the ¹H chemical shift of water peak became obscured by those of the methylene protons on the polystyrene backbone, which ranged from ca. 1.1 to 2.5 ppm, and higher concentrations yielded viscous solutions. The cmc values for some similar block ionomers, such as PS-b-PANa in THF, have been evaluated by SLS and

Table 7.2. Composition, Polydispersity Indices (P.I.) and Mole % of the Ionic Block for the Block Ionomers

Composition	P.I.	mol %
		Ionic Block
PS(x)-b-PMANa(y)		
440- <i>b</i> -40	1.09	8
440- <i>b</i> -18	1.09	4
310- <i>b</i> -42	1.20	12
310- <i>b</i> -17	1.19	5
PS(x)-b-PANa(y)		
380- <i>b</i> -27	1.10	7
660- <i>b</i> -21	1.05	3
PS(x)-b-PA		
600- <i>b</i> -34		5
PS(x)-b-P4VPMeI(y)		
470- <i>b</i> -26	1.10	5
600- <i>b</i> -37	1.10	6

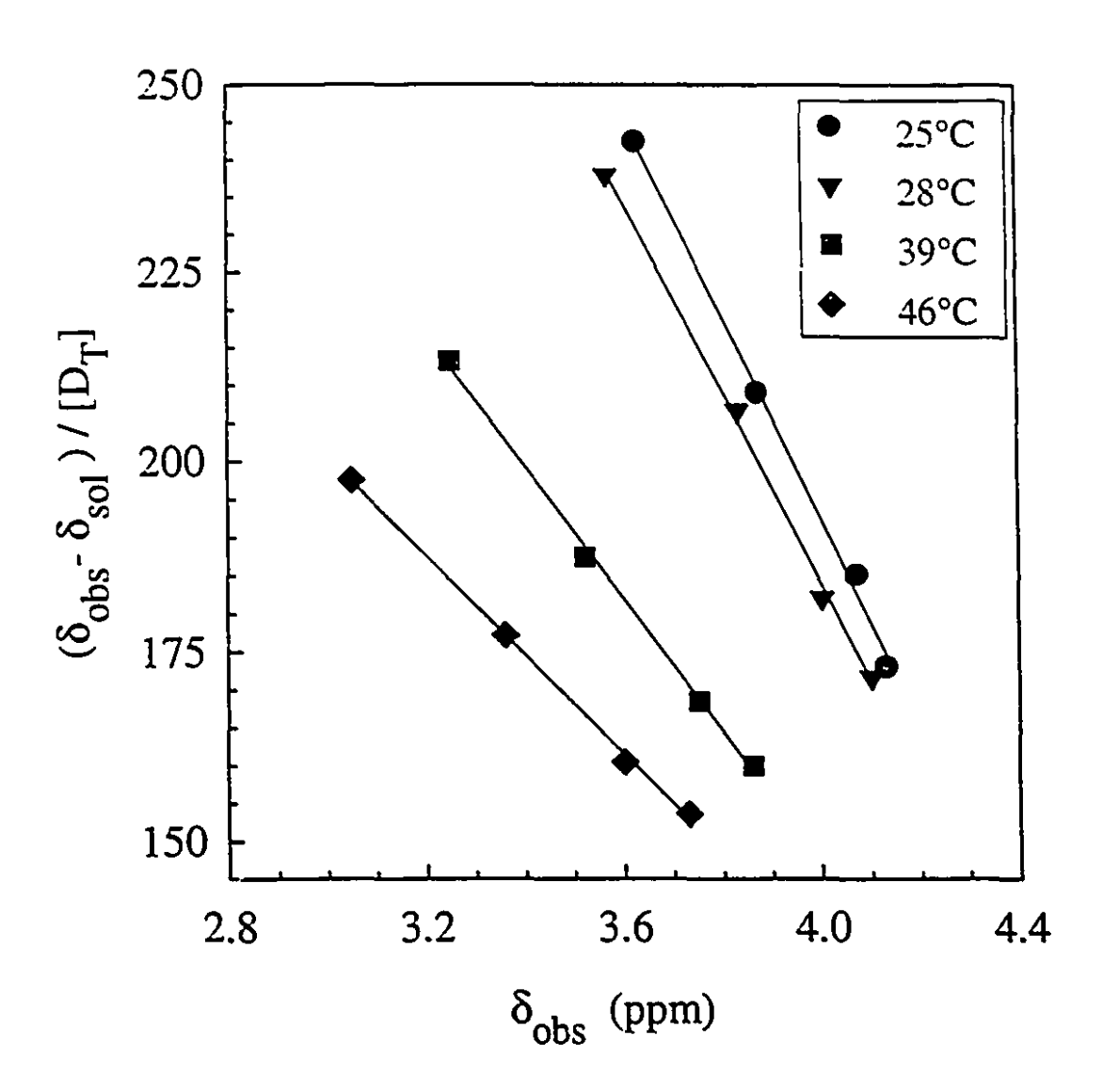


Figure 7.5. Typical evaluation of the distribution coefficients of water for PS(310)-b-PANa(17) in toluene-d8 at different temperatures.

were found to be in the range of 10-6 g/g.54 In comparison, the concentrations used in the present experiments were between 0.04 and 0.01 g/g, clearly much higher than these cmc values. Therefore no corrections for the cmc's were required.

The thermodynamic parameters of water transfer were evaluated according to eq. 6 from the distribution coefficients for water at different temperatures. Figure 7.6 shows the plot of ln K versus the inverse temperature, for the reverse micelles having an ionic core composed of either PMANa or PANa, represented by hollow and filled symbols, respectively. The solid line represents the linear regression through all the data, which had a correlation coefficient of 0.95; the dashed lines represent the 99% confidence intervals.

An interesting observation, which can be made from this plot, is that the values for K can all be represented by a single line within the confidence intervals, independent of the nonionic and ionic block lengths. Several conclusions can be drawn from this observation. First, the lack of dependency of K on the PS block length suggests that the corona dimension and thickness do not affect the distribution of water. Therefore, the PS corona does not present any appreciable barrier to the solubilization of water into the core. This result would imply that the distribution of water is essentially governed by the unfavorable interactions of water and the toluene solvent phase, as was found in the previous paper. 41

Second, from the independence of K on the ionic block length, it can be concluded that the water in all the block copolymers is bound to the ionic core in a similar manner. The water in these reverse micelles would be expected to hydrate the sodium counterions and the carboxylate ionic groups, (COO-Na+) by ion-dipole interactions and H-bonding, respectively, in a fashion analogous to the hydration of AOT reverse micelle cores. If water were bound to different locations in the micelle core, the distribution coefficient would have different values, depending on the nature of the water interactions.

Another observation which can be made from Figure 7.6, is that there is no difference between the distribution coefficients of the block copolymers containing either PMANa or PANa as the ionic block. This result implies that the hydrophobic methyl group

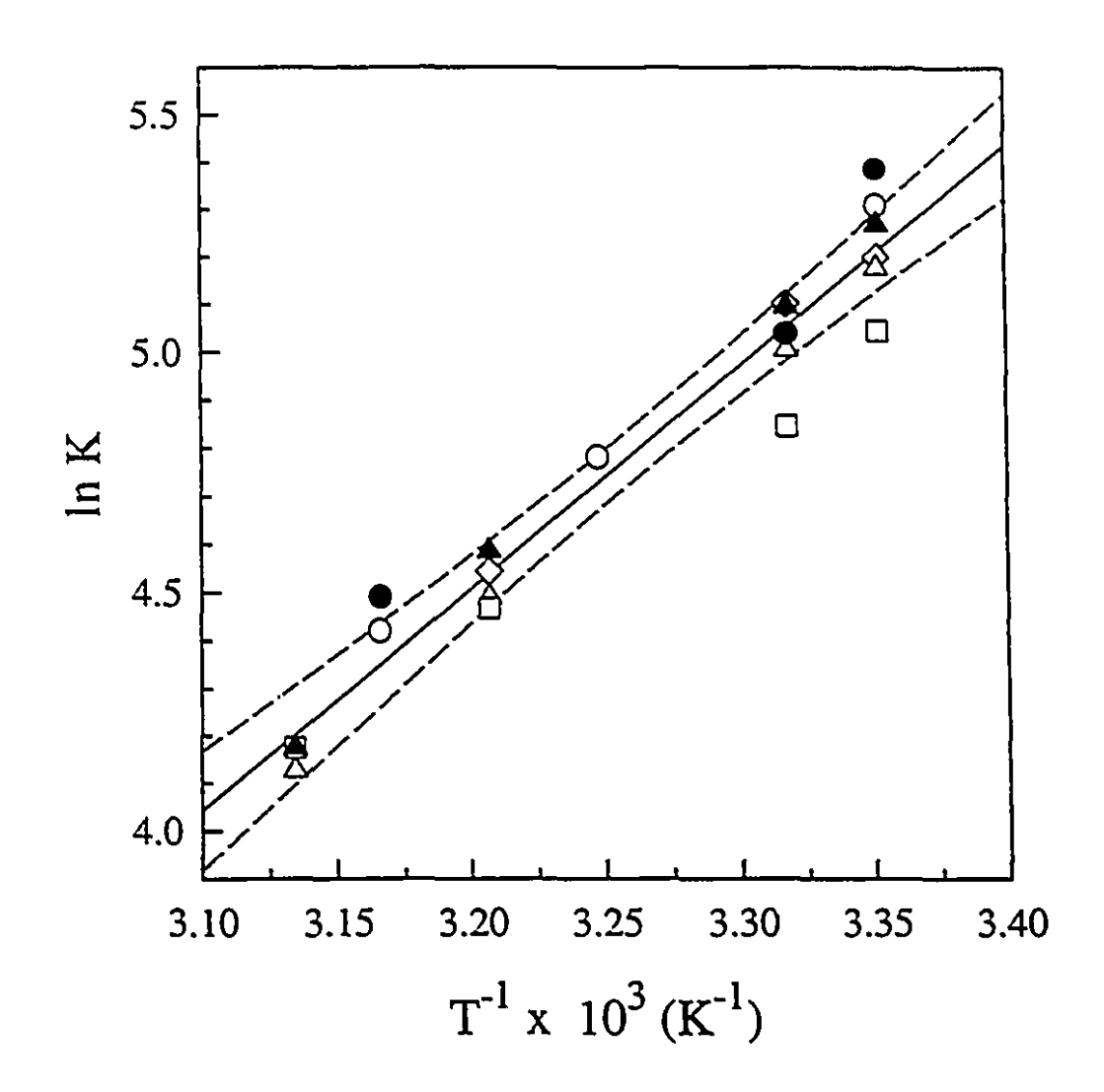


Figure 7.6. Plot of the ln of the distribution coefficients as a function of inverse temperature for PS(440)-b-PMANa(18) (O), PS(440)-b-PMANa(40) (◊), PS(310)-b-PMANa(42) (△), PS(310)-b-PMANa(17) (□), PS(382)-b-PANa(27) (●), and PS(660)-b-PANa(21) (s) block ionomers. The solid line represents the linear regression through all the data points and the dashed line is the 99% confidence interval

of the sodium methacrylate chain does not effect or hinder the binding of water at this R value compared to the structure of the sodium acrylate which has a proton in place of the methyl group. This result further supports the hydration mechanism in which only the COO-Na+ group is involved, as mentioned in the preceding paragraph.

The distribution coefficients of water in poly(styrene-b-4-vinylpyridinium methyl iodide) were evaluated for two samples, PS(470)-b-P4VPMeI(26) and PS(600)-b-P4VPMeI(37). The K values for these samples were also found to be independent of the PS and ionic block lengths. The values for K were found to be lower in PS-b-P4VPMeI than those in the PS-b-PMANa and PS-b-PANa reverse micelles (Table 7.3). Thus, less water is solubilized by these cationic reverse micelles than the anionic reverse micelles at the given temperatures. The amounts of water solubilized in the micelle cores for the different systems will be discussed in the following section.

7.4.1.3. Comparison of Thermodynamic Parameters for the Reverse Micelle Systems.

It is important to establish that the driving force for water solubilization in the cores of these reverse micelles is not due to saturation of water in the toluene phase. This can be determined by calculating, using eq. 4, the amount of water in the toluene phase (1-p) from the values of the distribution coefficients and the total amount of water added. For the present study, the amounts of water in toluene were evaluated to be below the maximum solubility of water in toluene⁵⁶ at the temperatures investigated for the AOT and the block ionomer micelles. Therefore, under the present experimental conditions, a true equilibrium exists between the water in the solvent phase and that in the micelle core.

The thermodynamic parameters for the transfer of water into the different reverse micelles investigated were evaluated from the temperature dependence of K according to eq. 6. For the block ionomer reverse micelle systems, the K values employed were those

determined from the linear regression including all the block copolymers containing the same ionic group (see e.g. Figure 7.6). Table 7.3 summarizes the thermodynamic parameters at 25°C for the different reverse micelle systems according to the various ionic groups (given here in parentheses), i.e. AOT (SO₃-Na⁺), PS-b-PANa and PS-b-PMANa (COO-Na⁺) and PS-b-P4VPMeI (N_{py}⁺(Me)I⁻), where N_{py}⁺(Me)I⁻ represents pyridine quarternized with methyl iodide.

The distribution coefficients of water were found to decrease in the following order: sodium sulfonates (SO₃-Na⁺) ~ sodium carboxylates (COO-Na⁺) > > pyridinium methyl iodide (N_{pv}+(Me)I-) (Table 7.3). This order reflects the decrease in the amount of solubilized water. Thus, in the above reverse micelle systems, PS-b-P4VPMeI solubilized the least amount of water compared to AOT, PS-b-PMANa, and PS-b-PANa. A similar trend has been observed previously in anionic and cationic surfactant reverse micelles having similar hydrocarbon groups but different polar head groups, e.g. AOT and bis(2ethylhexyl)ammonium bromide.55 It was found that the greatest variabilities in heats of solubilization of water appeared at low R values (< 1), where the solubilization depended significantly on the nature of the polar groups. In general it has been found that the olubilizing power, i.e., the maximum amount of solubilization and the strength of the solubilization followed the order anionics > cationics. The lower strength of solubilization in the cationic surfactants was due to weaker ion-dipole interaction compared to the anionic surfactant. This result shows that, in addition to the interactions between water and the toluene phase, the interactions between water and the core is also a major contributing factor to the partition of water.

It should be noted that according to the definition of R given in section 7.2.2., for a constant R value the amount of water added per unit weight of AOT is larger than that per unit weight of the block ionomers. For instance, for a constant AOT or block ionomer concentration of 0.03 g/g, the amount of water which is added per gram of solution for an R value of 6 is; 7.3, 2.9, 2.8, and 2.5 µL for AOT, PS-b-PANa, PS-b-PMANa, and PS-b-

Table 7.3. Thermodynamic Results for the Systems Studied as a Function of the Ionic Group Moeity at 25°C for a Constant Water Ratio of 6 and the Thermodynamic Parameters for the Transfer of Water from Toluene to a Water Phase

IONIC GROUP	K ^a (mol/kg) ⁻¹	ΔG _t ° (kJ/ mol)	ΔH _t ° (kJ/moi)	ΔS _t ° (kJ/molK)	TASt°a (kJ/mol)
SO ₃ -Na+	190 ^b	-13	-28	-0.051	-15
COO-Na+	190	-13	-38	-0.085	-25
N _{py} +(Me)I-	93	-11	-40	-0.098	-29
COO-Cs+	270	-14	-30	-0.055	-16
H ₂ O(tol)→ H ₂ O(bulk) ^c		-9	-30	-0.069	-21

^a Calculations performed with 3 significant figures. ^b Calculated using [D_M]

^c Calculated from data given in Tarassenkow et al., ref. 56.

4VPMeI, respectively. Therefore, AOT reverse micelles solubilize larger amounts of water than the block ionomer micelles. Also, from the definition of R, it is seen that for a constant concentration of block copolymer and a constant value of R, block ionomers with longer ionic blocks contain greater quantities of water compared to those with shorter ionic block lengths.

From the distribution coefficients, the free energies of water transfer from the solvent phase to the micelle cores (ΔG_t^0) were evaluated. The ΔG_t^0 values for the different reverse micelle systems are shown as a function of temperature in Figure 7.7. It should be noted that for AOT, the values plotted were those determined from the K values evaluated using $[D_M]$. ΔG_t^0 is a measure of the ease at which water can enter the micelle core. For the sulfonate and carboxylate ionic groups, the free energy at 25°C was found to be -13 kJ/mol; this shows that at this temperature, there is no difference in ΔG_t^0 whether water enters the core of the surfactant micelles, AOT, or the anionic block ionomer micelles. The free energy of transfer for the pyridinium methyl iodide ionic group is lower (-11 kJ/mol) than those of the anionic reverse micelles, as a consequence of the weaker solubilizing strength.

The free energy of transfer of water from toluene to the reverse micelle phase can be compared to that for the transfer of water from toluene to the bulk water phase $[\Delta G_t^o(\text{tol}\rightarrow\text{bulk H}_2O)]$. The value for the latter at 25°C was evaluated from the solubility of water in toluene⁵⁶ and was found to be -9 kJ/mol (Table 7.3). This value is slightly less negative than those of water transfer to the reverse micelle systems. This result suggests that it is more favorable for water to enter the core of the reverse micelles at R = 6, than it is for water to enter bulk water.

From the temperature dependence of ΔG_t^0 , the enthalpic (ΔH_t^0) and entropic (ΔS_t^0) contributions for the transfer process were determined. These values are given in Table 7.3; it can be observed that the transfer of water from toluene to the micelle core is governed by the favorable enthalpic contribution. This enthalpy of transfer is exothermic,

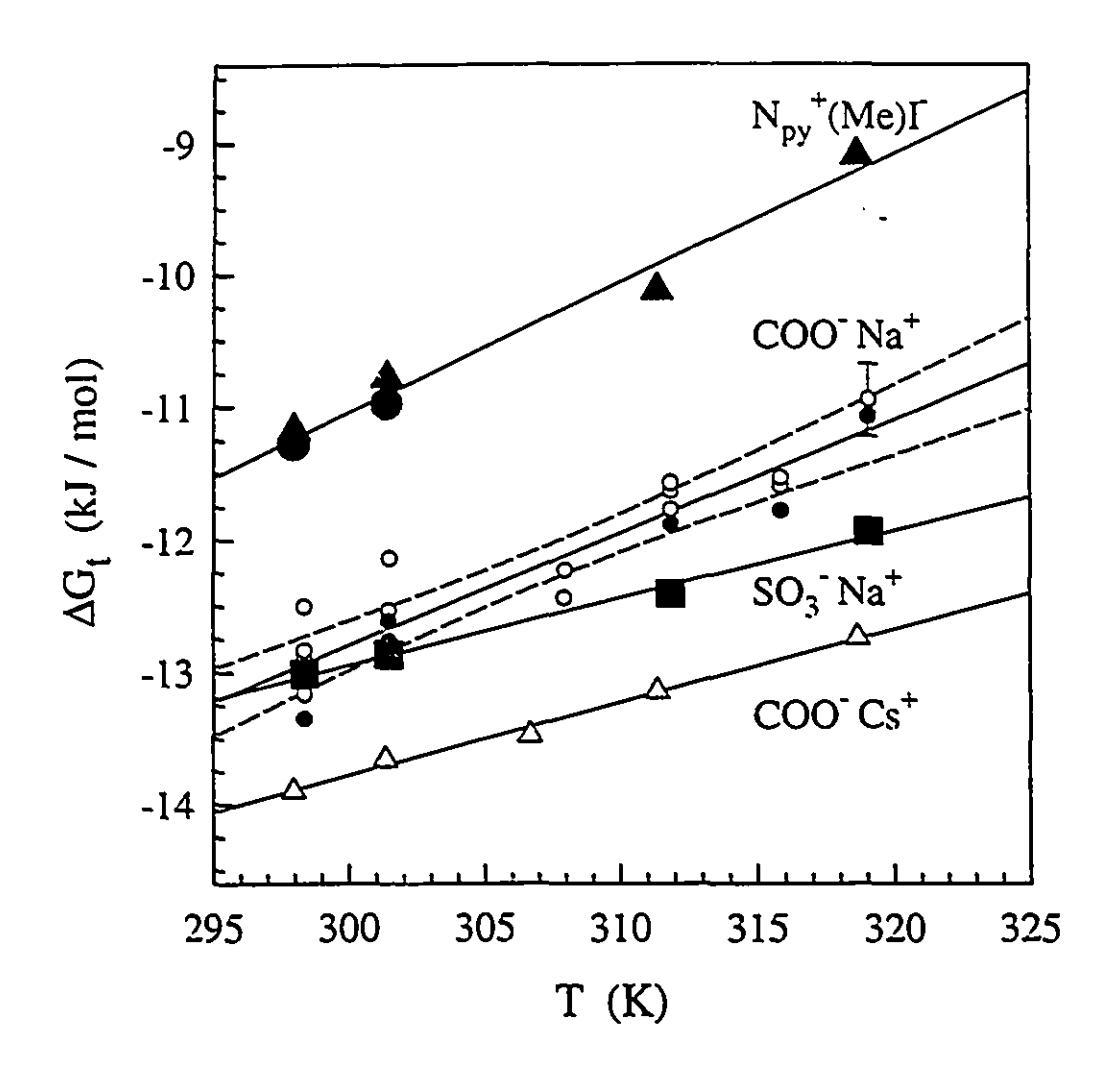


Figure 7.7. The free energy for the water transfer process as a function of temperature for different systems; polystyrene-b-poly(4-vinylpyridine) (\bullet , \bullet), polystyrene-b-poly(sedium methylacrylate) (\circ) and polystyrene-b-(sodium acrylate) (\bullet), and AOT (\blacksquare) in toluene-d8. The solid lines represent the linear regression through the respective reverse micelle systems.

since water in the micelle cores is more stable than that in the toluene phase. The entropic contribution to ΔG_t^o , which represents the degree of order in the system, is found to be negative. This result shows that water solubilized in the micelle cores is somewhat more structured than that in toluene, which is expected because of the stronger interactions of water with the counterions and the polar head groups.

It was observed that systems with larger $-\Delta H_t^o$ values had larger $-\Delta S_t^o$ values, i.e. the greater the interaction strength, the greater the ordering of water (Table 7.3). This feature in which the enthalpy and entropy compensate each other in order to create minor changes in the free energy has been found in other systems. For instance, a similar enthalpy - entropy compensation has been found for the transfer of organic molecules into aqueous solutions of cetyltrimethylammonium bromide (CTAB) micelles.⁵⁷ It has been suggested that such a relation may be due to experimental errors.^{57,58} However, much evidence has supported the existence of this compensation for a variety of processes involving small solutes and proteins in water solutions, for example, the solvation of ions, and it arises from the properties of water as a solvent.⁵⁸ In the present case, a plot of ΔH_t^o as a function of ΔS_t^o gave a linear relation with a correlation coefficient of 0.98 (graph not shown). The slope, or compensation temperature, and the intercept were 260 K and -16 kJ/mol, respectively.

As was done for the free energy (see above), the enthalpy and entropy for the transfer process can be compared to those of water transferred from the toluene phase to bulk water. These latter values were again determined from the temperature dependence of the solubility, in the range of 18 to 93°C , 56 and are given in Table 7.3. It was found that for AOT, the magnitudes of $\Delta H_t{}^{\circ}$ and $\Delta S_t{}^{\circ}$ were similar to those for the water transfer from toluene to bulk water. This result suggests that water solubilized in AOT is in an environment which is energetically and structurally very similar to that of bulk water. For AOT in toluene, it has been found that at R=4, the density of the water pool approaches that of bulk water. $S_t{}^{\circ}$ Thus, at R=6, it would be expected that the water solubilized in the

core interacts by hydrogen bonds with other similarly solubilized water molecules. On the other hand, for the block ionomer micelles, the ΔH_t^0 and ΔS_t^0 values are more negative than those for AOT and for the transfer of water from toluene to bulk water. This result indicates that water in the block ionomer micelles interacts more strongly and is more ordered than that in the AOT reverse micelles. Following from this result, it can be suggested that water which is transferred into the block ionomer micelles mainly hydrates the counterions and the ionic groups of the block forming the core. Therefore, a water pool most likely does not form in the block ionomer micelles at this R value. The possibility of a water pool formation in block ionomer micelles will be discussed in section 7.4.1.5.

7.4.1.4. Counterion Effect

The effect of Cs⁺ counterion on the transfer of water to a block ionomer micelle, PS(600)-b-PACs(34), was investigated for R=6. The thermodynamic parameters for the water transfer process are given in Table 7.3. The K value for the Cs⁺ carboxylate sample is higher than that for the Na⁺ carboxylate samples. For instance, the K values for the Cs⁺ and Na⁺ neutralized sample are 270 and 190 kg/mol, respectively. Therefore, larger amounts of water are transferred into the Cs⁺ neutralized core than the Na⁺ neutralized core. This result is in agreement with that observed for concentrated solutions of poly (acrylic acid) salts in which larger cations were found to hydrate more water than smaller cations. The values of ΔH_t^o and ΔS_t^o for the Cs⁺ neutralized sample are less negative than those of the Na⁺ neutralized samples. This result is expected and arises from the weaker ion-dipole interaction of Cs⁺ with water due to the larger Cs⁺ size.

7.4.1.5. Possible Structure of the Hydrated Core in Block Ionomers

From the above results, it is interesting to examine the possibility of forming a water pool in block ionomer reverse micelles. First, it is expected that at low values of R, water hydrates the counterions and polar head groups, as has been found in low molecular weight surfactant reverse micelles. For higher values of R, i.e. above the hydration requirements, it is expected that free water would emerge in the micelle cores. The presence of free water has been observed in AOT reverse micelles, in which the surfactant molecules form a monolayer effectively surrounding the water droplet. Block ionomer micelles, in contrast to those of AOT, contain more than one ionic group per chain. When the block ionomer is dissolved in an extremely unfavorable solvent for the block forming the core, the micelle core can be regarded as "frozen", i.e. the exchange of single chains between micelles is extremely slow.⁶¹ This aspect is particularly apparent for long ionic block lengths in which the glass transition (Tg) of the core is higher than room temperature. It is expected that the addition of water would decrease the T_g of the core and thus increase the exchange of chains between micelles. However, if this exchange is slow, then the single chains would not be able to associate further in order to form a monolayer which could surround the solubilized water, as in the AOT surfactants.

The absence of monolayer formation in reverse ionomer micelles containing water has been found in a recent study by SAXS.⁶² This study measured the core radius (R_c) of a PS-b-PACs reverse micelle as a function of R. The R_c values were found to increase for R values from 0 to 1.4, then remain constant from R values ranging from 1.4 to 10. This result is in contrast to that observed for AOT reverse micelles, in which the core radius has been found to increase progressively with R.¹⁶ As a result of the absence of monolayer formation in the ionomer micelles, the micelle core can be regarded as a hydrated ionic core and not a water pool. It is expected that a water pool could be formed

in block ionomer micelles if a cosurfactant were added, as has been found for other polymeric microemulsions.³⁵

It should be noted that for high block ionomer concentrations at $R \ge 10$ the solutions were found to be cloudy. These cloudy solutions appeared to be stable, and no precipitation of the block copolymers occurred. The ¹H NMR spectra for higher polymer concentrations showed the presence of two chemical shifts for water corresponding to that of solubilized and of bulk water. The presence of these two peaks suggests that the exchange between the two water phases is slow on the NMR time scale. It should be noted that this result is consistent with those previously observed for the formation of water in oil microemulsions, beyond the limit of water solubilization in the systems. ^{2,63} Thus R = 10 is expected to be the maximum threshold for water incorporation in the block ionomer micelles, after which an emulsion is formed.

7.4.2. Relaxation Studies of Nuclei in the Ion-Water Core

The molecular dynamics of the ionic cores of block ionomer micelles was investigated by multinuclei NMR relaxation measurements. Figure 7.8 illustrates the longitudinal and transverse relaxation rates (R₁ and R₂) for different water nuclei: ¹⁷O, ²H, and ¹H, and for the ²³Na counterion as a function of R in the PS(440)-b-PMANa(40) block ionomer. In general, the relaxation rates were found to decrease with R, indicating an increased mobility in the solubilized water molecules and the Na⁺ counterions. The mechanism for ¹H nuclei relaxation is by dipole-dipole coupling. Dipolar water-water effects can be distinguished from other relaxation processes by progressive substitution with deuterium which has been performed in studies of bulk water⁶⁴ and of water in reverse micelles. ^{11,65} The other nuclei investigated, ¹⁷O, ²H, and ²³Na relax by intramolecular electric quadrupole couplings.

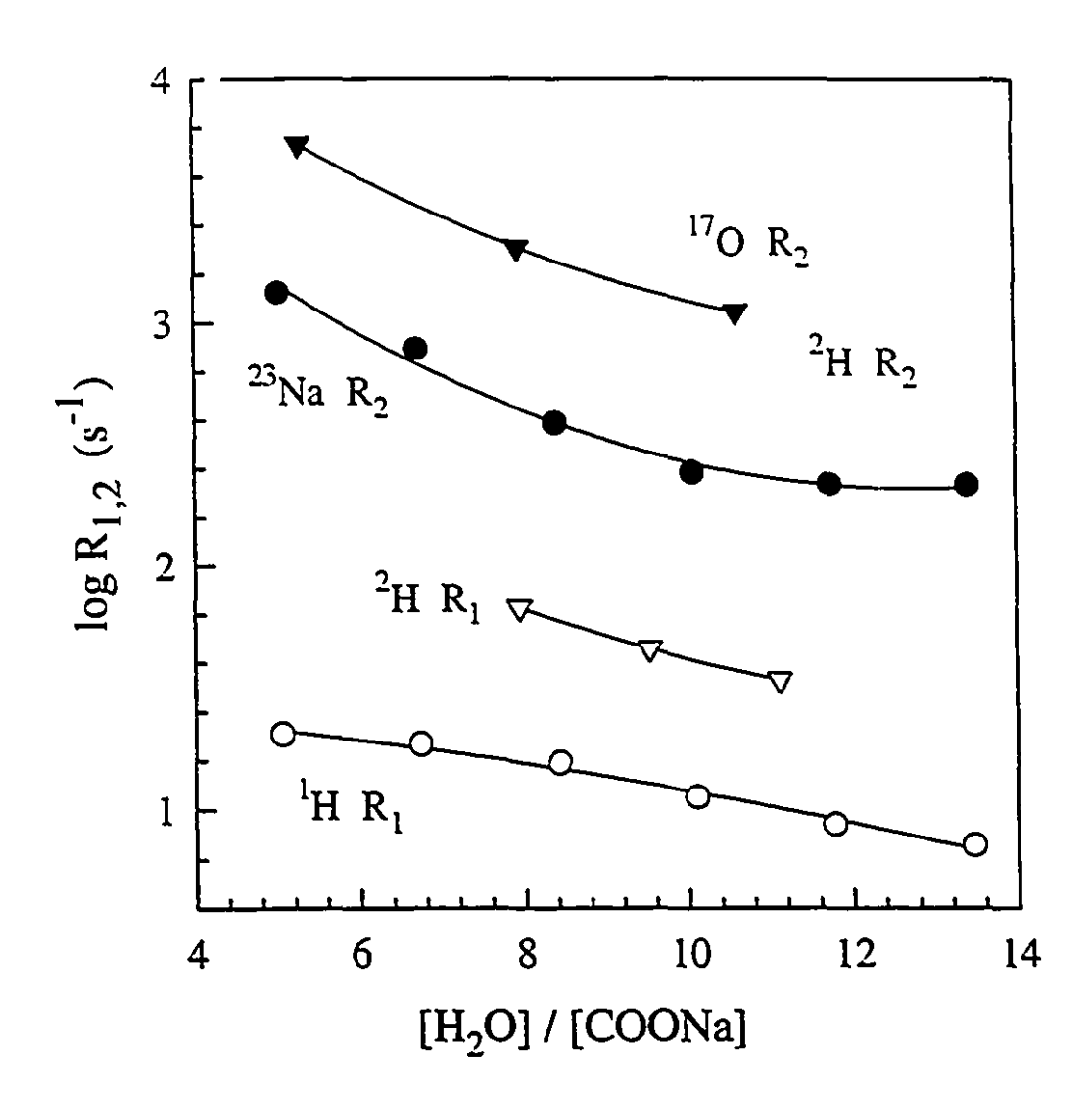


Figure 7.8. Relaxation rates of different nuclei in the aqueous core of PS(440)-b-PANa(40) reverse micelles.

y.

7.5. CONCLUSIONS

The distribution coefficient (K) of water partitioning between the toluene phase and the cores of reverse micelles formed from AOT and block ionomers was investigated at R = 6. For AOT, plots used to evaluate K, i.e. $(\delta_{obs} - \delta_{sol}) / [D_T]$ versus δ_{obs} were found to deviate from linearity near the cmc. When these plots were corrected for the cmc values, the plots became linear. The K constants determined from the slope of these linear plots and those using the initial slope of the nonlinear lines (i.e. not corrected for the cmc) at concentrations 10 times higher than the cmc, gave essentially the same values within experimental error. Therefore, the concentrations used in the determination of the K should be corrected for the cmc at low concentrations while above ca. 10 times the cmc, no corrections are needed.

An alternative method of determining the cmc's and the K values was by fitting plots of δ_{obs} versus [D_T]. The cmc's evaluated were found to agree with those determined from plots of the ¹H chemical shift of water at different surfactant concentrations. The K values were also found to agree with those determined from the slope of $(\delta_{obs} - \delta_{sol})$ / [D_M] versus δ_{obs} plots. The advantage of this method is that concentrations below the cmc are not required for the cmc evaluation.

The block ionomers studied were PS-b-PMANa, PS-b-PANa, PS-b-P4VPMeI and PS-b-PACs with varying nonionic and ionic block lengths. Since the cmc's were much smaller than the concentrations employed, the relations for K were found to be linear and no correction was required for the cmc. The K values for the PS-b-PMANa were found to be the same as those for the PS-b-PANa block ionomers. These values were also found to be independent of the ionic and nonionic block lengths.

The K values for the different reverse micelle systems were found to decrease in the following order according to the ionic groups, $COO^-Cs^+ > SO_3^-Na^+ \sim COO^-Na^+ > N_{py}^+(Me)I^-$. This result shows that the transfer of water is not only affected by the

interactions of water with the solvent, but that the nature of the interactions between the water and the core also significantly influences the transfer.

Thermodynamic parameters for the transfer process were evaluated from the temperature dependence of K. The enthalpy and entropy of transfer of water to the AOT reverse micelles and to PS-b-PACs was found to be similar to the transfer of water from a toluene phase to a bulk water phase. On the other hand, for the other block ionomer micelles the $-\Delta H_t^0$ and $-\Delta S_t^0$ values were found to be larger than those of AOT. The $-\Delta H_t^0$ and $-\Delta S_t^0$ values increased for the different reverse micelles according to the order: SO_3 -Na⁺ ~ COO-Cs⁺ > COO-Na⁺ ~ N_{py} +(Me)I⁻. This order reflects the stronger water interaction and greater ordering of the solubilized water in the cores of the block ionomers with the exception of PS-b-PACs in which the interaction was found to be weaker due to the larger Cs⁺ counterion size.

The mobility of water nuclei and of Na⁺ counterions was also investigated by multinuclei relaxation experiments for R values ranging from ca. 5 to ca. 14. In general, it was found that the relaxation rates decreased with R, indicating an increase in the mobility of these nuclei.

7.6. ACKNOWLEDGMENT

The authors would like to thank Dr. Alain Desjardins, Dr. Xing-Fu Zhong and Dr. Sunil K. Varshney, who synthesized the block copolymer samples in connection with other projects. The authors would also like to thank Dr. Francis Bossé for useful discussions. This work was supported by the Natural Sciences and Engineering Research Council of Canada (NSERC) and Le Fonds pour La Formation de Chercheurs et L'Aide à la Recherche (FCAR). K.K. is grateful for scholarship funding provided from NSERC and FCAR.

7.7. REFERENCES

- Martinek, K.; Levashov, A. V.; Khmelnitsky, Y. L.; Klyachko, N. L.; Berezin, I. V. Biochim. Biophys. Acta 1989, 981, 161.
- 2 Kithara, A. Adv. Colloid and Interface Sci. 1980, 12, 109.
- Fendler, J. H.; Fendler, E. J., Catalysis in Micellar and Macromolecular Systems;

 Academic Press: N. Y., 1975.
- Khmelnitsky, Y. L.; Levashov, A. V.; Klyachko, N. L.; Martinek, K. Russ. Chem. Rev.(Engl. Transl.) 1984, 319. (translated from Uspekhi Khimii 1984, 53, 545.)
- (a) P.L. Luisi and L. J. Magid, CRC Critical Reviews in Biochemistry 1986, 20,
 409. (b) Luisi, P.L.; Giomini, M.; Pileni, M. P.; Robinson, B. H., Biochim.
 Biophys. Acta 1988, 947, 209.
- El-Nokaly, M. A.; Piatt, D. M.; Charpentier, B. A., Eds.; *Polymeric Delivery Systems: Properties and Applications*; ACS Symposium Series 520; American Chemical Society: Washington, DC, 1993.
- Goto, A.; Harada, S.; Fujita, T.; Miwa, Y.; Yoshioka, H.; Kishimoto, H. Langmuir, 1993, 9, 86.
- (a) D'Aprano, A.; Lizzio, A.; Leveri, V. T. J. Phys. Chem. 1987, 91, 4749.
 (b) Goffredi, F.; Liveri, V. T.; Vassallo, G. J. Colloid Interface Sci. 1992, 151, 396.
 (c) Goto, A.; Yoshioka, H.; Kishimoto, H.; Fujita, T. Langmuir 1992, 8, 441.
- 9 Chachaty, C. Prog. Nucl. Magn. Reson. Spectrosc. 1987, 19, 183. and references therin.
- Wong, M.; Thomas, J. K.; Nowak, T. J. Am. Chem. Soc. 1977, 99, 4730.
- 11 Llor, A.; Rigny, P. J. Am. Chem. Soc. 1986, 108, 7533.
- Söderman, O.; Stilbs, P. Progress in NMR Spectroscopy 1994, 26, 445.

- (a) Hauser, H.; Haering, G.; Pande, A.; Luisi, P. L. J. Phys. Chem. 1989, 93,
 7869. (b) Christopher, D. J.; Yarwood, J.; Belton P. S.; Hills, B. P. J. Colloid Interface Sci 1992, 152, 465. and references therin.
- (a) Gaudel, Y.; Pammeret, S.; Yamada, N.; Migus, A.; Antonetti, A. J. Am.
 Chem. Soc. 1989, 111, 4974. (b) Belletete, M.; Durocher, G. J. Colloid Interface
 Sci. 1990, 134, 289. (c) Zhang, J.; Bright, F. V. J. Phys. Chem. 1991, 95, 7900.
- 15 Hauser, H.; Haering, G.; Pande, A.; Luisi, P. L. J. Phys. Chem. 1989, 93, 7869.
- Zulauf, M.; Eicke, H. F. J. Phys. Chem. 1979, 83, 480. (b) Day, R. A.; Robinson,
 B. H.; Clarke, J. H. R.; Doherty, J. V. J. Chem. Soc. Faraday Trans. I 1979, 75,
 132.
- 17 Assih, T.; Larche, F.; Delord, P. J. Colloid Interface Sci. 1982, 89, 35.
- 18 Chen, S. H. Ann. Rev. Phys. Chem. 1986, 37, 351.
- ¹⁹ Eicke, H.-F.; Rehak, J. Helv. Chim. Acta 1979, 59, 2883.
- Nagarajan, R.; Barry, M.; Ruckestein, E. Langmuir 1986, 2, 210.
- ²¹ Valint, Jr., P.L.; Bock, J. Macromolecules 1988, 21, 175.
- Tentisakis, A.; Hilfiker, R.; Chu, B. J. Colloid and Interface Sci. 1990, 135, 427.
- 23 Hurter, P.; Hatton, T. A. Langmuir 1992, 8, 1291.
- Kiserow, D.; Prochazka, K.; Ramireddy, C.; Tuzar, Z.; Munk, P.; Webber, S.E.
 Macromolecules 1992, 25, 461.
- ²⁵ Saito, Y.; Kondo, Y.; Abe, M.; Sato, T. Chem. Pharm. Bull. 1994, 42, 1348.
- 26 Kazanskii, K. S.; Dubrovskii, S. A. Adv. in Polym. Sci. 1992, 104, 97.
- (a) Calvert, T. L.; Phillips, R. J.; Dungan, S. R. AIChE J. 1994, 40, 1449.
 (b) Dualeh, A. J.; Steiner, C. A. Macromolecules 1991, 24, 112.
- 28 Dan, N.; Tirrell, M. Macromolecules 1993, 26, 637.

- Hurter, P. N.; Scheutjens, J. M. H. M.; Hatton, T. A. Macromolecules 1993, 26, 5030 and 5592.
- 30 Cogan, K. A.; Leermakers, F. A. M.; Gast, A. P. Langmuir 1992, 8, 429.
- 31 Boutillier, J.; Candau, F. Coll. Polym. Sci. 1979, 257, 46.
- 32 Candau, F.; Boutillier, J.; Tripier, F.; Wittman, J.-C. Polymer 1979, 20, 1221.
- 33 Candau, F.; Guenet, J.-M.; Boutillier, J.; Picot, C. Polymer 1979, 20, 1227.
- 34 Candau, S.; Boutillier, J.; Candau, F. Polymer 1979, 20, 1237.
- 35 Ballet, F.; Candau, F. J. Polym. Sci., Polym. Chem. Ed. 1983, 21, 155.
- 36 Riess, G.; Nervo, J.; Rogez, D. Polym. Eng. Sci. 1977, 17, 634.
- 37 Marie, P.; Gallot, Y. C.R. Acad. Sci. Paris 1977, C-284, 327.
- Marie, P.; Duplessix, R.; Gallot, Y.; Picot, C. Macromolecules 1979, 12, 1180.
- ³⁹ Cogan, K. A.; Gast, A. P. Macromolecules 1990, 23, 745.
- 40 Vagberg, L. J. M.; Cogan, K. A.; Gast, A. P. Macromolecules 1991, 24, 1670.
- Gao, Z; Desjardins, A; Eisenberg, A. Macromolecules 1992, 25, 1300.
- Desjardins, A.; van de Ven, T. G. M.; Eisenberg, A. Macromolecules 1992, 25, 2412.
- Zhong, X. F.; Varshney, S. K.; Eisenberg, A. Macromolecules 1992, 25, 7160.
- 44 Gao, Z.; Zhong, X.-F.; Eisenberg, A. Macromolecules 1994, 27, 794.
- Nguyen, D.; Zhong, X.-F.; Williams, C. E.; Eisenberg, A. Macromolecules 1994, 27, 5173.
- Sepulveda L.; Lissi E.; Quina F. Adv. Coll. Interface Sci. 1986, 25, 1-57
- 47 Kim, V.; Frolov, Y. G.; Kharlamova, I. M. Kolloidn. Zh. 1986, 48, 1210.
- Desjardins, A.; Eisenbeerg, A. Macromolecules 1991, 24, 5779.
- Zhong, X.-F.; Varshney, S. K.; Eisenberg, A. Macromolecules 1992, 25, 7160.

- Nguyen, D.; Varshney, S. K.; Williams, C. E.; Eisenberg, A. Macromolecules 1994, 27, 5086.
- 51 Kwan, C. L.; Atik, S.; Singer, L. A. J. Am. Chem. Soc. 1978, 100, 4783.
- 52 Yekta, A.; Aikawa, M.; Turro, N. J. Chem. Phys. Lett. 1979, 63, 543.
- 53 Giddings, L. D.; Olesik, S. V. Langmuir 1994, 10, 2877.
- 54 Khougaz, K.; Gao, Z.; Eisenberg, A. Macromolecules 1994, 27, 6341.
- (a) Kon-no, K.; Kitahara, A. J. Colloid Interface Sci. 1971, 35, 409.
 (b) Kon-no,
 K.; Kitahara, A. J. Colloid Interface Sci. 1971, 37, 469.
- Linke, W.F. Solubilities, Inorganic and Metal-Organic Compounds; American Chemical Society: Washington, D.C., 1958; vol 2, p.1135.
- 57 Larsen, J. W.; Magid, L. J. J. Phys. Chem. 1974, 78, 834.
- 58 Lumry, R.; Rajender, S. *Biopolymers* **1970**, 9, 1125.
- Day, R.; Robinson, B. H.; Clarke, J. H. R.; Doherty, J. V. J. Chem Soc. Faraday Trans. I. 1979, 75, 132.
- Hiraoka, K.; Yokoyama, T. J. of Polymer Science: Part B: Polymer Physics 1986,24, 769.
- Tian, M.; Qin, A.; Ramireddy, C.; Webber, S. E.; Munk, P.; Tuzar, Z.; Prochazka, K., Langmuir 1993, 9, 1741.
- 62 Nguyen, D.; Williams, C. E.; Eisenberg, A. In preparation.
- 63 Frank, S. G.; Shaw, Y.-H.; Li, N. C. J. Phys. Chem. 1973, 77, 238.
- 64 Smith, D. W. G.; Powles, J. G. Mol. Phys. 1966, 10, 451.
- Zhu, X. X.; Bardez, E.; Dallery, L.; Larrey, B.; Valeur, B. New J. Chem. 1992, 16,973.

CHAPTER 8

Conclusions, Contributions to Original Knowledge, and Suggestions for Future Work

8.1. CONCLUSIONS AND CONTRIBUTIONS TO ORIGINAL KNOWLEDGE

The following section describes the main conclusions and the contributions to original knowledge for each chapter. The section is divided into three parts summarizing, respectively, the results for block polyelectrolyte micelles in aqueous media (Chapter 3), the determination of critical micelle concentrations for block copolymers by static light scattering (Chapter 4) and the results obtained on reverse micelles in organic solutions (Chapters 4, 5 and 6).

8.1.1. Block Polyelectrolyte Micelles

Chapter 3 presented the first systematic study of the aggregation numbers, second virial coefficients and sizes of block polyelectrolyte micelles in aqueous media, i.e. in the absence of a co-solvent. The micelles were formed from the association of polystyrene-b-poly(sodium acrylate) (PS-b-PANa) block copolymers and several factors influencing their micellization were investigated by static light scattering (SLS). Initially, it was found that

gel-like particles formed upon sample dissolution. These aggregated particles were postulated to arise from the ionic interactions of the PANa coronal chains which most likely originated in the solid state. For a typical sample, PS(40)-b-PANa(520) it was found that as the sample was heated at 100 °C in a sealed ampoule, the scattered intensity and dissymmetry ratio decreased with heating time. For instance, after ca. 50 hours of heating, no further changes occurred in the scattered intensity. This disentanglement process was also investigated for samples with different PS and PANa block lengths. It was found that block copolymers with shorter PANa block lengths dissociated faster. The samples in the study were all heated for 5 days at 100° C in order to ensure a high extent of disentanglement.

The effects of the sodium chloride (NaCl) content on the micellar parameters were investigated for two samples, PS(6)-b-PANa(180) and PS(23)-b-PANa(300). It was found that the aggregation numbers (Nagg) increased with the salt concentration up to ca. 0.10 M NaCl. At higher salt contents, up to 2.5 M, the Nagg values remained constant. This result was consistent with the theory of Dan and Tirrell, which predicts that at moderately high salt concentrations micellar properties will be dominated by the insoluble block. The radius of gyration values (Rg) were independent of the salt concentration with the exception of PS(6)-b-PANa(180) in 0.025 M NaCi. The Rg of this sample at 0.025 M was ca. two times larger than that at higher salt concentrations. The second virial coefficient values (A2) for different salt concentrations were found to be similar to those reported in the literature for poly(sodium acrylate).

The effect of the soluble and insoluble block lengths on the aggregation behavior of PS-b-PANa was investigated in 2.5 M NaCl. It was found that the N_{agg} values were influenced much more by the insoluble block length than the soluble block length. The scaling relations of the star model and several mean field models were investigated in order to establish relations between the N_{agg} , the core radius (R_c) and the R_g values as a

function of the block lengths. In general, good agreement was obtained with these models.

The core radii values for the PS-b-PANa block copolymers in 2.5M NaCl solutions were compared with those determined for similar PS based block ionomers in the solid state. The core radii of the latter samples were evaluated from small angle X-ray scattering in an independent study. Good agreement between the two R_c values was observed. Based on this result, it can be concluded that the micelles in 2.5 M NaCl existed singly, i.e. that no supermicellar aggregates were present, and that the cores were solvent free, which is expected due to the unfavorable interactions between water and PS. The R_c values of the block polyelectrolyte micelles in 2.5 M NaCl solutions were found to be similar to those of a nonionic block copolymer system, polystyrene-b-poly(ethylene oxide) (PS-b-PEO) in water. This result shows that for these two PS based block copolymers in aqueous media, the nature of the soluble block does not seem to have a significant effect on the R_c or N_{agg} values.

8.1.2. Cmc Determination of Block Copolymer Micelles by SLS

Chapter 4 describes the development of a new method for the evaluation of the critical micelle concentrations (cmc's) of block copolymer micelles by SLS. In general, cmc values can be determined from the onset of the single chain region. However, this region is often unattainable because of the low magnitude of the cmc for block copolymer micelles. Up to now, current methods of cmc determination have employed the Debye equation which does not take into account the effects of polydispersity of the insoluble block on the cmc. Therefore, an improved method for the cmc determination of block copolymer micelles by SLS was presented in this chapter.

This method is based on a recent micellization theory of block copolymers, the mixed micelle model, which accounts for the effects of polydispersity. For instance, the

method considered the change of the total single chain concentration with total polymer concentration and the polydispersity of the insoluble block. The dependence of the cmc on the insoluble block length (N_B) was described by the following

$$\log(\text{cmc}) = a N_{\text{B}}^{1/3} + b$$

where a and b are constants. Once the a and b values are known, cmc values can be predicted for samples having different insoluble block lengths and different polydispersity indices.

The cmc values were evaluated for two systems, PS-b-PANa in tetrahydrofuran (THF) and polystyrene-b-poly(4-vinylpyridine) (PS-b-P4VP) in toluene. It was found that for a block ionomer series, PS(660)-b-PANa(x) where x was varied from 2.6 to 14 units, the cmc values could be evaluated by both the present method and the Debye equation. This result was attributed to the fact that the block ionomer samples had a narrow molecular weight distribution and a weak dependence of the cmc on the insoluble block length (a = -0.64). On the other hand, for PS(470)-b-P4VP(52), the dependence of the cmc on the insoluble block length was larger (a = -1.66) and only the proposed method was able to represent the cmc value. The polystyrene-b-polyisoprene (PS-b-PI) block copolymer system was modeled to show the effects of polydispersity on a system with a significant dependence of the cmc on the insoluble block length (a = -1.65). It was found that the Debye equation did not describe the cmc values and that the values depended on the range of points used in the evaluation.

8.1.3. Block Copolymer Reverse Micelles

Chapters 5 and 6 focused on the characterization of reverse micelles formed from PS-b-PANa and polystyrene-b-poly(acrylic acid) (PS-b-PAA) block copolymers in organic solvents. Chapter 4 presented the first systematic investigation of cmc values for block ionomer micelles in general and also for the nonionic PS-b-PAA block copolymer system.

This chapter was also the first to examine the effect of the PS and PANa block lengths on the aggregation of PS-b-PANa block ionomers in dilute solution by SLS. The novelty of the study in Chapter 5 was to probe the effects of different degrees of neutralization of the PAA core of PS-b-PAA block copolymer micelles by SLS and SAXS. The conclusions of these two chapters are given below.

The cmc values for PS(660)-b-PANa(x) and PS(660)-b-PAA(x), where x was varied from 2.6 to 18 units, was evaluated in different solvents by SLS. The cmc values for PS-b-PANa in toluene, THF and chloroform and those for PS-b-PAA in toluene were found to range from ca. 1 x 10^{-7} to 5 x 10^{-9} M. These values represent some of the lowest cmc values which have yet been reported in a systematic study of block copolymer micelles. The molecular weight distributions of the single chains and the micelle fractions were evaluated using the mixed micelle model and little segregation was found. This result was due to the small dependence of the cmc on the insoluble block length. The a and b constants which were evaluated for these systems as well as for others were correlated to the interaction parameters between the polymer forming the core and the solvent ($\chi_{core-sol}$). It was found that when $\chi_{core-sol}$ was large, the dependence of the insoluble block length was weak (small absolute value of a) and the cmc values were low (small value of b).

These block copolymer samples were also characterized by size exclusion chromatography (SEC) and dynamic light scattering (DLS). By SEC, the percent of micellized chains was determined. By using these values, the weight-average molecular weights (M_w) which were determined by SLS were corrected for the unmicellized polymer in order to evaluate the M_w for the micelles. From these later values, the aggregation numbers were calculated. The trends in N_{agg} as a function of insoluble block length were found to be opposite to those observed in the cmc values. The hydrodynamic radii of the PS(660)-b-PANa(x) block ionomers were found to be similar in toluene, THF, and chloroform since the expansion of PS is expected to be similar in these solvents.

The effect of the soluble and insoluble block lengths on the aggregation of PS-b-PANa in THF was investigated by SLS. A range of block ionomers was studied in which the PS and the PANa block lengths ranged from 190 to 2300 units and from 2.6 to 69 units, respectively. The soluble block length was found to influence the aggregation numbers significantly. Scaling relations were developed to describe the dependence of N_{agg} and R_c with the block lengths, $N_{agg} \propto N_{PANa}$ 0.5 N_{PS} -0.6 and $R_c \propto N_{PANa}$ 0.5 N_{PS} -0.2. The surface area per chain was found to be proportional to N_{PANa} as was predicted by the star model.

In Chapter 6, a description is given of the micellization of PS-b-PAA for different degrees of neutralization of the PAA block. The scattered intensity was monitored for a PS(600)-b-PAA(x) series where x was either 13, 34, or 45 units, as a function of the addition of cesium hydroxide (CsOH) in methanol. It was found that micellization began for these samples when the PAA chain was neutralized to the extent of 5 %. In another part of the study, PS(600)-b-PAA(34) and PS(600)-b-PAA(45) block copolymers were neutralized with CsOH to different degrees ranging from 5 to 150 %, freeze dried and redissolved in toluene. The N_{agg} and R_c values were then evaluated by SLS and SAXS, respectively. It was found that three regions could be distinguished, depending on the extent of neutralization of the PAA chain. In the first region, between 5 and 60 % neutralization, it was found that Nagg was constant and Rc increased. The Rc values increased due to the replacement of protons with Cs ions, which are larger in size. In the second region, between 60 and 100 % neutralization, Nagg was found to increase and Rc remained constant. In the third region, from 100 to 150 % neutralization, no further increase in Nagg occurred and Rc values increased, most likely due to the solubilization of excess Cs in the micelle core. To explain these results, it was postulated that the single chains and micelles were in a dynamic state at low degrees of neutralization (< 60%) and that for higher degrees, the dynamics were considerably reduced.

The focus of Chapter 7 was the solubilization of water into the cores of reverse micelles in toluene formed from a surfactant, sodium bis(2-ethylhexyl)sulfosuccinate (AOT), and from block ionomers having a nonionic soluble PS block attached to different ionic blocks. The block ionomers investigated were PS-b-PANa, PS-b-PMANa, PS-b-PACs, and polystyrene-b-poly(4-vinylpyridinium methyl iodide) (PS-b-P4VPMeI). This study represents the first which has examined the effects of a wide range of parameters, such as the effects of the block lengths, nature of the cores and the temperature, on the transfer of water in block ionomers. The thermodynamics of water solubilization was also evaluated for these systems.

The distribution coefficient (K) of water was determined from ¹H chemical shift measurements. It was found that for AOT reverse micelles, the K values were influenced significantly by the surfactant concentration range employed. For concentrations near the cmc, the plots used in the determination of K were non-linear and corrections for the cmc were required. The cmc values were determined experimentally from plots of the ¹H chemical shift observed as a function of the inverse surfactant concentration. Alternatively, it was found that using the initial slopes of the nonlinear plots at concentrations of ca. 10 times higher than the cmc, the K values could be evaluated. The values for K determined by these two methods were found to be agree withir experimental error.

For the block ionomer reverse micelles, it was found that the plots for the determination of K were linear. The linearity was due to the fact that the concentrations employed in the NMR studies were significantly higher than the cmc values. It was found that the K values for PS-b-PANa and PS-b-PMANa were the same and no block length dependence was observed. The K values for the different micellar systems were compared and found to decrease in the following order for the different ionic groups: COO-Cs+ > SO₃-Na+ ~ COO-Na+ > > N_{py}+(Me)I-, where N_{py}+(Me)I- represents pyridine quarternized with methyl iodide. This trend was explained by the stronger interactions of

water with the anionic reverse micelle systems compared to that with the cationic reverse micelle system. It was concluded that the interactions between water and the micelle core contribute significantly to the distribution of water.

The thermodynamic parameters for the water transfer process were evaluated from the temperature dependence of the distribution coefficients. It was found that for AOT, the enthalpy (ΔH_t^{O}) and entropy (ΔS_t^{O}) of transfer were similar to those calculated for the transfer of water from a toluene phase to a bulk water phase. On the other hand, for PS-b-PANa, PS-b-PMANa and PS-b-P4VPMeI, the interaction energy was found to be stronger (i.e. larger negative ΔH_t^{O} value) and the water structure was found to be more ordered (i.e. larger negative ΔS_t^{O} value). The ΔH_t^{O} and ΔS_t^{O} values for the cesium neutralized samples, PS-b-PACs, was found to be less negative compared to the sodium neutralized sample. This result was attributed to the weaker interactions of the larger Cs counterion with water compared to those of water with Na. An extropy-enthalpy compensation appeared to exist in the water transfer process. In the reverse micelle systems, an entropy-enthalpy compensation appeared to exist for the water transfer process.

The mobility of different nuclei in the block ionomer micelles was probed by multinuclei relaxation measurements. It was found that the mobility of the water nuclei (1H, 2H, and 17O) and the 23Na counterion increased with the addition of water.

8.2. SUGGESTIONS FOR FUTURE WORK

The effects of different preparation conditions on the micellization of the PS-b-PANa block polyelectrolyte samples can be examined. For instance, the block polyelectrolytes discussed in Chapter 3 of this thesis were prepared by dissolving the block copolymers in water and heating at 100°C for a few days. These micelles were postulated

to be in a thermodynamic equilibrium state since the glass transition temperatures of the PS cores were below 100°C. An alternative procedure would involve dissolving the block copolymers in a mixed solvent which is good for both blocks, such as a mixture of water and dioxane. In this solvent mixture, the block copolymer would be present as single chains. Micelle formation could then be induced by progressively removing the dioxane by stepwise dialysis. Comparison of the aggregation numbers, second virial coefficient values and sizes of the micelles prepared by these two different methods could then be made.

An interesting feature of block polyelectrolyte micelles which was described in Chapter 3 was the fact that the PANa chains in the corona appeared to be in a highly stretched conformation. It would be of interest to examine the extent of the stretching of these chains. For instance, the extension of the chains could be evaluated from the difference of the hydrodynamic radius of the micelle measured by dynamic light scattering (DLS) and the core radii calculated as described in Chapter 3.

This thesis also focused on the characterization of reverse block copolymer micelles. Several aspects regarding these micelles can be examined further. First, the effects of the solubilization of low molecular weight polar compounds, such as water and alcohols, and high molecular weight compounds such as polar homopolymers, on the cmc's, aggregation numbers and micelle sizes can be investigated by SLS as well as by DLS. Second, it would be of interest to determine the critical micelle temperatures (CMT's) by SLS of some nonionic block copolymer reverse micelles, such as PS-b-PVP. It should be noted that CMT's for block ionomer micelles would probably be unattainable because these values would be expected to be quite high. Third, the present studies concentrated on the micellization of spherical particles. By increasing the volume fraction of the block forming the core, it would be expected that different morphologies would form. For instance, the PS(190)-b-PANa(24) block ionomer, discussed in Chapter 5, was found to most likely form non-spherical micelles because of the relatively high percent of

the insoluble block. These non-spherical morphologies could be studied by transmission electron microscopy. In addition, measurements by SLS and DLS in combination could confirm the presence of the non-spherical morphology and would enable the characterization of a wide range of micellar parameters.

In Chapter 7, the hydrated ionic core of some block ionomers was discussed. A further step would be to investigate the solubilization of other substances in the hydrated cores. For instance, enzymes could be solubilized and their activity could be compared to results which have been obtained on similarly solubilized enzymes in surfactant reverse micelles. An advantage which could be envisaged in employing block ionomers would be the stability of these micelles as well as the size control of the cores. The latter fact is apparent since relationships have been developed between the block length and the core sizes.

Also, the formation of microemulsions in block ionomer reverse micelles can be explored. The microemulsions could be prepared for instance, by the addition of water and a cosurfactant such as an alcohol. The structure and the dynamics of the microemulsion can be examined by DLS and NMR measurements, respectively. A phase diagram for block ionomers in the presence of these two molecules can also be constructed.

Annex A

This program is used to determine the cmc values for block copolymer micelles.

```
These are the two Subroutines
 FileInput: Get the name of the input file
       The Input FILE name must have a ".pm" extension.
       Then FileInput reads the cx, KcRo, n0, Mm values
        cx: Experimental Concentration
        KcRo: Experimental KcRo Values
        n0: Number of Ionic Units
        Mm: Polymer MW
        npt%: Number of Data Points in the Set
 Limits: Input the Initial Values the Parameters
        amax: Maximum value for a (minimum = 0)
        bmax: Maximum value for b (minimum = -10)
         astep: Stepsize between iterations for a
         bstep: Stepsize between iterations for b
        HI: Polydispersity Index
         Ms: PS MW
DECLARE SUB FileInput ()
DECLARE SUB Limits ()
'These variables SHARED between the Main Program and the Subroutines
COMMON a%, b%, c%, d%, e%, f%, o%, npt%, Ms, HI, A2
COMMON bmin, bmax, bstep, amin, amax, astep, k10%
'I'm Initializing the Constants
k10\% = 10; k100\% = 100; k1000\% = 1000; k10000\% = 10000; maxit% = 15000
a\% = 1: b\% = 2: c\% = 3: d\% = 4: e\% = 5: f\% = 6: o\% = 0: npt\% = k100\%
'I'm Initializing the Variables
Khi2min = 10000: pi = 3.1416: Ms = 69000: HI = 1.1: A2 = 0\%
'Dimensions of the Arrays SHARED between the main Program and the Subroutines
DIM SHARED cx(npt%), KcRo(npt%), n0(npt%), Mm(npt%)
DIM SHARED see$(a%), file$(40), txt$(40)
'Dimensions of the Arrays for the Main Program
DIM r(k1000%), f(k1000%), Ci#(k1000%)
```

```
FileInput
Limits
'More Constants for the Calculation and get Initial Time
TIMER ON
PRINT "Time: "; TIME$
STtime = TIMER
fb1 = b\% * pi
fb2 = a\% / b\%
k3 = a\% / c\%
b = bmax + bstep
'This is where the b Loop Start
NewbValue: b = b - bstep: a = amax + astep
'This is where the a Loop Start
NewaValue: a = a - astep
Khi2 = 0\%
'Now for all the Data Set Points we minimize using X. GAO Equation
FOR j = a\% TO npt%
c = cx(i)
'The Contribution to the Summation must be decreased at low c values
'Test to find the right value of k%
k1 = k1000\%
IF c < .0000001 THEN
   k\% = k100\%
ELSE
  IF c < .000001 THEN
   k\% = e\%
  ELSE
   k\% = a\%
  END IF
END IF
'Calculate Sigma then More Constants for the Gaussian Distribution (GD)
sigma = (HI - a\%) ^ fb2 * n0(i)
sigma2 = sigma * sigma
```

```
fb3 = fb2 / sigma
 expo = b\% * sigma2
 m# = c
'Get Lower Limit of the Distribution, GD = Mean - (3 * sigma)
'Test if it is lower then 1 (gmin\% >= 1)
 g = c\% * sigma
 gmin\% = CINT(n0(j) - g)
 IF gmin% < a% THEN gmin% = a%
'Higher limit of the Distribution, GD = Mean + (3 * sigma)
 gmax\% = CINT(n0(j) + g)
 tst# = z# - a\%
'Flag ok% is set to FALSE. Set to TRUE after the Calculation of GD
'Flag it% controls the # of Iterations (Maximum # of Iterations = 15000)
 ok\% = o\%
 it\% = 0\%
HereWeGoAgain:
 it\% = it\% + a\%
 IF tst# < .00001 THEN
  m# = m# - m# / (k1 * k10000%)
 ELSE
  IF tst# < .0001 THEN
   m# = m# - m# / (k\% * k1000\%)
  ELSE
   IF tst# < .01 THEN
    m# = m# - m# / (k\% * k100\%)
   ELSE
    m# = m# - m# / (k\% * k10\%)
   END IF
  END IF
 END IF
 z# = 0\%
 IF ok\% = o\% THEN
  f1# = 0\%
  FOR I% = gmin% TO gmax%
   f(I\%) = fb1 ^-fb3 * EXP(-(I\% - nO(i)) ^ b\% / expo)
   f1# = f1# + f(1%)
   r(1\%) = 1\% ^(k3)
   Ci\#(I\%) = k10\% ^(-a * r(I\%) + b)
  NEXT 1%
  ok\% = a\%
 END IF
```

```
FOR I% = gmin% TO gmax%
  Y# = f(I\%) / fI# * c / (c + Ci#(I\%) - m#)
  2# = 2# + Y#
 NEXT 1%
 otst# = tst#
 tst# = z# - a\%
'Here we test if there is a variation between the current and previous z
'If the delta z is small, or the maximum # of Iterations is reach
'The minimum m# is found and the XGAO Minimization Process
' for the Data Point is over.
 IF it% > maxit% THEN GOTO finish
 IF ABS(tst# - otst#) >= .0000001 THEN GOTO HereWeGoAgain
finish:
'I have Found the Minimum for one data point.
'Print the result to screen then accumulate Khi2 for KcRo
 OldPastTime = PastTime
 PastTime = TIMER - STtime
 it = PastTime - OldPastTime
 PRINT
 PRINT "+*+**************************
 PRINT "C", "M"
 PRINT USING "+#.###^^^^ "; cx(j); m#
 PRINT "****************
 mc = m\#/c
 PRINT "mc= ": : PRINT USING "+#.###^^^ ": mc
 KcR = a\% / (Ms * mc + Mm(i) * (a\% - mc)) + b\% * A2 * cx(i)
 PRINT "KcR= "; : PRINT USING "+#.###^^^^ "; KcR;
 PRINT " KcRo= ":: PRINT USING "+#,###^^^ ": KcRo(i)
 PRINT "a: "; a, "b: "; b; " Data point: "; j
 PRINT CINT(it% / 150); "% Iterations in "; it; " seconds "
 PRINT "Total Time: "; PastTime / 60; "Minutes"
 Khi2 = Khi2 + (KcR - KcRo(i))^2 / KcRo(i) * KcRo(i)
NEXT i
'One set of Data is minimize for one pair of a and b values
Khi2 = ABS(Khi2)
'Test if the Khi2 is better then for the previous set of data
'If so keep Khi2, a and b values in Khi2min, al, bl, respectively.
'Output these values to screen and disk as a minimum.
```

```
'If it is not a minimum, output these values anyway, but not as minimum.
IF Khi2 < Khi2min THEN
 Khi2min = Khi2
 a1 = a: b1 = b
 BEEP: BEEP
 PRINT #b%.
 PRINT #b%, "=> Khi2 (Min) = "; Khi2min, "a= "; a1, "b= "; b1
 PRINT #b%, "Total Time: "; PastTime; " seconds"
 PRINT #b%.
*************************
 PRINT "=> Khi2 (Min) = "; Khi2min, " a="; a1, " b="; b1
 PRINT #b%.
ELSE
 PRINT
 PRINT "Khi2 = "; Khi2, " a="; a, " b="; b
 PRINT #b%, "Khi2 = "; Khi2, "a= "; a, "b= "; b
 PRINT #b%, "Total Time: "; PastTime; " seconds"
END IF
CLOSE (6%)
OPEN txt$ FOR APPEND AS #b%
'Test if the b interval has been scan. If True end program
IF b < bmin THEN
 PRINT #b%.
 PRINT #b%.
PRINT #b%, "Khi2 (Min) = "; Khi2min, " a="; a1, " b="; b1
 PRINT #b%.
*************************
 CLOSE (b%)
 GOTO That All Folks
END IF
'Test if the a interval has been scan. If TRUE move to next b value.
   if FALSE move on to the next a value
IF a < amin GOTO NewbValue
GOTO NewaValue
```

```
ThatAllFolks:
CLS
PRINT
PRINT "That's all Folks!"
PRINT "Hit a Key to Continue"
DO
BEEP
LOOP UNTIL INKEY$ <> ""
PRINT
PRINT
PRINT
PRINT
PRINT "Khi2min="; Khi2min, "a(best)="; a1, "b(best)="; b1
END
```

SUB FileInput SHARED npt%, cx, KcRo, n0, Mm, file\$, txt\$ SHARED 1%, b%, c%, d%, e%, o% CLS **PRINT: PRINT** INPUT "Enter Filename for the data (no .pm)"; file\$ **PRINT: PRINT** txt\$ = file\$ + ".pm" OPEN txt\$ FOR INPUT AS #1% npt% = 0%WHILE NOT EOF(a%) npt% = npt% + a%INPUT #a%, cx(npt%), KcRo(npt%), n0(npt%), Mm(npt%) WEND CLOSE #a% txtS = fileS + ".fit"OPEN txt\$ FOR OUTPUT AS #b% **END SUB**

```
SUB Limits
SHARED bmin, bmax, bstep, amin, amax, astep, Ms, HI, A2
SHARED a%, b%, e%, f%, o%, k10%, see$
TopaValues:
amin = 0\%
PRINT
INPUT "Input Maximum value of a (a>0)"; amax
INPUT "Input Minimum value of a (a>0)"; amin
INPUT "Input Step value of a "; astep
IF amin > amax THEN SWAP amin, amax
IF amin < 0\% THEN amin = 0\%
IF astep > amax - amin THEN astep = (amax - amin) / e%
PRINT "a (min) = "; amin, "a (max) = "; amax, "a step = "; astep
PRINT "These a Values are OK (Y)es or (N)o?"
DO
see$ = INKEY$
LOOP UNTIL see$ = "y" OR see$ = "Y" OR see$ = "N" OR see$ = "n"
IF see$ = "N" OR see$ = "n" THEN GOTO TopaValues
TopbValues:
bmin = -k10\%
PRINT
INPUT "Input Maximum value of b (b<0)"; bmax
INPUT "Input Minimum value of b (b<0)"; bmin
INPUT "Input Step value of b"; bstep
IF bmin > 0% THEN bmin = -bmin
IF bmin < -k10\% THEN bmin = -k10\%
IF bmax > 0\% THEN bmax = -bmax
IF bmin > bmax THEN SWAP bmin, bmax
IF bstep > bmax - bmin THEN bstep = (bmax - bmin) / e%
PRINT "b (min) = "; bmin, "b (max) = "; bmax, "b step = "; bstep
PRINT "These b Values are OK (Y)es or (N)o?"
DO
see$ = INKEY$
LOOP UNTIL see$ = "y" OR see$ = "Y" OR see$ = "N" OR see$ = "n"
IF see$ = "N" OR see$ = "n" THEN GOTO Topb Values
TopkkkValues:
PRINT
INPUT "Input Polydispersity Index (P.I.>1)"; HI
IF HI \leq= a% OR HI \geq= b% THEN HI = 1.1
PRINT
INPUT "Input PS MW (e.g. MW=69000)"; Ms
IF Ms \leq= a% THEN Ms = 69000
PRINT
INPUT "Input Second Virial Coefficient (e.g. A2=0)"; A2
PRINT "P.I. = "; HI, "PS MW = "; Ms, " A2 = "; A2
PRINT "These Values are OK (Y)es or (N)o?"
```

Annex A

DO
see\$ = INKEY\$
LOOP UNTIL see\$ = "y" OR see\$ = "Y" OR see\$ = "N" OR see\$ = "n"
IF see\$ = "N" OR see\$ = "n" THEN GOTO TopkkkValues
CLS
END SUB